Monitoring soil erosion and vegetation pattern related to microclimatic conditions in Icelandic and Fennoscandian tundra

Georg Kodl

A thesis submitted for the degree of PhD
at the
University of St Andrews

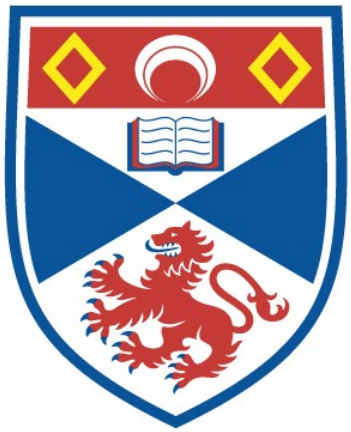

2025

Identifier to use to cite or link to this thesis:
DOI: https://doi.org/10.17630/sta/1221

DECLARATIONS

Candidate's declaration

I, Georg Kodl, do hereby certify that this thesis, submitted for the degree of PhD, which is approximately 60000 words in length, has been written by me, and that it is the record of work carried out by me, or principally by myself in collaboration with others as acknowledged, and that it has not been submitted in any previous application for any degree. I confirm that any appendices included in my thesis contain only material permitted by the 'Assessment of Postgraduate Research Students' policy.

I was admitted as a research student at the University of St Andrews in September 2020.

I received funding from an organisation or institution and have acknowledged the funder(s) in the full text of my thesis.

Date 06/01/2025 Signature of candidate

Supervisor's declaration

I hereby certify that the candidate has fulfilled the conditions of the Resolution and Regulations appropriate for the degree of PhD in the University of St Andrews and that the candidate is qualified to submit this thesis in application for that degree. I confirm that any appendices included in the thesis contain only material permitted by the 'Assessment of Postgraduate Research Students' policy.

Date 06/01/2025 Signature of supervisor

Permission for publication

In submitting this thesis to the University of St Andrews we understand that we are giving permission for it to be made available for use in accordance with the regulations of the University Library for the time being in force, subject to any copyright vested in the work not being affected thereby. We also understand, unless exempt by an award of an embargo as requested below, that the title and the abstract will be published, and that a copy of the work may be made and supplied to any bona fide library or research worker, that this thesis will be electronically accessible for personal or research use and that the library has the right to migrate this thesis into new electronic forms as required to ensure continued access to the thesis.

I, Georg Kodl, confirm that my thesis does not contain any third-party material that requires copyright clearance.

The following is an agreed request by candidate and supervisor regarding the publication of this thesis:

Printed copy

No embargo on print copy.

Electronic copy

No embargo on electronic copy.

Date 06/01/2025 Signature of candidate

Date 06/01/2025 Signature of supervisor

Underpinning Research Data or Digital Outputs

Candidate's declaration

I, Georg Kodl, understand that by declaring that I have original research data or digital outputs, I should make every effort in meeting the University's and research funders' requirements on the deposit and sharing of research data or research digital outputs.

Date 06/01/2025 Signature of candidate

Permission for publication of underpinning research data or digital outputs

We understand that for any original research data or digital outputs which are deposited, we are giving permission for them to be made available for use in accordance with the requirements of the University and research funders, for the time being in force.

We also understand that the title and the description will be published, and that the underpinning research data or digital outputs will be electronically accessible for use in accordance with the license specified at the point of deposit, unless exempt by award of an embargo as requested below.

The following is an agreed request by candidate and supervisor regarding the publication of underpinning research data or digital outputs:

No embargo on underpinning research data or digital outputs.

Date 06/01/2025 Signature of candidate

Date 06/01/2025 Signature of supervisor

ABSTRACT

The Arctic tundra, a key regulator of the global carbon cycle that stores nearly half of the world's below-ground organic carbon, is increasingly threatened by soil erosion driven by climate change and anthropogenic activity. Topography moderates these impacts on small spatial scales by creating microclimates that shape biogeomorphological processes and the distribution of barren and vegetated areas. Seasonal variations further influence these dynamics, adding to the complexity of monitoring and assessing landscape resilience under growing environmental pressures.

This research addresses two key questions: How can we best monitor tundra environments? Where and how will different tundra environments respond to changing climatic conditions?

Fieldwork was conducted in Svalbarðshreppur, Iceland and Kilpisjärvi, Finland during the growing seasons of 2021-2023. Methods included remote sensing data from multispectral uncrewed aerial vehicle (UAV) surveys, optical satellites (Landsat, Sentinel-2, PlanetScope) and digital elevation models derived from UAV, aerial LiDAR (light detection and ranging) and ArcticDEM. Soil moisture and temperature sensors were deployed along mesotopographic transects, together with vegetation surveys, to provide ground-level information.

Findings revealed limitations of common satellite systems for soil erosion monitoring due to spectral confusion caused by shrub expansion. The Shannon Evenness Index was introduced to identify suitable spatial resolutions for environmental monitoring, revealing that a resolution of <3 m is necessary in Iceland to minimise excessive mixed pixels. Seasonal microclimatic conditions and topographic position influenced the distribution of land cover and plant structure. In summer, soil moisture impacted plant species richness and distribution, with increased water stress observed on ridge positions. In winter, snow cover duration (SCD), associated with thermal insulation and wind protection, was a determining factor on the distribution of barren and vegetated areas. In Finland, an SCD of approximately 155 days was identified as a tipping point, beyond which snow cover shifts from benefiting vegetation to suppressing it.

ACKNOWLEDGEMENTS

I would like to thank the people who helped and supported me throughout my PhD journey and helped me to achieve this work. First and foremost, I extend my gratitude to my supervisor team Richard, Tobias and Nick.

Richard Streeter you have been the cornerstone of this journey, and I am immensely thankful for the opportunity and the help you have provided. Your guidance has been invaluable, striking a nice balance between offering direction when needed and allowing me the freedom to make my own decisions throughout the process. Your mentorship, coupled with your good humour and pleasant company, has made this experience both enriching and enjoyable. It has truly been a pleasure to work with you.

I am very thankful to Tobias Bolch for providing me the opportunity to come to St Andrews and for the warm welcome during the challenging COVID-19 period. I fondly recall our first meeting, which included a memorable swim in the Scottish sea - a truly delightful introduction to Scotland! Your support in remote sensing has been vital for this journey. Thank you for your insightful advice and the enriching conversations we have shared along the way.

I would like to express my sincere gratitude to Nick Cutler. Though not initially part of my official supervision team, you became a vital pillar in the success of this project. Your advice, reviews, and recommendations have been instrumental in shaping this work. Your contributions have been crucial in transforming this thesis into the formidable piece of research it has become. Thank you for your resolute support and guidance throughout this journey.

I am grateful to William McCarthy for being a hero in my time of need. At the start of my PhD, when faced with uncertainties regarding UAV processing equipment, you provided crucial support. Upon returning from my first trip in Iceland, I found myself unable to process the gathered data. Your generosity in allowing me to use your lab computer was a lifesaver, preventing what could have been a significant setback in my research.

Thanks to Willem Koster for being my companion upon my arrival in St Andrews. Your presence and helpfulness in navigating my new surroundings were greatly appreciated. I am particularly grateful for our memorable trip to Iceland and the great music we shared during our long drives across the country. A standout moment was our arrival in Iceland, where we found ourselves in quarantine in Vogar. In a serendipitous twist, The Lord of the Rings was airing on Icelandic television that week while we could observe the glowing, erupting volcano on the horizon

outside our room. This unique confluence of fiction and nature created an unforgettable experience that I will always cherish.

During my PhD journey, I had the chance to build a collaboration with Finnish colleagues, which turned out to be a very fruitful and exciting experience. Julia, Pekka, and Miska's work was very inspirational on my research journey. I never would have thought back then that I'd be working with you later and that you'd show me around picturesque Kilpisjärvi. I was truly amazed by the fantastic research you are doing and your kindness and connection to nature. Finland definitely has a special place in my heart now.

I was lucky to have the opportunity to work in the field with Julia Kemppinen. I particularly appreciate learning so much about the lovely tiny plants of Kilpisjärvi! Thank you very much for all your help and advice along the way.

I also had the chance to spend time with Pekka Niittynen in Kilpisjärvi. Thanks for the great talks we had and for sharing good times in the best sauna I had the chance to experience!

I was fortunate that Miska Luoto hosted me at the University of Helsinki for a couple of weeks. I want to greatly thank you for such kind hospitality, for showing me the beautiful nature around Helsinki, and for our inspiring talks.

I would also like to thank Hildur and Siggi for their great hospitality at Grásteinn in Iceland. They made me feel at home during my stay, and I enjoyed the most delicious breakfast every day. I always looked forward to coming back. Thank you for letting me study your wonderful land.

Yuri Gorokhovich played a less direct role in my thesis process, but his contribution was nonetheless important. I am deeply grateful for bringing this position to my attention and for your support in helping me to get it. Our conversations were always enriching, both personally and intellectually.

Last but not least, I want to thank my parents, Helena and Jiří Kodl. Without their continuous support and having my back in difficult times, I wouldn't be here.
Děkuji vám, že jste vždy se mnou / Dziękuję, że zawsze jesteście ze mną.

FUNDING ACKNOWLEDGEMENTS

The PhD was funded by the St Andrews World Leading Scholarship. The research visit and fieldwork conducted in Finland was funded by the Scottish Alliance for Geoscience, Environment & Society (SAGES) Saltire Award (2022). Santander Research Mobility award supported a field trip to Iceland (2022). Smaller grant schemes from Scottish Arctic Network (ScAN) and SAGES provided financial support for conferences.

Fagradalsfjall volcano, Iceland. 21 August 2021

“I wish it need not have happened in my time,” said Frodo.
“So do I,” said Gandalf, “and so do all who live to see such times. But that is not for them to decide. All we have to decide is what to do with the time that is given us.”

— J.R.R. Tolkien

TABLE OF CONTENTS

TABLE OF FIGURES

LIST OF TABLES

LIST OF ABBREVIATIONS

DEM – Digital Elevation Model

DSM – Digital Surface Model

FVC – Fractional Vegetation Cover

LiDAR – Light Detection And Ranging

LS – Landsat

Ls-Veg – Low-stature Vegetation

Ms-Shrub – Medium-stature Shrub (=dwarf birch)

NDVI – Normalized Difference Vegetation Index

NDRE – Normalized Difference Red Edge

NIR – Near Infrared

NMDS – Non-metric Multidimensional Scaling

PFT – Plant Functional Type

PS – PlanetScope

RE – Red Edge

RECI – Red Edge Chlorophyll Index

RENDVI – Red Edge Normalized Difference Vegetation Index

S2 – Sentinel-2

SCD – Snow Cover Duration

SM – Soil Moisture

ST – Soil Temperature

SOC – Soil Organic Content

SWC – Soil Water Content

UAV – Uncrewed Aerial Vehicle

PUBLICATION AND CONTRIBUTIONS

The third Chapter was published and based on the following article:

Kodl, Georg; Streeter, Richard; Cutler, Nick; Bolch, Tobias (2024): Arctic tundra shrubification can obscure increasing levels of soil erosion in NDVI assessments of land cover derived from satellite imagery. In *Remote Sensing of Environment* 301, p. 113935. DOI: 10.1016/j.rse.2023.113935.

The specific tasks and support in data collection provided by each person for this thesis are outlined:

1. Richard Streeter assisted with fieldwork in Svalbarðshreppur, Iceland (2021) and Kilpisjärvi, Finland (2022), specifically with drone surveys and deploying soil moisture and temperature probes.
2. Julia Kemppinen helped with the vegetation composition survey and with sampling and processing of the leaf information in the lab of *Betula nana* in Kilpisjärvi (2022) (Chapter 5.3.2.2). She also provided support in deploying and managing the soil logger from the field site in Kilpisjärvi.
3. Pekka Niittynen processed the snow cover duration (SCD) data for Svalbarðshreppur and from Kilpisjärvi (Chapter 4.3.4). He assisted with the software processing of leaf information (Chapter 5.3.2.2). He also helped in retrieving the soil logger from the field site in Kilpisjärvi.

CHAPTER 1: INTRODUCTION

1.1 TUNDRA: A BIOME IN TRANSFORMATION

The Arctic tundra, once a symbol of untouched wilderness, is now at the forefront of dramatic ecological transformations due to anthropogenic pressures and climate change (IPCC 2023; Post et al. 2019). The transformation of the Arctic tundra is not only altering its physical landscape but also has profound implications for its ecological functions and global climate regulation.

The tundra, a treeless biome covering approximately 10% of the Earth's land surface, plays a crucial role in the global climate system and provides essential ecological functions (Thomas 2020; Callaghan et al. 2004). This biome is found in two distinct areas: the high-latitudes of the northern hemisphere, known as the Arctic tundra, and on the tops of mountains, referred to as the Alpine tundra. It is the coldest of all biomes and its landscapes are shaped by the cryosphere and are characterised by extremely low temperatures, low precipitation, poor nutrient availability, and short growing seasons (Thomas 2020).

The tundra biome supports a diverse array of flora and fauna adapted to the cold environment, including unique vegetation like endemic mosses, lichens, graminoids, and dwarf shrubs (Walker et al. 2016), which are crucial for various forms of wildlife, including migratory birds and home to ungulate herbivores such as the caribou, muskox and reindeer (Meltofte 2013). Functionally, the tundra is a critical global climate regulator. It plays a crucial role in the global climate system, as it stores significant amounts of carbon in its permafrost and peatlands (Schuur et al. 2015), with its soils containing approximately half of the estimated global below-ground organic carbon pool (Tarnocai et al. 2009). Moreover, its expansive snow-covered landscapes and light coloured vegetation contribute significantly to the Earth's albedo effect, reflecting solar radiation and thus influencing global temperature patterns (Euskirchen et al. 2016; Sturm et al. 2005).

Beyond its environmental impact, the Arctic tundra holds profound cultural and economic significance for indigenous populations, such as the Sami of Fennoscandia, who have thrived in these extreme conditions for millennia, developing unique cultural practices tied closely to the land. This biome, therefore, is not only a critical component of the

Earth's ecological health but also a vital cultural heritage site that necessitates careful management and protection to ensure its preservation for future generations (Nuttall 1998).

Biogeomorphological feedbacks and Microclimate

The Arctic tundra ecosystem's response to climatic changes is governed by a complex interplay between biological and geomorphological factors. Biogeomorphological processes, which involve the interactions between living organisms and the physical landscape, can either mitigate (e.g., through species richness) or promote (e.g., via productivity or disturbance gradients) vegetation responses to climatic warming. These processes create a patchwork of microhabitats with distinct ecological conditions, leading to multiple ecological states transitions within a small area (Lara et al. 2020; Niittynen et al. 2020a).

Biogeomorphological feedbacks play an important role in Arctic vegetation dynamics, exhibiting both positive and negative effects. Positive feedbacks, like snow trapping by shrubs, can promote replacement of graminoid to shrub dominated tundra (Sturm et al. 2001), or the cryogenically formed patterned-ground features can promote tall shrub recruitment (Frost et al. 2013). Conversely, negative feedbacks, such as soil erosion, can reduce plant vitality (Cutler et al. 2023), or the expansion of thermokarst features e.g. resulting in more abundant small ponds, greater microrelief, more active lakeshore erosion and increased landscape and habitat heterogeneity (Raynolds et al. 2014). These geomorphological processes have diverse ecological impacts. For instance, disturbances were shown to promote species richness. However, the response to climate change varies across ecosystems. Vegetation in productive, low-altitude sites (such as herb-rich deciduous forests) shows higher sensitivity to warming. In contrast, alpine tundra vegetation demonstrates more resilience, partly due to the buffering effects of grazing (Virtanen et al. 2010).

The tundra biome is characterised by its highly fragmented environment (Virtanen & Ek, 2014). This fragmentation is primarily formed due to the interaction between landscape curvature and weather conditions, creating microclimates (Fig. 1). Microclimates are localised atmospheric conditions that differ from the surrounding area (Suggitt et al. 2011) and influence various environmental properties, such as soil type, sun and wind exposure, soil moisture and temperature, snow distribution, nutrient availability, pH

levels, and microbial activity (van Zuijlen et al. 2020; Kemppinen et al. 2019; Cutler 2011; Sturm & Wagner 2010). These differences in microclimate create niche habitats and influence the productivity, distribution, and structure of vegetation (Kemppinen & Niittynen 2022; Suvanto et al. 2014). Microclimatic winter thermal conditions have been identified as the most important environmental variable for vascular plant richness in the Fennoscandian tundra and plant species occurrence in all Arctic sites (Niittynen et al. 2020a). These conditions are strongly controlled by snow depth and snow cover duration, and their distribution is influenced locally by topographic variability (Niittynen et al. 2020a). Additionally, tundra microclimates affect geomorphological processes, such as wind and fluvial erosion, and frost activity (Giaccone et al. 2019), and mediate the impact of grazing and disturbance recovery (Mörsdorf et al. 2021).

Understanding the role of topography in tundra environments in forming microclimates and its impact on the tundra landscape can therefore help in understanding the biome's past, present, and future development. These fine-scale dynamics can be revealed in UAV imagery (Assmann et al. 2020), but are not captured in lower-resolution satellite datasets, introducing uncertainty into assessments of the tundra's current and future states (Myers-Smith et al. 2020; Lara et al. 2018).

Changing environmental conditions

The Arctic is warming at a rate up to four times higher than the global average (Rantanen et al. 2022), exacerbated by Arctic Amplification (Rantanen et al. 2022; Chylek et al. 2022). This rapid warming is primarily triggered by a decline in sea ice cover, which lowers the albedo of the north pole and further amplifies warming. This process has been the dominant radiative feedback mechanism affecting the region over the last few decades (Letterly et al. 2018). As a result, more frequent, longer, and more intense Arctic marine heatwaves have occurred in recent years, and an increase in their frequency is expected (Barkhordarian et al. 2024; Smith et al. 2023). These heat waves put significant stress on cold-dependent regions, leading to uncertain outcomes for the Arctic ecosystems (Smith et al. 2023).

As the climate becomes warmer and wetter in the Arctic, vegetation cover and ecosystem function will respond (Weijers et al. 2018; Vuorinen et al. 2017; Myers-Smith et al. 2011). This vegetation change manifests as Arctic greening which is associated with increased vegetation cover, shrub expansion, and higher biological productivity. On the other hand,

Arctic browning is associated with plant damage or loss of vegetation cover (Myers-Smith et al. 2020). In the context of remote sensing, the terms "Arctic greening" and "browning" refer to specific phenomena derived from observing spectral trends in satellite data (Myers-Smith et al. 2020). "Greening" indicates a positive trend in vegetation indices, suggesting an increase in plant growth, biomass, or photosynthetic activity (Phoenix and Bjerke 2016; Epstein et al. 2015; Xu et al. 2013; Jia et al. 2003). Conversely, "browning" indicates a negative trend in vegetation cover, plant health and productivity. Despite increasing summer air temperatures, the lack of a greenness trend could be attributed to limitations imposed by indirect drivers such as local microclimatic variability, confounding factors such as patchy vegetation and bare ground or greening (e.g., plant productivity) and browning (herbivory) effects that annul each other (Berner et al. 2020). An analysis across the whole Arctic using Landsat satellite data with 30 m spatial resolution from 1985 to 2016 revealed that 37.3% of the Arctic has greened, 4.7% has browned, and 58% has shown no change (Berner et al. 2020), highlighting the complexity of vegetation responses to climate change.

Widespread changes in Arctic vegetation in response to climate change have been documented (Elmendorf et al. 2012; Myers-Smith et al. 2011), from the northward spread of taller shrubs and trees to shifts in plant species composition, with increases in vascular plants and decreases in non-vascular species like moss and lichen (Harris et al. 2022; IPCC 2019; Myers-Smith et al. 2015; Walker et al. 2006). Notably, Greenland has experienced a doubling of vegetation cover from the late 1980s to the late 2010s, primarily due to wet heath development along receding lakeshores and changes associated with latitude (Grimes et al. 2024). Arctic greening was also associated, with summer warming, which has been identified as a key driver of widespread, albeit not uniform, greening in the Arctic tundra biome, linked to increased plant productivity of graminoids and shrubs, as well as overall ecosystem productivity (Berner et al. 2020).

While there is a general uptrend in Arctic vegetation greenness, "browning" represents the minority of the Arctic tundra areas where vegetation suffers from physical damage or mortality due to extreme events, e.g. wildfire, drought, insect and fungal pests, leading to decreased productivity (Myers-Smith et al. 2020; Bjerke et al. 2014; Bokhorst et al. 2009). Regions in West Greenland and across Iceland are experiencing vegetation loss, mainly due to aeolian soil erosion and unstable soils (Heindel et al. 2015; Arnalds 2015). Land

use practices, especially animal husbandry, are crucial components in managing and shaping Arctic landscapes. Overgrazing can lead to reduced vegetation cover and productivity if biological thresholds for sustainable usage are exceeded (Barbero-Palacios et al. 2024; Mörsdorf et al. 2021; Marteinsdóttir et al. 2017; Forbes & Kumpula 2009; Simpson et al. 2001).

Despite the increasing knowledge about Arctic greening and browning trends, it remains challenging to derive comprehensive conclusions about the environmental state, such as changing biodiversity, biological productivity, or geomorphological activity, and whether these processes change homogeneously over the landscape. While remote sensing has provided valuable insights into large-scale vegetation changes, the majority of the Arctic tundra remains "spectrally stable" reported in multiple studies using NDVI (Callaghan et al. 2022 and references therein), meaning that no significant changes in spectral reflectance have been detected. This spectral stability, however, does not necessarily imply ecological stability, as there is still little understanding of the ecological implications of these spectral trends.

The vast expanse of the Arctic and the challenges associated with remote sensing and ground observations introduce uncertainties regarding the causes of spectral change or stability in specific regions. While these trends provide valuable insights into the changing Arctic tundra at a large-scale, they do not capture the spatially variable outcomes at small to medium scales. The Arctic is characterised by high spatial variability, with local factors such as topography, soil conditions, hydrology, herbivory and microclimate significantly influencing the extent and nature of vegetation changes at a fine spatial scale (Bjorkman et al. 2018; Tape et al. 2012). This spatial heterogeneity is further compounded by the resolution limitations of current remote sensing data, which may not adequately capture the complex mosaic of ecological changes occurring at smaller scales.

Resilience and Tipping points

Understanding the response of the tundra landscape to rapid environmental changes is critical, given that landscapes possess resilience thresholds that govern their adaptability to these changes (Walker et al. 2004; Holling 1973). Each system has a stable state, but changing environmental conditions can lead the system to 'flip' to a new state with different ecosystem functions and biological productivity (Scheffer et al. 2001). The response of the tundra landscape to changes in macroclimate and land use practices is

significantly influenced by topography. Topographic features mediate these changes, leading to highly heterogeneous responses across the landscape (Fig. 1) (Suggitt et al. 2011; Aalto & Luoto 2014). This heterogeneity means that certain areas within the Arctic may reach ecological tipping points sooner than others, particularly those already under stress (Pichon et al. 2024). Consequently, this can result in the coexistence of multiple stable states within the landscape (Rietkerk et al. 2021), or, in extreme cases, complete ecosystem collapse (Rietkerk et al. 2004; Arnalds et al. 2001). Understanding the resilience and potential tipping points of the tundra landscape is essential for assessing altering ecosystem services provided and developing appropriate management strategies (Bennett et al. 2015). To effectively assess tundra's landscape resilience and identify early warning signals of major ecosystem shifts (Kéfi et al. 2014), it is crucial to implement precise monitoring systems in these remote areas.

Monitoring and Remote sensing

The advent of remote sensing technologies has revolutionised our ability to study and monitor tundra ecosystems on a global scale, overcoming the limitations of traditional research methods. Prior to this technological breakthrough, tundra research relied heavily on field surveys, which, while valuable, were necessarily restricted in both spatial extent and temporal coverage. The deployment of satellite sensors like MSS, TM, and ETM+ aboard the Landsat series (from 1972) and the Advanced Very-High-Resolution Radiometer (AVHRR; from 1982) aboard NOAA satellites, and the Moderate Resolution Imaging Spectroradiometer (MODIS; from 1999) aboard NASA's Terra and Aqua satellites has transformed tundra research by delivering global datasets with varying spatial, temporal, and spectral resolutions (Myers-Smith et al. 2020). The Landsat series provided multispectral imagery at moderate spatial resolution of 30-60 m but infrequent revisits of ~16 days, while the coarser 1 km AVHRR sensor and MODIS with 250 m to 1km spatial resolution offer daily global coverage (NASA, 2024; NOAA, 2024). These satellite systems have allowed us to derive vegetation indices such as normalized difference vegetation index (NDVI) which are proxies of photosynthetic activity and used indirectly as a measure of biological productivity (Fitter & Raffaelli 1999; Goward et al. 1991). This set the baseline for long-term studies and has provided unparalleled insights into land cover and biophysical changes across the Arctic over the decades (Stow et al. 2004).

However, challenges persist in upscaling and effectively integrating satellite data with ground-based observations, primarily due to mismatches in the spatial and temporal scales of the datasets, which complicate analysis and synthesis efforts (Miles & Esau 2016; Bhatt et al. 2013). Moreover, trends in NDVI data produced from different satellite datasets or using different methods do not always correspond at a given location (Tian et al. 2015; Guay et al. 2014), making it challenging to distinguish ecological change from differences due to methods and sensor/platform-related issues when interpreting localised spectral signals.

Spatial scale is a crucial factor to consider in tundra monitoring, as satellite data often miss the fine-resolution details essential for reflecting the tundra's fragmented nature (Räsänen et al. 2019; Virtanen & Ek 2014). To address this issue, Earth observation must be coupled with ground-truthing data to understand and validate the received spectral signals in space (Bartsch et al. 2016; Raynolds et al. 2012). Understanding the potential capacity and limitations of these monitoring systems is essential for accurate interpretation and decision making (Laidler et al. 2008; Stow et al. 2004).

Failure to account for scale issues can introduce uncertainties and lead to potentially serious misinterpretations, which can have detrimental consequences such as missing ecological tipping points (Kéfi et al. 2014; Rietkerk et al. 2004). Remote sensing data are used to validate environmental models and monitor real-world changes, making the availability of the most accurate products a necessity (Pettorelli et al. 2014). These data inform global and local policy stakeholders and guide land use practices, underlining the importance of reliable and precise monitoring at appropriate scales (Arnalds & Barkarson 2003). Efforts to bridge the gap between satellite observations and ground-based measurements are crucial for developing a comprehensive understanding of the tundra's complex dynamics and ensuring informed decision making in the face of rapid environmental change (Eischeid et al. 2021; Siewert & Olofsson 2020; Assmann et al. 2019).

Ground validation

Remote sensing enables the scaling of tundra vegetation measurements from landscape to global scales (Stow et al. 2004). To achieve this with high accuracy, datasets at multiple spatial scales are required. These datasets capture fine-scale vegetation patterns and connect them to broader landscape, regional, and global processes.

Advancements in uncrewed aerial vehicle (UAV) technology, along with reduced costs, present promising avenues for bridging the gap between in-situ observations and space-derived data (Assmann et al. 2020; Cunliffe et al. 2020). Due to the very-high resolution of cm-scale, data from UAVs provide a close approximation to ground-truth while covering a suitable spatial extent to capture landscape-forming processes. Early (mid-2010s) UAV surveys of vegetation used a digital RGB camera mounted on a quadcopter and photogrammetry techniques (Fraser et al. 2016). Since then, market and technology evolved quickly with smaller specialised UAVs using multispectral bands, but also hyperspectral and LiDAR systems that allowed monitoring of fine-scale environmental processes and validate satellite imagery (Eischeid et al. 2021; Siewert & Olofsson 2020; Sotille et al. 2020). However, several obstacles still need to be overcome to fully harness the potential of UAVs in tundra research, including limited flight endurance, payload restrictions, severe weather conditions, inaccessible terrain, and data processing requirements (Poley & McDermid 2020; Assmann et al. 2019).

Despite these challenges, UAVs have enhanced the validation of satellite data and facilitated detailed studies of local environmental processes (Eischeid et al. 2021; Siewert & Olofsson 2020; Sotille et al. 2020). For instance, Sotille et al. (2020) used UAV data to demonstrate that scale-dependency varies significantly across areas and seasons in the Arctic, complicating generalisations and highlighting the importance of validating satellite datasets. The integration of UAV data with satellite imagery and field observations has substantially improved our approach to monitoring and understanding the heterogeneous tundra ecosystem, offering novel insights into its complex dynamics and potential responses to environmental changes.

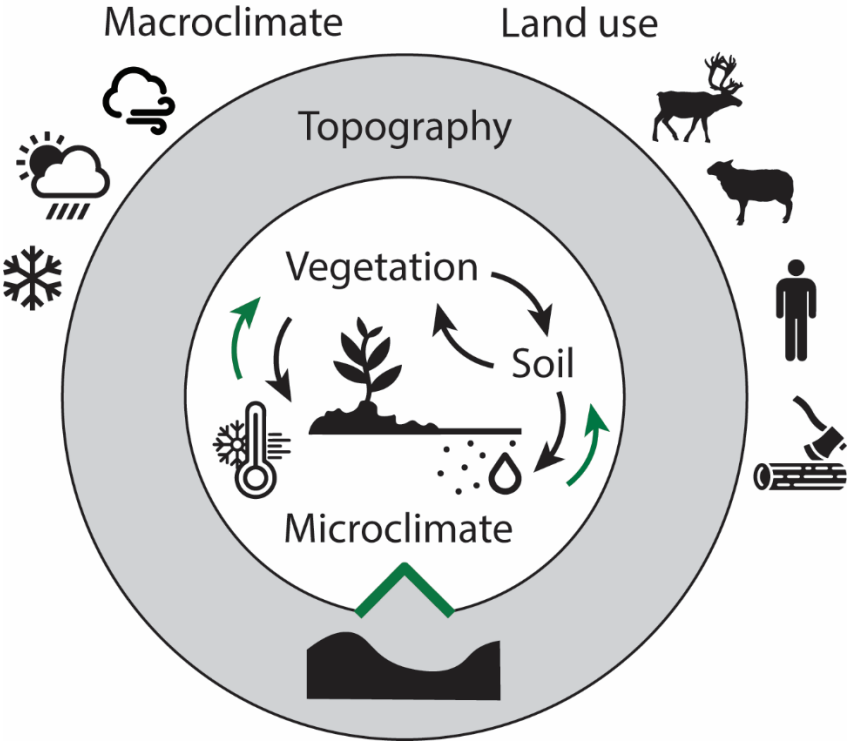

Fig. 1 Illustration of the mediating qualities of topography on macroclimate and land use influences on microclimate, vegetation, and soil. The green arrows indicate the research focus of this study.

1.2 CHALLENGES AND RESEARCH QUESTIONS ADDRESSED IN THE THESIS

Studying long-term ecological changes presents several difficulties due to the complexity of the involved systems and the extended time spans that need to be considered. Two major challenges arise 1) the lack of detailed knowledge about all the influencing components and 2) the scarcity of suitable datasets to infer biophysical variations from change detection.

A particularly important process that can result from abrupt environmental change is soil erosion. Soil erosion is a multifaceted process influenced by various factors, such as climate, topography, soil properties, land cover, and land use practices (Poesen 2018). The interplay between these factors can result in non-linear and unpredictable erosion patterns over time (García-Ruiz et al. 2015), making it difficult to understand and predict the long-term dynamics of soil erosion. Given the complexity of the systems involved and the limitations in studying the entire chain of interrelated environmental variables, focusing on controlling factors, such as topography, can provide valuable insights (Fig. 1).

Topographic heterogeneity can explain patterns of vegetation response to climate change (Bueno de Mesquita et al. 2018). While climatic conditions and land use are fundamental drivers of landscape development and productivity, topography mediates all of these factors and thus affects biotic and abiotic processes (Fig. 1) (Raynor et al. 2021; Dialynas et al. 2016; Suvanto et al. 2014). Understanding how minor changes in terrain can affect microclimate, vegetation, and soil formation through biogeomorphological processes allows to comprehend better the spatial controls of landscape development and predicting future changes.

Moreover, the extended time spans required to observe significant changes in soil erosion or ecology pose another obstacle. The limited availability of data across time and space further complicates the study of these phenomena, as the available datasets do not necessarily cover the temporal and spatial scales required. Validating satellite imagery presents an additional hurdle, as it requires high-resolution spatial data and on the ground knowledge. By integrating multiple datasets, including very-high resolution multispectral UAV data, satellite data with larger spatial extent and temporal range, in-situ soil loggers with high-temporal resolution, and collected vegetation data, this allows landscape formation processes to be studied in more detail.

The main aims of the thesis are (I) to assess accuracy of monitoring capabilities using Earth observation data and (II) to understand the microclimatic winter and summer conditions and their influence on land cover formation in the tundra.

The first aim addresses the scaling biases encountered when using satellite data for monitoring soil erosion in Iceland, in order to determine the most appropriate spatial resolutions for this task (Chapter 3). This involves the following research questions:

1) Does Arctic greening occur at the Icelandic study sites and is it associated with observed changes in vegetation cover?
2) Which current satellite systems are best suited for tundra land cover monitoring?
3) What are suitable spatial resolutions of remote sensing data to mitigate scaling biases?

The second aim is to investigate how winter microclimate conditions affect the distribution of barren cover at the study locations in Iceland and Finland (Chapter 4).

To address this, the research questions are:

4) How is the distribution of barren cover related to terrain curvature?
5) How is the distribution of barren cover related to the snow cover duration (SCD)?
6) What are the soil thermal microclimatic conditions during the winter season?

The second aim is to investigate how microclimatic conditions during the summer growing season affect vegetation cover and vitality at study locations in Iceland and Finland (Chapter 5).

The research questions for this aim are:

7) What is the vegetation distribution in relation to terrain curvature?
8) How does the plant vigour/morphology for common plant functional types (PFT) vary according to different topographic positions?
9) How does topography affect spatial distribution of soil moisture?
10) How does soil moisture relate to land cover pattern?

Given the variability of the tundra biome across different environments, investigating the microclimatic influence on land cover in multiple locations, is beneficial to understand how these relationships may vary in different environments. To address this, Chapters 4 and 5 focus on studying the relationship between microclimate and land cover in both Iceland and Finland. The scaling biases discussed in Chapter 3 have been examined solely in Iceland, as its simple land cover and clearly defined patches provide an ideal setting for investigating this phenomenon. By conducting research across different tundra environments and at various scales, this thesis aims to contribute to a more holistic understanding of the complex interactions between physical and ecological processes shaping the tundra landscapes.

1.3 SITE SELECTION – ICELAND AND FENNOSCANDIA

Svalbarðshreppur in Iceland and Kilpisjärvi in Fennoscandia were chosen as research sites for this study due to the potential they offer for understanding ecosystem development, particularly in the context of soil erosion processes and microclimatic conditions in tundra environments. This section describes why these two regions were chosen for this study.

The Arctic tundra is subdivided into several zones based on latitude and elevation: sub-Arctic, low-Arctic, high-Arctic, and oro-Arctic in mountainous areas (Fig. 2). Although there is no universal agreement on the exact boundaries between these zones, Iceland is

generally considered sub-Arctic tundra due to its low tree cover and tundra-like vegetation, despite having a slightly milder climate than other sub-Arctic regions.

Before the Norse settlement in the 9th century CE, Icelandic climax vegetation, consisting of *B. pubescens*, *Salix,* and *Juniperus* woodland, was part of the Fennoscandian sub-Alpine birch-forest belt (Dugmore et al. 2005). However, after centuries of detrimental land use practices, Iceland's vegetation is now predominantly composed of low-growing shrubs, grasses, mosses, and lichens, with very few trees, reflecting the plant life found in sub-Arctic tundra regions.

The oro-Arctic zone in Fennoscandia begins at the elevation where the tree line of the Taiga, or boreal forests, ends. Beyond the Kola Peninsula in northeastern Fennoscandia, the ecoregion transitions into the low-Arctic, extending deep into Russia. The high Arctic tundra can be found in regions such as Greenland and Svalbard.

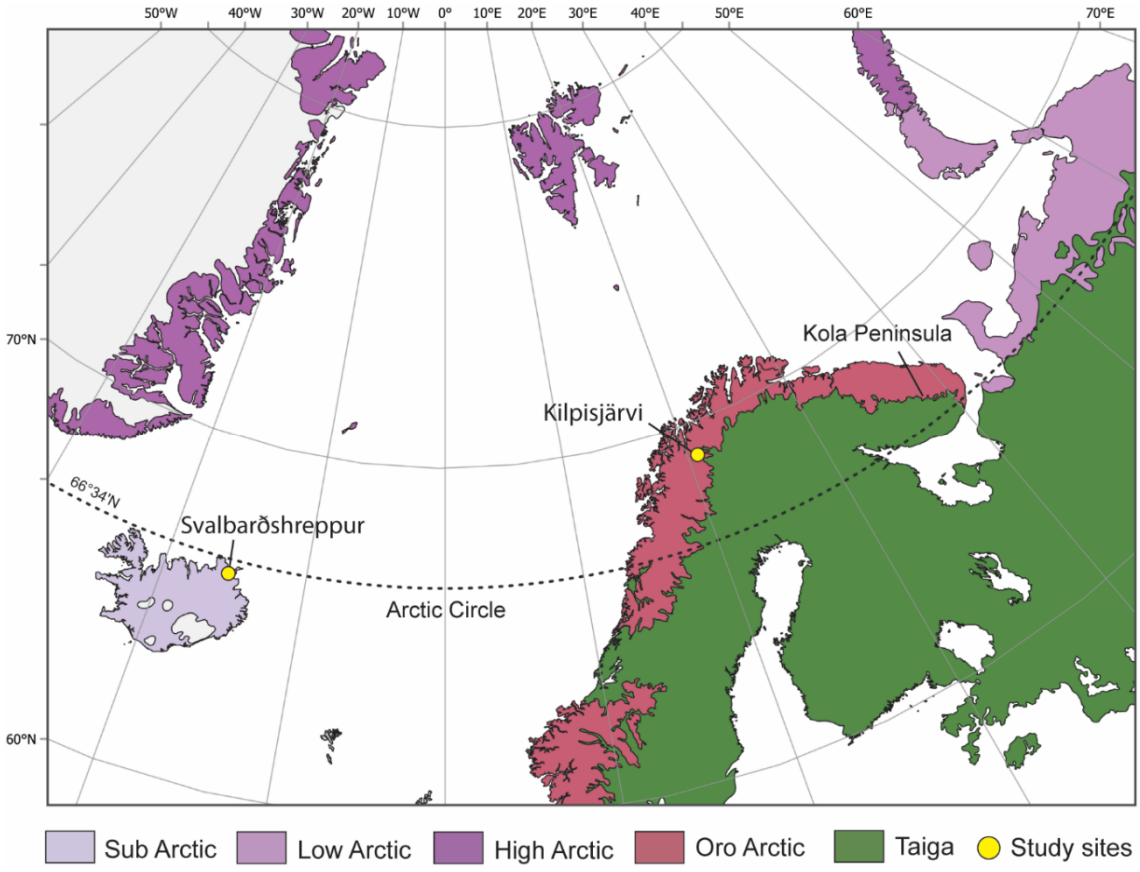

Fig. 2 Arctic map with terrestrial ecoregions (modified after The Nature Conservancy (Dec 14, 2009); developed originally by Olson & Dinerstein (2002), Bailey (1995) and Environment Canada (Wiken, 1986))

Iceland, with its severely degraded landscapes (Arnalds et al. 2023), provides a distinctive opportunity to study ecosystem development and soil erosion processes by achieving a balance between the complexity of natural systems and the manageability of scientific analysis. Land degradation refers to the deterioration of land quality and productivity, leading to a reduction in the land's capacity to support ecosystems and provide ecosystem services. It encompasses various forms of environmental degradation, such as soil degradation (e.g., loss of organic matter, nutrient depletion), vegetation degradation (including deforestation, overgrazing, or the spread of invasive species), water resource degradation, and biodiversity loss.

Iceland's biota is relatively simple due to its isolated oceanic location, high-latitude, glaciation history, and land use practices (Sadler 1999; Steindorsson 1962) and thus serves as an ideal model system to study land cover patterns, microclimates, and to assess monitoring capabilities. Functional land cover refers to the categorisation of land surface based on its ecological functions and the services it provides, such as habitat provision, carbon sequestration, or water regulation. In Iceland, these functional land cover types are irregularly scattered across the landscape, varying in shape, size, form, and abundance, with distinct boundaries between barren areas, shrubs, and low-growing vegetation. In this context, the term 'barren areas' refers to regions where vegetation cover is not present, either due to soil erosion exposing the underlying soil or, if further deflated, the glacial till beneath, or due to the presence of non-vegetated rocks/boulders. Additionally, human impact on the island has been relatively short-lived, and well documented in detailed historical records, with most of the major changes to vegetation cover occurring since its settlement in 870 CE (Streeter et al. 2015; Simpson et al. 2001).

The primary cause of land degradation in Iceland is considered to be the destruction of woodlands through deforestation, which led to a transition to simpler ecological states. This transition was further exacerbated by high grazing pressure, advancing the deterioration of soil and vegetation cover (Barrio et al. 2018; Thorsson 2008; Dugmore et al. 2000). Additionally, climate cooling caused multiple degradation phases in 5000BP, 2500BP, and the 16th century (Ólafsdóttir and Guòmundsson 2002).

Extensive research has been conducted on the social, historical, and environmental drivers of erosion in Iceland (Barrio & Arnalds 2023; Arnalds et al. 2023; Cutler et al. 2023; Dugmore et al. 2020; Barrio et al. 2018; Dugmore et al. 2009a; Thorsson 2008; Ólafsdóttir

& Guòmundsson 2002; Arnalds et al. 2001; Simpson et al. 2001), with some studies using and assessing remote sensing techniques to study soil erosion (Cutler et al. 2023; Fernández et al. 2023; Fernández et al. 2022; Streeter & Cutler 2020; Dugmore et al. 2020; Raynolds et al. 2015; Thorsson 2008). While there is still debate about the primary drivers, their relative importance, and the cascading effects on land degradation, there is agreement that the combined effect of natural processes and human interventions has promoted and accelerated erosion (Streeter et al. 2015) and that the drivers of soil erosion have changed over time and in different regions of Iceland (Streeter & Dugmore 2014). However, there is still limited understanding of the spatial distribution and future development of barren areas (Streeter & Cutler 2020).

Microclimatic studies in Iceland have been limited, with research conducted on grazing recovery (Mörsdorf et al. 2021), vegetation primary succession on young lava flows (Cutler 2011), and microclimatic conditions in woodland and scrub cover (Sjogren 1973). While it is acknowledged that small-scale topography can influence the resilience of vegetation to soil erosion (Arnalds 2015), no studies have investigated this relationship in detail.

Fennoscandia, constitutes the northernmost parts of continental Europe and is characterised by the Fennoscandian Shield, a stable and ancient segment of the Earth's crust consisting of Precambrian crystalline rock formations (Lidmar-Bergström & Näslund 2002). The Fennoscandian Shield spans Norway, Sweden, Finland, and parts of Russia (Karelia and the Kola Peninsula). The landscape has been heavily shaped by glacial activity during the Pleistocene ice ages, resulting in features like glacial valleys, kettle holes, moraines, eskers, and erratics (Stroeven et al. 2016; Kleman et al. 1997). The Scandinavian Mountains, also known as the Scandes, run along the western coast of the Scandinavian Peninsula, stretching from southern Norway to the North Cape up to the east of the Kola peninsula, forming the Oro-Arctic-Alpine tundra landscapes (Birks 2008). Together with Iceland, Greenland, and Svalbard, it is one of the few places in Europe where the Arctic tundra biome can be found and connecting with the low-Arctic tundra in Russia to the east (Fig. 2).

Fennoscandian tundra, connected to the broader Arctic, serves as a valuable study area for comparing and understanding tundra environments. Unlike Iceland, which is an isolated volcanic island with unique characteristics, Fennoscandia's tundra is more representative of the wider Arctic biome in terms of its flora, fauna, and climate, making it

a useful reference point for understanding the ecology and dynamics of tundra ecosystems.

The Kilpisjärvi region in northern Finland, known as a biodiversity hotspot in the Scandes, due to its strong environmental gradients and geodiversity (Kauhanen 2013). Located close to the University of Helsinki's Biological research station in Kilpisjärvi village (Fig. 11), the region has been the focus of decades-long intensive studies on various topics. Early research focused on fauna, particularly known for lemmings (Valanne et al. 1968; Aho & Kalela 1966), while more recent studies have covered a wide range of subjects, including plant ecology (Kemppinen et al. 2021; Kemppinen et al. 2019), bio-geomorphology (Aalto et al. 2021; Aalto & Luoto 2014; Suvanto et al. 2014), geodiversity (Salminen et al. 2023), permafrost (Gisnås et al. 2017; King and Seppälä 1987), snow-plant interactions (Niittynen et al. 2020b, 2018) and microclimate (Peña-Aguilera et al. 2023; Tyystjärvi et al. 2022; Kemppinen & Niittynen 2022). There has been substantial research on microclimate ecology in the Kilpisjärvi region, and also how topography drives vegetation pattern and geomorphic activity (Kemppinen et al. 2022; Niittynen et al. 2020a; Kemppinen et al. 2019; Riihimäki et al. 2017; Suvanto et al. 2014; Hjort & Luoto 2009). However, the relationships between topography, microclimatic conditions and barren cover distribution have not yet been fully established.

Iceland and Fennoscandia offer unique opportunities to study ecosystem development, soil erosion processes, and microclimatic conditions in tundra environments. The combination of their distinct characteristics, extensive research history, and the potential for comparative analysis makes them ideal research sites for this study, with the aim of contributing to a better understanding of the spatial distribution and future development of barren areas, as well as the relationships between microclimatic conditions and vegetation patterns in the Arctic tundra.

1.4 THESIS OUTLINE

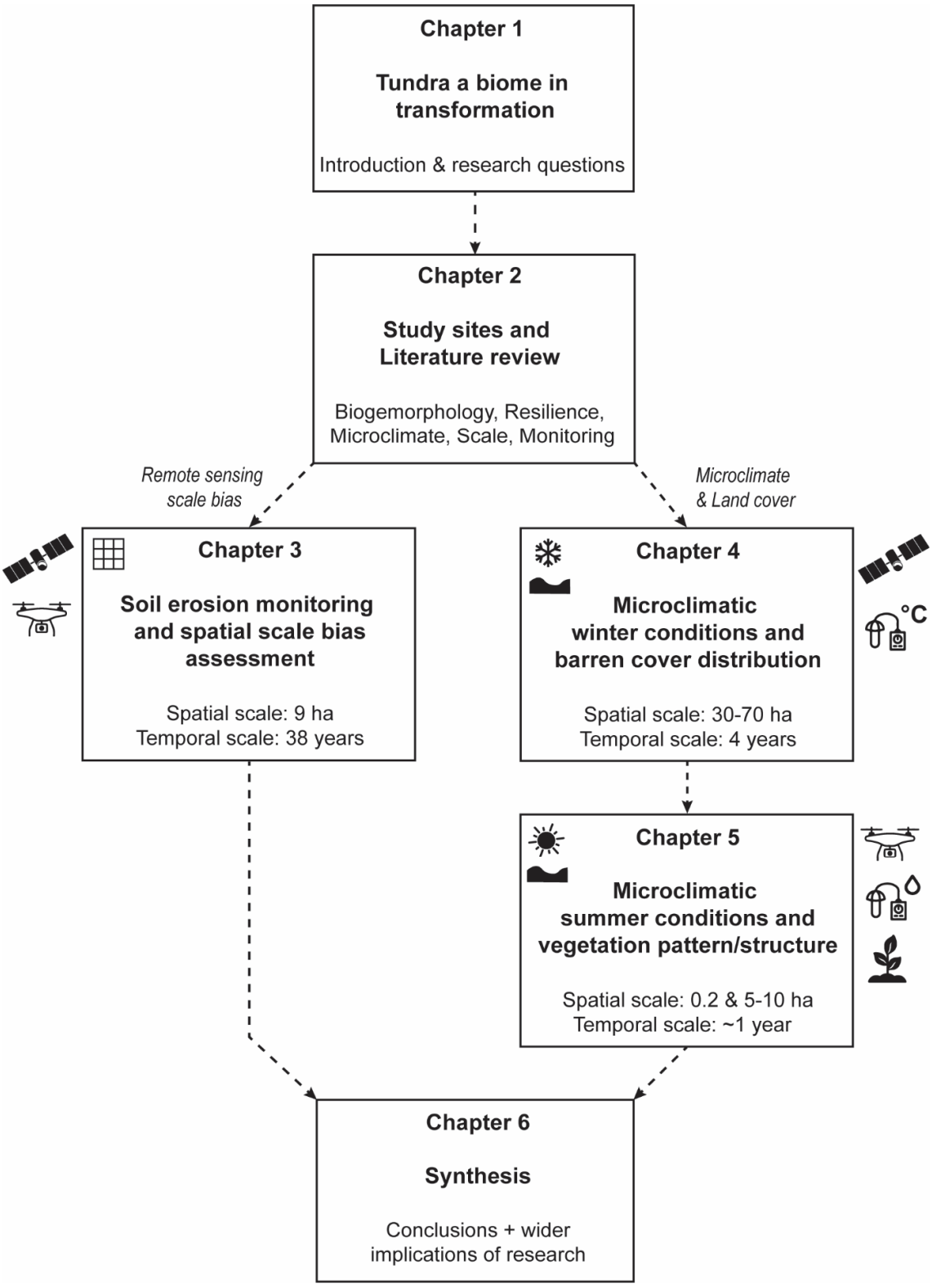

Fig. 3 Flowchart illustrating the structure of the thesis.

The thesis progresses from the introduction to explore various topics in subsequent chapters.

Chapter 2 introduces the concepts of biogeomorphology and their application to the research areas. It explores the role of topography as a driver of microclimate and how summer and winter conditions influence biogeomorphological processes. The chapter then presents the study sites in Iceland and Fennoscandia and discusses the concepts of tipping points and landscape resilience in relation to these areas. It then addresses the issue of observation scale and how it can distort our perception of reality on the ground. Finally, the chapter concludes with an overview of the history and methods of Arctic monitoring.

Chapter 3 addresses the challenge of monitoring soil erosion in high-latitude areas, where shrub expansion can cause spectral changes that lead to spectral confusion and obscure vegetation cover loss. It presents UAV survey data collected from the field, which is then compared with commonly used satellite imagery for tundra monitoring. A novel metric is introduced to determine the appropriate spatial resolution needed to avoid spectral mixing the studied environment. The aim is to enhance understanding of soil erosion monitoring by choosing suitable satellite imagery and highlighting potential biases that may arise.

Chapter 4 examines the spatial distribution of barren cover at sites in Iceland and in Finland, and explores the role microclimatic winter conditions play in the distribution. It examines the relationship between mesotopography, SCD and fractional vegetation cover (FVC). High-resolution satellite/aerial data (2-3 m) are used to investigate this. Additionally, microclimatic soil temperature conditions are evaluated and related to the land cover distribution.

Chapter 5 investigates the spatial distribution of vegetation composition and vigour on a local and landscape scale and the microclimatic summer conditions play in the distribution. It explores the relationships between vegetation cover, mesotopography and soil moisture. Additionally, plant traits of dwarf birch trees have been examined, to assess plant morphology and validate remote sensing data. A combination of multispectral UAV data, with soil instrumentation and vegetation data enabled to study these dynamics on a fine-scale.

Chapter 6 concludes this thesis and summarises the answers to the main research questions set out in chapter 1. It synthesises the results from Chapters 3–5, outlining best practices for tundra satellite monitoring and identifies key drivers of barren and vegetated cover in tundra environments. It presents a conceptual microclimate-vegetation model for Iceland and Fennoscandia based on findings from Chapters 4 and 5, and discusses the broader implications of the research.

1.5 DATASETS USED IN THE THESIS

To study biogeomorphological processes influenced by microclimatic conditions, a comprehensive dataset with a wide range of temporal and spatial resolutions, and also incorporating ground data for validation purposes, was acquired (Fig. 4). Overview of data used in the study is shown in Table 1.

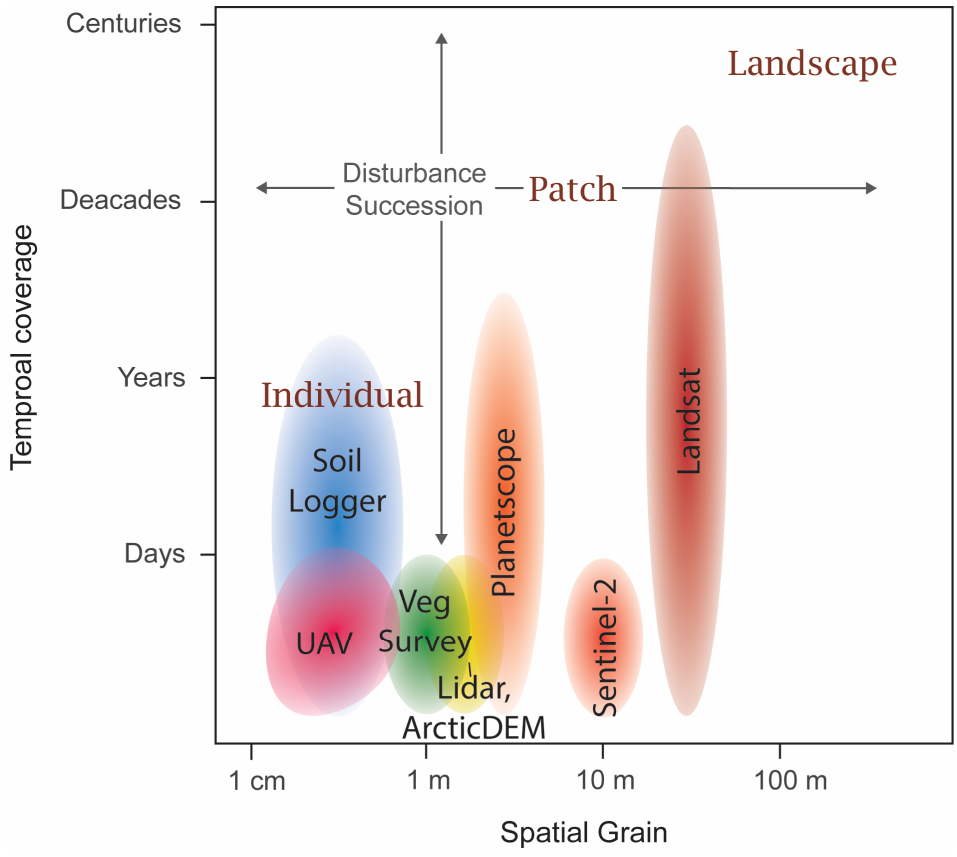

Fig. 4 Spatial and temporal resolution of datasets used in the study. This Figure illustrates the relationship between the size of the observed resolution (spatial grain) and the length of observation (temporal coverage) across various datasets. "Individual" refers to processes affecting single plants or small objects, "Patch" includes areas larger than 1m² and less than 100m², and "Landscape" encompasses areas greater than 100m². Disturbance succession indicates the sequential increase in the area of disturbance from individual to landscape scale over time. Datasets are labelled based on the acquisition instruments/methods, such as "Veg Survey" for vegetation surveys.

Advances in satellite technology have provided researchers with high-resolution spatial data that are continuously collected over extensive areas with different temporal and spatial scales. The most common satellite imagery with suitable resolutions to resolve high-latitude landscapes, provide frequent acquisition, and is freely accessible are from the NASA-led Landsat mission, ESA's Sentinel-2, and PlanetScope's CubeSats. The longest available satellite imagery with medium-resolution (30 m) is available from Landsat 5-9, starting from 1984, which is the baseline used here to assess Arctic greening trends at the study sites. All of these datasets are used in Arctic tundra studies (Andreatta et al. 2022), and here, these datasets are assessed for their suitability in environmental monitoring of the tundra. PlanetScope data have been further used in Chapter 4 to derive snow cover duration (SCD) and fractional vegetation cover (FVC).

Topographic information was derived from the widely used ArcticDEM in Arctic research, processed using high-resolution stereo imagery and accessed through the Polar Geospatial Center of the University of Minnesota (www.pgc.umn.edu/data/arcticdem/). The ArcticDEM has notable limitations, especially in steep topographic terrain, due to noise introduced by variations in image quality, differences between sunlit and shadowed areas, and step artifacts caused by vertical calibration discrepancies (Morin et al. 2016). Additionally, aerial LiDAR data from the National Land Survey of Finland were used, as they provided better data quality, particularly in the mountainous region of Kilpisjärvi.

To gain a comprehensive understanding of complexity in the natural environment, it is essential to employ a multi-faceted approach that combines earth observation with on-site field studies (Lenton et al. 2024).

Close-Range Remote sensing

UAVs offer a means to bridge remote sensing data obtained from space and ground data, as they provide a suitable spatial extent and resolution to study landscape development. In this study, multispectral UAV imagery was obtained to validate the coarser-resolved satellite imagery and create detailed land cover maps for fine-scale spatial pattern analysis. The UAV data facilitated the measurement of the spectral response of individual plant species or plant functional types (PFTs), group of plant species with similar functional characteristics and responses to environmental conditions, indicating their vigour by acquiring pure pixels. Additionally, photogrammetric procedures enabled the production of high-resolution digital surface model (DSM) maps of the study sites.

The DJI Phantom 4 Multispectral UAV system was used, equipped with five multispectral sensors capturing the centre frequency of the bands Blue (λ=450 ± 16 nm), Green (λ=560 ± 16 nm), Red (λ = 650 ± 16 nm), Red-edge (λ=730 ± 16 nm), and Near-infrared (λ=840 ± 26 nm), alongside an RGB sensor for visible light imaging. Each 1/2.9-inch CMOS sensor has an effective pixel resolution of 2.08 MP. The system is equipped with a sunlight sensor, enabling internal correction for changes in light intensity during flight.

Ground collected data

Remote sensing provides valuable large-scale data for Arctic monitoring, but it has limitations. Satellite imagery is typically acquired daily or weekly, and the Arctic's prolonged darkness in the winter and frequent cloud coverage further hinder consistent observation using passive remote sensing. Thus, passive remote sensing cannot capture dynamic microclimate variations throughout the day or season. To address these limitations, a multi-scale approach is necessary. Soil instruments have been deployed to record temperature and moisture along a mesotopographic transect (metre-scale) at hourly intervals, allowing for fine-scale monitoring of microclimatic conditions during both growing and winter seasons. The combination of broad-scale remote sensing data with high-temporal-resolution, point-scale sensor measurements enables a more nuanced and complete investigation of Arctic microclimatic systems. This integrated approach bridges the gap between large-scale patterns and localised environmental variations, providing a richer dataset for understanding the complex dynamics of tundra ecosystems.

To enable the classification of land cover orthomosaics, vegetation surveys were carried out to collect point locations of PFTs. Additionally, a vegetation composition survey with 1×1 m quadrats was conducted just above the deployed soil sensors. From these surveys, we can infer whether vegetation composition is adapting to topographic position. Further, it enables the assessment of whether the change in vegetation composition is related to microclimatic variables such as soil temperature or moisture. In Finland, plant trait measurements of the dwarf birch (*Betula nana*) have been collected, helping to interpret the spectral changes visible from UAV imagery.

Table 1 Overview of datasets used in the study. Datasets marked with an asterisk (*) were collected and processed by myself. The rest was acquired externally through freely accessible data or collaboration.

Dataset	Use	Source (Year)
Topography		
ArcticDEM	TPI	WorldView-1,2,3 (2012-2017); Photogrammetry
Aerial LiDAR	TPI	National Land Survey of Finland (2016)
UAV*	TPI, DSM for LC classification	UAV survey (2021+2022); Photogrammetry
Vegetation / Soil		
Landsat	NDVI time series	Google Earth Engine; Nasa – USGS (1984 – 2022)
Sentinel-2	NDVI	ESA – Copernicus (2022)
PlanetScope	NDVI, FVC	Planet (2017 -2022)
UAV*	NDVI, NDRE, RENDVI, LC map	UAV survey (2021 + 2022)
Land cover datapoints*	LC classification	Land cover survey (2021+2022)
Vegetation composition*	NMDS	Vegetation survey (2022)
Plant trait*	Shrub height, Leaf area + weight	Measuring and Sampling (2022)
Microclimate		
Soil temperature*	GDD, FDD, CV	Soil probes (2021-2023)
Soil moisture*	Quartile regression, CV, Mean, NMDS	Soil probes (2021-2023)
PlanetScope	Snow cover duration (SCD)	Planet (2017-2022)

CHAPTER 2: LITERATURE REVIEW AND STUDY SITES

2.1 BIOGEOMORPHOLOGY

Biogeomorphology seeks to understand how biotic factors interact with abiotic processes to create and shape landscapes. By integrating knowledge from geomorphology, ecology, and soil science, biogeomorphology provides a comprehensive framework for understanding the evolution and functioning of Earth's surface in response to the interplay between living organisms and their physical environment (Corenblit et al. 2011; Marston 2010; Viles 2020).

In the context of the Arctic tundra, biogeomorphology plays a crucial role in understanding the interactions between the stressful abiotic conditions and the resilient biotic communities that shape this-ecosystem. It is often associated with thermokarst formation and carbon dynamics (Lara et al. 2020), shrubification (Kemppinen et al. 2021; Myers-Smith & Hik 2018; Fraser et al. 2014), grazing (Barbero-Palacios et al. 2024), snow effects (Rixen et al. 2022; Happonen et al. 2019), landscape formation and vegetation change (Kemppinen et al. 2022; Kemppinen et al. 2019; Virtanen et al. 2010; Hjort and Luoto 2009; Aalto et al. 2021).

For instance, the root systems of tundra plants help stabilise the soil, reducing erosion and promoting the formation of soil organic matter (Wang et al. 2017; Iversen et al. 2015). Moreover, the presence of dense shrub patches can alter the patterns of snow accumulation and melt, leading to changes in soil moisture, nutrient availability, and surface runoff (Sturm et al. 2001). Shrubs also insulate the ground during winter, resulting in warmer soil temperatures under the snowpack (Kropp et al. 2021). Displacement of tundra by forest / woody shrubs decreases local albedo, enhancing lower atmospheric temperatures and accelerating climate warming during the high radiation late snow season (Zhang et al. 2013); this effect is partially offset by negative feedback from increased evapotranspiration (Matthes et al. 2012). In general, dwarf shrubs have been shown to make tundra soils drier, colder, and less rich in organic carbon (Kemppinen et al. 2021). Remarkably, lichens have been found to buffer the tundra microclimate more effectively than the largely expanding dwarf birch (*Betula Nana*) by reducing temperature daytime highs and raising nighttime lows during the summer (Mallen-Cooper et al. 2021). Lichens also tended to reduce soil moisture by intercepting rainfall, which influences

competition with vascular plants in areas where summer rainfall is low (Mallen-Cooper et al. 2021).

Herbivores play an important role in shaping the structure and function of tundra ecosystems. Different types and combinations of herbivores exert additive or compensatory effects, and these effects can change depending on the environmental conditions (Barbero-Palacios et al. 2024). For example, intense grazing can result in significantly higher soil temperatures, likely leading to increased measured soil N concentrations and litter decomposition rates (Olofsson et al. 2004). The grazing and trampling activities of large herbivores can alter vegetation composition, increasing nutrient cycling rates and plant uptake, leading to changes in vegetation composition from lichen and moss dominated to higher productive grass dominated tundra (Petit Bon et al. 2020; van der Wal 2006). Kaarlejärvi et al. (2017) showed that a warming trend in the presence of herbivores can lead to increases in plant species richness, which may have mixed effects in the tundra ecosystem. While greater species diversity could enhance ecosystem resilience, it may also favour the spread of shrubs and other competitive species, potentially altering the balance of tundra vegetation and impacting biodiversity. Depending on the landscape resilience and the carrying capacity of the ecosystem, overgrazing can lead to the reduction of soil stability and increase erosion susceptibility. This can lead in the worst case to the degradation of the whole landscape, from a vegetated to a barren system, such as witnessed in Iceland, from historical overgrazing (Barrio et al. 2018; Arnalds 2000a).

2.1.1 Iceland - Soil erosion

Soil erosion is a major environmental concern in Iceland, driven by the interaction of society, economy, climate and the natural environment (Barrio and Arnalds 2023; Dugmore et al. 2020). Gaining insight into the present land condition of Iceland requires an understanding of the biotic and abiotic environmental systems and historical land-use practices (Greipsson 2012; Arnalds & Barkarson 2003).

During the early Holocene, as the glaciers retreated after the Younger Dryas stadial (ended around 11,700 years ago), vegetation gradually covered Iceland (Ólafsdóttir et al. 2001; Rundgren and Ingólfsson 1999). Paleoecological evidence suggests that by the time of Norse settlement (ca. 870 AD), over 60% of Iceland was covered by vegetation, with birch forests accounting for 25-40% of the land area (Eysteinsson and Aradottir 2003;

Ólafsdóttir et al. 2001; Bergpórsson 1996; Sigurdsson 1977). Today, according to the Nytjaland database, only 45% of the country is vegetated, with more than half classified as poor heathland (Gisladottir et al. 2014). Approximately 30% of the land is classified as barren deserts, 12% as poorly vegetated with limited plant productivity, and only 1% of natural birch forest remains (Traustason & Snorrason 2008). While reforestation efforts have been ongoing since the mid-20th century, challenges like grazing pressure, volcanic activity, soil erosion, and a harsh climate persist. Restoration strategies are evolving, shifting from agronomic approaches to more ecological methods that emphasize native species and low-input techniques. However, large-scale restoration remains difficult due to the vast extent of degraded land and limited resource retention and limited ecosystem functioning (Aradóttir 2003).

Paleoecological studies suggest that during the Holocene, three major erosion periods occurred: around 5000 BP, 2500 BP, and in the 16th century, all possibly linked to climatic deterioration (Ólafsdóttir & Guòmundsson 2002; Ólafsdóttir et al. 2001). However, only the latter period showed particularly high erosion rates, coinciding with the onset of the Little Ice Age (ca. 1250-1850 AD) and extensive land degradation and land cover change that accelerated after the Norse settlement. The cooling climate during the Little Ice Age increased environmental stress on vegetation cover, while anthropogenic impact reduced the soil stability, particularly in highland areas (Fig. 5) (Streeter et al. 2012; Geirsdóttir et al. 2009). This combination of factors exacerbated soil erosion, evidenced by paleoenvironmental and archaeological studies (Eddudóttir et al. 2020; Streeter et al. 2015; Dugmore et al. 2005). The settlement period, marked by the Landnám tephra layer (ca. 870 AD), saw rapid deforestation, with some areas experiencing total loss of woodland within decades, while others underwent more gradual decline over centuries (Streeter et al. 2015). The introduction of grazing animals, such as sheep and goats, led to increased soil erosion, particularly in deforested and highland areas (Dugmore et al. 2005).

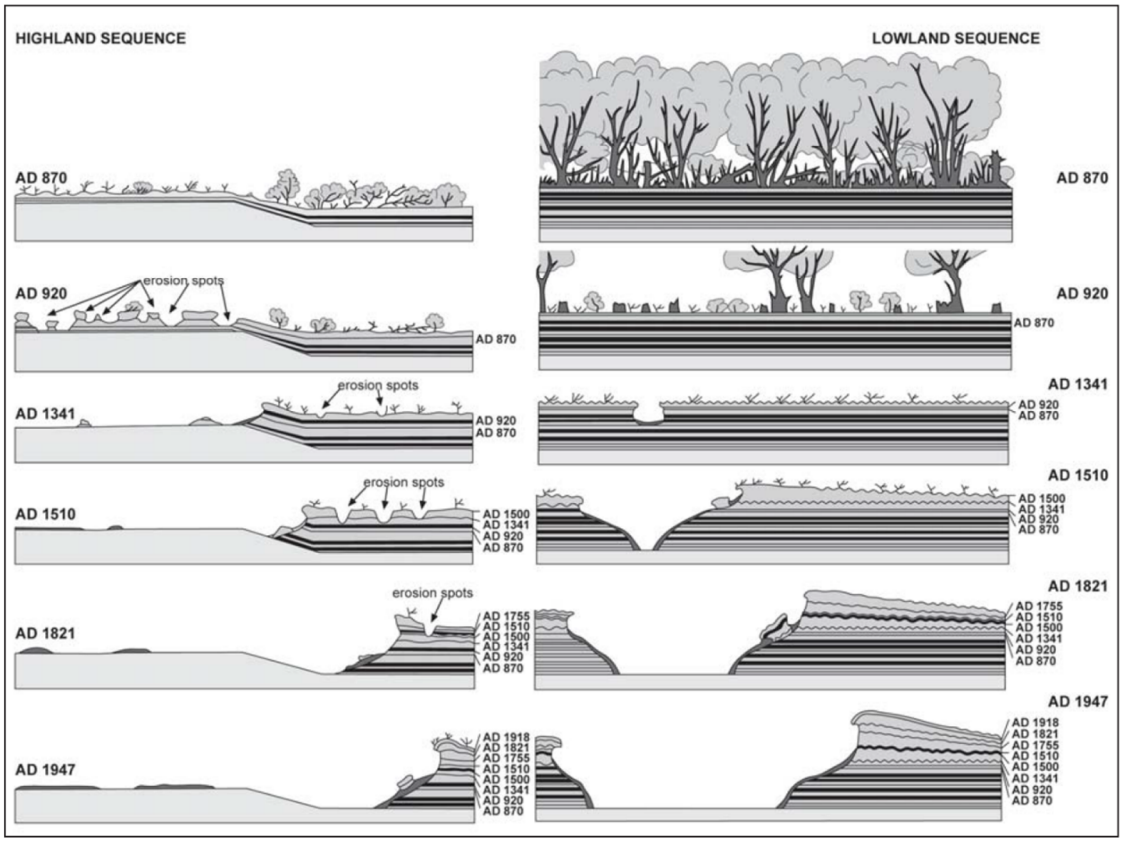

Fig. 5 Historical landscape development in Iceland: Deforestation and soil erosion leading to the formation of erosion spots and Rofabarðs in the low- and highlands (from Dugmore et al. 2009a).

Soil erosion in Iceland is driven by the interaction of natural processes and anthropogenic practices. Natural factors such as tephra fall, frost, strong winds, floods, and drifting sands, combined with human activities like deforestation and unsustainable animal grazing, have accelerated erosion (Greipsson 2012; Simpson et al. 2001; Arnalds 1987). The relative importance of these drivers varies spatially and temporally (Streeter et al. 2015; Dugmore et al. 2009a). These processes are interconnected and can have cascading effects, making the Icelandic landscape highly susceptible to erosion and challenging to revegetate (Mörsdorf et al. 2021; Barrio et al. 2018; Arnalds 2015; Thorsson 2008; Gísladóttir 2001).

Andosols, a type of soil that are expansive in Iceland, are characterised by their distinctive properties, including high water retention, low bulk density, and aggregate cohesion. These properties make Andosols susceptible to various erosion processes, such as aeolian (wind-driven), fluvial (water-driven), and frost-related erosion (Arnalds 2015).

The processes contributing to soil erosion in Iceland are diverse and interconnected. The majority of the erosion is attributed to aeolian processes. Strong prevailing winds detach soil particles through saltation and suspension, facilitated by the low bulk density and cohesion of Icelandic soils, leading to sand encroachment and burial of vegetated areas (Kok et al. 2012; Gisladottir et al. 2005; Arnalds et al. 2001). Frost activity is also prevalent in Iceland's periglacial environment, characterised by frequent freeze-thaw cycles. Temperatures around the freezing point and high-water retention capacity promote cryoturbation, leading to differential frost heave and needle-ice formation. These processes contribute to the destabilisation of topsoils and hinder revegetation (Arnalds 2015; Thorsson 2008). Overgrazing has negatively impacted the ecosystem by altering plant communities, through selective grazing, and disrupting the vegetation cover through trampling, increasing erosion risk, particularly at higher altitudes, and in the volcanic zone, where plant productivity is lower (Barrio et al. 2018; Marteinsdóttir et al. 2017; Thorsson 2008; Gísladóttir 2001). Volcanic activity, including lava flows, tephra deposition, and associated floods, can intensify land degradation, with the impact varying depending on the existing vegetation cover and prevailing wind patterns (Arnalds et al. 2013; Greipsson 2012). Fluvial processes, driven by soil characteristics, high precipitation rates, and snowmelt, promote sediment removal through rain-splash, sheet erosion, rill and gully formation, and flooding events (Arnalds et al. 2001). While the primary drivers and their relative importance are debated, it is agreed that the combined effect of natural processes and human interventions has promoted and accelerated erosion (Streeter et al. 2015), with drivers changing over time and across different regions of Iceland (Streeter & Dugmore 2014).

It has been shown that soil erosion can also have a feedback effect on vegetation. In southern Iceland grassland close to erosion fronts exhibit lower plant vitality due to water stress. Soil hydrology was disrupted near the erosion front, resulting in lower soil moisture levels and increased variability (Cutler et al. 2023). This hydrological disruption, coupled with other potential causes such as nutrient loss, reduced soil structure stability, and exposure to harsher microclimatic conditions, stresses plants, affecting their physiology and initiating a feedback mechanism that facilitates the propagation of soil erosion.

Typical landforms occur in Iceland associated with soil erosion including erosion spots and Rofabarðs (Fig. 5, 6). Erosion spots form when vegetation cover is breached, mainly

triggered by animal husbandry, cryogenic, or aeolian activity, exposing soil that is highly susceptible to further erosion (Arnalds 2015; Thorsson 2008). These spots range in size from a few square centimetres to several hundred square meters (Fig. 6a) (Streeter and Cutler 2020; Arnalds 2015; Dugmore et al. 2009b; Gísladóttir 2001). Typical hummocks, which are small-scale dome-shaped mounds (Icelandic: thúfur) of about 0.5-1.5 m in diameter and 0.1-1 m in height (Thompson et al. 2022a), contribute to the erosion spot formation (Fig. 6b). These thúfur are formed by frequent freeze-thaw cycles and winter precipitation, which contribute to the churning of the topsoils. Grazing animals putting their feet down between the thúfur can lead to the gradual upward push of soil around depressions, further contributing to thúfur formation (Arnalds 2015). These protruding landforms from the ground are susceptible to disruption of vegetation cover through trampling from grazers or exposure to erosive forces, which can be the initiation of erosion spot formation (Thorsson 2008).

Other common landforms in Iceland are Rofabarðs, which are thick soil escarpments associated with multiple erosion processes (Fig. 6c) (Arnalds 2000b). These processes include e.g. water erosion, formation of water ponds, or cryoturbation from needle-ice formation that loosens the topsoil. The propagation of the erosion front is attributed to the vertically exposed Andosols that are prone to redistribution by wind. Strong winds and rain-splash detach the soil particles from the soil profile, undermining the vegetation cover and leading to its collapse under its own weight, further promoting soil erosion (Fig. 5) (Dugmore et al. 2020; Arnalds 2000b). These features are common in the Icelandic landscape, particularly in areas with loose, unconsolidated soil, usually soils formed post-Landnám due to higher sediment accumulation from erosion, and sparse vegetation cover (Dugmore et al. 2020).

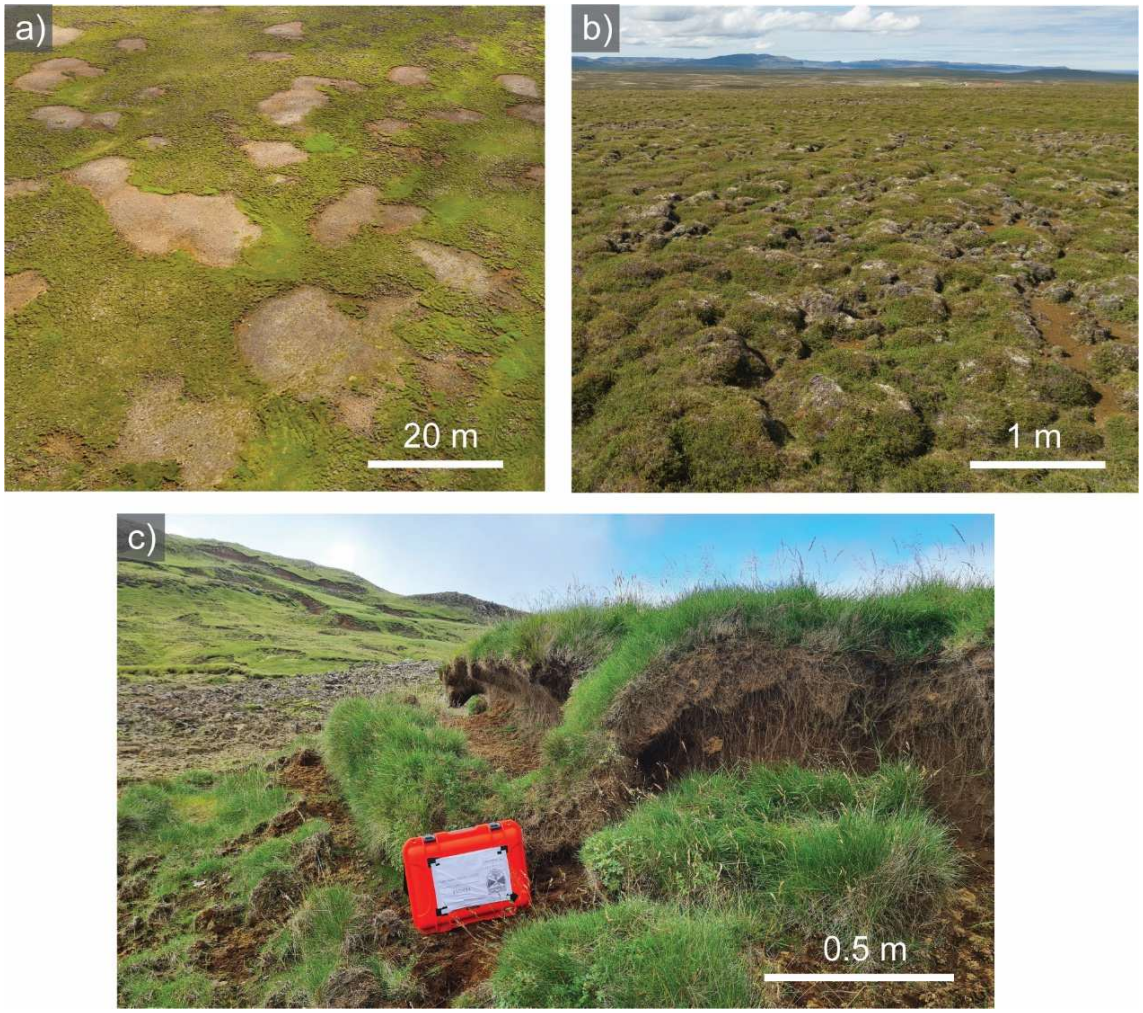

Fig. 6 Landforms of Iceland. a) Erosion spots, b) Thúfur patterned landscape with forming erosion spots in the centre and right, c) Rofabarð.

While there is good understanding how soil erosion spots form and develop, there is less knowledge about the spatial distribution of more stressful areas in the landscape that are particularly vulnerable to erosion. Streeter & Cutler (2020) demonstrated that small erosion spots tend to form in close proximity to larger ones. This pattern can be explained by distance-weighted feedback mechanisms, where the presence of an erosion spot in one area affects nearby regions. As vegetation is lost, the soil becomes more vulnerable to wind and water erosion, and nearby areas, especially those already degraded or under stress, are more likely to experience increased erosion pressure. This cascading effect leads to clusters of erosion spots that grow and spread based on their distance from one another, a process reinforced by low vegetation recovery in degraded areas with unstable soils (Streeter & Cutler 2020; Rietkerk & van de Koppel 2008). Thus, erosion patterns in

Iceland are largely driven by these distance-weighted feedback loops, where proximity to already eroded areas increases the likelihood of further soil degradation.

The disruption of vegetation cover through practices such as grazing (Barrio et al. 2018; Thorsson 2008) or proximity to large erosion spots (Streeter & Cutler 2020) exposes the underlying soil to frost activity and wind deflation. In Iceland, this is particularly detrimental as the unstable soils are easily deflated and hinder revegetation until bare rock is exposed. This results in extensive barren areas with low soil cover and organic carbon (Arnalds & Kimble 2001), which is crucial as intact soil and vegetation cover mediates many of the chemical, physical, and biological processes of soil (Óskarsson et al. 2004). Furthermore, soil erosion (=reduction of vegetation cover) disrupts soil hydrology (Cutler et al. 2023) and reduces the cooling effect provided by vegetation, especially during summer drought (Rietze et al. 2024). This leads to higher land surface temperatures and increased desiccation, creating less favourable growing conditions.

2.1.2 Fennoscandia - Ecosystem changes

The Fennoscandian oro-Arctic tundra faces multiple environmental and ecological pressures closely linked to its biogeomorphological characteristics. Factors such as permafrost thaw, overgrazing, shrubification, and shifts in snow cover patterns significantly affect both the function and biodiversity of the tundra and the geomorphological processes shaping its landscape (Lagergren et al. 2024; Niittynen & Luoto 2018; Vuorinen et al. 2017; Mod & Luoto 2016; Aalto & Luoto 2014). In particular, the Kilpisjärvi region, recognised as a biodiversity hotspot, has been the focus of numerous biogeomorphological studies.

Topography has shown to have an indirect influence on vegetation patterns and biomass in that area (Riihimäki et al. 2017; Suvanto et al. 2014). The most important drivers of above-ground biomass were identified as soil characteristics and soil moisture. Geomorphological processes typically decreased plant biomass through mechanical disturbance (Suvanto et al. 2014). Le Roux & Luoto (2014) found that all geomorphological processes (cryoturbation, nivation, deflation, solifluction, and fluvial) were important in determining the fine-scale distributions of some species to different extents. Aalto et al. (2021) highlighted the importance of cryogenic processes shaping vegetation and biomass patterns and suggested that cryogenic land surface processes play a crucial role

in shaping future patterns of tundra biomass, provided that climate warming does not significantly reduce cryogenic ground activity.

The study by Hjort & Luoto (2009) investigated the relationship between vegetation–cryoturbation interaction in the Kilpisjärvi area. They found that vegetation cover and the total above ground biomass were among the most important single predictors, with important consequences for the periglacial processes under global climate change. Improved growing conditions may first increase cryoturbation in sparsely vegetated areas, but further vegetation growth and treeline advance could stabilise periglacial features and reduce geomorphic activity (Hjort & Luoto 2009).

Olofsson et al. (2001) investigated the impact of reindeer grazing on biogeomorphological processes in the Kilpisjärvi area. High levels of reindeer grazing can lead to reduced vegetation cover and increased soil erosion due to the trampling action of reindeer hooves. However, moderate grazing levels were found to promote primary productivity by enhancing nutrients from feces and urine, creating an organic nutrient pool. The study also showed that trampling disturbs the bryophyte carpet, causing the soil microclimate to become drier and warmer, allowing for shifts from moss to graminoid cover with higher biomass productivity (Olofsson et al. 2001). The tipping point between beneficial and detrimental grazing depends on both grazing intensity and seasonality. Grazing practised during vulnerable seasons, such as early spring and winter, can shift the balance toward ecosystem degradation.

Climate change is influencing the biogeomorphological dynamics in the Kilpisjärvi region, altering vegetation dynamics and soil properties. Virtanen et al. (2010) found that climate sensitivity varies among vegetation types, with productive low-altitude deciduous forests more affected by warming than alpine tundra. Alpine tundra, however, can be buffered by grazing, as the reduction of ericoid shrubs benefits the expansion of graminoids and small herbaceous species. The study also noted that geomorphological disturbances accelerate vegetation change under warming, while high biodiversity stabilises these ecosystems. Warming temperatures have been shown to lead to the expansion of woody shrub and tree cover, a process known as 'shrubification'. This vegetation shift has shown to reduce soil moisture and temperatures, and lower organic carbon in the soils (Kemppinen et al. 2021).

Snow cover pattern have also shown to influence vegetation pattern. Aalto & Luoto (2014) showed that high-latitude earth surface processes are extremely sensitive to climate variation. Happonen et al. (2019) and Niittynen et al. (2020a) highlighted the importance of snow as a control of vegetation pattern in Kilpisjärvi and across different Arctic tundra zones.

2.2 TUNDRA MICROCLIMATE

A microclimate is a localised set of atmospheric and environmental conditions that differ from the broader regional or surrounding climate. These small-scale variations in factors such as local-temperature, water levels, wind exposure and solar radiation can significantly influence the structure and function of ecosystems. These distinct environmental conditions are crucial in influencing species individuals, populations, communities and ecosystems and their processes on a small-scale (Fig. 7) (Kemppinen et al. 2024).

Traditional climate data, such as annual, seasonal, or monthly averages, often focus on temperature and precipitation. However, these metrics may not adequately capture ecologically important aspects of the Arctic climate that are relevant to various biological, biogeochemical, or geomorphological processes. Examples of such aspects include snow cover depth and duration, rain-on-snow events, water vapor pressure deficit, and extreme wind events, which may not be fully represented by the more commonly used climate statistics (Rantanen et al. 2023).

Local climatic variability is primarily mediated by topography, vegetation and soil, and the presence of water bodies, that can create distinct microclimatic conditions (Bramer et al. 2018). This multifaceted role of topography shapes the microclimates that, in turn, dictate the dynamics within plant communities and soil processes (Fig. 1). Topography affects various biotic ecosystem processes that influence nutrient cycling, soil nutrient availability, and ecosystem productivity (With 2019), but also abiotic drivers such as soil erosion through aeolian or cryogenic processes (Le Roux & Luoto 2014). Florinsky & Kuryakova (1996) highlights the influence of topography on vegetation cover properties, indicating how the physical landscape directly impacts plant distribution and abundance (Fig. 7). In Kilpisjärvi mesotopographic gradients, referring to landforms in tens of meters such as ridges and hollows (Waddington & Roulet 1996), have been identified as major

driver of species richness and occurrence. Winter thermal conditions, controlled by snow cover, were particularly important for vascular plant distribution and soil moisture for bryophytes richness. Summer thermal conditions were less relevant for species richness but showed similar importance to other variables for species occurrence (Fig. 7) (Niittynen et al. 2020a). The close relationship between topography, microclimate, and vegetation is also evident in intraspecific trait patterns, reflecting adaptations to localised environmental conditions (Kemppinen & Niittynen 2022; Fan et al. 2020).

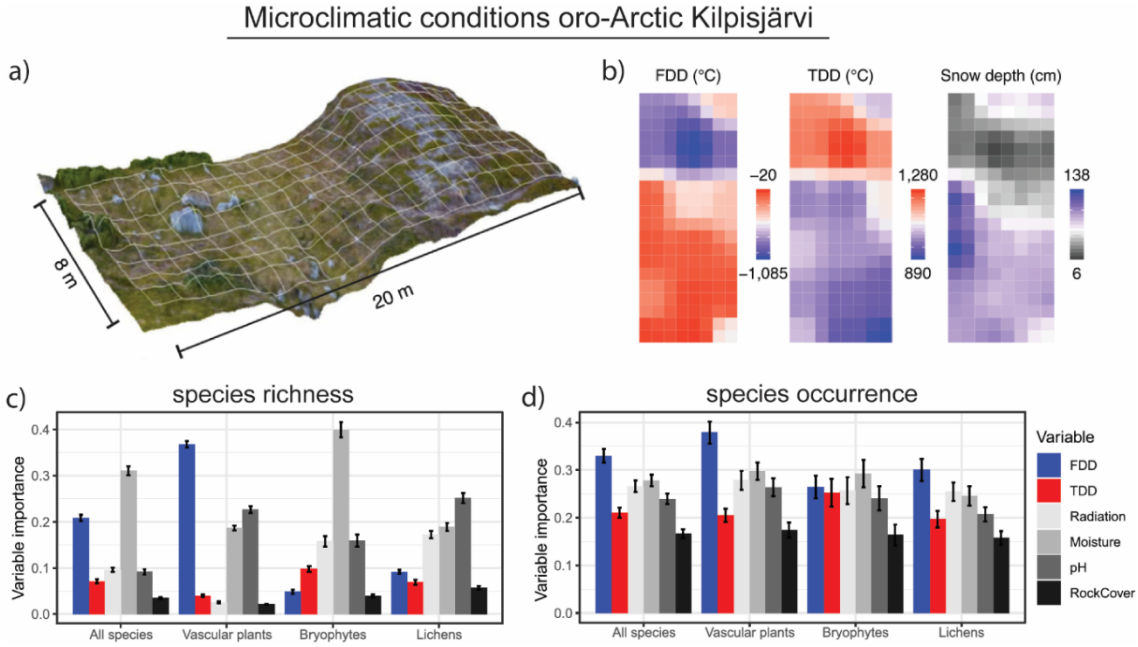

Fig. 7 Microclimatic conditions in oro-Arctic Kilpisjärvi and influence on vegetation. a) An example of microclimate grid in Kilpisjärvi shaped by mesotopographic gradients, imaged in RGB. b) Microclimatic variables show considerable variation in winter and summer soil temperatures (FDD and TDD) and snow depth. c, d) Variable importance values of species richness and species occurrence models. Thermal stress experienced by vegetation during winter season, was quantified using the freezing degree days (FDD), which is the sum of daily soil temperatures below 0 °C. Conversely, the overall summer thermal conditions, the thawing degree days (TDD) were calculated. It is the sum of daily soil temperatures above 0 °C and serves as a proxy for the energy available to plants and the duration of the growing season (from Niittynen et al. 2020a)

Moreover, topography's influence extends to biomass production and nutrient cycling, crucial components of ecosystem productivity and health. Biomass accumulation and distribution are significantly affected by topographical features, which in turn influence soil nutrient availability and cycling processes (Riihimäki et al. 2017; Suvanto et al. 2014; Fisk et al. 1998). Stewart et al. (2014) and Fisk et al. (1998) have further identified topography as a key driver of atmospheric nitrogen exchange and nitrogen cycling within Arctic tundra ecosystems. These processes are vital for maintaining the fertility of the soil and supporting primary productivity. Livensperger et al. (2019) demonstrated how

microclimate variations can influence senescence, affecting the lifecycle of plants and their ecological roles. Lastly, the role of microtopography in primary succession, was documented by Cutler (2011) demonstrating its governing role in the initial establishment of vegetation on newly formed or exposed surfaces.

Herbivores interact with microclimatic environments by influencing plant and soil properties. They are drawn to areas with favourable microclimatic conditions, such as wind-protected hollows with high biomass productivity, where their feces and urine further enrich the nutrient pool and promote vegetation growth (Barbero-Palacios et al. 2024). In winter and early spring, herbivores often graze on snow-free ridges, increasing pressure on these low-productivity areas and exacerbating soil erosion and compaction. This reduction in aboveground biomass decreases snow accumulation in winter and lowers soil moisture in spring (Yan et al. 2019). Grazing can intensify freeze-thaw processes by reducing vegetation cover, which normally insulates the soil. As a result, exposed soil warms more quickly during the day and cools faster at night, leading to shorter frozen periods and extended freezing and thawing cycles (Wang et al. 2023). These seasonal grazing effects can alter microclimatic conditions and hinder vegetation recovery, particularly in vulnerable tundra ecosystems.

Microclimatic conditions, particularly soil moisture and temperature, play a crucial role in shaping local landscape structure and development by influencing various biogeomorphological processes that vary across seasons. During the growing season, local vegetation distribution is primarily controlled by water availability, as it is essential for plant growth and development, alongside soil nutrients, microorganisms, and sunlight (Spitzer et al. 2022; Kemppinen et al. 2019). In winter, when vegetation is dormant and does not require resources for growth, the focus shifts to the role of thermoregulation by snow in providing shelter from damaging frost activity and blizzards (Fig. 8). This was also found by Niittynen et al. (2020a), who demonstrated that winter temperature conditions were related to fine-scale patterns in tundra vegetation, whereas summer temperature conditions explained coarse-scale patterns.

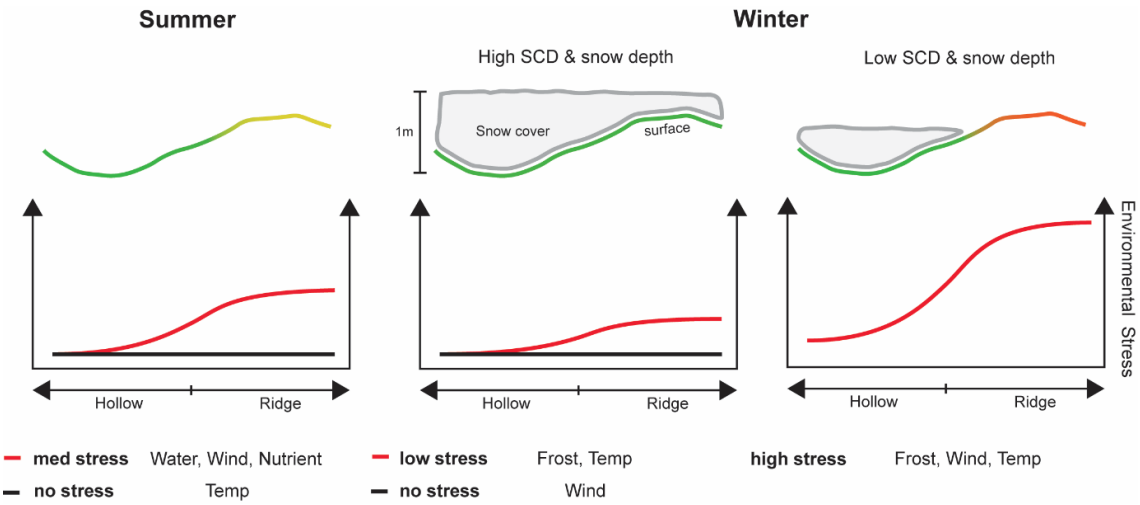

Fig. 8 Microclimatic controls and environmental stress factors in hollows and ridges during growing season in summer and the winter period with low and high snow cover. In the summer, during the growing season, soil moisture and nutrients are the largest limitations to growth. While in the winter, no growth occurs, and harsher conditions prevail; therefore, geomorphological processes mediated through snow cover are the decisive factors (Pirk et al. 2023; Aalto et al. 2021; Callaghan et al. 2011b).

2.2.1 Microclimatic soil moisture conditions

Water is essential for vegetation growth, functioning, and distribution, acting as a limiting resource, stress factor, and disturbance agent (Grime 1977). In cold regions, the role of water in tundra ecosystems has gained attention due to global change (Bring et al. 2016) and has been recognised as the primary factor influencing local vegetation patterns in high-latitude regions (Kemppinen et al. 2019).

Plant species have unique hydrological niches, enabling co-existence within communities (Silvertown et al. 2015) and shaping species distributions and diversity across gradients (Le Roux et al. 2013). Tundra plants have shallow roots (Iversen et al. 2015), relying on a thin topsoil layer recharged by precipitation, groundwater, and meltwaters (Barichivich et al. 2014).

The influence of water on tundra vegetation is further supported by several other studies. Campbell et al. (2021) found that water is an important driver of greening in the high-Arctic, mediated by terrain characteristics and moisture conditions. Berdanier and Klein (2011) demonstrated that plants at high elevations exhibit interactive responses to soil moisture and growing season length, with both factors independently and jointly affecting biomass production. In the Fennoscandian mountain tundra, spatial variability in water availability has a more significant impact on the fine-scale species distribution across three taxonomic groups (vascular plants, mosses, and lichens) than temperature

(Kemppinen et al. 2019). Kemppinen et al. (2019) highlighted the varying responses to water related variables within and between these groups, with vascular plants showing the strongest response to water availability, followed by mosses and lichens. High temporal variability in soil moisture, including cycles of waterlogging and rapid drying, can expose vegetation to physiological stress (Trahan & Schubert 2016). Vegetation stress has been observed at the erosion front, where disruptions in soil hydrology through soil erosion have led to high soil moisture variability, as observed in studies conducted in Iceland (Cutler et al. 2023). Water availability and variability can induce vegetation stress and mechanical disturbance in tundra ecosystems, but also facilitate growth, emphasising the importance of incorporating water as a key factor in species distribution models for all groups.

Soil moisture plays an important role in modulating the contrasting phenomena of greening and browning in the Arctic. While warmer temperatures can promote shrub encroachment and the "greening" of the Arctic landscape (Weijers et al. 2018), the response is mediated by soil moisture conditions (Myers-Smith et al. 2015), which may amplify the greening effect. Conversely, shifts towards wetter and warmer conditions have also been linked to "browning," characterised by plant dieback (Lara et al. 2018). This phenomenon is attributed to reduced photosynthesis under increased water stress (Angert et al. 2005), which can be triggered by extreme events like droughts (Bjerke et al. 2017; Phoenix & Bjerke 2016). In high-altitude and high-latitude systems, rising temperatures are likely to increase the dependence of vascular plant patterns on hydrological conditions (Winkler et al. 2016; Crimmins et al. 2011).

However, predicting the impact of climate change on plant available water is challenging, as the microclimate influencing soil moisture conditions may be highly decoupled from the macroclimate (Aalto et al. 2018). This decoupling underscores a significant uncertainty, particularly in projecting future hydrological cycle (Bring et al. 2016) and accurately modelling local soil moisture distribution (Kemppinen et al. 2018). While water distribution is known to follow topography, its response is very different based on the environment and climate. Fine-scale topographic features not apparent in lower resolved remote sensing data complicate the modelling soil moisture distribution. Different soil properties across high-latitude regions and geomorphology play a crucial role in hydrology and differ across the tundra biome, which cannot be accurately assessed remotely.

Understanding the fine-scale spatial distribution of soil moisture and its role in controlling plant growth or vegetation stress is essential for predicting how the land cover structure may change in response to climate change. This critical aspect will be further investigated in this thesis.

2.2.2 Microclimatic snow cover and temperature conditions

Harsh winter conditions are a defining feature of tundra ecosystems and have been identified as the strongest environmental variable related to the fine-scale patterns in Arctic tundra vegetation (Niittynen et al. 2020a; Chernov 1988; Walker et al. 1993).

The complex relationship between snow cover and ecosystem dynamics in alpine and polar regions is well documented (Pirk et al. 2023; Bokhorst et al. 2016). Snow acts as a protective blanket against erosive forces, shielding vegetation and soils from frost as desiccating and abrasive winds. Snow cover plays a vital role in thermoregulating freezing temperatures and fluctuations, protecting from detrimental freeze and thaw events, mitigating the risk of cryogenic damage (Kearney 2020). Snow also protects against wind and detrimental blizzards, that can cause widespread damage to vegetation (Bykov et al. 2022; Bokhorst et al. 2009). The absence of snow cover leaves plants vulnerable to damage from sub-zero ambient temperatures, drastic temperature fluctuations, winter desiccation, recurring freeze-thaw cycles, and abrasion by windblown ice particles until fresh snow covers the system (Jones 2001; Sonesson & Callaghan 1991). Freezing damage can result from dehydration that exceeds cell tolerance, surpassing the limits of deep supercooling, and the persistence of freezing induced embolisms within xylem vessels (Pearce 2001).

Moreover, snow cover provides soil moisture at the onset of the growing season, influencing plant growth, community composition, phenology, carbon sequestration, and microbial diversity in these sensitive environments (Zinger et al. 2009; Jones 2001). The timing and duration of snow cover can have contrasting effects. While early meltwater release can promote a shift towards shrub-dominated vegetation due to increased moisture availability (Rixen et al. 2022), persistent deep snowpacks that last into summer can impede vegetation growth through the process of nivation (Aalto et al. 2021)

Even subtle variations in topography can significantly influence the spatial distribution of snow patches (Sturm & Wagner 2010; Brown & Ward 1996), with hollows acting as

accumulation zones and ridges experiencing wind driven snow erosion. Consequently, future changes in snow distribution patterns – and their impact on the formation of barren patches – are expected to exhibit high spatial variability, posing challenges for predicting ecosystem responses in these environments.

Arctic winter temperatures are warming more rapidly than summer at about five times the global average rate (Zhang et al. 2021). In recent years, many regions across the Arctic have experienced a decrease in snow cover duration (SCD), resulting in significant reductions in the extent of snow cover during May and June (Derksen & Brown 2012). High-latitude maritime areas are particularly affected, with predicted SCD declines of 30–40% by 2050 (Callaghan et al. 2011c). Shorter SCD is a key driver of biodiversity loss in the Arctic (Niittynen et al. 2018). However, while SCD is expected to continue declining, some parts of the Arctic are projected to witness an increase in snow depth (Brown & Mote 2009).

2.3 STUDY AREAS

2.3.1 Iceland: Svalbarðshreppur

The Icelandic sites selected for this study are located in the northeast of the country (66° 09' N, 15° 30' W) in the former municipality Svalbarðshreppur, which since 2022 has been combined to a larger municipality called Langanesbyggð, close to the village Þórshöfn. The elevation increases gradually from the coast to inland: the lowest site is close to sea level with the furthest site inland (14 km) is at an altitude of 180 m. Iceland is located on the Mid-Atlantic Ridge and above a hotspot, fuelling its growth and resulting in frequent volcanic activity (Thordarson & Larsen 2007). The selected study area was chosen to be distant from the volcanically active region, to minimise the impact of volcanic activity on soil erosion (Raynolds et al. 2015). However, the area does receive tephra falls from larger volcanic eruptions (Woollett et al. 2014).

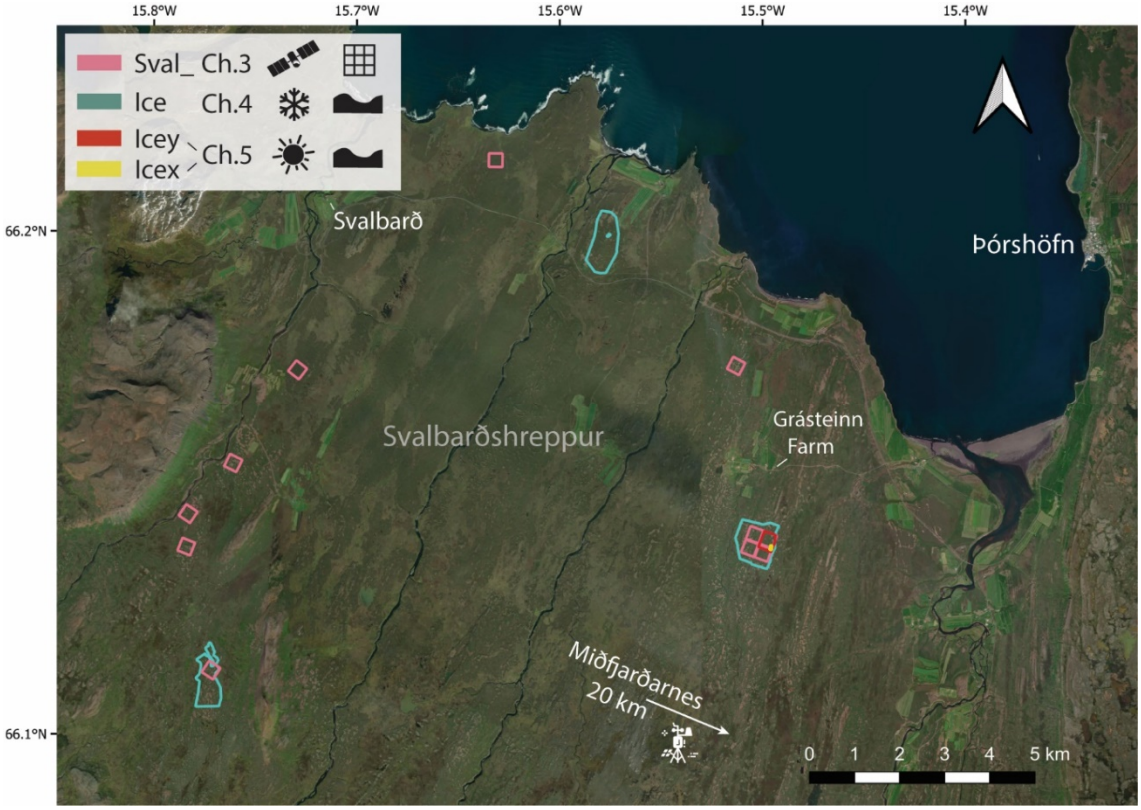

Fig. 9 Overview study sites in the former municipality of Svalbarðshreppur and characteristics of the research area. Grásteinn Farm served as the base and lodge where surveys were planned, while Miðfjarðarnes indicates the location of the weather station. The legend indicates the naming of the sites, the chapters in which they are used, and the research objectives, highlighted by different colours. (Bing Maps, retrieved 5 April 2024)

Climate

Northern Iceland has a cool, maritime climate and is characterised by strong winds, frequent precipitation, mild winters and cool summers (Ólafsson et al. 2007; Arnalds 2004). Due to the influence of the "Icelandic low", which brings frequent low atmospheric pressure, the region experiences persistently high wind speeds (Ólafsson et al. 2007). Despite its northern latitude, Iceland has a relatively mild climate due to the Gulf Stream, making it between polar and temperate conditions (Bjornsson et al. 2007). The mean annual temperature is about 4 °C, in the winter the monthly mean temperature drops down to -4 °C and during the summer goes up to 10 °C (altitude 25 m above sea level, from Miðfjarðarnes the nearest station with detailed monthly records, approximately 21 km SE of the closest study site) (Veðurstofa Íslands, 2024) (Fig. 10). The precipitation in the north is between 500 to 1000 mm a^{-1}, which is lower than in the south ~2000 mm a^{-1}, due to lack of orographic influence (Crochet et al. 2007). The mean wind speed is high in the region and has increased since the early 2000s from an average 4 to 6 m s^{-1} (Fig. 10).

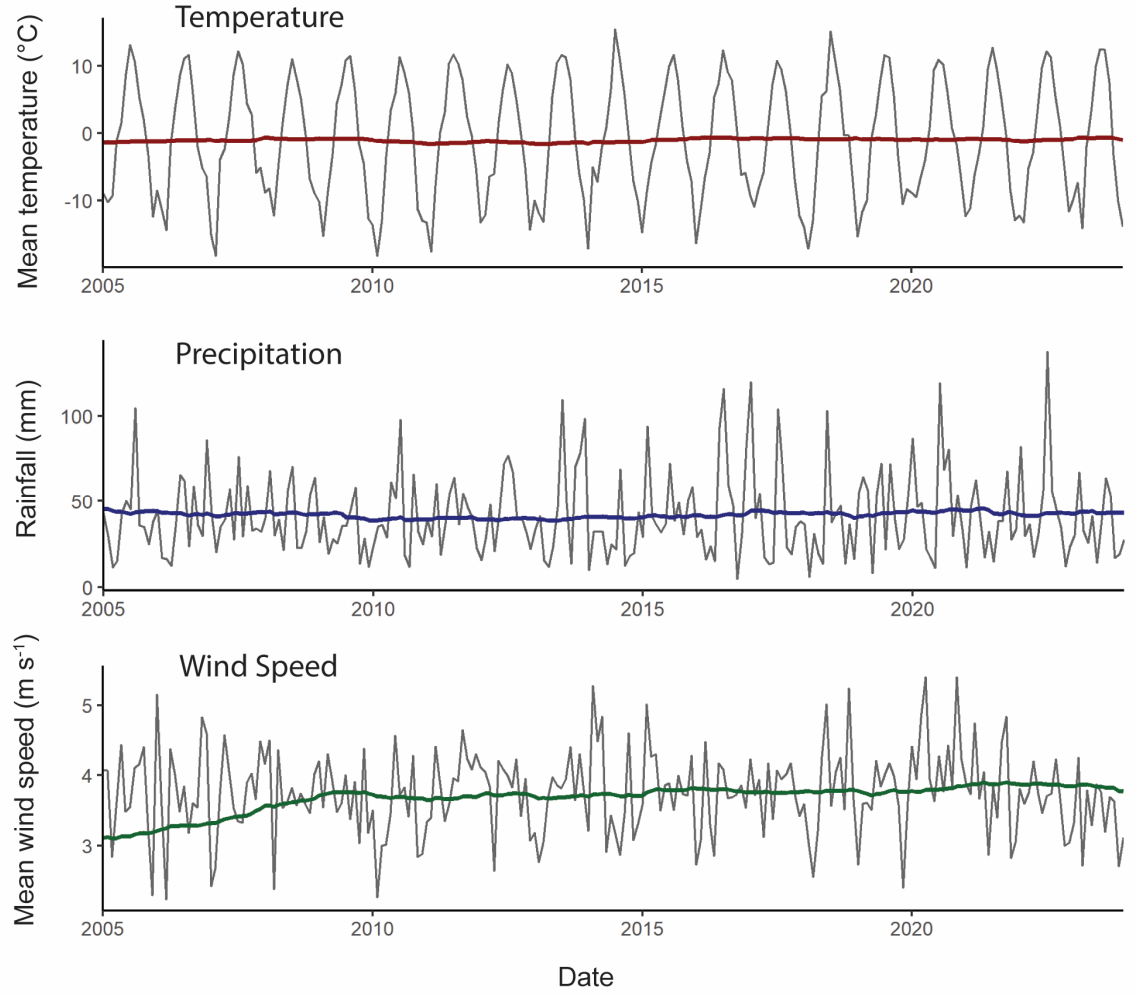

Fig. 10 Climatic data from the Miðfjarðarnes weather station, 2005 – 2024. The data have been smoothed using a five-year running average in each case (starting from 2000).

Vegetation

Iceland has five major natural vegetation types: birch woodlands, wetlands, moss/lichen dominated fields, poor heathland, and rich heathland. Heathlands and grasslands are the most abundant, often used as grazing areas, and are linked to soil erosion (Barrio et al. 2018; Thorsson 2008). In the study area, poor heathland dominates (defined as where grazing plants are not as abundant as in the rich heathland (<10 %) (Arnalds 2015), with rich heathland found in protected or less grazed areas, and scattered wetlands located in low-lying areas.

The study area falls into the low-shrub tundra sub-zone (Walker et al. 2005) and it can be described as a dwarf shrub heath environment with erosion spots scattered across the landscape of different sizes from cm to 10s meters (Fig. 6a). Dwarf shrub heath is characterised by a hummocky surface, with drought-resistant species on the hummock

tops such as moss (*Racomitrium lanuginosum)*, lichen or Crowberry (*Empetrum nigrum)* and graminoids and forbs in the depressions, creating a micro-scale mosaic of patches (Fig. 6b) (Gísladóttir 2001). Dwarf shrub heath and poor heathland are the most susceptible vegetation types to erosion spot formation, which is why they are the subject of this research (Gísladóttir 2001; Aradóttir et al. 1992; Kolasa 1989).

Soils

Iceland's soils are primarily Andosols, formed from volcanic materials deposited by wind after the retreat of the Pleistocene glacier (Arnalds 2004). These soils consist of silt-sized particles derived from fine-grained basaltic tephra, which weather quickly to form clay minerals which have an amorphous or poor crystalline structure (Arnalds 2015). Andosols are thixotropic, meaning they can retain large amounts of water without reaching the plasticity limit, but release water when disturbed by physical force (Arnalds 2015). This property, expressed by very high liquid limits, contributes to their susceptibility to frost heave, rain splash, running water, and slope failures (Arnalds 2000b). Additionally, Andosols have a very low bulk density (~0.8 g cm^{-3}) and low aggregate cohesion, making them prone to wind redistribution (Arnalds 2015).

Soil thickness varies across Iceland, ranging from a few decimetres to more than 2 meters. This variation is primarily governed by age, sediment accumulation and erosion. In the lowlands, soils tend to be thicker due to earlier ice recession, and soil profiles gradually increase in thickness towards higher altitudes. Soil cover is also controlled by prevailing wind patterns and proximity to active volcanic zones and glaciers, which serve as sediment sources (Arnalds 2015; Ólafsdóttir & Guòmundsson 2002).

Landforms and Terrain

The landscape has a multi-scale topographic structure. In the range of 0.5-1 km, the lower elevated areas are waterlogged peatlands dominated by graminoids, while the higher elevated areas exhibit typical mixed tundra vegetation and have eroded surfaces. The higher areas are further structured into undulating mounds with a diameter of 20-100 m and a height of 1-3 m, and thúfurs of about 0.5 m in diameter and 0.3 m in height.

Land use

The study is located within unfenced rangelands, which were historically grazed by sheep. During the grazing season (May–September), sheep roam freely across these rangelands. Sheep numbers in Iceland today have halved since the late 1970s from 900,000, with the introduction of livestock quotas in 1984 (Marteinsdóttir et al. 2017). This decline is also believed to be reflected in the study area, as evident from the observed small numbers of sheep used for the comparatively large rangelands. Additionally, highly detrimental winter grazing is no longer practiced in the area (Sigurður Þór Guðmundsson, pers. com.) and the rest of Iceland, due to improved access to winter fodder, which led to the gradual abandonment of winter grazing and reduced grazing pressure around farms (Barrio et al. 2018).

2.3.2 Fennoscandia: Kilpisjärvi

The main study site in Fennoscandia is located next to the Saana mountain in northern Finland (69° 03' N, 20° 50' E), close to Kilpisjärvi village. The mean altitude is 660 m above sea level. The region is defined as oro-Arctic, sometimes as sub-Arctic tundra, located in the mountainous northern part of the Scandes (Virtanen et al. 2016). The main biomes in Fennoscandia include the boreal forest (Taiga) and the tundra. Much of Fennoscandia is covered by boreal forests, characterised mostly by coniferous trees like spruce, pine, fir and deciduous birch. In the northernmost and highest parts of Fennoscandia, when crossing the tree line, the landscape transitions into tundra ecoregion (Fig. 2, 11) (Walker et al. 2005). The tundra ecosystem in Kilpisjärvi is marked by strong environmental gradients and geodiversity. It is known for its high arctic-alpine biodiversity and considered one of the biodiversity hotspots in the Scandic mountains, also attributed to the presence of dolomite layer (Kauhanen 2013).

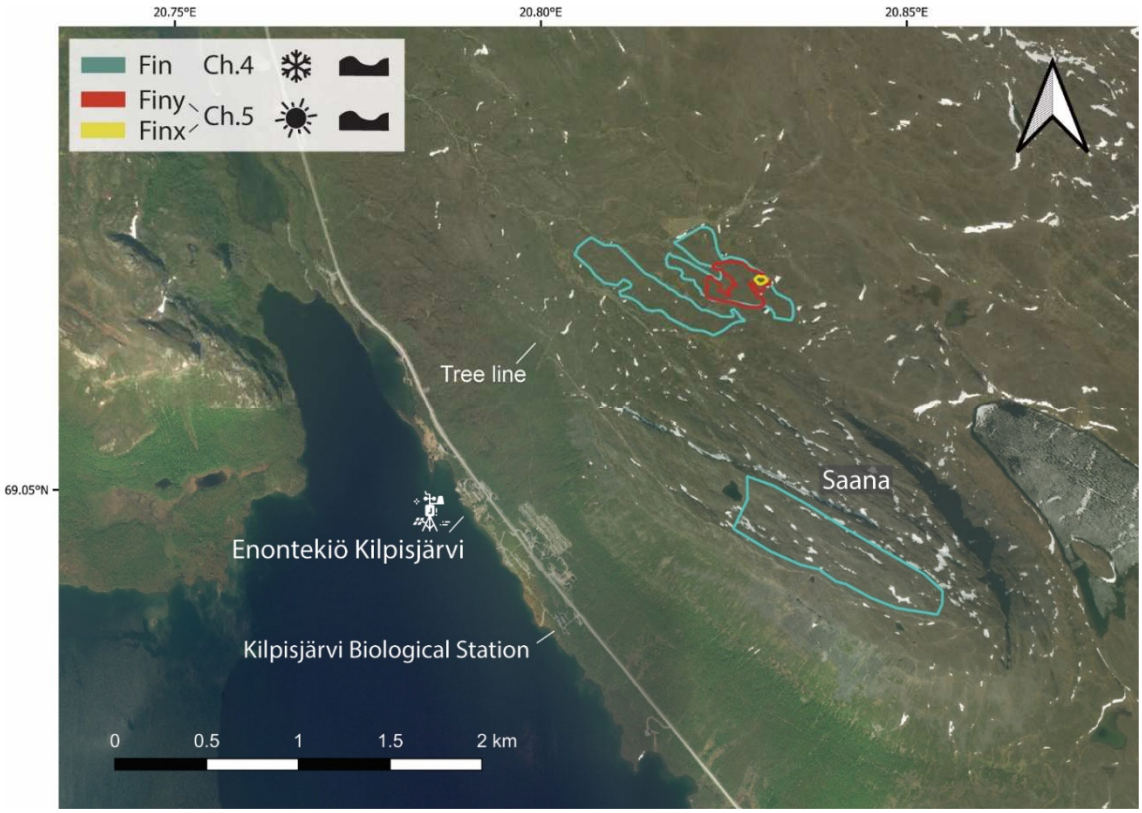

Fig. 11 Overview study sites around Kilpisjärvi and characteristics of the research area. Weather station is located in Enontekiö Kilpisjärvi. The legend indicates the naming of the sites, the chapters in which they are used, and the research objectives, highlighted by different colours. (Bing Maps, retrieved 5 April 2024)

Climate

Kilpisjärvi has a cool, maritime/continental climate with strong winds and low precipitation. The mean annual temperature is about -1.5 °C, with monthly mean temperatures dropping to -15 °C in winter and rising to 12 °C in summer (altitude 500 m above sea level, from the Enontekiö Kilpisjärvi weather station, approximately 2 km SW of the study site) (Ilmatieteen laitos 2024) (Fig. 13). The nearby Scandinavian mountains cause a rain shadow effect, limiting the mean annual precipitation (Kauhanen 2013). The precipitation is moderate at about 500 m a^{-1}, with rain becoming the dominant form of precipitation compared to snow (Kivinen et al. 2012). The mean wind speed is high in the region and has increased since the early 2000s from an average 3 to 3.5 m s^{-1}. The wind speed at the study sites is likely higher, due to the elevated position.

Vegetation

The diverse ecosystems around the Saana Nature Reserve situated in the Kilpisjärvi region, are segmented by altitude and range from mountain birch forests at low altitudes

(480-600 m) to alpine tundra above 600 m (Fig. 12) (Ahti et al. 1968, Eurola 1999). Floral composition and diversity are influenced by factors such as the northern location, altitudinal variation, alkaline-rich bedrock, harsh winters, snow distribution, proximity to the Atlantic Ocean, and the microclimate of sheltered valleys (Kauhanen 2013). The oro-Arctic zone, above the mountain birch forest, features dwarf birch (*B. nana*) and willow (*Salix spp*.) shrubs, transitioning to alpine tundra dominated by dwarf shrubs like *Salix herbacea*, *Cassiope tetragona*, *Diapensia lapponica*, and *Loiseleuria procumbens* (Austrheim et al. 2010). The alpine area is further divided into low oro-Arctic, middle oro-Arctic (850-900 m), and high oro-Arctic zones (1100-1200 m), with the study area encompassing only the low and middle oro-Arctic zones. Studies have shown the importance of earth surface processes in these zones, that drive plant richness and composition (Le Roux und Luoto 2014), biomass pattern (Aalto et al. 2021) and plant traits (Kemppinen et al. 2022).

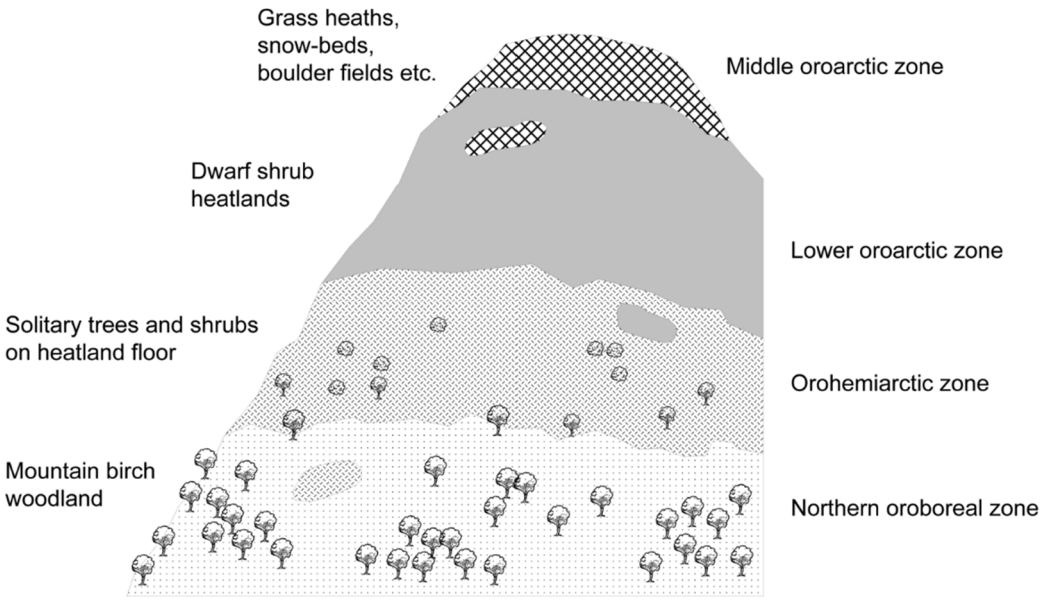

Fig. 12 Altitudinal vegetation zones in Kilpisjärvi region (from Kauhanen 2013)

Soils

The tundra soils in the Kilpisjärvi region exhibit distinct physicochemical characteristics across different ecosystems (barren, heathland, meadow, and fen) and depths (organic and mineral layers) (Pessi et al. 2022). The soils can be classified as mineral or organic based on their biological material content (Strahler & Strahler 2005). Mineral soils form

when rock breaks down into aggregates, with large aggregates creating well-drained soils containing gaps filled with water, air, and plant roots (Huggett & Cheesman 2002). Organic soils form when the accumulation of organic matter, such as plant litter, exceeds its decomposition rate. Low temperatures slow down soil microbial activity and decomposition rates, leading to the accumulation of organic carbon in the soil (Hugelius et al. 2014). In the drier areas, the soils are typically thin, measuring only a few centimetres in thickness, and are classified as mineral-rich Cryosols. In contrast, soils near water sources have a higher organic matter content and are thicker (Kumar et al. 2016; Kauhanen 2013).

In the mineral layer, soil characteristics remain relatively consistent across ecosystems, while notable differences emerge in the organic layer. Fen soils display higher pH, moisture, and nitrogen content, while both fens and meadows exhibit lower C:N ratios compared to heathland and barren land (Pessi et al. 2022). The barren, heathland, and meadow soils are characterised as drier, oxic upland soils, contrasting with the continuously water-logged and anoxic conditions found in fen soils due to their lower topographic position. These drier tundra soils are generally low in N, and the plants growing in these soils can experience N limitation. Heathlands, in particular, exhibit large variability in N content on a small spatial scale, suggesting that N availability may be influenced by factors such as microtopography or vegetation composition. Rapid increases in N availability can occur across all tundra soils during events such as the spring melting season (Pessi et al. 2022). The presence of diverse animal species and complex vegetation contributes to the high microbial variation observed in these soils (Kauhanen 2013).

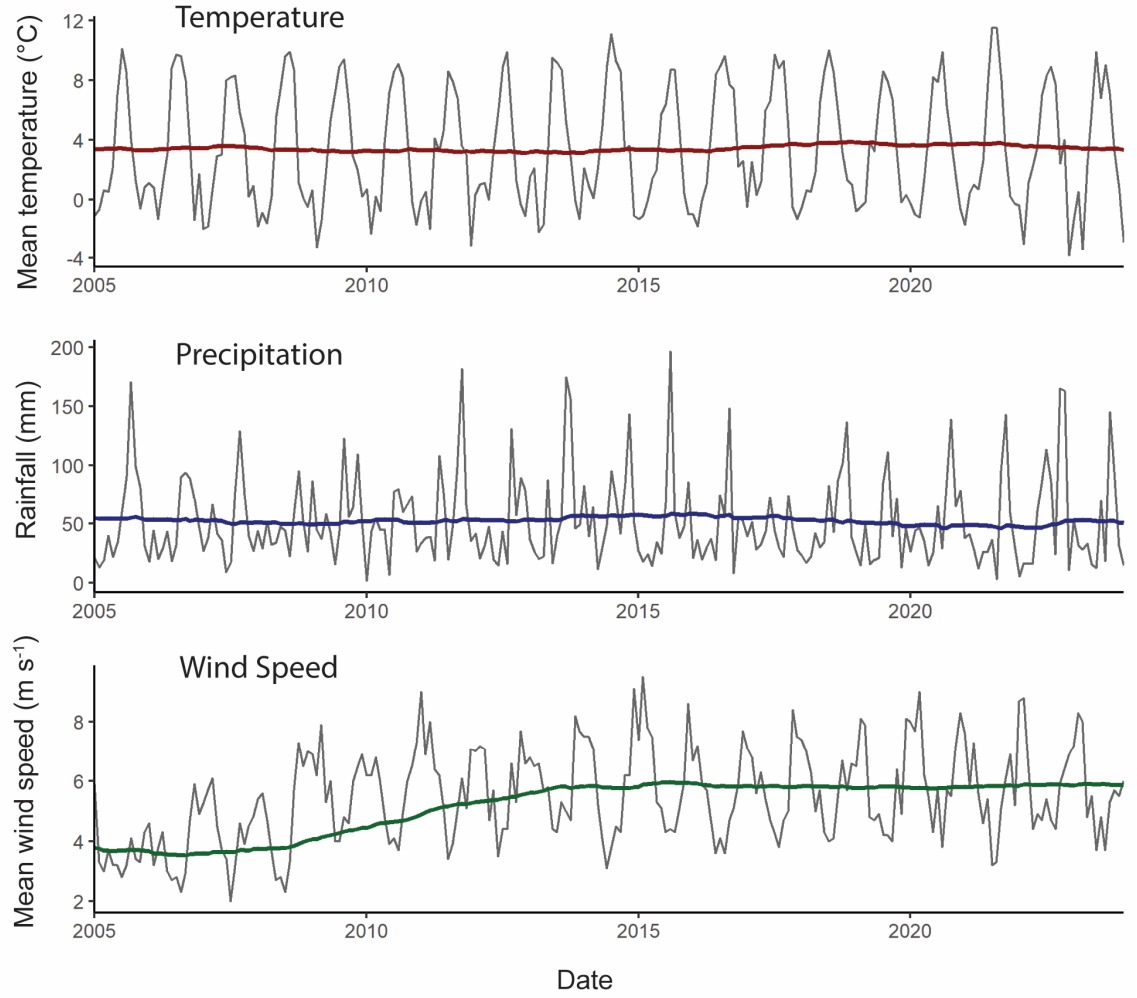

Fig. 13 Climatic data from the Enontekiö Kilpisjärvi weather station, 2005 – 2024. The data have been smoothed using a five-year running average in each case (starting from 2000).

Terrain

The studied landscape is on a moderate slope and transitions from the tree line to a shrub-dominated landscape. With further increase in elevation, the shrub sizes decrease, and turning into grass and heath-dominated areas (Fig. 12). The area is covered with undulating mounds with a diameter of 10-60 m and a height of 1-3 m. On top of the undulating ridges cryogenic features such as hummocks and deflated areas are found. Hollows are either barren, or partially or fully vegetated depending on the snow cover duration in these pockets.

Land use

The land use in the Kilpisjärvi region is characterised by reindeer herding, tourism, and recreational activities, with minimal infrastructure development (Kauhanen 2013).

Reindeer herding, primarily managed by Sámi people in Fennoscandia, has a long history, with 40% of the land designated for grazing (Huntington 2013). Migratory patterns vary across the region, with most districts following seasonal migrations between the coast and mountains, while some practice year-round grazing (Pape & Löffler 2012). Competing land-use activities are increasingly putting pressure on extensive grazing, affecting reindeer behaviour, herding practices, and grazing patterns (Tømmervik et al. 2012). Sustainable winter grazing efforts have led to the recovery of lichen-dominated tundra heaths and increased vascular plant cover (Tømmervik et al. 2012). Herbivory has accelerated short-term nutrient cycling rates in these ecosystems, modifying plant-community nutrient dynamics in tundra-grasslands (Petit Bon et al. 2020). However, a majority of the grazing land is exposed to cumulative pressures, (including tourism, infrastructure, forestry, and climate change), and if the expansion of these pressures leads to grazing abandonment in disturbed areas and intensification in others, it could irreversibly change the Fennoscandian mountain landscape (Stoessel et al. 2022).

2.4 TIPPING POINTS AND RESILIENCE

The concept of tipping points and landscape resilience has gained importance in the understanding of the dynamics of complex systems, particularly in the context of environmental and ecological processes. Tipping points refer to critical thresholds beyond which a system undergoes an abrupt and potentially irreversible change, transitioning to a new state or regime (Fig. 14a) (Scheffer et al. 2001; Rietkerk et al. 2004). These thresholds represent the limit of a system's capacity to absorb disturbances, beyond which feedback mechanisms amplify changes, pushing the system away from equilibrium.

Landscape resilience, on the other hand, is the capacity of a landscape or ecosystem to absorb disturbances and maintain its fundamental structure, functions, and processes. This capacity is shaped by factors such as biodiversity, connectivity, and spatial self-organisation, which allow the system to reorganise and adapt to changing conditions without crossing tipping points (Fig. 14b,c) (Rietkerk et al. 2021). Identifying thresholds and understanding landscape resilience is crucial for predicting and mitigating undesirable shifts and providing valuable insights about managing landscapes under increasing environmental pressures.

Turing patterns are regular spatial patterns that can emerge in systems where two interacting components, such as vegetation / land cover types, spread at different rates. These patterns form due to the interplay between short-range positive feedback (activation) and long-range negative feedback (inhibition) between the components. The classical view suggests that these self-organised patterns can serve as early warning signals for an approaching tipping point, where a system may transition to an alternative stable state once a critical threshold is crossed (Fig. 14).However, the concept of multistability of Turing patterns, associated with the presence of a "Busse balloon" in parameter space, proposes that self-organised patterns can arise in localised regions before the tipping point and persist beyond it (Fig. 14b). This allows the system to gradually adjust to changing conditions and avoid catastrophic shifts. The Busse balloon represents a range of conditions under which multiple stable patterned states can coexist. Furthermore, the multistability of coexistence states suggests that after a perturbation, the system may allow alternative stable states to coexist in different spatial regions (Fig. 14c). This spatial coexistence enhances the system's resilience by preventing a complete system collapse, as the effects of the perturbation remain localised. These concepts highlight the potential for sudden shifts in environmental conditions while also recognising the landscape's ability to maintain resilience through spatially driven mechanisms. As a result, systems prone to tipping points may be more resilient to global stressors than currently recognised (Rietkerk et al. 2021).

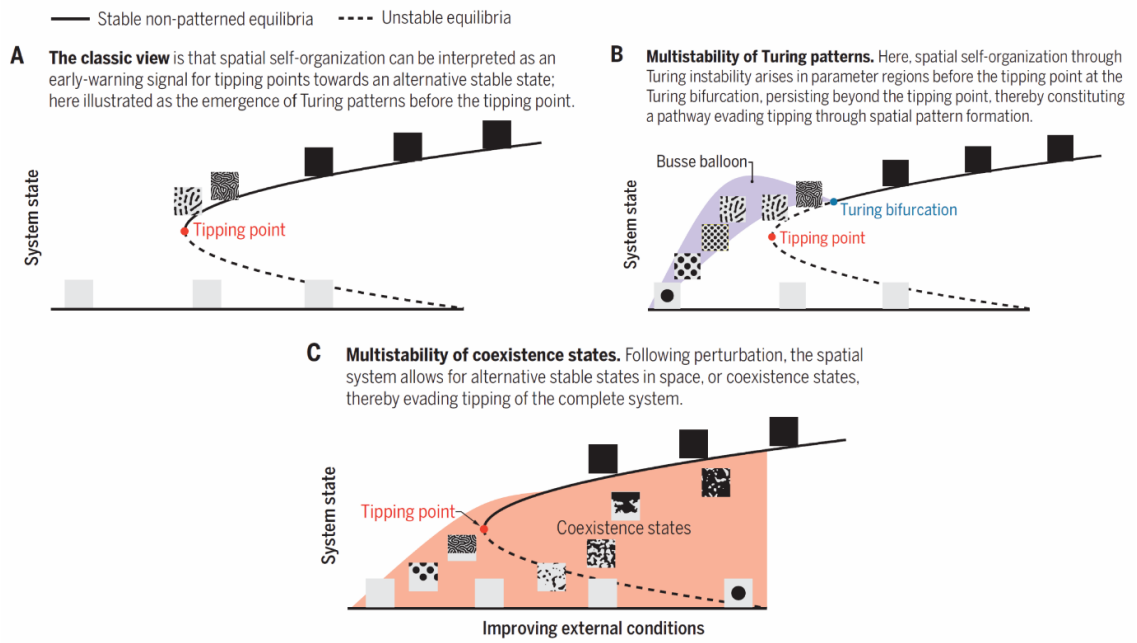

Fig. 14 Mechanisms tipping points and the evasion of them in complex systems. (A) Classic view. (B) Multistability of Turing patterns within Busse balloons, supported by models and satellite observations. (C) Multistability of coexistence states, where spatial patterns emerge before the tipping point and persist beyond it, providing an alternative pathway to avoid collapse (from Rietkerk et al. 2021).

In ecosystems characterised by regular spatial structures, such as the patterned vegetation observed in drylands (Buxton et al. 2022), processes of spatial self-organisation can give rise to multiple alternative stable pattern states under low rainfall conditions. This phenomenon may provide a mechanism for ecosystems to circumvent tipping points and the consequent rapid deterioration of ecosystem services (Rietkerk et al. 2021). The interaction between plants and soil, known as plant-soil feedback, is a critical factor in driving spatial self-organisation and has an impact on community assembly and resilience in both above- and below-ground areas (Inderjit et al. 2021). For example, in Namibia, fairy circles have been linked to ecohydrological feedbacks that create self-organised vegetation patterns driven by water stress (Getzin et al. 2022). While extensive research has been conducted on the resilience of patterned vegetation in dryland savannas, the Arctic tundra has received comparatively little attention, despite permafrost soils (Lenton et al. 2024).

In the Arctic tundra, abrupt ecological transitions related to permafrost thaw, the transition to a shrub-dominated ecosystem or – in the case of Iceland – desertification. Tundra shrub expansion (Martin et al. 2017) competes with local vegetation by shading and resource competition (Kemppinen et al. 2021). Darker shrubs absorb more thermal

radiation than mixed tundra vegetation, facilitating heating (Myers-Smith et al. 2011; Loranty et al. 2011). Herbivores like reindeer can reduce deciduous shrub cover through selective browsing, increasing the abundance of evergreen dwarf shrubs, potentially slowing down carbon cycling and increasing soil carbon storage. However, the majority of the carbon is stored in permafrost, and thawing threatens to release half of this stored carbon through collapsing ground, rapid erosion, and landslides (Turetsky et al. 2019).

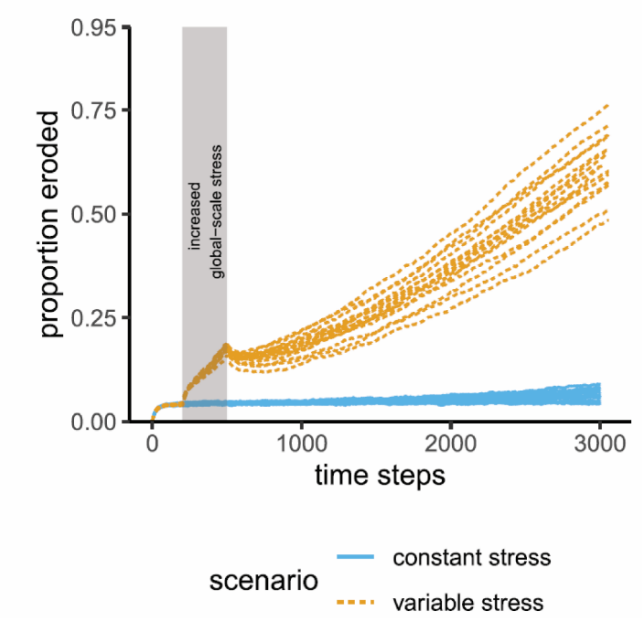

Fig. 15 Progression of total eroded area from a model run simulating erosion in Iceland. The graph presents the progression of erosion under two scenarios: one with constant low global-scale stress (solid blue lines) and the other with variable global-scale stress (dashed orange lines), where high global-scale stress is applied for time steps 200–500. The results demonstrate that once erosion reaches a certain threshold—approximately 15% of the total area—it continues to expand, regardless of global-scale stress levels (Streeter and Cutler 2020). This suggests a potential irreversible tipping point, where erosive forces exceed the landscape's capacity for recovery through revegetation, ultimately leading to desertification, even if conditions, such as climate or grazing pressure, improve.

In the highly geomorphologically active environment of Iceland, soil erosion poses a threat to ecosystem stability. Centuries of deforestation and overgrazing have left large areas susceptible to severe wind erosion, stripping away the susceptible volcanic soils (Barrio et al. 2018; Arnalds 2015). In the study by Streeter and Cutler (2020), the authors developed a cellular automata model to simulate soil erosion and revegetation processes in Iceland, incorporating both global-scale and local-scale probabilities of revegetation, with the local-scale probability dependent on the vegetation status of adjacent cells. The simulations revealed that once erosion patches reach a sufficient size, they continue to grow independently of external environmental conditions, aligning with observations in Iceland where erosion has been challenging to halt or reverse, even after the complete

removal of grazing (Barrio et al. 2018; Marteinsdóttir et al. 2017). The authors suggest that there may be a threshold in the proportion of eroded land, between 15-35% (Fig. 15) (Streeter & Cutler 2020; Thorsson 2008), beyond which erosion becomes extremely difficult to reverse, transforming Iceland's remaining vegetated areas into barren landscapes (Ólafsdóttir & Guòmundsson 2002; Arnalds 2000a). This desertification process can be observed further inland in the barren highlands of Iceland. Despite the long history of erosion in northeastern Iceland, completely eroded sites are uncommon, suggesting that either the eroded area increases at an extremely slow rate or that sites show some level of responsiveness to global-scale stressors (Streeter & Cutler 2020). It could also be an indication of multistability of coexistent states by evading potential tipping points by spatial pattern formation, of completely vegetated or barren cover (Fig. 14c) (Zelnik & Meron 2018), which is an important knowledge gap to explore. There is little understanding as to whether transitioning to a new ecological stable state through desertification is the sole outcome in Iceland or if spatial pattern formation offers a pathway to landscape resilience in response to global stressors such as changing climate or grazing. For this we need to better understand the underlying forces and interactions between them.

2.5 ADVANCES AND CHALLENGES IN REMOTE SENSING FOR ENVIRONMENTAL MONITORING

Remote sensing has become a crucial tool for monitoring environmental changes, offering insights into key environmental variables such as soil moisture, snow cover, vegetation health, and land cover distribution. These capabilities are vital for addressing the impacts of climate variability and anthropogenic activities in both Arctic and non-Arctic regions. Despite significant advancements, challenges persist, particularly in addressing spatial resolution limitations, mixed pixels, data integration, and the need for ground-truthing.

Soil moisture is a critical environmental variable for hydrology, agriculture, vegetation health, and climate interactions. Remote sensing technologies like Microwave sensors, including radar (active sensors) and radiometers (passive sensors), are well suited for estimating soil moisture due to their sensitivity to soil moisture content and their ability to penetrate clouds. For example, NASA’s SMAP mission utilizes L-band microwaves to generate global soil moisture products with spatial resolutions ranging 1 – 36 km

(Entekhabi et al. 2010; Portal 2020). However, the coarse resolution of microwave sensors limits their applicability in heterogeneous regions where finer detail is required. Optical and thermal sensors offer higher spatial resolution, estimating soil moisture indirectly through vegetation indices and surface temperature variations (Jackson et al. 2004). However, these methods face challenges in regions with persistent cloud cover, aerosol interference, and complex topography (Ghilain 2019). Recent innovations in data fusion and downscaling aim to combine the moisture sensitivity of microwave sensors with the spatial detail of optical sensors, enhancing soil moisture mapping for applications such as agricultural monitoring and flood prediction (Peng et al. 2017). Promising advancements include integrating Sentinel-1 radar and Sentinel-2 optical data, enabling soil moisture monitoring at a 10 m spatial resolution, which shows significant potential for addressing these limitations (Atar, 2024). However, ground validation is essential for ensuring confidence in remote soil moisture assessments, particularly in heterogeneous landscapes where soil moisture dynamics exhibit significant spatial and temporal variability, leading to large uncertainties (Dorigo et al. 2011).

Monitoring snow cover is a critical application of remote sensing, fundamental to understanding hydrological cycles, assessing climate change impacts and understanding microclimates (Zhao et al. 2020; Rango 1997). Optical sensors, such as those on MODIS (250–500 m resolution) and Landsat (30 m) platforms, are widely used to map snow cover extent due to their ability to distinguish snow from other land cover types based on spectral reflectance in the visible and near-infrared bands (Hall et al. 2002). However, these sensors often struggle to differentiate snow from clouds, especially in persistently cloudy regions. Microwave sensors, such as AMSR-E (5 – 56 km) and Sentinel-1 (10 m), overcome this limitation by detecting snow cover under cloud cover and estimating snow water equivalent (SWE). Their ability to penetrate clouds and snowpacks minimizes confusion between clouds and snow, a common issue with optical data (Tsang et al. 2022; Dietz et al. 2012). Advances in data fusion techniques now combine optical and microwave datasets, improving snow cover mapping accuracy and resolution while addressing challenges such as cloud interference and spatial detail limitations. Furthermore, new high-resolution platforms like Planet, offering 3 m resolution, enhance the ability to monitor snow cover distribution and dynamics in heterogeneous terrains with greater detail (Kemppinen & Niittynen 2022).

Vegetation health monitoring is a key application of remote sensing, using vegetation indices like the Normalized Difference Vegetation Index (NDVI) and Normalized Difference Red Edge (NDRE) to quantify plant vigour and chlorophyll content by analysing differential reflectance in red and near-infrared bands (Tucker, 1979). Multispectral imaging captures data in broad wavelength bands, while hyperspectral imaging provides finer spectral resolution through numerous narrow and contiguous bands, enabling more accurate analysis of vegetation properties such as species composition and stress levels, including onboard UAV systems (Putkiranta et al. 2024). Despite its advantages, hyperspectral imaging is less versatile than multispectral systems due to higher costs and bulkier equipment, with current operational satellites like the Italian PRISMA (30 m) and German EnMAP (30 m) not yet readily available to the wider research community (Musacchio et al. 2024; Beamish et al. 2020). Platforms like MODIS and Landsat facilitate time series analyses, offering insights into seasonal and long-term vegetation dynamics, including phenological changes and disturbances like droughts, deforestation, and soil erosion (Huang et al. 2020; Žížala et al. 2019)

Understanding spatial patterns and land cover distribution within ecosystems is crucial for biodiversity conservation and ecosystem management. Remote sensing enables land cover classification and ecosystem mapping through supervised and unsupervised methods, with unsupervised methods commonly applied in areas where prior knowledge is lacking, and supervised methods used in areas with known land cover types, providing more accurate and reliable results (Lu & Weng 2007). Traditional classification methods like Maximum Likelihood Classification (MLC) and Minimum Distance Classifiers (MDC) have been widely used in remote sensing but often struggle with non-linear relationships and high-dimensional data compared. The integration of machine learning algorithms, such as Random Forests (RF) and Support Vector Machines (SVM), has significantly enhanced the accuracy of these classifications by identifying complex patterns in high-dimensional data (Pal, 2005). These are among the most common and reliable algorithms for remote sensing applications. Although neural networks, including deep learning methods such as Convolutional Neural Networks (CNNs), can further improve classification accuracy, their computational intensity often limits their practical application, and established methods like RF or SVM show often better or comparable performance in land-use and land-cover (LULC) classification (Vali et al. 2020).

Despite these advancements, challenges remain. Mixed pixels, which occur when a single pixel contains multiple land cover types, are a persistent issue, particularly in coarse-resolution imagery. Techniques such as spectral unmixing aim to address this by decomposing pixels into their constituent components, but these methods are computationally demanding and rely on accurate endmember identification (Keshava & Mustard, 2002). UAV systems are increasingly valuable in overcoming these limitations by providing high-resolution data that bridges the gap between satellite-based remote sensing and ground-based observations. UAVs enable the collection of higher resolved spatial information, reducing the prevalence of mixed pixels and enhancing the accuracy in environmental monitoring (Eskandari et al. 2020). Their flexibility and ability to capture data at various scales make them a crucial tool for improving accuracy of environmental assessments and refining spectral unmixing techniques.

2.6 SCALE

Scale includes the observation scale, which is the spatial extent of the study area, the measurement scale, which is referred to as spatial resolution or 'grain', and the operational or intrinsic scale of a landscape at which processes occur (Romano et al. 2023). The representation of spatial landscape features and processes is inextricably linked to the spatial resolutions at which they are monitored. A spatial resolution different from the actual functional structure of the landscape, without taking into account scaling effects, can lead to distortions that affect our interpretation and give us a false picture of the environmental status (Fig. 16).

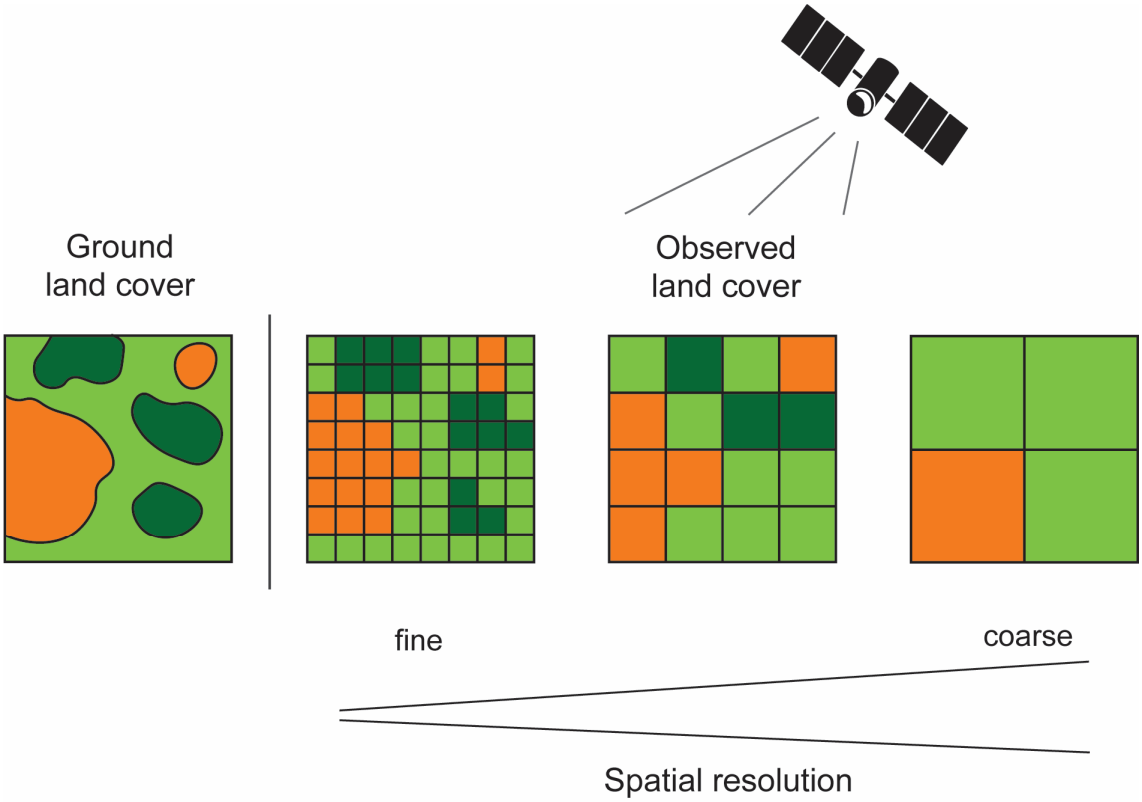

Fig. 16 Illustration of the effects of spatial resolution on observed land cover patterns. The ground land cover (left) represents the true spatial distribution of three land cover types. As the spatial resolution of the observation instrument becomes coarser (from left to right), the observed land cover patterns become increasingly generalised and less representative of the actual ground conditions.

Satellite-derived vegetation indices, such as NDVI, are commonly used to monitor Arctic greening and browning trends over decades (Guay et al. 2014; Raynolds et al. 2013; Forkel et al. 2013). Similar methods have been applied to track global land-cover change dynamics and assess their drivers (Song et al. 2018). In China, NDVI analyses have been used to study temporal and spatial vegetation changes, examining dynamics influenced by land-use and land-cover changes, climate, and anthropogenic factors (Yao 2021; Wang et al. 2019). However, interpreting these trends is challenging due to the complexities of Arctic ecosystems and limitations of satellite data (Myers-Smith et al. 2020). Spectral greening and browning may not always correspond to in-situ observations of vegetation change (Pattison et al. 2015; Raynolds et al. 2013; Frost et al. 2014), as non-biological factors like snow cover, surface water, and soil moisture can influence the measured greenness (Liu et al. 2017; Riihimäki et al. 2017; Raynolds & Walker 2016; Gamon et al. 2013). Additionally, satellite records may not accurately capture plant phenology and growing season length changes at high-latitudes (Myers-Smith et al. 2020). Comparisons between satellite-derived productivity trends and ground-based measurements are

complicated by the lack of in-situ data at an annual resolution and low sampling replication across the landscape (Berner et al. 2018; Myers-Smith et al. 2015; Elmendorf et al. 2012). Additionally, the fine-scale variability of land cover and the range of biogeomorphological processes in the Arctic increase the difficulty of studying these changes using Earth observation data. For instance, the UAV study by Assmann et al. (2020) revealed that the spatial variation of Dryas-Vetch and Tussock-Sedge Tundra was about 0.5 m, highlighting the need for high-resolution data to capture such fine-scale heterogeneity.

The issue of scale in remote sensing has been a longstanding challenge (Woodcock & Strahler 1987). Monitoring fragmented high-latitude environments is particularly complex, as determining whether spectral changes are driven by plant productivity or land-cover changes remains difficult (Myers-Smith et al. 2020). This raises important questions about the spatial resolutions best suited for studying these processes and the differences in monitoring capabilities among imaging sensors (Stow et al. 2004). Remote sensing is critical for the detection of various tipping phenomena, early warning systems, changing resilience, and interactions between tipping systems (Lenton et al. 2024). Therefore, to improve monitoring and research capabilities, we need a better understanding of scaling biases and how they influence the interpretation of satellite-derived vegetation indices and their relationship to on the ground vegetation change in the Arctic (Beamish et al. 2020; Laidler et al. 2008). This understanding will also help validate satellite imagery and ensure that the data accurately represents the complex ecological processes (Sotille et al. 2020). These represent critical knowledge gaps that merit further exploration.

2.7 ARCTIC MONITORING

Accurate monitoring of Arctic ecosystems is crucial for several reasons. It allows the tracking of land cover changes related to vegetation change, particularly shrubification, and of land degradation such as soil erosion, permafrost thaw, and fire. It also helps in understanding the underlying processes and predicting future developments. This is especially important given the region's rapid transformation and the uncertain consequences that accompany it (Vincent et al. 2011). Such knowledge is essential to protect the Arctic, adapt effectively to ongoing changes, and develop sustainable practices for land use.

The history of monitoring the Arctic tundra dates back to the early 20th century. Early monitoring efforts relied on traditional methods, such as field observations, specimen collections, and manual measurements of physical and biological parameters (Callaghan et al. 2004). These labour intensive approaches provided valuable insights into the ecology and dynamics of the Arctic but were limited in their spatial and temporal coverage.

As technology advanced, monitoring methods evolved to include more sophisticated tools and techniques. In the 1950s and 1960s, aerial photography became an important tool for mapping the Arctic landscape, allowing researchers to cover larger areas and study vegetation patterns, permafrost distribution, and glaciers (Liljequist 1993; Hobson 1981). Environmental monitoring has been a long-standing concern in Iceland, leading to early efforts in conducting aerial surveys to improve soil erosion mapping (Arnason & Benediktsson 1999). Systematic surveys for cartographic purposes were conducted by the Danish since the 1937-38 (Aldred et al. 2010). However, aerial surveys were still limited by weather conditions, high costs, and the need for extensive ground-truthing.

The advent of satellite remote sensing in the 1970s marked a breakthrough. Satellites, most prominently the Landsat series, provided regular, high-resolution imagery of the entire Arctic region, enabling researchers to track changes in vegetation cover, phenological changes, snow and ice extent, and other key indicators of ecosystem health (Beamish et al. 2020; Bhatt et al. 2010).

Hyperspectral sensors, capable of collecting data across hundreds of narrow spectral bands, have emerged as a powerful tool for studying the biophysical features of the tundra. Field spectrometry allowed for the identification and mapping of specific plant species, soil properties, and other ecosystem characteristics (Bratsch et al. 2016; Davidson et al. 2016), providing new insights into the biodiversity, ecological function, and biogeochemical cycling of Arctic tundra ecosystems (Beamish et al. 2020). Future satellite hyperspectral missions such as the SBG (NASA) (Thompson et al. 2022b) and CHIME (ESA) (Rast et al. 2021), with global coverage, frequent acquisitions and suitable spatial resolutions (30 m), are expected to significantly advance monitoring capabilities at the end of 2020's. Building on the capabilities of current hyperspectral missions like EnMap (DLR) and PRISMA (ASI), which are already providing valuable datasets.

Active sensing systems such as Light Detection and Ranging (LiDAR) and the Synthetic Aperture Radar (SAR) satellite systems, have proven to be valuable tools in polar research. SAR has the ability to monitor structural changes independent of cloud cover and illumination and is used for monitoring permafrost, water bodies, and land cover (Beamish et al. 2020; Michaelides et al. 2019; Bartsch et al. 2016; Widhalm et al. 2017). LiDAR is the most accurate instrument for measuring vertical structure and has shown great promise in providing precise topographical data and indirectly vegetation characteristics, such as shrub and tree biomass and plant functional types (Beamish et al. 2020; Langford et al. 2016; Greaves et al. 2015).

In recent years, the use of UAVs has also gained traction in high-latitude research. UAVs equipped with high-resolution RGB, multispectral, hyperspectral and LiDAR sensors can provide data at fine spatial scales, bridging the gap between satellite remote sensing and ground-based observations (Anderson & Gaston 2013). These platforms offer a cost-effective and flexible alternative to traditional aerial surveys, allowing researchers to collect data on demand and in remote or inaccessible areas of the Arctic (Assmann et al. 2019). UAVs are useful for monitoring biomass, plant composition, plant traits, phenology, productivity, detecting vegetation damage, and erosion but also for mapping topography and snow accumulation (Lamare et al. 2023; Thomson et al. 2021; Fraser et al. 2016). For example, Eischeid et al. (2021) conducted a multispectral UAV study in Spitsbergen, demonstrating its efficacy mapping vegetation disturbance caused by herbivory (goose grubbing) and winter damage (rain-on-snow and freeze-thaw) in high Arctic tundra. Fraser et al. (2016) successfully estimated shrub biomass and mapped fine-scale vegetation using UAV photogrammetric methods with a quadcopter and a high-resolution RGB camera in Tuktoyaktuk, Northwest Territories. Likewise, Orndahl et al. (2022) obtained promising results in fine-scale PFT mapping and estimating biomass from digital surface model (DSM) using UAV photogrammetry and multispectral imagery in northwest Canada.

Despite the many advantages of remote sensing, traditional field-based monitoring methods remain essential for validating satellite data and providing detailed, local site-specific information on environmental properties such as soils, biodiversity, plant physiology and climate. Field surveys of plant and animal communities provide valuable data on species composition, abundance, and distribution that cannot be obtained

through remote sensing alone (Christensen 2013). These surveys often involve the use of standardised sampling techniques, such as plot-based vegetation assessments, transect counts, and mark-recapture studies, which allow researchers to quantify changes in biodiversity over time and across different habitats (Magurran et al. 2010). Similarly, measurements of soil properties, such as carbon and nutrient cycling, microbial activity, and permafrost, rely on the collection of physical samples and the use of specialised instruments that cannot be deployed remotely (Schuur et al. 2015).

Similarly, ground-based measurements of climate variables as soil temperature, and moisture, light, humidity, and nutrient cycling are critical for modelling the complex interactions between land and climate (Lembrechts & Lenoir 2020). In recent years, the use of small, affordable sensors for monitoring the microclimate and soil properties of the Arctic tundra has become increasingly important (Kemppinen et al. 2024). These sensors, known as microloggers, can measure a wide range of environmental variables, such as air and soil temperature, humidity, soil moisture, and solar radiation, at high-temporal and spatial resolutions (Maclean et al. 2021; Lundquist & Lott 2008). By deploying networks of these sensors across the landscape, researchers can capture the fine-scale variability in microclimate conditions that is often missed by larger, more widely spaced monitoring stations (Niittynen et al. 2024; Ashcroft & Gollan 2012). Combined with vegetation data, they can provide comprehensive understanding of small-scale ecological adaptations to climatic changes.

In recent years, there has been a growing recognition of the importance of integrating traditional and modern monitoring methods to gain a more comprehensive understanding of the Arctic tundra. This has led to the development of collaborative monitoring networks, such as the Circumpolar Biodiversity Monitoring Program (CBMP), which brings together scientists, indigenous communities, and other stakeholders to share knowledge and coordinate monitoring efforts across the Arctic (AMAP 2017).

The Arctic's vast areas are often not readily accessible due to underdeveloped infrastructure and political boundaries, limiting research to isolated sites. Metcalfe et al. (2018) identified significant spatial biases in Arctic field sampling and study citations, with under-sampling and under-recognition of colder, rapidly warming, and sparsely vegetated sites, primarily in the Canadian high-Arctic Archipelago and the Russian Arctic coastline, potentially biasing scientific understanding of Arctic climate change. By combining

various monitoring approaches, encompassing different spatial and temporal scales and including local populations' knowledge, scientists can develop a more comprehensive understanding of the Arctic tundra's particularly understudied regions and inform effective conservation and management strategies.

CHAPTER 3: ARCTIC TUNDRA SHRUBIFICATION CAN OBSCURE INCREASING LEVELS OF SOIL EROSION IN NDVI ASSESSMENTS OF LAND COVER DERIVED FROM SATELLITE IMAGERY

3.1 INTRODUCTION

The Arctic tundra has warmed two to four times faster than the global average in recent decades (Rantanen et al. 2022; Post et al. 2019). This warming has led to profound ecological changes, including the encroachment of woody shrub species ('shrubification') with associated geomorphological changes (Kemppinen et al. 2021; Myers-Smith et al. 2011). Changes in vegetation composition and structure are likely to influence slope stability and processes of soil degradation/erosion and vice versa (Kemppinen et al. 2022; Eichel et al. 2016; Marston 2010). However, uncertainties remain over the interaction between ecological and geomorphological processes in a rapidly changing climate (Niittynen et al. 2020a). Large-scale changes in vegetation structure are commonly inferred from remote sensing data, notably the normalized difference vegetation index (NDVI). However, these assessments are complicated by several factors, including the influence of mixed pixels including multiple land cover, atmospheric conditions, soil background effects, and seasonal variations in vegetation (Giri et al. 2013; Huete et al. 2002; Huete & Tucker 1991). Additionally, NDVI tends to saturate in areas with dense vegetation, making it less effective for distinguishing between different levels of high biomass (Sims & Gamon 2002). The calibration of medium resolution remote sensing data with finer-resolution imagery derived from uncrewed aerial vehicles (UAVs) offers a way forward. This paper will address the interpretation of NDVI values derived from satellite platforms by comparing high- to mid-resolution remote sensing NDVI scenes from Landsat-8 (L8, spatial resolution 30 m), Sentinel-2 (S2, 10 m) and PlanetScope (PS, 3 m) with collected very-high-resolution (0.05 m) multispectral data acquired using a UAV. In addition, the effect of different scales on the spectral mixture of pixels is tested by using classified landscapes from the UAV images.

Satellite monitoring indicates widespread long-term greening trends across a majority of the circumpolar Arctic within the period (1982–2017), reflecting an increase in vegetation productivity (Bhatt et al. 2017; Ju & Masek 2016; Xu et al. 2013), and in some cases a shift

in plant dominance, in particular to an increase in shrub biomass (Weijers et al. 2018; Forbes et al. 2010).

A warmer, wetter climate is likely to lead to the expansion of shrubs with upright growth forms in the tundra ('shrubification': (Myers-Smith & Hik 2018; Martin et al. 2017; Tape et al. 2012)), as growth conditions ameliorate. It is estimated that >50% of the tundra biome will be replaced by woody shrubs by 2050 (IPCC 2019). Shrubification will result in increased canopy cover and woody root mass, which will reduce surface wind speeds, intercept rainfall and bind soils to the substrate. These processes would tend to reduce soil erosion. The magnitude of this effect is not yet clear (Heindel et al. 2017); it is therefore essential to monitor shrubification if we are to understand geomorphological changes – including soil erosion – and ecological changes including vegetation cover in high-latitude areas.

Soil erosion is a major problem in Iceland, due to a combination of fine, low-cohesion soils, high winds, grazing pressure and frequent freeze-thaw cycles (Arnalds 2015; Dugmore et al. 2009). Vegetation cover is a particularly important control on erosion rates, because plants have the potential to reduce soil loss. A key metric is the ratio of vegetated to eroded area (Streeter & Cutler 2020; Barrio et al. 2018; Thorsson 2008). At critically low values of this ratio, a tipping point may be reached, and rapid soil erosion can lead to irreversible desertification (Rietkerk et al. 2004) (Ch. 2.4).

The obvious way to measure large-scale changes in tundra cover is remote sensing, but the unique characteristics of tundra landscapes complicates the estimation of land cover change. Tundra ecosystems are highly fragmented compared to other biomes (Virtanen & Ek 2014). They consist of a mosaic of different vegetation, geomorphic formations and water bodies and are characterised by multiple scales of landscape heterogeneity (Stow et al. 2004; McFadden et al. 1998). This heterogeneity is a result of combined factors related to the harsh Arctic climate. The sparse vegetation cover is susceptible to physical forces such as wind and frost activity. Combined with seasonal and longer-term changes, it affects soil properties and causes small-scale variations in vegetation and land cover (Virtanen & Ek 2014).

The most commonly used indicator of photosynthetic activity is the NDVI, as it can be easily calculated from the near-infrared (NIR) and red spectral bands, which have been observed from space since the 1970s (Myers-Smith et al. 2020). The applicability of NDVI

for the detection of vegetation cover has been demonstrated in the Arctic and Antarctic environments (Sotille et al. 2020; Fretwell et al. 2011; Laidler et al. 2008). Yang et al. (2020) suggest that deciduous shrub cover has a significant impact on spectral reflectance, particular in the NIR range. Shrub cover has higher NIR reflectance than other tundra vegetation because shrubs typically have a denser, more complex canopy structure and larger leaf area, which enhances NIR scattering. Additionally, compared to low-lying tundra vegetation like mosses and lichens, shrubs reduce soil exposure and maintain more biomass, leading to greater overall NIR reflectance. Increases in shrub cover therefore should lead to higher NIR to R ratio reflectance; in contrast, eroded terrain will have much lower values. The use of NDVI to infer land surface change may therefore be complicated if shrubification occurs at the same time as soil erosion. In this scenario, increased shrub vitality (and higher NIR reflectance) might mask an increase in eroded terrain (with an associated decrease in NIR reflectance) (Fig. 17).

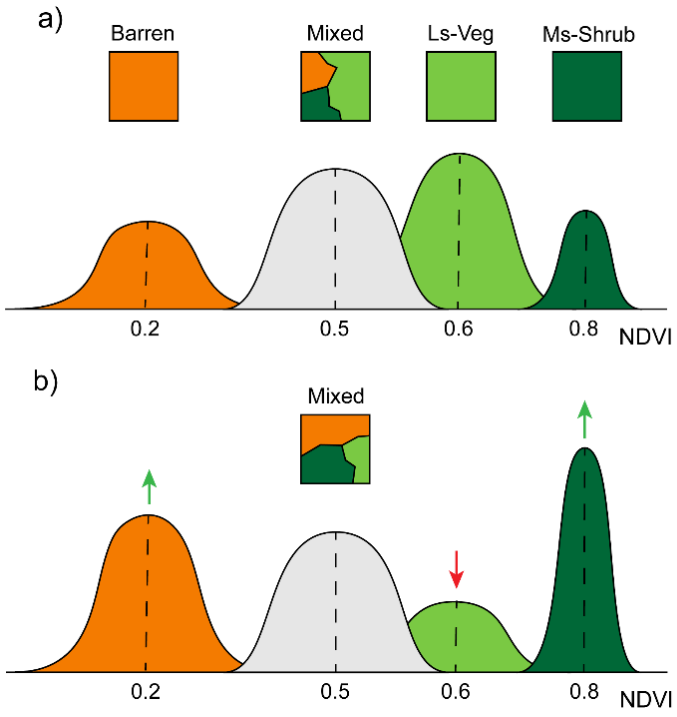

Fig. 17 Spectral confusion caused by mixing of land cover types. a) The three functional land cover type Barren, Low-stature Vegetation (Ls-Veg) and Medium-stature Shrub (Ms-Shrub) are contributing to the spectral mixing of a sensed pixel shown in grey. b) Barren and Ms-Shrub cover is increasing over time while Ls-Veg cover decreases, but the pixel NDVI value stays the same. Simultaneous changes in cover composition may mask each other, thereby impeding observations of land cover change at coarse spatial resolution (after Campbell 2011).

As Fig. 17 demonstrates, large-scale Arctic monitoring studies run the risk of inferring wrong ecological trends from datasets with coarse spatial resolution. In the study of Ju &

Masek (2016) in Canada and Alaska, NDVI trend analysis between AVHRR and Landsat showed broadly similar large-scale trends but differed considerably from regional trend patterns. Siewert and Olofsson (2020) showed in a study for northern Sweden that when decreasing resolution from UAV imagery to satellite scale, the mean NDVI remained stable, but the biomass and gross primary productivity (GPP) calculated from NDVI were underestimated due to non-linear relationship between remote sensing products, ecosystem processes, and spatial heterogeneity. The study showed that at coarse spatial resolutions the link between NDVI and biomass differs to that existing at fine resolutions. Similarly, research from Assmann et al. (2020) in Herschel Island, Canada, revealed that the peak in spatial variation is around 0.5 m, at which resolution ecological information within plant communities are studied best. When upscaling to moderate grain resolution (~10-30 m) (i.e. those typically returned by satellite platforms), vital information was lost.

It is still not well understood how spatial aggregation influences the observed ecological heterogeneity in the various Arctic environments (Beamish et al. 2020). The spatial resolution and sensors used for monitoring are fundamentally related to how we can see and interpret the earth's surface. One way to address the issues associated with coarse-scale satellite measurements, is to calibrate readings with fine-scale observations acquired from UAVs. Reduction in the size and cost of UAVs made them more accessible to the research community, allowing the acquisition of very-high-resolution and radiometrically corrected multispectral imagery in remote areas. These data can be used together with field knowledge to compare and evaluate the validity of satellite products.

The major aim of our study was to understand how scale and sensor can affect estimations of vegetation cover. We suspected that ongoing soil erosion would not be visible in coarse-scale satellite data, due to climate-driven increases in photosynthetic activity. To investigate this, we carried out a multispectral UAV survey in 2021 at an actively eroding tundra rangeland in Iceland. We conducted a land cover classification from UAV imagery and compared the land cover maps to high- to mid-resolution (3-30 m) satellite imagery. Finally, we explored how different spatial resolutions affect spectral mixture and the consequent information loss, aiming to identify optimal spatial resolutions required for effective monitoring of the Arctic tundra.

3.2 STUDY SITE

The research was conducted at 12 study sites of 300 × 300 m, located in NE-Iceland (Fig. 18a). Sites were selected based on the criteria of low topographic variation, homogeneous vegetation cover, and similar hydrologic conditions. We aimed to cover areas in different degradation stages (Fig. 18b). The surveyed sites were located within unfenced rangelands. During the grazing season (May–September) sheep roam freely across these rangelands, except for the As-farm site, where grazing is only practiced in late summer. Sheep numbers across Iceland have declined hugely from the late 1970s (Marteinsdóttir et al. 2017), and we believe that our sites exhibit a similar trend of declining sheep numbers. Stocking densities were very low: we rarely saw sheep during our fieldwork and if we did, they were in small groups of just a few individuals.

The closest weather station with a long-term record is located in Raufarhöfn, about 30 km NW from the study sites (NE for site As). During the observation period between 1949–2008 the mean annual temperature was 2.5°C and the mean annual precipitation 680 mm, both with an increasing trend since 1980s (Veðurstofa Íslands, 2022) (Fig. A1 in Appendix).

The study area can be characterised as Dwarf shrub heath. The landscape is dominated mainly by medium-stature deciduous shrubs below 60 cm in height, mostly dwarf birch (*Betula nana*) (Fig. 18c). Also notable is the low-growing deciduous bog bilberry (*Vaccinium uliginosum*) and evergreen crowberry (*Empetrum nigrum*). Dwarf willow (*Salix herbacea*) is present but rarer due to grazing. Non-shrubby plants include graminoids (sedges, grasses and rushes), forbs, mosses and lichen (Fig. 18d). Plant community composition and susceptibility to erosion is strongly controlled by metre-scale mesotopographic variation (slope, topographic position index, aspect, elevation), which influences hydrology, snow cover, wind exposure and other environmental variables.

The studied landscape is characterised by numerous erosion patches, ranging in size from 1 cm^2 to 10s m^2, embedded in a tundra vegetation matrix (Fig. 18b). The larger erosion patches can be stable over long periods of time from decades to centuries (Streeter & Cutler 2020). Soils in this area of Iceland are Andosols, which mainly derive their properties from volcanic ejecta. They have a high-water retention capacity and are particularly susceptible to disturbances such as cryoturbation and aeolian erosion

(Arnalds 2015). Actively deflating areas consist of silt-sized soil particles, with remnants of vegetation cover but no secondary vegetation regrowth (Fig. 18e). Fully deflated areas consist of glacial till and have a darker appearance (Fig. 18f). On this eroded cover, recolonising vegetation is commonly established between or below the larger debris, this is mainly stress resistant vegetation such as lichen, moss, biocrust and to a smaller extent, graminoids and low-growing shrubs.

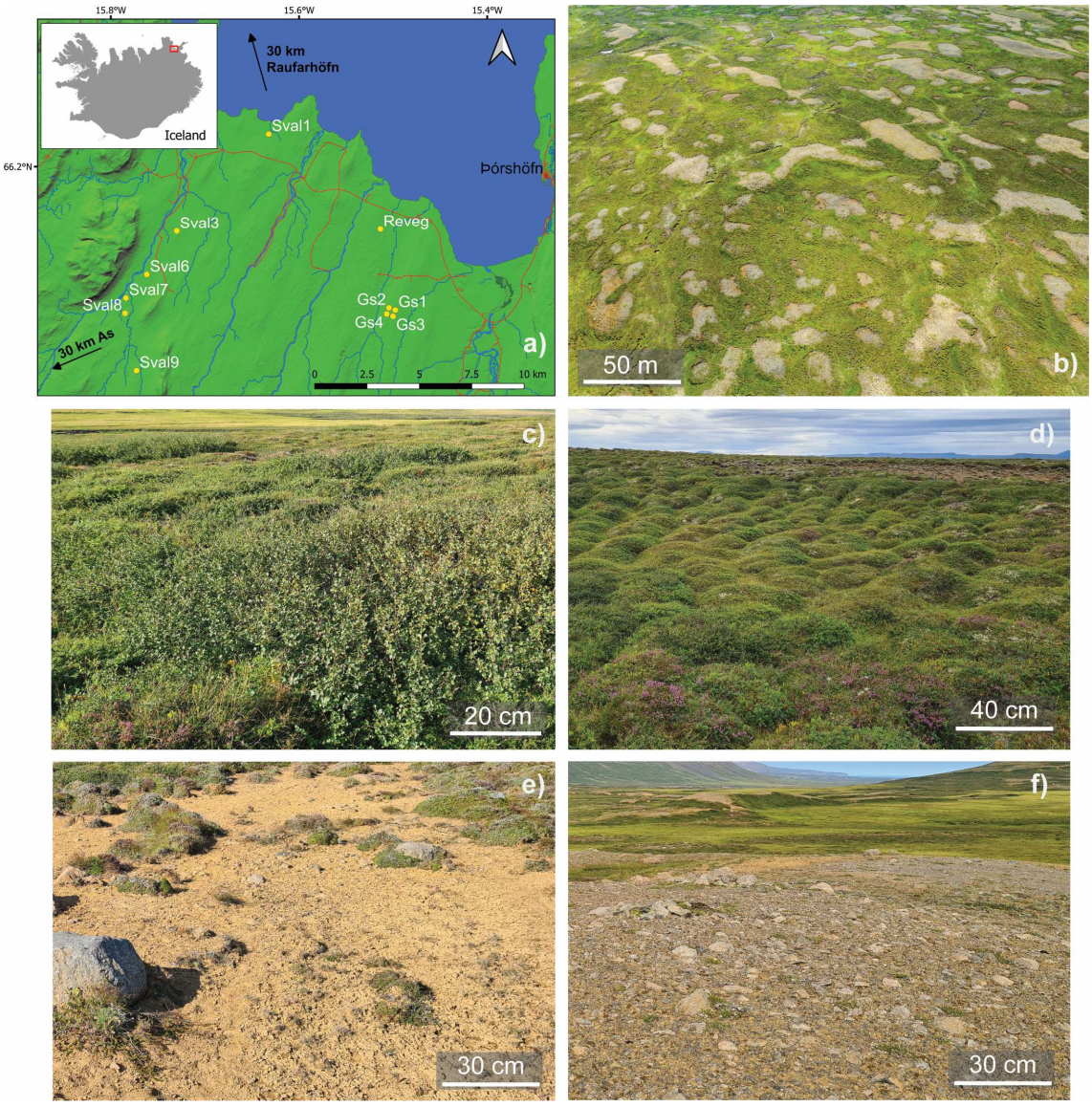

Fig. 18 a) Location of study sites surveyed in 2021 in NE-Iceland. b) UAV photo taken around location Gs2, showing a mosaic of eroded area (light tone) and tundra vegetation. c) Ms-Shrub land cover class with uniform patches of taller growing dwarf birch. d) Homogenous Ls-Veg land cover class showing a mixture of graminoids, forbs, low-stature shrubs, moss and lichen. e) Barren land cover with exposed Andosols in the foreground and remnant vegetation cover. f) Deflated barren land cover with rock debris and recolonising vegetation.

3.3 MATERIALS AND METHODS

3.3.3 Satellite data

We compared Landsat-8 (L8), Sentinel-2A (S2), and PlanetScope (PS) satellite data with higher resolution data acquired with a UAV Phantom 4M 5-band multispectral sensor (Table 2). Cloud or haze free scenes were selected that were closest to the UAV acquisition period (Table 3). All downloaded scenes were analysis-ready orthorectified products and atmospherically corrected data, representing bottom of atmosphere reflectance images and analysis ready (Level 2, Table A1 in Appendix).

Table 2 Characteristics of the remote sensing platforms used in the study. Scene identifiers used for the analysis can be found in the Appendix.

REMOTE SENSING IMAGERY METADATA						
Platform	Phantom 4m	PlanetScope	Sentinel-2	Landsat-8	Landsat-7	Landsat-5
Sensor	/	PSB.SD	MSI	OLI	ETM+	TM
Spatial resolution	~0.04 m	3 m	10 m	30 m	30 m	30 m
Processing level	/	L3B	L2A	L2	L2	L2
Band Red	650 ± 16 nm	665 ± 15 nm	665 ± 15 nm	660 ± 13 nm	660 ± 30 nm	660 ± 30 nm
Band NIR	840 ± 26 nm	865 ± 20 nm	833 ± 53 nm	865 ± 14 nm	835 ± 65 nm	830 ± 70 nm
Radiometric resolution	16-bit	12-bit collected (scaled to 16-bit)			8-bit	8-bit
Repeated coverage	/	Daily	5 days	8 days[1]	16 days	16 days
Zenith view angle	0°	1-5°	7.7°	0°	0°	0°
In operation	/	Since 2016	Since 2015	Since 2013	Since 1999	1984–1995
Equatorial crossing[2]	11:00–15:30[3]	9:30–11:30	10:30	10:00	10:00	9:45

[1]with Landsat 9 since October 2021; [2]Solar noon at study site 13:00; [3]UAV acquisition time

Furthermore, we used Landsat-5/7/8 imagery to plot a NDVI time series, to test whether continuous soil erosion is evident in the surveyed sites from 1984 until 2022. We extracted Landsat Collection 2 Tier 1 TOA reflectance data, using Google Earth Engine (GEE) Code Editor (Table A2 in Appendix). Tier 1 includes Landsat scenes with the highest available data quality and are considered suitable for time series analysis. Top-of-Atmosphere (TOA) data were used as they were the only data collection complete on GEE for the Landsat series. In an earlier study, Xu et al. (2014) noted that OLI NDVI shows high consistency with ETM+ in areas of dense vegetation but requires further calibration for low vegetation regions to ensure accuracy. However, more recent studies have demonstrated strong agreement between ETM+ and OLI sensors using Level 1 TOA reflectance data, as well as consistency with in-situ measurements (Teixeira Pinto et al. 2020; She et al. 2015).

The sensor wavelength range from Landsat-5/7 differs to that of Landsat-8 in the NIR band but the centre frequencies are similar (L8: 865nm, L7: 834nm, L5: 830nm). Collection 2 post-processed products are well radiometrically characterised and inter-calibrated across the different Landsat instruments (Landsat collection 2, 2021), ensuring data products for similar wavelengths are producing similar responses.

The use of NDVI in this study is justified by its widespread application, which facilitates comparisons with existing literature on Arctic greening and vegetation cover changes, providing insights across different contexts. Despite its limitations – such as a tendency to mask low extremes in mixed pixels and sensitivity to soil background (Montandon & Small 2008) – NDVI remains the most widely used metric for monitoring vegetation dynamics due to its simplicity, robustness, and compatibility with global datasets.

3.3.4 NDVI and aerial imagery trends

To understand vegetation trends in our study region we calculated the mean NDVI for each site considering only the growing season from June to September between 1984 and 2022.

Each script used for GEE included a feature collection that extracts data from each site on a specific date, a function that calculates the mean NDVI and a mask function that excludes all classified 'Cloud', 'Cloud Shadow', 'Dilated Clouds' and 'Cirrus' pixels from the provided '*QA_Pixel*' band. NDVI values <0 were excluded. Datapoints that had values <0.3 NDVI were manually checked to account for scenes that were not filtered by the cloud mask. 668 datapoints were retrieved from 492 Landsat scenes. Over 90 points were excluded due to cloud coverage or georeferencing issues found in L5 data.

3.3.5 Multispectral UAV data collection

A UAV survey with a multispectral camera was conducted across the study area, in the later part of the growing season (23 Aug – 2 Sept 2021) (Table 3). A DJI Phantom 4 with built-in multispectral sensor (P4m) quadcopter was used, which is equipped with six imaging 1/2.9” CMOS sensors, including five monochrome bands Blue (B) (450 nm ± 16 nm); Green (G) (560 nm ± 16 nm); Red (R) (650 nm ± 16 nm); Red-edge (RE) (730 nm ± 16 nm); Near-infrared (NIR) (840 nm ± 26 nm) and one RGB sensor. The sensors have a global shutter and 2.08 MP (1600 × 1300) resolution, a field of view of 62.7° and a focal length of 5.74 mm; autofocus was set to ∞ and the aperture to f/2.2. The P4m camera generated

results comparable to the widely applied Parrot Sequoia+ camera. Flight planning and execution followed the recommendations of the HiLDEN drone network protocol (Assmann et al. 2019). A reflectance target (Mapir Inc., San Diego) was imaged before, during and after the survey for radiometric calibration. The image that best represented the average light conditions during the survey for each site, was used for radiometric correction when generating orthomosaics in Pix4D. GCPs were used to georeference the orthomosaic of each site. Six to eight ground control points (GCPs) were selected prior to the flight and geolocated with a Spectra Precision ProMark 120 GPS system (Spectra Geospatial, Westminster CO) (Table 4). The mean geolocation error for each GCP in horizontal and vertical directions was about HMRS/VMRS = ~0.5 m.

Table 3 Name, centroid location of the surveyed sites and date of acquisition for utilised remote sensing imagery for direct comparison with the UAV acquired data.

Platform			**UAV**	**PlanetScope**	**Sentinel-2**	**Landsat-8**
Site	Lat	Lon	Date			
Gs1	66.140	-15.495	23/08/21	01/09/21	01/09/21	08/08/21
Gs2	66.141	-15.502	23/08/21	01/09/21	01/09/21	08/08/21
Gs3	66.137	-15.498	23/08/21	01/09/21	01/09/21	08/08/21
Gs4	66.138	-15.504	25/08/21	01/09/21	01/09/21	08/08/21
Reveg	66.175	-15.512	30/08/21	01/09/21	01/09/21	08/08/21
Sval1	66.215	-15.631	30/08/21	01/09/21	01/09/21	08/08/21
Sval3	66.173	-15.727	31/08/21	01/09/21	01/09/21	08/08/21
Sval6	66.154	-15.758	31/08/21	01/09/21	01/09/21	08/08/21
Sval7	66.144	-15.780	01/09/21	01/09/21	01/09/21	08/08/21
Sval8	66.137	-15.781	01/09/21	01/09/21	01/09/21	08/08/21
Sval9	66.113	-15.768	25/08/21	01/09/21	01/09/21	08/08/21
As	66.030	-16.393	02/09/21	01/09/21	01/09/21	31/08/21

The survey was flown along parallel flight and at an above ground altitude of 70 m, resulting in an average ground sampling distance of ~4 cm (Table 4). Images were acquired with 80% front and side overlap and within 2 hours of solar noon. Site Gs4 was surveyed in the morning due to time constraints, resulting in considerable shading effects from thúfurs. However, these shadows did not affect the NDVI values as the calculation involves a ratio, which inherently normalises such variations. Survey details and weather conditions during each flight were recorded (Table 4) (UAV survey details in Appendix).

Table 4 Flight protocol and weather conditions for UAV survey in Iceland 2021.

Flight-ID	Altitude [m]	Start	End	GCP	Cloud conditions
Gs1,2	70	12:19	13:51	6	Scattered stratus & cumulus cover - sun partly obscured
Gs3	70	13:53	14:36	8	Stratus - sun obscured
Gs4	70	08:23	09:06	8	Clear sky to haze
Sval9	70	14:20	15:05	6	Haze
Sval1	70	11:03	11:52	6	Cumulus - sun obscured
Reveg	70	14:11	15:26	7	Cumulus - over most sky (alternating with sun)
Sval3	70	10:55	11:55	6	Thin cirrus - sun not obscured
Sval6	70	14:37	15:12	8	Thin cirrus - sun obscured (alternating with sun)
Sval8	70	11:35	12:18	7	Haze
Sval7	70	14:30	15:15	6	Haze
As	70	11:26	12:25	7	Thin cirrus - sun obscured, later half stratus cover

The UAV data were processed in Pix4D Mapper (Pix4D SA, Switzerland). Photogrammetric procedures were applied along with georeferencing based on the GCPs and radiometric calibration based on photographs of the calibration targets. The processed output comprised a digital surface model (DSM) from Structure from Motion protocols and orthomosaics for each individual band. Furthermore, the NDVI was calculated as the normalised difference between the NIR and red band (equation 1).

(1) $$\boldsymbol{NDVI = \frac{NIR - Red}{NIR + Red}}$$

3.3.6 Land cover classification and landscape characteristics

The aim of the land cover classification is to distinguish the following land cover categories: barren, mixed low-stature vegetation (including moss, lichen, graminoid, forbs, low-stature shrubs) and medium-stature shrub (namely *Betula nana* or dwarf birch). These classes were chosen to investigate the impact of the dwarf birch, a characteristic shrub of the Arctic tundra, on the overall spectral mix of the landscape, as this species has a high NDVI due to its thick canopy and spectral characteristics compared to other vegetation and spreads extensively. An advantage is that the dwarf birch is easily distinguishable in UAV imagery from other vegetation due to its growth form.

A ground vegetation survey was carried out in June 2022 to collect point coordinates of land cover types for supervised classification. The survey was conducted at the sites Gs1

and Gs3, for their representativeness and accessibility using a Spectra Precision ProMark 120 GPS system. A judgmental sampling method was applied, wherein land cover were selected based on expertise and judgment, aiming for a representative sampling and spatially equal distribution. Point coordinates of the following land cover classes were collected: barren cover, mixed low-stature vegetation (bog bilberry and crowberry), graminoids, forbs, moss, lichen, and medium-stature shrub (dwarf birch). 73 Ls-Veg, 51 Ms-Shrub and 36 Barren data points were collected (160 in total within an area of 15 ha).

To increase the amount of training samples to train the classification model, the identified land cover from the high-resolution orthomosaic were then used to create training and validation datasets for the classification. As the land cover types were consistent and readily distinguishable across the two ground surveyed sites, we were able to manually select the training data for the other sites from the very-high-resolution, orthomosaics from the UAV data. The relatively simple configuration of the landscape - i.e. three distinct and qualitatively different types of land cover - meant that our simplified classification system worked well for our sites (Krenz et al. 2019). The sampled land cover data was split into 70% training and 30% validation data.

The following workflow was applied for the classification (Fig. 19):

All processed orthomosaics were clipped to 300 × 300 m, resampled to 5 cm spatial resolution using bilinear interpolation, and merged into one file. Bilinear interpolation is a resampling method that uses the distance-weighted average of the four nearest pixel values to estimate a new pixel value (Campbell 2011). We applied the Random Forest (RF) algorithm (Belgiu & Drăguţ 2016) and trained an individual model using the multi-spectral bands (B, G, R, RE, NIR), the NDVI and the DSM for each of the 12 sites. While other classification algorithms, such as Support Vector Machines (SVM) and k-Nearest Neighbors (k-NN), were considered, RF was selected for its proven robustness, ability to handle high-dimensional data, effectiveness in managing non-linear relationships, and superior classification accuracy demonstrated in comparative testing.

The Orfeo ToolBox (OTB) was used in QGIS (3.22) for the classification workflow. Image statistics were computed and included in the model. Training and validation data for each individual class and site was created based on the ground land cover survey and visual interpretation of the very-high-resolution UAV imagery. The maximum tree depth was set to 5, the minimum number of samples per node to 10, and the maximum number of trees

to 100. Additionally, the clustering of possible values for the categorical variable into K clusters was set to 10.

Afterwards, the *ImageClassifier* was applied using the trained RF model, image statistics and processed layers for each site. Subsequently for accuracy assessment, a Confusion Matrix was computed with the validation data and the F-score and Kappa were calculated for each site (Table 2). Both are established metrics in classification assessment, the F-score, a measure that balances precision and recall, often used to evaluate the performance of binary classification models. Kappa, or Cohen's Kappa, is a statistic that measures inter-rater reliability for categorical items, comparing the observed agreement with the expected agreement by chance (Campbell 2011). Finally, a majority filter with a 5 × 5 kernel was applied (using SAGA 7.8.2) to minimise scattered misclassified individual pixels. These datasets were the basis for the following analysis.

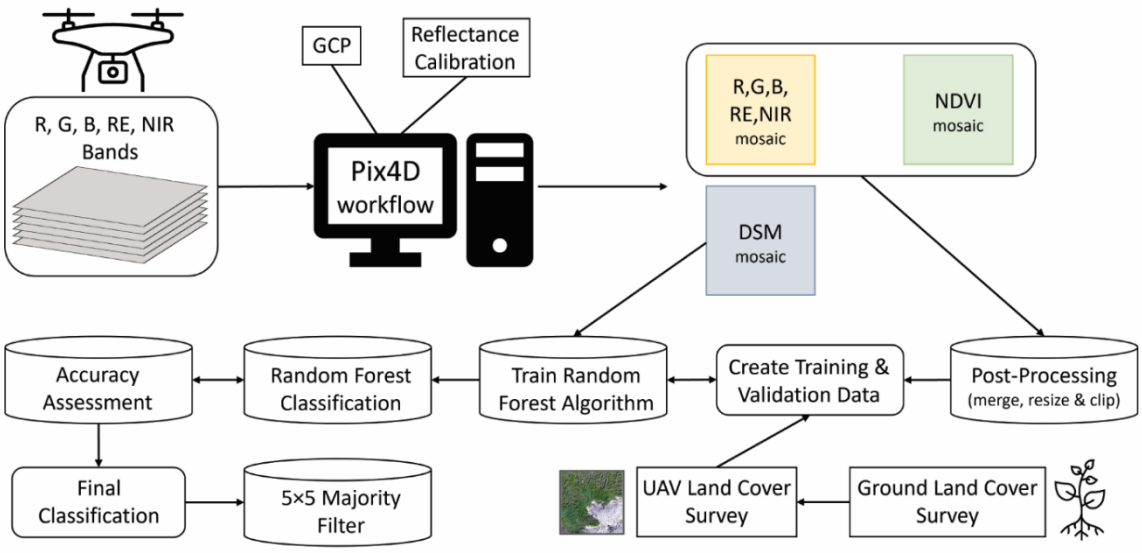

Fig. 19 Workflow for processing and classification of UAV imagery.

The probability density function (PDF) was calculated to estimate the distributions of bare or shrub patch sizes collected from all sites, providing insight into the landscape structure (Moreno-de Las Heras et al. 2011). The PDF gives the probability that a patch has a given area, P (Patch = a). The patch area for each class was calculated using *landscapemetrics* (Hesselbarth et al. 2019) package (1.5.7) in R. Patches were defined that were connected within the eight-neighbor rule. For the PDF, regular bins were created from log-transformed data, with a bandwidth of 0.15. Using log-transformed data has been shown

to reduce noise occurring at the tail of the curve and underestimating small values with high frequencies (White et al. 2008).

3.3.7 NDVI and land cover assessment across sensor scales

To assess the land cover composition for a NDVI value, we compared NDVI pixels for each satellite with the underlying land cover classified from the UAV.

NDVI raster derived from satellites were clipped to the size of the study sites and vectorised so that each pixel is labelled and represents a polygon with the NDVI value. Zonal statistics were then calculated for each polygon (representing a NDVI pixel) and the land cover composition within.

3.3.8 Determination of mixed pixels and the best suitable scale

To compare how different remote sensing datasets capture the landscape we plotted NDVI histograms and visually compared the different remote sensing products for site Sval3. The site was chosen because it has a moderate amount of barren land with patches of different sizes evenly distributed across the landscape.

Each environment has an inherent structure consisting of functional land cover types. These vary in shape, size and position in the landscape. To be able to accurately monitor changes in land cover types, a suitable spatial scale is necessary.

To assess the right spatial scale for our degraded tundra environment, we calculated the Shannon evenness index (SHEI) (Vajda 1950). SHEI is a diversity metric used in ecology to assess composition and richness in an area (Gergel & Turner 2017). The function calculates the amount of different land cover types (m) in an area and their relative abundances (P_i). It is calculated by dividing the Shannon diversity index (SHDI) by its maximum (ln (m)) (equation 2). The output ranges between 0 and 1. In our example, 0 means only one land cover class is present in a pixel and 1 indicates that all land cover classes are present at the same proportional abundance within a pixel.

SHEI can be calculated as:

(2) $$\boldsymbol{SHEI} = \frac{\boldsymbol{SHDI}}{\boldsymbol{max(SHDI)}} = \frac{\sum_{\boldsymbol{i=1}}^{\boldsymbol{m}} (\boldsymbol{P_i} * \boldsymbol{\ln}\,(\boldsymbol{P_i}))}{\boldsymbol{ln(m)}}$$

The SHEI was calculated for different grid sizes corresponding to different remote sensing spatial resolutions of (0.5, 1, 3, 5, 10, 20, 30, 100, 150 meter). An empty grid was created with the extent of the studied site and specific spatial resolutions. The SHEI was calculated for each grid cell fully within the area of land cover classification. The mean of all SHEI values for a specific spatial resolution and site was calculated and plotted (Fig. 20).

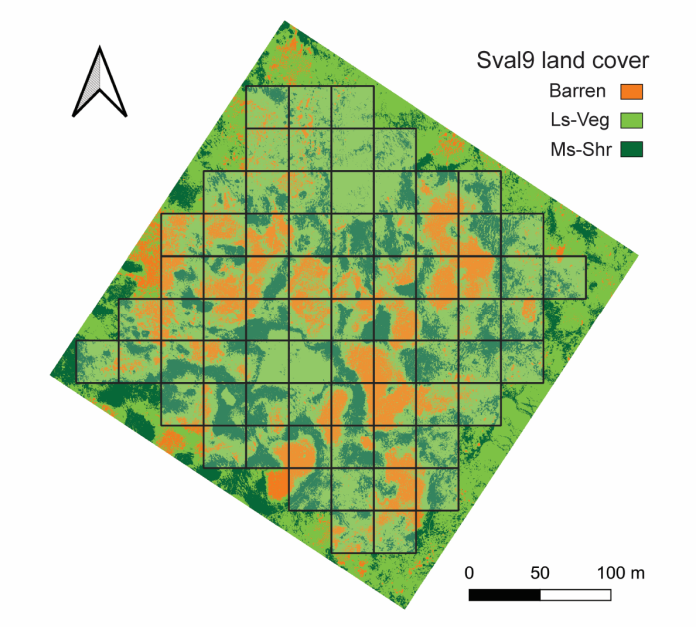

Fig. 20 Example of SHEI calculation at a 30 m grid cell resolution for site Sval9. Only grid cells fully covered by the land cover map were included. The SHEI was calculated for each grid cell, and the mean of all grid values per site was determined.

3.4 Results

3.4.1 NDVI and land cover trends

Analysis of the NDVI time series reveals a greening trend from 1984 until present for most of the sites (Fig. 21). The sites As, Reveg and Sval6,9 show a slight decline since 2017, while Gs1,3 and Sval1,8 show no change since 2017. The Reveg site was artificially treated with fertiliser and seeds from the early 1990s (Sigurður Þór Guðmundsson, pers. com.) and therefore shows a steeper increase in the 1990s and 2000s.

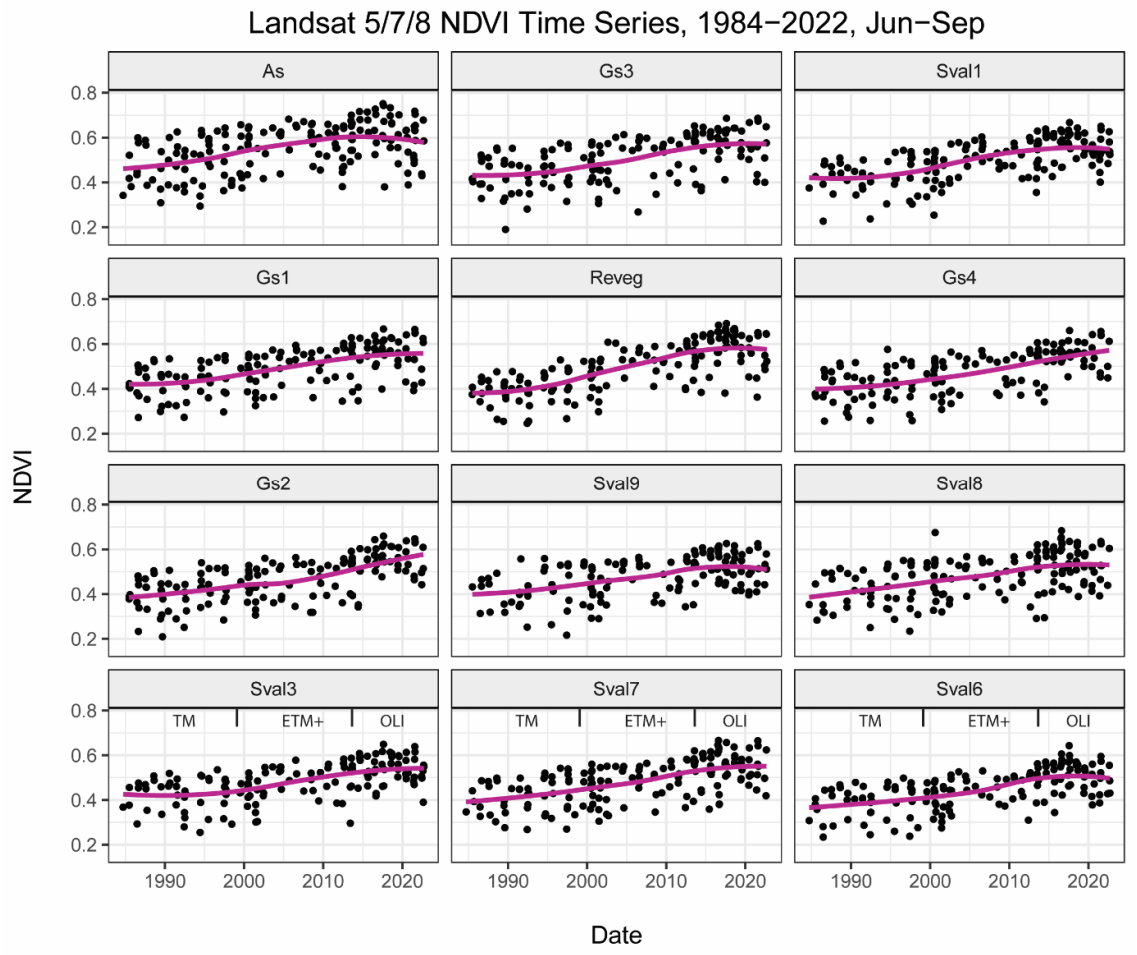

Fig. 21 NDVI time series of all surveyed sites from 1984 until 2022 over the growing season Jun-Sep from Landsat 5/7/8 imagery, ordered from top-left to bottom-right according to increasing barren area. Pixel covered in clouds or shadows were excluded. A steady increasing greening trend is observable. Some sites show a decreasing or lateral trend since 2017. The labels at the bottom of the three lower plots indicate the time periods during which different sensors on Landsat satellites were used: 'TM' for Landsat 5, 'ETM+' for Landsat 7, and 'OLI' for Landsat 8. This delineation is consistent across all plotted sites.

To get a qualitative perspective on long-term land cover changes at our sites, we compared multiple greyscale aerial photographs downloaded from Land Surveying Service in Iceland (lmi.is) (Table A3 in Appendix) with recent UAV imagery. The images cover the study area in July 1980, with an image resolution of ~0.73 m per pixel. To illustrate the changes in land cover in the study region, an example area was selected at Sval3, for visual comparison. The historical aerial photo was manually co-registered, using six GCPs and a 2nd order polynomial transformation to the UAV image.

At several locations in Sval3 it can be observed that previously vegetated areas have turned into barren land (Fig. 22, yellow arrow). Further expansion of shrub cover is also visible, though more difficult to distinguish (red arrow). Densification of vegetation cover

and secondary regrowth of eroded patches could also contribute to a greening trend, but this is not visible in the comparison.

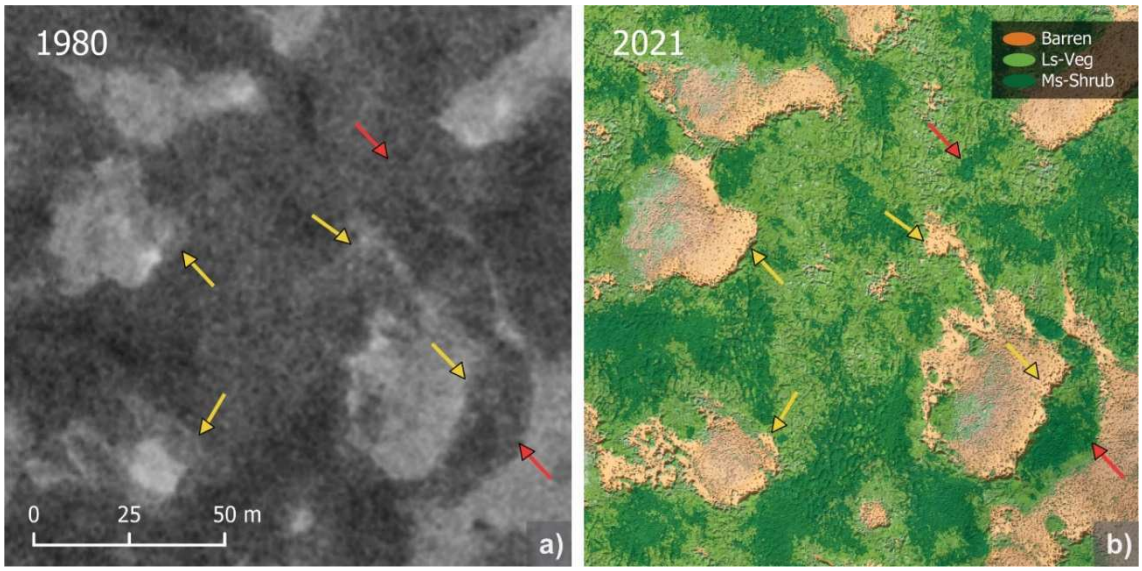

Fig. 22 Comparison of site Sval3 of a) a monochrome aerial photograph (taken in July 1980) with (b) RGB UAV imagery (taken in August 2021) overlaid with a classified land cover map. In panel a) the dark shaded areas represent shrub cover, grey represents vegetation cover and light grey barren areas. Visible changes in texture and tone likely caused by soil erosion is indicated by yellow arrows; red arrows indicate shrub expansion. The arrows are at the same location in both images.

3.4.2 Land cover classification and landscape characteristics

Overall, the RF classification showed good accuracies with kappa values >0.8 (Table 2). An example of a classified site (Sval3) is shown with the corresponding RGB image (Fig. 23). The F-score for the low-stature vegetated class returned the lowest values among the classes with average values around 0.84. The highest F-score at Sval8 and Sval9 was derived from a boggy area where extensive, uniform graminoid cover was classified easily by the model (Table 2). Lower F-values resulted from homogeneous vegetation cover which was harder to classify.

Due to the late stage of the growing season during the UAV survey, the leaves of some shrubs had turned yellow, mainly observed on a few shrubs in site As, which resulted in some misclassification. Shading effects were mainly caused by thúfurs; this also caused some misclassifications where non-shrubby vegetation was assigned to the shrub class. The shrub class showed high accuracies. This is attributed to the contrast between the shrubs and surrounding vegetation, in terms of stature and texture. The relatively high NDVI values of the low-growing deciduous shrub bog bilberry and graminoids, resulted in

some minor misclassification as the shrub class. The barren class achieved highest scores (Table 2), attributed to the comparatively strong correlation to NDVI and NIR.

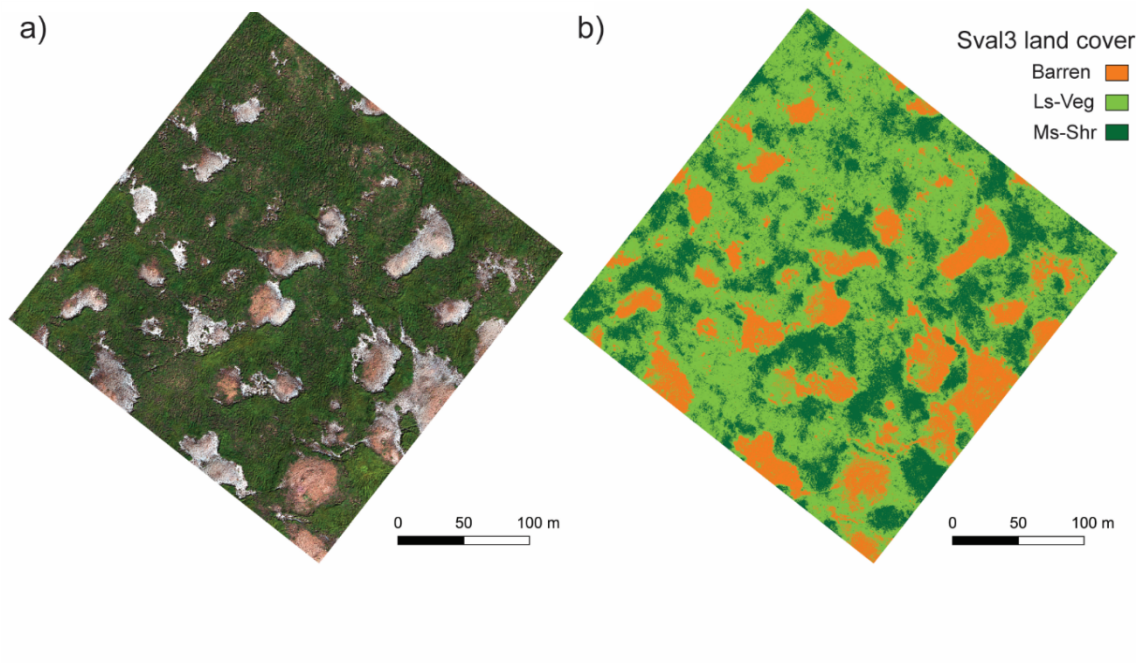

Fig. 23 Site Sval3 a) UAV RGB image b) classified land cover. North is up the page.

Table 5 Results of the percentage of land cover classification for Barren, Low-stature Vegetation (Ls-Veg) and Medium-stature Shrub (Ms-shrub) classes, and the accuracy of classification.

Percentage land cover and classification precision							
Site	**Barren %**	**F-score**	**Ls-Veg %**	**F-score**	**Ms-Shrub %**	**F-score**	**Kappa**
As	1	0.97	53	0.78	45	0.96	0.82
Gs3	4	0.96	63	0.84	33	0.87	0.83
Sval1	6	0.96	68	0.83	25	0.90	0.85
Gs1	11	0.99	57	0.87	32	0.92	0.87
Reveg	12	0.96	50	0.92	37	0.91	0.89
Gs4	14	0.96	55	0.90	31	0.94	0.89
Gs2	16	0.98	53	0.88	31	0.95	0.90
Sval9	16	0.98	60	0.96	24	0.95	0.95
Sval8	17	0.96	56	0.96	27	0.95	0.94
Sval3	18	0.99	58	0.91	24	0.92	0.90
Sval7	19	0.99	47	0.92	34	0.96	0.92
Sval6	30	0.98	43	0.88	27	0.92	0.90
Mean	14	0.97	55	0.89	31	0.93	0.89

The sizes of barren and shrub patches varied greatly among the sites ranging from 0.0025 m^2 (pixel resolution) to 7045 m^2 for barren patches (with the largest one found in the most eroded site, Sval6), and 0.0025 m^2 to 18,864 m^2 for shrub patches (the largest of which were found in the least eroded site, As). In contrast, at the sites As and Gs3 the largest barren patches reached only up to 370 m^2 and 379 m^2, respectively, and the largest shrub patch in Sval1 was 824 m^2 (Table 3).

The PDF for low eroded (<=6%) and high eroded (>10%) sites followed different distribution patterns. In contrast, the PDFs for the shrub class had similar distribution patterns across all sites (Fig. 24). The patch size analysis demonstrated that a significant majority of barren and shrub patches falls below the detectability threshold for most satellite platforms (as indicated by the dashed lines in Fig. 24). Specifically, 83% of the shrub patches and 78% of the eroded patches were below the 0.5 m threshold. At 3 m spatial resolution, around 2% of barren and shrub patches were the same size or larger than the pixel size, while with 10 m spatial resolution, only 0.3%. At 30 m resolution, 0.2% in high eroded areas and 0.025% in low eroded areas and 0.06% for shrubs were higher than the pixel size.

The PDF of barren and shrub patches show an upward trend from the smallest patch size (one pixel 0.0025 m^2) to a peak size of about 0.1 m^2 for shrub patches and 0.04 m^2 for

barren patches. It should be noted that the majority filter reduced the number of the smallest patch sizes, which explains the initial upward trend. Beyond these sizes, the probability decreases with increasing patch size until 100 m^2, at which point the distribution patterns of low eroded and high eroded areas begin to diverge. Low eroded areas experience a further decline in patch probability, while high eroded areas maintain a consistent probability up to a size of 1000 m^2, followed by a decline. Shrub patches exhibit a smooth decreasing trend, with patch sizes in the upper range exceeding 10,000 m^2 (Fig. 24).

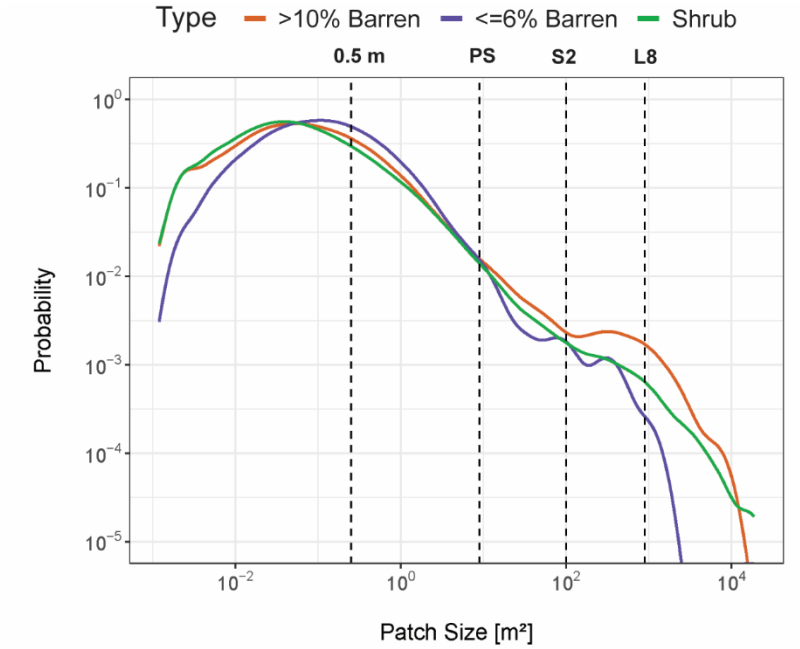

Fig. 24 Probability density function for patch sizes. Dashed lines show the spatial resolution for 0.5 m pixel, PlanetScope (PS), Sentinel-2 (S2) and Landsat (LS).

3.4.3 Variations in NDVI across sensor scales

The mean NDVI values are similar for UAV, PS, S2 and L8 platforms to a certain extent (Table 6). However, PS showed consistently higher values between 0.3-0.9 NDVI compared to UAV. S2 mostly matched or slightly exceeded the UAV values of 0.2-0.3 NDVI. L8 data exhibited higher values of 0.5-1.0 NDVI, with the exception of site As, which can be explained by the scene acquisition earlier in the growing season (Table 3).

Mean NDVI values of each site do not always correlate well with proportions of land cover. This can be seen by comparing Sval1 (0.64 NDVI, Barren 6%, Ms-Shrub 25%), Gs2 (0.64 NDVI, Barren 16%, Ms-Shrub 31%) and Sval7 (0.66 NDVI, Barren 19%, Ms-Shrub 34%). For

these three sites, mean NDVI value was essentially the same, whilst the relative proportion of barren and shrub cover varied. However, shrub cover didn't always correlate exactly with NDVI as seen on Sval3 (0.66 NDVI, Barren 18%, Ms-Shrub 24%) and Sval7 (0.66 NDVI, Barren 19%, Ms-Shrub 34%).

Table 6 Mean NDVI values for each site and remote sensing dataset. Additionally, the total Barren and Medium-stature Shrub (Ms-Shrub) area, the largest and mean Barren and Ms-Shrub patch size is shown.

	As	Gs3	Sval1	Gs1	Reveg	Gs4	Gs2	Sval9	Sval8	Sval3	Sval7	Sval6
UAV	0.74	0.7	0.64	0.67	0.68	0.68	0.64	0.63	0.66	0.66	0.66	0.57
PS	0.83	0.78	0.73	0.75	0.72	0.73	0.73	0.68	0.7	0.7	0.69	0.63
S2	0.77	0.73	0.68	0.7	0.69	0.69	0.68	0.66	0.68	0.66	0.69	0.61
L8	0.74	0.78	0.73	0.75	0.73	0.74	0.74	0.70	0.72	0.71	0.74	0.67
Total Barren %	1	4	6	11	12	14	16	16	17	18	19	30
Total Ms-Shrub %	45	33	25	32	37	31	31	24	27	24	34	27
Barren max patch size [m^2]	370	379	1005	2133	3521	1884	2568	1748	6886	2303	2465	7045
Barren mean patch size [m^2]	0.43	0.91	0.68	1.55	1.52	2.48	2.2	1.5	2.72	3.68	2.38	3.14
Ms-Shrub max patch size [m^2]	18,864	1742	824	2014	7619	6057	3538	3730	14,650	1480	6063	2867
Ms-Shrub mean patch size [m^2]	1.79	1.02	0.6	1.17	1.93	1.43	1.68	1.32	1.83	1.09	1.89	1.13

The NDVI map comparison illustrates how different remote sensing (RS) products resolve a fragmented and eroded landscape (Fig. 25a). The patchiness and distribution of the barren areas are clearly visible in the UAV image. With increasing scale, the smaller patches become less apparent, although they are still visible to certain extent at PS resolution, which shows low contrast between barren and vegetated areas. Larger patches are still visible in the S2 scene, although the edges of the barren patches are blended with the vegetation cover. In the L8 scene, only large barren patches are evident in the lower part. The rest of the barren patches in the centre of the area are not visible.

The UAV NDVI histogram exhibited a wide range of 0.92 and a bimodal distribution, which is not reflected in the satellite data (Fig. 25b). NDVI values from S2 showed the highest dynamic range - 0.58 - compared to PS and L8 that had a similar narrow range of approximately 0.4, despite the large difference in spatial resolution. While PS and L8

showed similar maximum NDVI values to S2, the NDVI lower values were not represented (Fig. 25b).

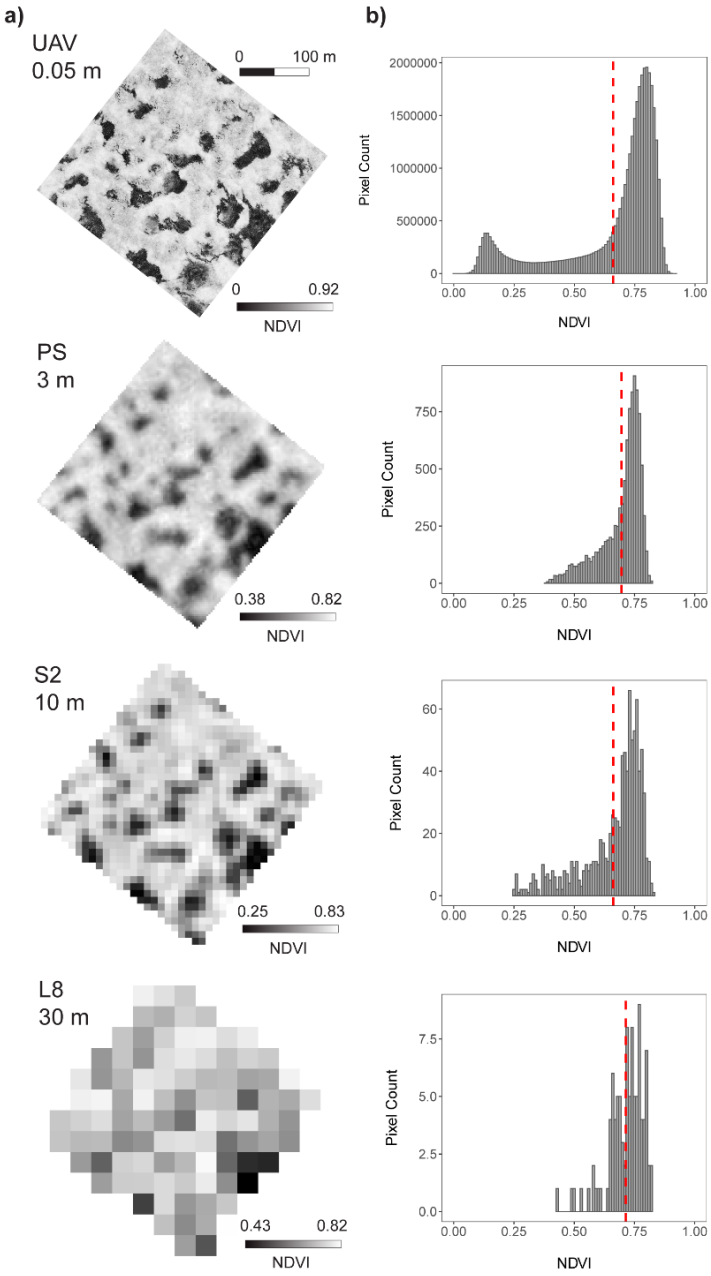

Fig. 25 a) NDVI landscape and b) histogram comparison between different remote sensing datasets from site Sval3. The red dashed vertical line indicates the mean NDVI. North is up the page.

3.4.4 Correspondence between land cover and NDVI

All RS products displayed a similar pattern of correspondence of NDVI values to percentage of land cover (PLC), although they differed significantly in their dispersion (Fig. 26, 26, 27).

The NDVI to land cover distribution is explained in more detail for S2, as it correlated best between PLC and NDVI, had the highest dynamic range and a sufficient number of pixels (Fig. 26). NDVI values of fully barren pixels ranged from 0.15 to 0.38, LS-Veg ranged from 0.6 to 0.72, and Ms-Shrub ranged from 0.8 to 0.86 (Fig. 26a, b, c). As the barren cover decreased, the NDVI gradually increased until it reached 0.6, representing the absence of barren cover (Fig. 26a). The plot for the Ls-Veg class showed a peak at the centre of the NDVI spectrum (Fig. 26b). Before and beyond this range, there was a sharp drop in vegetated coverage, suggesting an increase in PLC of Barren cover and Ms-Shrub. No Ms-Shrub cover was observed up to an NDVI of 0.4, after which there was a slight increase in PLC up to 0.68 (Fig. 26c). Thereafter, the PLC increased sharply until it reached its maximum extent.

It is noteworthy, that due to the wide vertical dispersion, a value of 0.6 NDVI could represent 0% or up to 62% barren cover in Fig. 26d, three sample pixels are shown that have the same NDVI with very different land cover compositions. Vertical dispersion is highest for the Ls-Veg class at 0.66 and Ms-Shrub at 0.76. Large variability at this range for the Ls-Veg is influenced by varying degrees of Barren and Ms-Shrub cover. The large dispersion of Ms-Shrub could be related to plants that were misclassified from the Ls-Veg class with different NDVI values.

Horizontal dispersion varied across the classes and was highest for the Ls-Veg class at 50% PLC ranging from 0.4-0.8 NDVI. This was expected as various plants with different spectral reflectance characteristics were included in the class. The dispersion for the Barren class at 50% PLC was 0.4-0.63 NDVI, while for the Ms-Shrub class, was the lowest, ranging between 0.7-0.8 NDVI.

L8 plot showed very similar pattern to S2, but they did not include NDVI values <0.3 (Fig. 27). This is likely influenced by the insufficient amount of pure Barren cover pixels. The PS also didn't show any NDVI value <0.35 and had large vertical dispersion at 0.6 NDVI for Barren and Ls-Veg class and at 0.75 for Ls-Veg and Ms-Shrub class (Fig. 28).

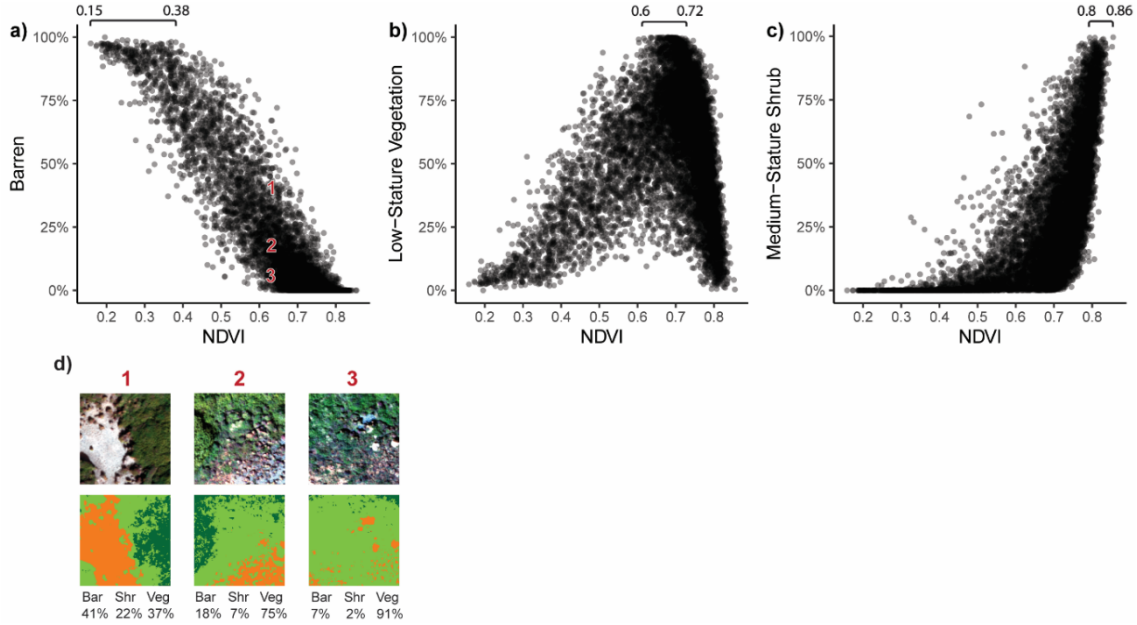

Fig. 26 Representation of Sentinel-2 (S2) NDVI pixels and corresponding percentage of land cover (PLC) classified from UAV. Each datapoint represents a S2 pixel plotted from all sites. The lines above show the NDVI range for fully covered pixels per land cover. a) For Barren, b) Ls-Veg and c) Ms-Shrub cover. d) Upper panel RGB image, lower panel land cover classification, for three selected pixels of edge length 10 m with NDVI value of 0.61. The sample pixels illustrate a large variability in land cover composition for a specific NDVI value. The pixels are highlighted in the Barren graph a).

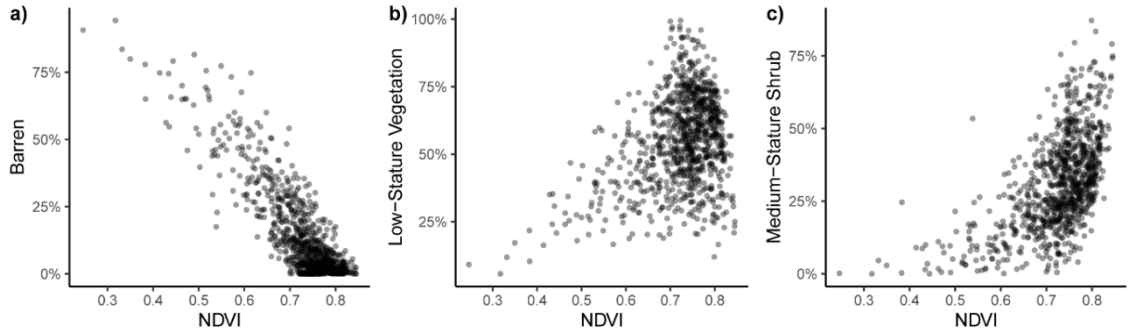

Fig. 27 Representation of L8 NDVI pixel and corresponding PLC classified from UAV. Each datapoint represents a L8 pixel plotted from all sites. a) For Barren, b) Ls-Veg and c) Ms-shrub cover

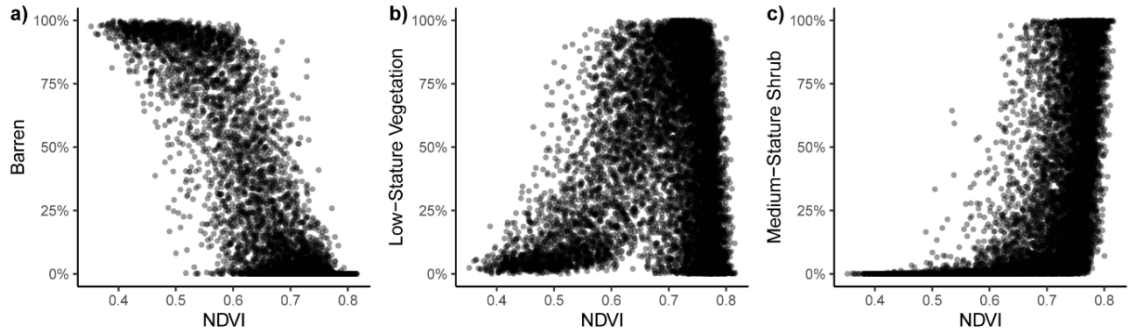

Fig. 28 Representation of PS NDVI pixel and corresponding PLC classified from UAV. Each datapoint represents a PS pixel plotted from site Sval7 a) For Barren, b) Ls-Veg and c) Ms-shrub cover.

3.4.5 Correspondence between sensor grain-size and land cover

The mean SHEI landscape metric showed a rapid increase up to 3 m and a slow increase at larger spatial resolutions (dashed line in Fig. 29). The mean reached the vertical asymptote at 0.5 m, with the lowest mean SHEI score 0.34. Sites with low and high amounts of barren cover differed in their pattern.

The moderately to highly barren sites from Gs1 onwards followed a similar pattern with SHEI continuously increasing with spatial resolution. At a scale up to 3 m, the SHEI increased sharply to 0.6 and then rose moderately up to 50 m with values >0.8. Subsequently the SHEI is increased slowly, reaching a horizontal asymptote at 100 m.

The values for sites with low barren cover rose sharply from 0.5 m, eventually peaking at 3 m with 0.65-0.7 SHEI for Gs1, Sval1 and Gs3. Values for site As continued to increase up to 20 m reaching 0.8. Thereafter, the sites levelled off at 50 m at 0.7 SHEI (Table A4 in Appendix).

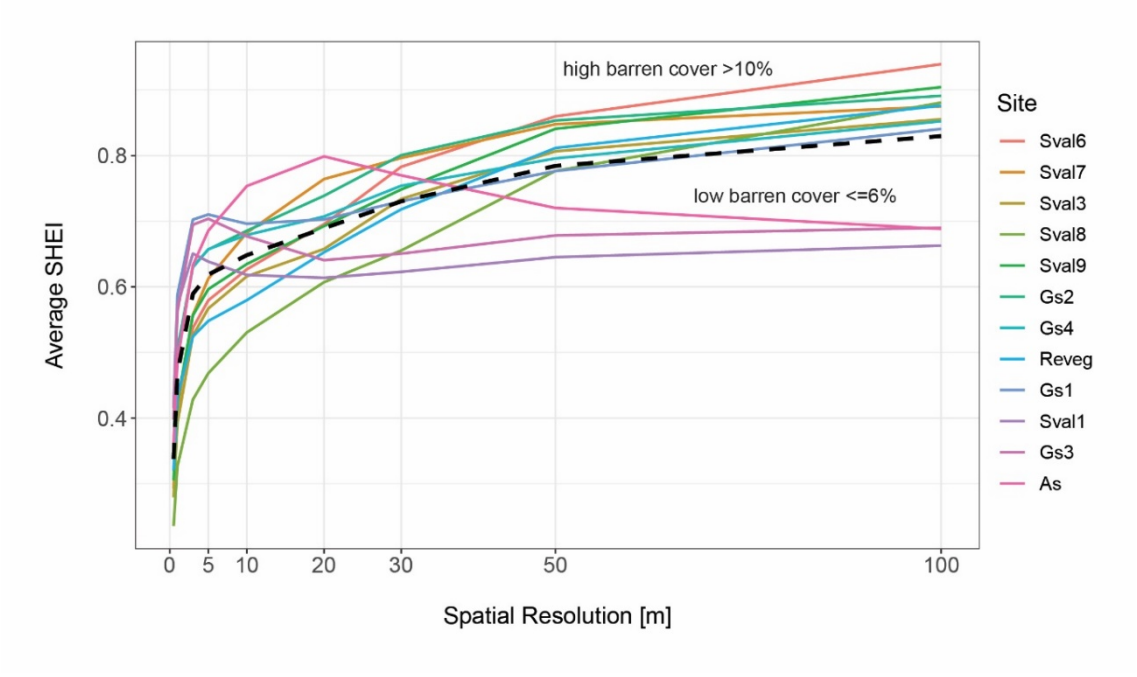

Fig. 29 Graph showing SHEI for different sites and spatial scales. The sites in the legend are sorted by decreasing barren cover. The black dashed line is the mean of all sites.

3.5 Discussion

We set out to 1) explore the biases occurring from satellite monitoring in degraded Arctic landscapes and 2) determine which spatial resolution is most useful in evaluating

vegetation cover and landscape health in fragmented tundra landscapes. We found that Arctic greening likely associated with shrubification can lead to spectral confusion, which can obscure soil erosion processes and confirmed the importance of considering multiple spatial scales when monitoring land condition in Iceland. GróLind, Iceland's first long-term vegetation and soil monitoring program, was initiated in 2017 and uses satellite imagery, UAVs, and on-site analyses to estimate land condition and predict areas at risk (Arnalds et al. 2023; Marteinsdóttir et al. 2021). Our findings should give confidence that the use of 10 m resolution S2 data will result in a sufficient accurate indication of land condition resolving larger erosion spots (although <=3 m resolution would be better), but suggests that the use of coarser resolution products may be problematic due to the difficulties of mixed spectral signatures and the potential for masking increases in barren cover. Additionally, the S2 data have suitable temporal and spatial coverage, advantages over the sub 3 m products.

3.5.1 NDVI time series

The mean NDVI has increased on our study sites over the last four decades (Fig. 21). This trend was validated using MODIS data, which corroborated the NDVI increases observed in Landsat data over the same period and area. Such a greening trend could indicate an amelioration of the environment, an increase in vegetation productivity, or shifts in vegetation structure and composition or an increase in vegetation cover and a decrease in barren land. There has been an overall greening of tundra vegetation across the circumpolar Arctic in the last four decades and a direct link between warming air temperatures and vegetation greening has been reported (Myers-Smith et al. 2011; IPCC 2019; Raynolds et al. 2013; Bhatt et al. 2010).

However, the comparison of aerial images from 1980 and a recent UAV image (Fig. 22) reveals that soil erosion continued on our study sites, which was evident on all study plots when comparing aerial photographs, i.e. vegetation cover was lost across the region in that time period.

If the increase in NDVI we observed was not due to increased vegetated area, it must have been caused by changes in vegetation productivity, structure or composition. Studies have demonstrated correlations among greenness in the Arctic with air temperature and aboveground biomass (Xu et al. 2013; Ju & Masek 2016; Bhatt et al. 2017), and prolonged

growing seasons that are shifting plant phenology (Post et al. 2018; Oberbauer et al. 2013).

On our sites, the NDVI values of the shrub class were found to be higher than those of the surrounding vegetation (Fig. 26). Combined with our observations indicating shrub growth (Fig. 22), with other studies demonstrating that shrub growth in the Arctic tundra was closely linked to spectral greening (Pattison et al. 2015; Fraser et al. 2014; Forbes et al. 2010), leads us to conclude that the increasing NDVI trend at our sites was mainly driven by the expansion of shrub patches, although other contributing factors cannot be excluded and are likely of lesser significance.

This time series has a low spatial resolution (size of study sites, 300 × 300 m), encompassing various erosion patches and vegetation cover across the entire study site. It underscores the significance of pixel resolution relative to the patch size, revealing that when pixel resolution is larger than the studied patch dimensions, the spectral confusion of distinct land covers, for example erosion and shrub patches, hinders the detection of land cover changes. This confusion arises as multiple concurrent trends either counteract one another, or a dominant trend (shrubification) obscures a weaker signal (soil erosion).

3.5.2 Land cover and NDVI correspondence

Overall, the NDVI values for Barren, Ls-Veg, and Ms-Shrub cover were similar across the L8, S2, and PS datasets. However, significant differences were observed in the distribution of PLC vs NDVI values, as dynamic range (Fig. 25,Fig. 26, Table 6) and in minor variations in the mean NDVI values.

Surprisingly, the percentage of land cover classified as barren exhibited a higher degree of dispersion (Fig. 26a) than expected, considering the distinct spectral differences in NDVI between vegetated and non-vegetated surfaces. This could be related to the broader definition of barren land, which could have included some remnant vegetation or different stages of soil deflation in barren land types (darker and brighter appearance), leading to some variability in that class (Fig. 18e, f). However, the variance in NDVI remained relatively consistent across the full range of Barren PLC, likely because the variability due to the mixed land cover will be similar across different PLC values.

The satellite platforms returned very wide range of values for the Ls-Veg class (Fig. 26b, Fig. 27b, Fig. 28b). This is because this class encompasses many different plant types -

including low-growing, deciduous and evergreen shrubs, graminoids, forbs and mosses - each with their own distinct spectral characteristics. Sub-dividing this class might help to reduce variance in future analyses. However, this would be challenging in Iceland because the vegetation cover displays high alpha (plot-level) diversity but low beta (between-plot) diversity. In other words, a diversity of plant species at a fine spatial scale combines to form homogeneous vegetation at a landscape scale.

The dynamic range provides an indication of how much information is retained and differs significantly among the RS products. PS and L8 had a low dynamic range, mainly missing the lower NDVI values (Fig. 25b) compared to S2, leading to lower contrasting imagery which limits its use for accurate classification of land cover and deriving biophysical parameters. No satellite image was able to detect the bimodal distribution visible in the UAV histogram (Fig. 25b), due to pure pixels representing Barren only at smaller pixel size.

We observed high dispersion of NDVI vs PLC, which was strongest for PS. For regional scale (10s km^2) studies this dispersion can average out, however for landscape scale (100s m^2) studies with coarser resolutions this dispersion could skew interpretation of the data. This is particularly notable in the L8 data (Fig. 27a), where we observed up to a 60% variation in the percentage of Barren cover between pixels that had similar NDVI values (0.54–0.55). This indicates that even small differences in NDVI within this range can correspond to substantial variability in Barren land cover, complicating data interpretation at finer scales.

The mean NDVI values varied slightly across the RS datasets, with S2 resembling the UAV values most closely (Table 6). Various factors, such as band-pass differences among sensors (Ke et al. 2015), bidirectional reflectance influenced by viewing angles (Song & Woodcock, 2003), and differences in acquisition dates, could contribute to the observed variations in NDVI values. Slight differences in acquisition dates can have a significant impact in Arctic locations due to the short growing season (Myers-Smith et al. 2020). This explains the consistently higher NDVI values in the L8 data, which are 2-3 weeks earlier and closer to the peak growing season compared to the UAV acquisition, except for site As (2 days difference to UAV acquisition) which had the same value as the UAV. The variability in PS data can be either related to the sensor quality, affected by the varying viewing angles of PS platforms, which varied between 1-5°, or differences in NIR and R spectral ranges (Table 2). Frazier and Hemingway (2021) demonstrated that the

radiometric and geometric quality of PS imagery doesn't match that of traditional systems such as Landsat and Sentinel-2, and it is not always "analysis ready", often requiring additional correction and postprocessing. Hence, Sentinel-2 data can be the better choice even though the spatial resolution is lower.

3.5.3 Mixed pixel and spatial resolution

The second aim of the study was to identify the most appropriate spatial resolutions to study a degraded Icelandic tundra environment. In doing so, we assessed the effectiveness of commonly used remote sensing datasets in detecting geomorphologically relevant land cover categories.

We chose to categorise three functional land cover types and these categories proved effective in our study environment. It's important to note that one of our categories - eroded terrain - has limited extent across the Arctic. While our land cover classification may need adaptation to areas that lack eroded terrain, the analytical approach using SHEI to assess spatial resolution remains the same. The importance of spatial resolution can be illustrated by comparing the mean SHEI metrics calculated for lower eroded areas (barren cover <=6%) and higher eroded areas (barren cover >10% of total). Both types of terrain exhibit sharp rises in SHEI as spatial resolution increased, up to a size of ~3 m (Fig. 29). At larger spatial resolutions, mean SHEI diverged. On lower eroded areas, mean SHEI peaked at spatial resolutions of 3-5 m, declined slightly, then levelled-out; on higher eroded terrain, mean SHEI kept increasing to an asymptote at 100 m spatial resolution, as it captured more and more cover variation.

SHEI is a metric of the diversity of cover within a grid cell. Low SHEI values indicate low diversity, i.e. overwhelming dominance of a single cover type. Hence low values are present at low spatial resolutions, as pure pixels are possible. High SHEI values indicate a variety of cover types with approximately equal proportional coverage. Thus, we expect low SHEI values with small grid cells (the cells can only encompass a single cover type) and increases in SHEI as spatial resolution decreases and increasingly large grid cells encompass multiple, contrasting patches.

On our sites, SHEI increased predictably with spatial resolution for the higher eroded areas. Finer spatial resolutions only detected one land cover type and mean SHEI is low; mean SHEI increased as larger grid cells encompassed both barren and vegetated cover,

until the resolution approximated the size of the largest patches and increasing the grid dimension did not capture any further diversity.

On the less eroded sites, variation within the vegetation cover - particularly the presence of small patches of shrubs - led to a different pattern. Small spatial resolution still resulted in low mean SHEI. But a spatial resolution around 3 m was able to encompass small patches of shrubs and barren terrain, leading to a peak in mean SHEI at these scales. As spatial resolution decreased, the cells became dominated by non-shrubby vegetation and mean SHEI decreased.

Our study demonstrates the limitations of coarse resolution datasets for studying complex ecological-geomorphology processes such as soil erosion at a landscape scale. The Landsat data (30 m resolution) proved inadequate for detecting small-scale vegetation changes (shrub expansion) and the emergence of small erosion patches, as these features were merged in a single mixed pixel (Fig. 25a). Furthermore, our research indicates that SHEI based on high-resolution imagery could be a valuable tool for understanding land cover change.

3.5.4 Remote sensing recommendations for soil erosion monitoring

Monitoring the extent of barren cover from coarse resolution satellite products is challenging, especially in a fragmented Arctic landscape. Our study demonstrated the importance of considering spatial resolution when assessing soil erosion and vegetation change. Landsat spatial resolution is not sufficient to capture important ecological and geomorphological changes. Using inappropriate datasets with coarse spatial resolution may result in underestimation of the extent of soil erosion and crucial threshold-crossing events being missed.

High-resolution information on sub-pixel heterogeneity is essential for accurate interpretations. Integration of UAV imagery with field knowledge provides a valuable solution by capturing data at a scale comparable to ground based observations. This approach enhances the comprehension of spectral variations at coarse spatial resolutions, by validating satellite datasets and facilitating the development of scaling functions. Ultimately, this enables more precise and reliable long-term monitoring of land cover change. This is in line with Sotille et al. (2020), where the authors compared S2, L8 and UAV-derived data in a study of Antarctic vegetation cover. In their study, the use of

UAV data improved the accuracy of vegetation cover estimation, due to higher spatial resolution and greater discrimination of areas that appeared to be homogeneous in lower resolution imagery.

Newer satellite platforms will assist with efforts to monitor soil erosion and vegetation change in a warming Arctic, due to higher spatial resolutions, availability of multiple spectral bands and spatial coverage. Studies have shown that S2 and PS are effective in detecting the extent of vegetation cover compared to L8 (Andreatta et al. 2022). The use of red-edge bands – available in S2 and PS – permits the accurate separation of barren and vegetation cover, allowing for more precise mapping capabilities (Andreatta et al. 2022; Fernández et al. 2022). Caution should be taken in the selection of PS products due to variations in radiometric and geometric quality (Frazier & Hemingway 2021) and lower dynamic range. Confidence in using PS for intra-patch monitoring can be enhanced through detailed comparative studies with higher-quality datasets, time series analysis to assess temporal consistency, and ground truthing to evaluate accuracy in fine-scale monitoring. Additionally, sensitivity testing can quantify the impact of PS's lower radiometric and geometric quality, while data fusion with higher-quality sensors like S2 could improve its accuracy (Fricker et al. 2019). However, even platforms such as S2 or PS might not be sufficient to monitor the development of small shrub/erosion patches, which are critical for environmental assessment in Iceland (Cutler et al. 2023, Streeter & Cutler 2020). The dynamic behavior of small patches can be an indicator of important ecological/geomorphological processes, revealing potential tipping points in the landscape development that may not be apparent in widely used RS products due to their limited spatial resolution. Very-high-resolution imagery, like that from the Pléiades Neo mission and WorldView 3/4, offers the potential to pan-sharpen multispectral imagery from 1.2 to 0.3 m spatial resolution and to study small-scale land cover changes more accurately on a local scale.

Clearly, each RS platform has its advantages and disadvantages. The future of remote sensing will lie in the combination of various systems. PS is useful in resolving small-scale features on a local scale, but shortcomings in consistent image quality limit its use for spectrally complex land cover discrimination and time series analysis. Due to the use of a constellation with different sensors on board. Landsat will continue to be an important dataset for long-term time series analysis along with Visible Infrared Imager-Radiometer

Suite (VIIRS), Sentinel-3 OLCI and Moderate Resolution Imaging Spectroradiometer (MODIS) for monitoring large areas. Caution should be taken when interpreting large-scale monitoring studies in locations where small-scale ecological and geomorphological processes scale-up to landscape-level features. In the long-term, the S2 mission is likely to prove the best platform for tundra environmental monitoring, as it offers frequent image acquisition, excellent sensors, and variety of spectral bands at suitable spatial resolutions. To enhance reliability of coarse satellite datasets in highly fragmented environments, we recommend complementing it with UAV imagery for validation.

CHAPTER 4: SNOW COVER DURATION AND MESOTOPOGRAPHY SHAPE BARREN COVER PATTERNS

4.1 INTRODUCTION

Snow cover plays a crucial role in shaping land cover structure in tundra biomes (Pirk et al. 2023; Niittynen et al. 2020a; Niittynen et al. 2018; Bokhorst et al. 2016). Vegetation growth in the tundra is constrained primarily by the availability of moisture and nutrients, surface energy balance, and soil temperatures (Rixen et al. 2022; Le Roux et al. 2013), but also by exposure to geomorphic forces (Hjort & Luoto 2009; Aalto et al. 2017). Mott et al. (2018) highlighted that the snowpack provides essential protection to plants from frost, dehydration, and mechanical damage caused by wind-blown ice particles. An absence of snow cover during the winter can result in reduced plant productivity and – if conditions are particularly stressful – the creation of barren patches where vegetation cover is thin or dies off (Bokhorst et al. 2009). Meso-scale topographic variation on the order of 1-3 m height difference and 20-100s of meters lateral extension and as typically found in post-glacial environments. This mesotopographic variation is closely related to microclimatic variation and snow cover patterns effectively controlling wind exposure, cryogenic activity and soil temperature (Fig. 30).

Land cover in the tundra is changing rapidly as the climate changes (Rixen et al. 2022; Myers-Smith et al. 2015; Myers-Smith et al. 2011). Arctic winter temperatures are warming more rapidly than summer at about five times the global average rate (Zhang et al. 2021). Precipitation regimes are also changing; for example, high-latitude maritime areas, including coastal Alaska and northern Scandinavia, are projected to experience a 30-40% decline in snow cover duration (SCD) by 2050 (Callaghan et al. 2011c). Climate change of this magnitude will stress tundra ecosystems and drive changes in land cover and plant structure (Wang et al. 2020; Happonen et al. 2019; Callaghan et al. 2011b). While the general trend is towards warmer conditions, Arctic regions will continue to experience severe cold periods and a likely increase in extreme weather (Markkula et al. 2019; Furberg et al. 2018; Overland et al. 2016). Weather extremes may result in atypical precipitation during periods of extreme cold, abrupt shifts in temperature and increased incidence of freeze-thaw events. Choler (2018) noted that the benefits of favourable summer conditions are often diminished by sub-zero temperatures in spring, leading to

reduced growth despite extended growing seasons. This effect is likely to vary spatially: tundra areas close to the sea will experience less variability and less stressful conditions than those inland (Wegmann et al. 2018).

The increased ecological stress induced by climate change means that some parts of the tundra will be vulnerable to land degradation. Areas where grazing on marginal land has been practiced – such as in parts of Iceland and Greenland – will be particularly vulnerable (Dugmore et al. 2009; Massa et al. 2012). Some areas may see an increase in barren cover. Barren cover typically arises either from soil erosion or the absence of vegetation. The susceptibility of soil cover to erosive forces is a function of soil characteristics (Batista et al. 2023), vegetation cover, climatic and hydrological conditions (Subhatu et al. 2018), and land use (Barrio & Arnalds 2023; Archer & Stokes 2000).

The relationship between snow cover and ecosystem variables is well-established (Pirk et al. 2023; Bokhorst et al. 2016; Billings 1973). Snow cover is a crucial factor, particularly during snow accumulation when ground temperatures decouple from air temperatures at snow depths between 15-80 cm (Kivinen & Rasmus 2015). Snow protects vegetation and soils against desiccating and erosive winds (Sturm et al. 2001) and it stabilises temperature fluctuations (Grünberg et al. 2020; Niittynen et al. 2020a). Furthermore, SCD has shown to be a key variable affecting ecosystem function and plant diversity pattern (Niittynen et al. 2020b, 2018). The reduction of snow cover and winter warming events could contribute to the increase of cryogenic damage from frost activity and extreme blizzard events in the short term (Fig. 30). In the long-term geomorphological features resulting from periglacial processes are on the decline in the Arctic and get stabilised by vegetation (Aalto et al. 2017). However, winter warming events, without protective snow cover, can lead to the dieback of shrubs (Bokhorst et al. 2009), and thermal erosion where permafrost is present is particularly threatening coastal regions (Kizyakov & Leibman 2016).

Snow cover supplies moisture to the soil at the start of the growing season, affecting plant growth, plant community composition, phenology, and carbon sequestration and microbial diversity in alpine tundra soils (Zinger et al. 2009; Williams et al. 2009; Litaor et al. 2008). Changes in meltwater release timing can lead to a shift from forb-dominated to shrub-dominated vegetation due to drought stress (Rixen et al. 2022), thus affecting

vegetation structure and soil stability. Conversely, deep snowpacks that persist into summer can restrict vegetation growth, a process known as nivation (Aalto et al. 2021; Hall 1998).

Snow cover patterns are closely related to mesotopography variability; even minor topographical variations can have a major impact on the distribution of snow patches (Sturm & Wagner 2010; Williams et al. 2009; Litaor et al. 2008; Brown & Ward 1996). Snow is likely to accumulate in hollows and blow off ridges, resulting in a heterogeneous snow cover distribution. Areas with low topographic variability are more easily blanketed by snow, whereas regions with high topographic variability require more snow cover to completely cover the ridges.

In addition to influencing snow cover patterns, micro to mesotopographic variations also affect land cover patterns. During the summer, ridges experience higher stress due to reduced soil moisture and nutrients, as well as increased wind exposure. This differentiation between hollow and ridge positions intensifies in the winter with the impact of snow cover (Fig. 8). Snow-covered ridges endure little to no stress, while uncovered ridges experience high stress from various factors, including cryogenic processes, temperature fluctuations and wind exposure (Fig. 30). The combination of these factors leads to distinct land cover patterns that are strongly influenced by the interplay between topography and snow cover dynamics. Future changes in patterns of snow distribution – and the impact this has on the formation of barren patches – is likely to be highly variable in space.

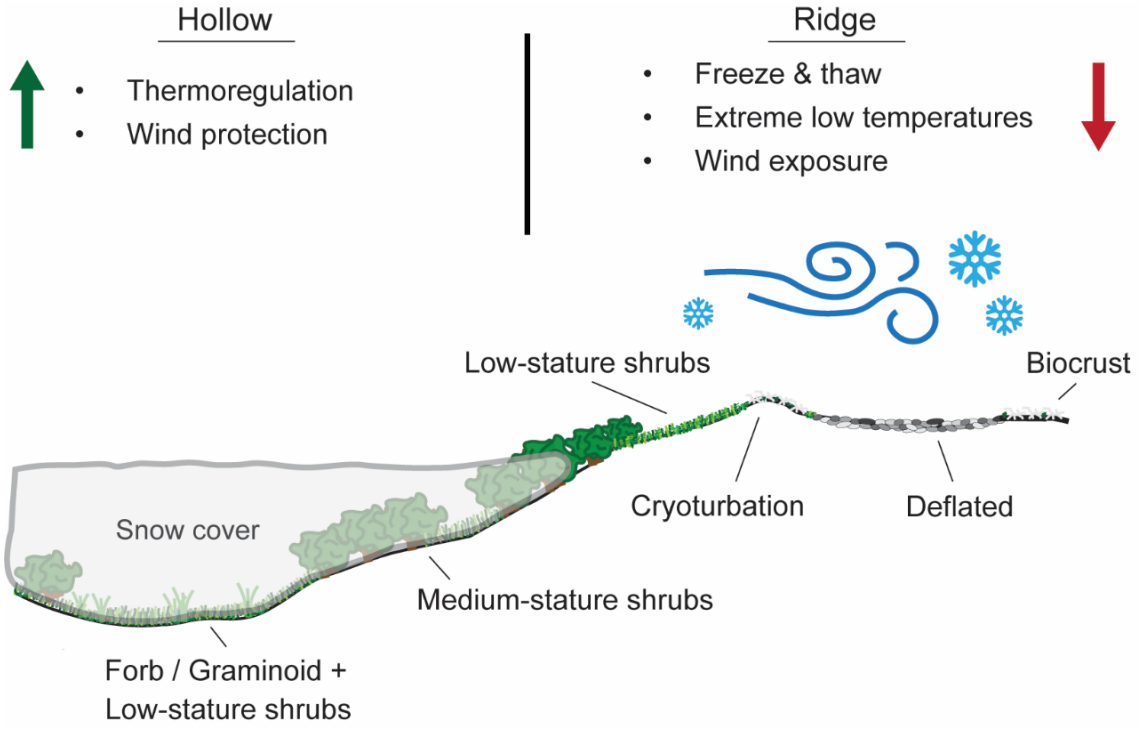

Fig. 30 Illustration about how mesotopography is controlling winter microclimatic conditions and land cover distribution.

Therefore, understanding the interplay between snow cover, mesotopography, soil erosion and vegetation growth is vital for comprehending landscape development in warming tundra regions. This interaction has far-reaching implications, including the loss of soil carbon and reduced biological productivity from the erosion of topsoil, constraints on vegetation growth and soil stability, biodiversity loss driven by increasing environmental stress factors, and disruptions in soil hydrology caused by changes in meltwater dynamics and soil cover.

However, the relationship between microclimatic winter conditions formed by meso-scale landforms and the spatial structure of land cover (vegetation and barren patches) of the tundra lacks comprehensive understanding. This reveals a critical knowledge gap, creating the need for further exploration. To address this gap, this chapter examines the relationships among snow cover duration, mesotopography – expressed with the Topographic Position Index (TPI) - and barren cover, deriving information from high-resolution (2-3 m) satellite imagery. To explore the link between snow cover and soil conditions, we supplemented remotely sensed data with field-based measurements of soil temperature along mesotopographic transects, to better understand how snow cover duration influences cryogenic processes and landscape structure (Fig. 2).

We hypothesised that:

- Barren cover is strongly associated with SCD and TPI (Fig. 30).
- There is a threshold for SCD associated with increasing barren or vegetative cover.
- During winter, ridges experience lower temperatures and greater temperature variability compared to hollows (Fig. 30).
- SCD is likely a better predictor of barren cover than TPI, due to its amplification of mesotopographic influence exemplified in (Fig. 30).

We conducted studies in two regions: northern Iceland and northern Finland. Although the study sites in Finland experience harsher winter conditions and generally steeper topography compared to those in Iceland, both regions share comparable vegetation composition and grazing pressure. Stocking densities are managed in both Iceland and Finland, with relatively low densities spread over extensive areas. While we aimed to select sites with similar conditions for comparability, it is important to acknowledge that the sites in Finland and Iceland are not directly comparable due to differences in climatic conditions, topography, soil characteristics, land-use history, and local flora and fauna. Despite these differences, the contrasting Arctic locations provide valuable opportunities to assess each region individually, offering insights into potential climate transitions and their effects on Arctic ecosystems. To account for local variations, we further subdivided these areas based on environmental gradients, such as proximity to the sea (Iceland) and altitude (Finland).

In this chapter, we utilised high-resolution (2-3 m) satellite imagery to calculate Fractional Vegetation Cover (FVC) (in the year 2022), SCD (calculated from 2017 – 2022), both from PlanetScope data and TPI from aerial Lidar data in Finland (2016) and ArcticDEM from (2018). The FVC serves as a metric of barren area. This spatial information was complemented with data from soil temperature loggers arranged along microtopographic transects. The integration of high spatial resolution remote sensing datasets, with high temporal resolution measurements of soil data (two winter seasons 2021 – 2023) in the field was designed to yield a comprehensive understanding of how winter conditions and landscape morphology influence barren cover formation in these areas of sub-Arctic tundra.

4.2 STUDY AREA

The aim was to investigate the effects of SCD and TPI on barren cover across diverse tundra environments and climatic conditions. Accordingly, three study sites were selected in northeastern Iceland and two in northern Finland. This selection was made to determine whether the relationships between the analysed parameters differ according to the degree of environmental stress gradient. In Iceland, the sites varied in their distance from the sea and their altitude (Table 7). In Finland, the study areas were differentiated based on altitude, with one site situated on the side and another at the top of Saana Mountain. In both study regions, waterlogged areas and zones near river systems were excluded to ensure comparability of hydrological regimes. Steep terrain was also avoided to maintain consistency across the study sites.

Table 7 Details to location and climatic characteristics of studied sites. Average values from climatic variables derived from WorldClim version 2.1 climate data for (January 1970-2000) with 1 km spatial resolution (Fick & Hijmans 2017). Tavg = Average air temperature (°C) of coldest annual quarter, Prec = Precipitation (mm) of coldest annual quarter. Tmin-Tmax-Wind = Lowest and highest Temperature (°C) and wind speed (m s-1) in the coldest month January.

	Size [km^2]	Mean Altitude [m]	Min – Max Altitude [m]	Distance to the sea [km]	Tavg [°C]	Tmin [°C]	Tmax [°C]	Wind [m s-1]	Prec [mm]
Ice1	0.66	50	30- 70	2	-1.3	-4.3	1.5	6.5	175
Ice2	0.73	80	60- 100	4	-1.5	-4.5	1.4	6.4	173
Ice3	0.52	160	140- 180	13.4	-2.1	-5	0.8	6.6	161
Fin1	0.27	650	600- 700	44 km Fjord,	-12.5	-18	-8.2	2.5	107
Fin2	0.32	940	860- 1020	130 km Sea	-12.6	-17.9	-8.3	2.6	121

4.2.1 Iceland

In Iceland, the three study sites are located in Svalbarðshreppur (Fig. 31a) (Chapter 2.3.1, p. 37). The sites are located in unfenced rangelands, where sheep roam freely during the May to September grazing season. The average temperature in the coldest annual quarter decreases with increasing distance from the sea from -1.3 to -2.1. The min and max temperature in the coldest month January is between -5 to -4.5 °C and 0.8 to 1.5°C. The wind speed is around 6.5 m s^{-1} and precipitation around 170 mm in January.

The vegetation is primarily composed of medium-stature deciduous shrubs, such as dwarf birch (*Betula nana*), along with bog bilberry (*Vaccinium uliginosum*) and crowberry (*Empetrum nigrum*), interspersed with graminoids, forbs, mosses, and lichens (Fig. 31c).

The landscape is characterised by the presence of scattered erosion patches consisting of barren cover within a vegetated matrix. The total barren area varies from 4 to 30% (Chapter 3.4.3, p. 78) depending on sea proximity and historical grazing pressure. The size of the erosion patches ranges from 1 cm^2 to hundreds of square meters (Fig. 31b), these patches have shown stability over long periods (Streeter & Cutler 2020).

The soil type is predominantly Andosol, consisting of silt-sized particles derived from volcanic ejecta. They exhibit high levels of water retention capacity and low cohesiveness, making them particularly vulnerable to cryoturbation from freeze-thaw cycles and redistribution by aeolian activity (Arnalds 2015). In our area, the thickness of the soil varies by about 1 meter, being deeper in hollows and shallower at ridges. In areas of active deflation, we find soil particles with remnant vegetation cover, whereas fully deflated areas consist of glacial till with recolonising vegetation—mostly lichen and moss along with some graminoids and low shrubs—located amongst the gravel.

Soil erosion in Iceland is primarily driven by aeolian processes, although factors such as cryoturbation and grazing also reduce soil stability (Barrio et al. 2018; Arnalds 2015; Thorsson 2008). These processes involve the redistribution of the underlying soil, leading to the undercutting of vegetation cover. This results in the vegetation collapsing into erosion patches under its own weight, due to the lack of support from the soil beneath (Fig. 32a). The orientation of erosion fronts is significantly influenced by the prevailing winds (Dugmore et al. 2020), which predominantly originate from the sea to the north (Sigurður Þór Guðmundsson, pers. com.) (Fig. 31d).

4.2.2 Finland

In Finland, our two study sites are situated near Kilpisjärvi (Fig. 31e) (Chapter 2.3.2, p. 41), Fin1 next to Saana and the other Fin2 on top of Saana Mountain. These sites lie within unfenced rangelands, frequented by reindeer during the growing season.

The average temperature in the coldest annual quarter is-12.5 °C. The min and max temperature in the coldest month (January) is between -18°C and -8.2 °C. Fin2 likely experiences lower temperature in the Winter, as evident by the higher presence of exposed rock and lower vegetation cover. The average wind speed is around 2.5 m s^{-1} and precipitation between 107-121 mm in January (Table 7).

The site falls within the boreal zone (Walker et al. 2005), although due to their elevated position, the study sites exhibit characteristics of the low-shrub tundra sub-zone (Fig. 31f). At Fin1 the vegetation consists of medium-stature deciduous shrubs like dwarf birch and juniper, with willows present to a greater extent in sites with high moisture availability. The dominant species are accompanied by low-stature shrubs such as bog bilberry, crowberry, and blue heath (*Phyllodoce*), as well as a mix of graminoids, forbs, mosses, and lichens. As in Iceland, plant productivity and community composition – as well as susceptibility to soil erosion – are strongly influenced by microtopographic variations (Fig. 31e) (Kemppinen et al. 2022; Suvanto et al. 2014). The Fin2 area – which exemplifies a high-Arctic environment – has sparser vegetation cover and thinner soils, with vegetation primarily comprising of low growing stress-tolerant species, such as crowberry, mosses and lichens.

Barren cover in the Finnish landscape is less prevalent than at the Iceland sites, primarily affecting ridge tops and covering areas up to a few square meters. The soils are characterised as Cryosols, which have low water retention capacity and are less prone to aeolian erosion due to their cohesiveness. A notable difference from the Icelandic sites is the presence in Finland of a dense moss/lichen biocrust that helps to prevent soil erosion (Fig. 32b).

Fig. 31 Overview of site location and photographs of site characteristics. a) Location of sites, b) aerial view , c) landscape and d) soil erosion front in Iceland. e) Location of sites, f) aerial view , g) landscape Fin1, h) landscape Fin2 and i) barren to vegetation cover transition topview, in Finland. (a) & e) retrieved from Bing Maps, 8 November 2023)

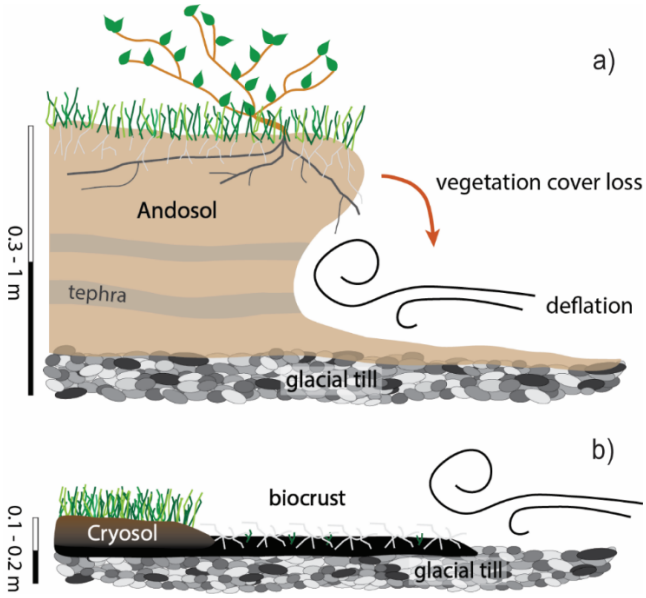

Fig. 32 Soil erosion process in a) Iceland. Andosols are prone to particle distribution by aeolian activity. Undercutting of vegetation cover leads to the detachment of the topsoil cover. b) Finland. The Cryosols on the Finnish sites have higher cohesiveness than the Icelandic Andosols and partial protection from a moss/lichen biocrust.

4.3 Data and Methods

4.3.1 Remote sensing data

To explore the relationships among fractional vegetation cover (FVC), snow cover duration (SCD) and topographic position index (TPI), we used high-resolution satellite imagery and aerial LiDAR data (Table 2). PlanetScope (PS) imagery from the SuperDove satellite, equipped with PSB.SD sensor, includes eight bands with a 3 m spatial resolution. The Near-Infrared (NIR) and Red-Edge (RE) bands were used to derive FVC during the 2022 growing season (see Table 8), using vegetation index RECI serving as a reliable predictor of vegetation density. SCD data were derived from 80 images in Iceland and 306 in Finland, covering in total four winter seasons (Table 8).

To obtain topographical information we used datasets from aerial LiDAR survey and the Arctic DEM datasets. The ArcticDEM is a high-resolution digital surface model (DSM) of the Arctic (>60°) with a 2 m spatial resolution, primarily using stereo imagery from Worldview-1, 2, 3, and some from the GeoEye-1 platforms (Porter et al. 2018). Candela et al. (2017) compared ArcticDEM's accuracy with ICESat data and high-resolution airborne LiDAR datasets, finding an average accuracy of -0.01 m ± 0.07 m for ArcticDEM. They concluded that it is suitable for analysis without additional corrections. The Finnish

national DEM produced by the National Land Survey of Finland is also available at 2 m spatial resolution and is based on nationwide LiDAR campaigns.

The LiDAR data were obtained from the National Land Survey of Finland. The scanning of the area was performed (16–17 August 2016) with a Leica ALS60 laser scanner. Flight altitude was 2950 m a.s.l. (c. 2200 m above ground), beam divergence (1/e2) was 0.22 mrad, and the maximum scan angle was 20°. Nominal pulse spacing in the study area was 1.3 m. Accuracy statistics for the LiDAR data have not been provided, but it is considered to be of higher quality than the ArcticDEM.

Table 8 Remote sensing datasets used for analysis including acquisition/product dates.

	FVC	SCD	TPI
Iceland	PlanetScope (3m) 17.08.2022	PlanetScope (3m) 2019 – 2022	ArcticDEM (2m) 27.06.2018 (Version 3)
Finland	PlanetScope (3m) 30.07.2022	PlanetScope (3m) 2017 – 2021	Aerial LiDAR (2m) 17.08.2016

4.3.2 Fractional vegetation cover

FVC serves as an indicator for the level of barren land cover. From the PS 8-band product both NIR and RE bands were used to calculate the Red Edge Chlorophyll Index (RECI) (equation 3) (Gitelson et al. 2003). RECI is a vegetation index sensitive to changes in chlorophyll content; it can indicate the density of vegetation. Andreatta et al. (2022) demonstrated that RECI is the best predictor of FVC as – unlike NDVI - it does not saturate at higher values. UAV surveys were conducted during the growing season in August 2021 in Iceland and 2022 in Finland. Land cover surveys conducted at the same time enabled supervised classification (Chapter 3.3.6, p. 69; Chapter 5.3.3.2, p. 140). The generated classified land cover maps of 5 cm resolution and other commonly used vegetation indices derived from multispectral drone datasets enabled us to validate the PlanetScope data. The minimum value $\mathbf{RECI_{Bar}}$, indicates completely barren land, and the maximum value $\mathbf{RECI_{Veg}}$, indicates complete vegetation cover of any sort. The lowest RECI value with complete vegetation cover (excluding biocrust) was identified (Table 9) to calculate the FVC (equation 4). In Iceland, FVC measurements were consistent across sites as the values were similar. However, in Finland, adjustments for min and max RECI values for each site were necessary, due to variations in vegetation density across different landscapes.

The higher plant diversity in Finland introduced some uncertainty in FVC measurements compared to Iceland, resulting in larger variability of FVC represented by a RECI value. Adjustments were necessary for each site due to variations in vegetation density and composition for sites Fin1 and Fin2. This difference stemmed from Fin2's lower plant diversity and the dominance of the prostrate shrub crowberry, which has lower RECI values than the medium-stature dwarf birch found in Fin1 and Iceland. The presence of biocrust and lichens in rocky, barren areas further complicated FVC estimation due to their higher RECI signals, leading to these areas being identified as partly vegetated.

(3) $$\boldsymbol{RECI = \left(\frac{NIR}{Rededge}\right) - 1}$$

(4) $$\boldsymbol{FVC_{RECI} = \frac{RECI - RECI_{Bar}}{RECI_{Veg} - RECI_{Bar}}}$$

Table 9 Upper and lower RECI values for completely barren and vegetation areas, to calculate the fractional vegetation cover calculation.

	RECI values for FVC	
Land cover	$\mathbf{RECI_{Bar}}$	$\mathbf{RECI_{Veg}}$
Ice1-3	0.5	2.0
Fin1	0.8	2.0
Fin2	0.15	1.1

4.3.3 Topographic indices

The TPI developed by Weiss (2001) is a quantitative metric used to divide the terrain into features such as hollows and ridges, which can generate variations in microclimatic conditions. TPI operates by comparing the elevation of each cell in a digital elevation model (DEM) to the average elevation of surrounding cells within a specified neighbourhood (equation 5; Fig. A2). The equation represents TPI_i represents the at location *i*, where Z_0 is the elevation of the point of interest, Z_n are the elevations of the surrounding *n* points, and *n* is the total number of surrounding points used to calculate the average elevation. Allowing the TPI to indicate whether the point is higher (ridge) or lower (valley) relative to its surroundings and widely used to classify various landforms (Jenness 2006). In our case we only distinguished between (< 0 TPI = Hollow, > 0 TPI =

Ridge) determined by whether the cell's elevation is higher, lower, or similar to its neighbours. For our study, we aimed to capture the meso-scale curvature variation of the landscape within both Iceland and Finland in the best possible detail. To achieve this, we tested multiple kernel sizes in each area and ultimately selected a kernel size of 20 × 20 meters for both locations. This kernel size allowed us to effectively capture the distinct hollows and ridges in the landscape, as it resulted in the largest TPI differences between these positions. We found that smaller kernel sizes tended to reflect smaller landscape features and miss larger mesotopographic features stretching tens of meters horizontally. On the other hand, larger kernel sizes rendered the mesotopographic features less pronounced, resulting in less variability between hollows and ridges. The selected kernel size of 20 × 20 meters struck a balance between these factors, representing best the mesotopographic landforms in the study areas.

Likely due to the lower quality of the ArcticDEM, the Icelandic TPI exhibited a speckle pattern. To remove this granular noise, a 5 × 5 Majority filter was applied. The TPI layer was subsequently co-registered to the FVC and SCD in both study regions. Iceland is characterised by smoother topography compared to Finland. Typical TPI values for both sites are shown in Fig. 33. A TPI value of 1 indicates that the focal point is 1 meter higher than its surrounding 20-meter area.

(5)
$$TPI_i = Z_0 - \frac{\sum_{1-n} Z_n}{n}$$

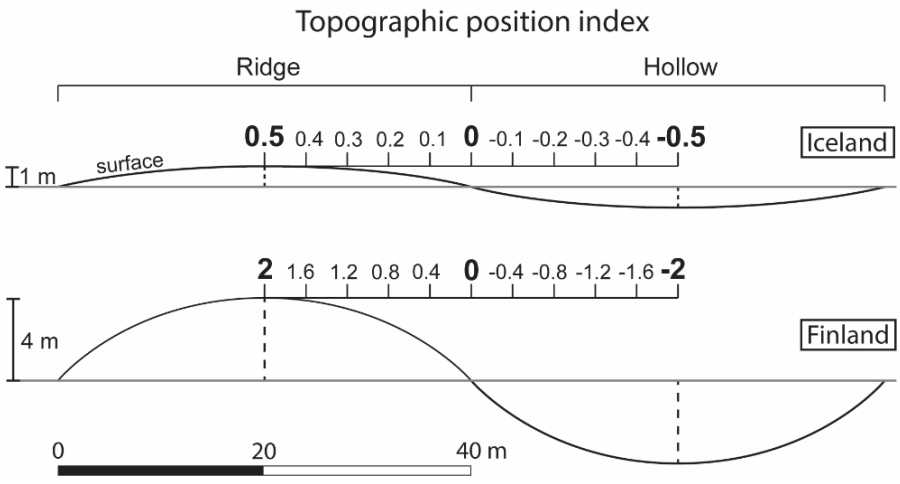

Fig. 33 Sketch illustrating typical TPI values in Iceland (upper panel) and Finland (lower panel). The sketch is vertically exaggerated. Hollows and ridges are delineated on the panels.

To better understand the irregularity of the terrain or here referred to as surface roughness on each site, the Terrain Ruggedness Index (TRI) was generated from the DEM. The TRI quantifies the amount of elevation difference between adjacent cells in a digital elevation grid, providing a measure of terrain heterogeneity (Riley et al. 1999). It is calculated by determining the largest inter-cell difference between a central pixel and its surrounding cells. A TRI value of 1 means that the central pixel is elevated 1 m relative to the surrounding pixels. A TRI value of 0 represents completely flat terrain, indicating no elevation difference between adjacent cells. Higher TRI values indicate more rugged or irregular terrain, while lower values suggest smoother or more homogeneous surfaces.

4.3.4 Snow cover duration

The detailed method used to derive the snow cover duration map for Kilpisjärvi is described in Kemppinen and Niittynen (2022), and calculations for Iceland followed the same procedure. In short, we first downloaded PlanetScope images that were mostly cloud free over the study areas and manually digitised cloud masks to remove the clouds. The spatial accuracy was enchained by cross-coregistering the images by comparing the images to monthly median mosaic images with the coregisterImages function from RStoolbox R library (Leutner et al. 2019). Next, we fitted a Random Forest classifier to classify each pixel in the images to snow, land or water (Liaw & Wiener 2002). Lastly, the RandomForest model classifications were used in a pixel-wise binomial generalised linear model which determined the average melting date for each pixel (Kemppinen & Niittynen 2022). In Kilpisjärvi, the melting date was determined as the date where the modelled snow probability dropped first time below 0.5. However, in Iceland the spring snow melt timing was often less clear (new-snow events occurred long after the first melts) and varied more across years. To account for these fluctuations, we calculated the average melting date by summing the snow probabilities for each day from January 1st to June 31st and identifying the date when the cumulative snow probability reached its midpoint. This method provides a more nuanced and realistic estimate of the melting date under Iceland's variable snow conditions. While both methods generally yield similar results, the cumulative approach was better suited to Iceland's unpredictable snow patterns. Due to the polar night, satellite imagery is not available before mid-February. All sites were considered to be under snow before mid-February, which can lead to overestimation of

SCD in some extremely early melting locations, which were however considered rare in both study areas.

4.3.5 Relationships between FVC, SCD and TPI

To understand the distribution of FVC and SCD at each site, we created density plots for both variables. For comparison between variables, boxplots were used to illustrate variability and general relationships. The independent variables, TPI and SCD, were segmented into bins. TPI was divided into intervals of 0.1 in Iceland and 0.3 in Finland, accounting for the broader range of TPI values on the Finnish sites. SCD was categorised into 3 SCD bins, reflecting a similar SCD range in Iceland and Finland. To examine the impact of SCD on FVC in contrasting topographic features, the dataset was divided into hollows and ridges based on TPI values (< 0 = Hollow, > 0 = Ridge). Subsequently, we created separate plots comparing FVC against SCD for hollows and ridges in both Iceland and Finland. The Loess function was applied (Cleveland & Devlin 1988) to illustrate these relationships, which is particularly effective for examining complex, non-linear relationships with high variability, as it reveals underlying trends without relying on strict parametric assumptions.

4.3.6 TPI and SCD distribution for barren and vegetated cover

The aim of this analysis was to classify land cover as either 'barren' or 'vegetated' based on FVC thresholds and to investigate the distribution patterns of these land cover types in relation to SCD and TPI across our study sites. By doing so, we aimed to enhance our understanding of the predictability of barren and vegetated land cover using SCD and TPI. Land cover was classified for each 9 m^2 pixel, where pixels with FVC less than 10 or 20% were categorised as 'barren', and pixels with FVC exceeding 10 or 20% were categorised as 'vegetated'. The different FVC thresholds for land cover classification were used to account for various types of disturbed land cover, such as bare rock, lichen-covered rock, and biocrust. Following this categorisation, density plots were generated for both TPI and SCD to contrast the distribution patterns of barren and vegetated land cover.

4.3.7 Microclimatic soil data

We established two transects consisting of six PB-5001 soil temperature probes connected to three Tinytag Plus 2 data loggers (Tinytag, Chichester, UK) in August 2021 (Iceland) and July 2022 (Finland). These were arranged along a topographic elevation

gradient ranging from 1 to 1.5 meters and along a horizontal distance of 11 to 24 m (Table 10). The first probe (St1) was located in the hollow, and the final probe (St6) was positioned at the ridge, with intermediate probes spread between the height extremes. At each probe site, we carefully removed the topsoil and installed the sensors at a depth of 8 cm in Iceland and about 3 cm in Finland, due to different soil thickness. The soil depth was chosen as it represented the root depth of the present vegetation. The topsoil was then replaced over the sensors to ensure complete coverage while preserving the integrity of the vegetation cover. Soil temperature readings were recorded hourly from 1 September 2021 to 30 September 2022 in Iceland, and from 16 July 2022 to 26 September 2023 in Finland. Subsequently, the soil data for the winter seasons of 2022 and 2023, spanning from November to mid-May (when air temperature is often below 0°C), were compiled. One sensor in the hollow and one at the ridge were plotted for each winter season to visualise the temporal variation of hollow and ridge positions. Additionally, statistics such as median, minimum, maximum, and variance were calculated for each entire winter season for all probes.

Table 10 Information about the probe deployment and sensing period for Iceland (Icex1) and Finland (Finx).

Transect Logger	Transect length	Height range	Probe depth	Sensing period
Icex1 St	10.8 m	1.1 m	8 cm	27/08/2021 – 19/09/2023
Finx St	23.5 m	1.6 m	~3 cm	23/07/2022 – 15/11/2023

The growing degree days (GDD) were calculated to assess summer thermal conditions, and are defined here as the sum of daily soil temperatures above 0°C. This sum indicates the amount of energy available to plants during the growing season. As a counterpart for winter conditions, freezing degree days (FDD) were quantified to reflect the severity of winter conditions affecting vegetation, based on the sum of daily soil temperatures below 0°C. Both metrics have been associated with species richness and abundance (Niittynen et al. 2020a).

4.4 RESULTS

4.4.1 Site characteristics

Each study area had around the following number of cells (9 m^2): Ice1 (73,000), Ice2 (81,000), Ice3 (57,000), Fin1 (30,000), Fin2 (33,000). The distribution of FVC, SCD, and TPI cell values revealed different environmental conditions along the increasing environmental stress gradient from Ice1 to Ice3 in Iceland and from Fin1 to Fin2 in Finland (Fig. 34 and TableA6, A7, A8 in Appendix). Iceland experienced a range of SCD from 50 (close to the coast) to 138 days (further inland), while Finland had a SCD range from 122 to 192 days, increasing with altitude. The mean FVC across each site decreased with increasing distance away from the sea and elevation: 72% in Ice1, 69% in Ice2, 62% in Ice3, 46% in Fin1, and 34% in Fin2 (Fig. 34b). The Icelandic landscape is characterised by a smoother terrain, with TPI values around ±0.5, in contrast to the more rugged Finnish terrain (TPI values around ± 2-3).

The range of TPI values indicated lower topographic variation in Iceland, with minimum and maximum values of -1.5 and 1.8. Typical TPI values in Iceland range from -0.5 to 0.5, with maxima up to -0.7 to 0.7 in Ice3 (Fig. 33c). In contrast, Finland displays greater topographic variability, with TPI values ranging from -5.5 to 6.4. Typical TPI values varied more significantly between the Finnish sites, from -2 to 2.5 in Fin1 and from -4 to 5 in Fin2.

The mean surface roughness values in Iceland are around 0.4, while Fin1 is 0.7 and Fin2 1.1 (Fig. 34d). A higher irregularity at the Finnish sites compared to Iceland, could indicate a higher landscape fragmentation and thus microclimatic variability.

SCD data revealed an increase in line with the stress gradient (increased distance to sea/elevation), ranging from 50 to 138 days in Iceland and 122 to 195 days in Finland (Fig. 34a). Ice1 exhibited the narrowest range of SCD values, starting at 50 days and peaking at 65 before levelling off at 80, with a mean of 69 days. Ice2 and Ice3 demonstrated a wider distribution of values, with a peak of 97 for Ice2 and 104 for Ice3 and mean SCDs of 93 and 103 days, respectively. Fin1 displayed a more concentrated distribution, peaking at 155 days, with a mean of 152. Fin2's pattern more bell-shaped, with a wider distribution of values, peaking at 158 days, which is also the mean value.

Mean FVC decreased with increasing stress (Fig. 34b). All sites feature pixels that are either completely barren or fully covered with vegetation, as they include RECI values for barren and fully vegetated. The Icelandic sites display a bimodal distribution of FVC values: one peak is the local maxima around 80% FVC, and the other occurs at the point of full vegetation cover. The Icelandic sites show a gradual decrease of FVC peak distribution, with Ice1 exhibiting two peaks at fully vegetated areas and at 81%, while Ice2 and Ice3 have one maxima at 79% and 69% FVC, respectively. Finnish sites, however, have a single maxima which occurs at lower values of FVC, peaking at 41% for Fin1 and 31% for Fin2, before gradually decreasing in frequency.

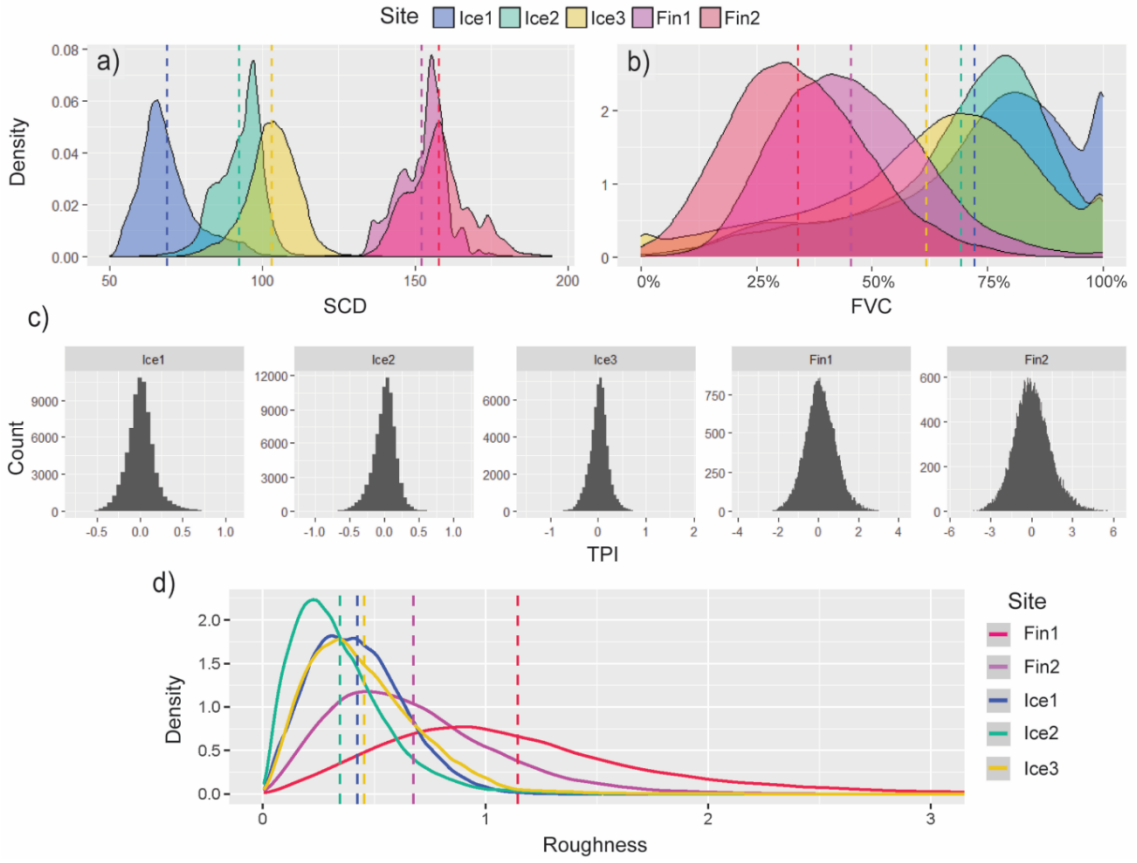

Fig. 34 Density plots and histogram for various parameters. a) Density plot for snow cover duration (SCD) and b) fractional vegetation cover (FVC). Histogram displaying the Topographic Position Index (TPI) distribution across each site, with a bin width of 0.05. d) Density plot for surface roughness (TRI). Dashed lines in each plot indicate the mean value of the respective parameter for each site. The bandwidth used in each density plot follows the Gaussian kernel density estimation method as proposed by Silverman (1986).

4.4.2 Relationship between SCD, TPI and barren cover

All sites in Iceland (Ice1, Ice2, and Ice3) and two in Finland (Fin1 and Fin2) displayed a negative relationship between TPI and SCD, albeit with varying slopes depending on the stress gradient (Fig. 35a). Notably, Ice1 had the steepest slope, indicating high sensitivity within the range of < -0.25 and > 0.5 TPI, and levels out above 0.5 TPI. In Finland, Fin1 showed a gradual decrease in SCD with increased topographic exposure, whereas Fin2 levels out at 0.5 TPI (Fig. 35a).

At Icelandic sites, particularly Ice1, there was a nearly linear decrease in FVC with increasing TPI (Fig. 35b). FVC at the Ice2 and Ice3 sites exhibited either a plateau or a slight downward trend up to 0 TPI, followed by a sharp decline. Both Finnish gradients, Fin1 and Fin2, showed an initial increase in maximum FVC values up to 0 TPI. However, Fin1 exhibits a generally horizontal relationship, attributed to the large variability of high and low FVC values in hollows. Above 0 TPI, both Finnish sites demonstrate a decreasing trend in FVC with increasing TPI.

In the Icelandic context (Ice1, Ice2, and Ice3), a positive relationship is observed between FVC and SCD, with FVC generally increasing as SCD increases. (Fig. 35c). Ice1 in particular showed a marked increase in FVC up to 68 SCD, followed by a more gradual rise. In Finland, Fin1 exhibited an initial increase, peaking in vegetation cover at around 160 SCD, before declining as SCD increased further. In contrast, Fin2 peaked at the lowest SCD, with its median gradually decreasing over time. However, around 160 SCD,

the outliers for both sites exhibited the highest variability and FVC values.

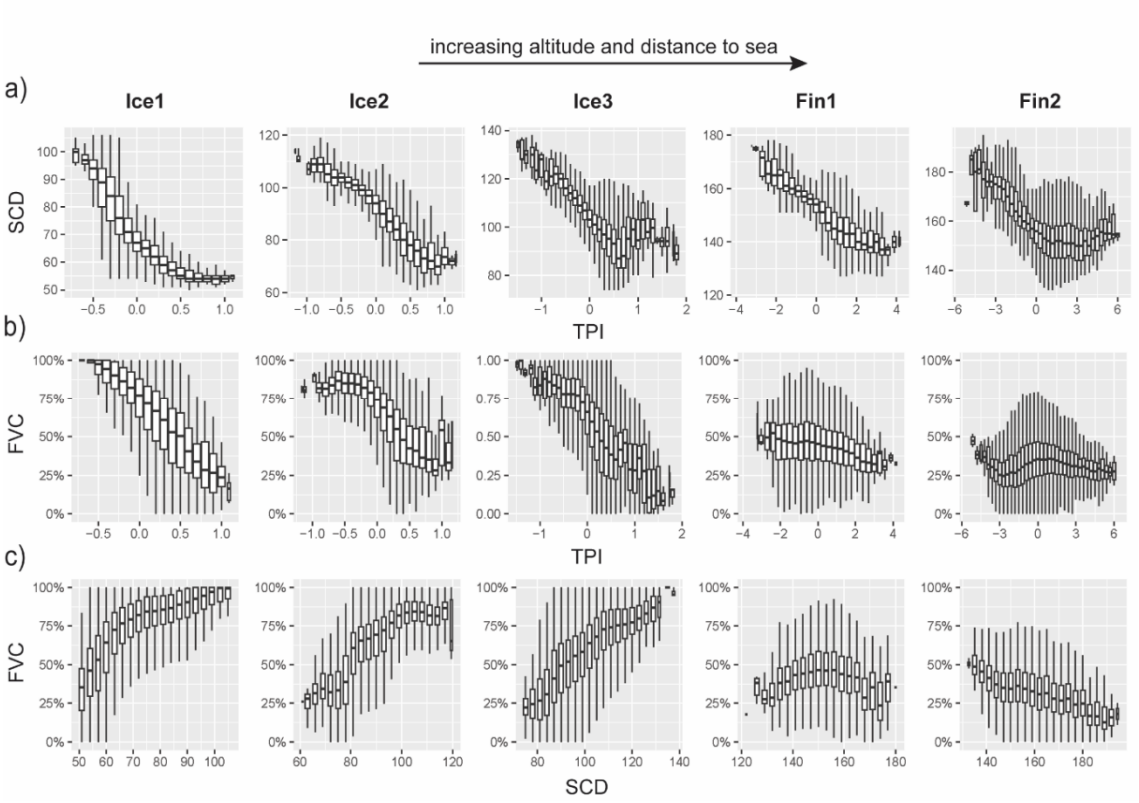

Fig. 35 Spatial Relationships between a) SCD versus TPI (cutwidth 0.1 TPI in Ice and 0.3 TPI in Fin), b) FVC versus TPI (cutwidth 0.1 TPI in Ice and 0.3 TPI in Fin), c) FVC versus SCD (cutwidth 3 SCD) for each site with increasing environmental gradient.

4.4.3 FVC vs SCD in hollow and ridge position

In hollow areas, Ice1 and Ice2 exhibited a sharp increase in FVC with rising SCD to an asymptote (Fig. 36a). At Ice3 the rate of FVC increase was more gradual, missing lower SCD values. For Fin1 and Fin2, SCD and FVC were overall negatively correlated, yet they displayed contrasting patterns at low SCD values (<145). Fin2's FVC increased up to an SCD value of 150, peaking alongside Fin1, before both began to decrease (Fig. 36a).

In ridge locations, SCD and FVC are positively correlated for Ice1, Ice2, and Ice3 (Fig. 36b). In the case of Fin1 and Fin2, ridge locations exhibited a different pattern to hollows (Fig. 36). At Fin1, FVC increased up to a SDC value of 150, then levelled-off at higher values. At Fin2 there was a continuous decrease in FVC as SDC increased.

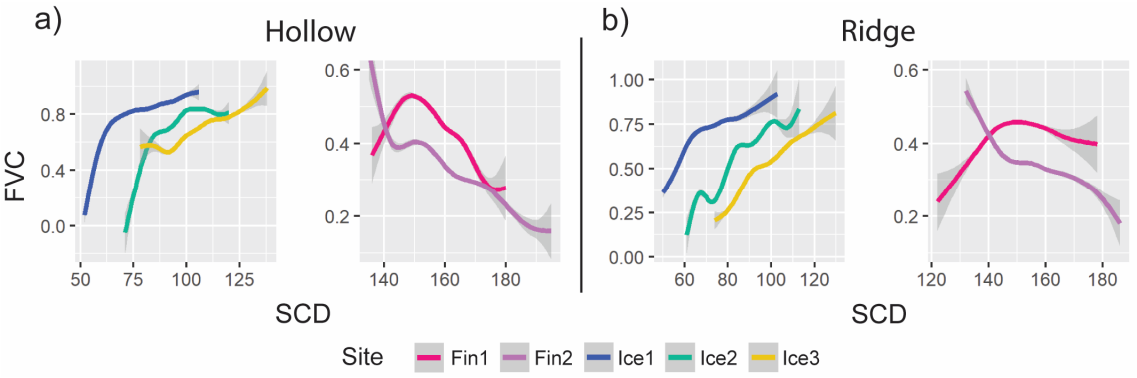

Fig. 36 SCD vs FVC split by topographic position in Iceland and Finland. The dataset is split based on Hollow < 0 TPI and Ridge > 0 TPI. The greyed area represents 95% confidence interval of the loess function.

4.4.4 TPI and SCD distribution of barren and vegetated land cover

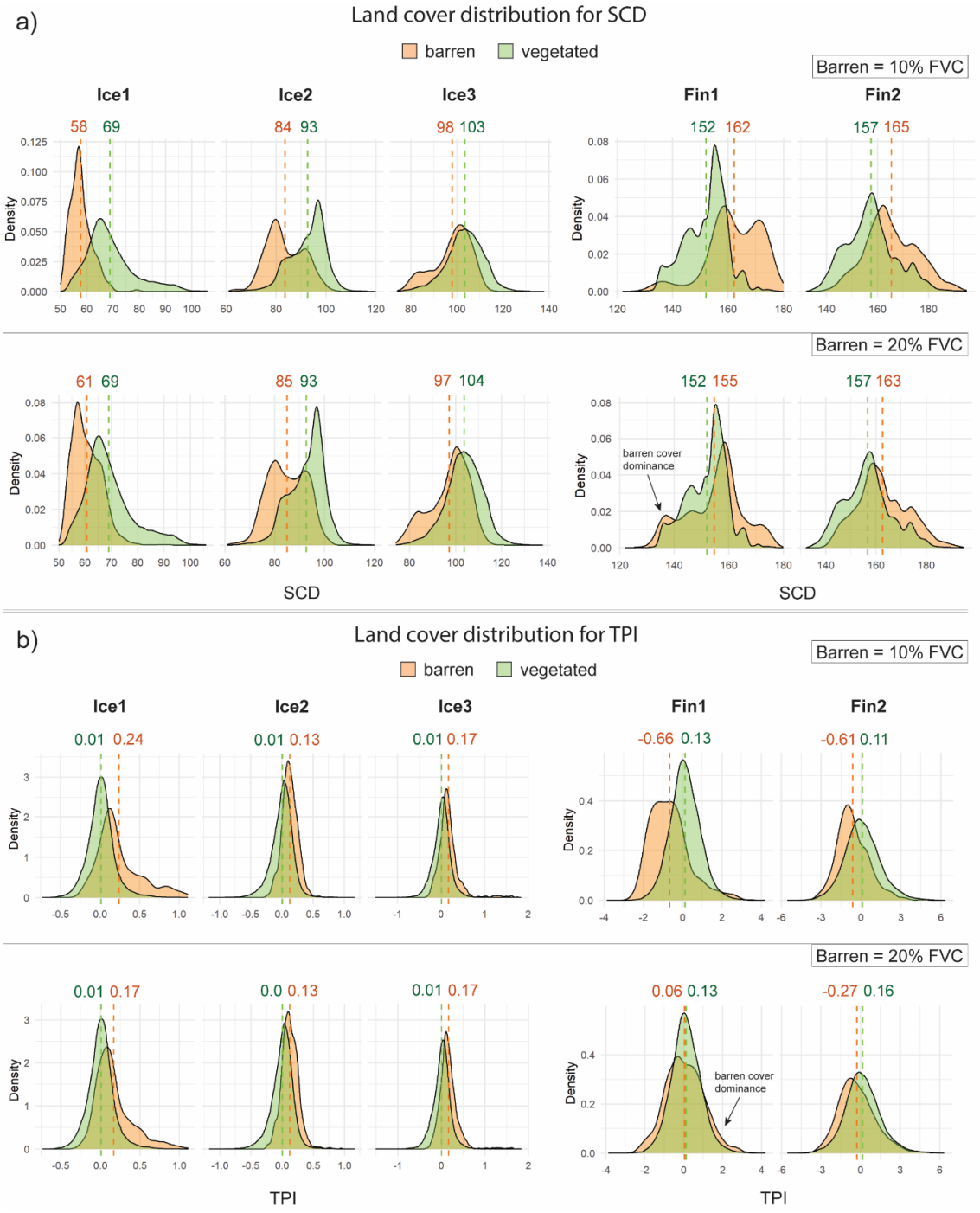

Fig. 37 Density plot displays the distribution of a) TPI and b) SCD, for barren (orange) and vegetated (green) land cover. The dashed lines indicate the mean for each land cover class, site and variable. An FVC of 20% covers all values below it, including the data from 0-10% Barren.

In Iceland the distribution of TPI and SCD showed a marked division between barren and vegetated cover (Fig. 37). In contrast, the Finnish landscape presented a more complex scenario: the differences in TPI are subtler, yet the variability in SCD is notably different.

In the Icelandic context, TPI values revealed a distinct division: areas with TPI values less than 0 are predominantly vegetated, while regions where TPI exceeds 0 were more frequently characterised by barren cover. This pattern is mirrored in the distribution of SCD, where a clear division is observed: low SCD correlates with high barren cover density, and high SCD aligns with extensive vegetated cover.

Conversely, the landscape dynamics in Finland exhibited a more nuanced pattern. At Fin1, the distribution between barren and vegetated cover differed for barren cover classified <10% and <20% FVC. <10% FVC has a distinct pattern, where barren cover occurs in the hollows and high SCD. Whereas at <20% FVC, barren cover occurred at ridge position and low SCD values.

At Fin2, the trend diverged; low TPI values were associated with more barren cover, while higher FVC values dominate in the TPI range of 0 to 1. The relationship with SCD at Fin1 showed a stark contrast: barren cover is predominantly observed at the extreme ends of the SCD spectrum, particularly at values below 142 and above 158. In contrast, at Fin2, vegetated cover was more common at SCD values below 158, with barren cover becoming prevalent when SCD values exceed 158.

4.4.5 Soil Temperature

The calculated site characteristics for the soil temperature probes showed differences between Iceland and Finland. In Iceland, there was an irregular decrease in FVC from the fully vegetated hollow to the eroded ridge, dropping from 100% to 76% FVC, and a gradual decrease in SCD from 101 to 93. The TPI ranges only from -0.3 to -0.1. Field observations indicated that the top sensor is located on a ridge, but the ArcticDEM may not be accurate enough to reflect this variation. In contrast, in Finland, both the hollow and ridge positions exhibited relatively low FVC values, with a maximum FVC in the hollows of 50% and minimum of 25%. Here, the SCD sharply decreased from 157 to 135 at the ridge top, and the TPI values showed a wider range, from -1.2 to 1.8.

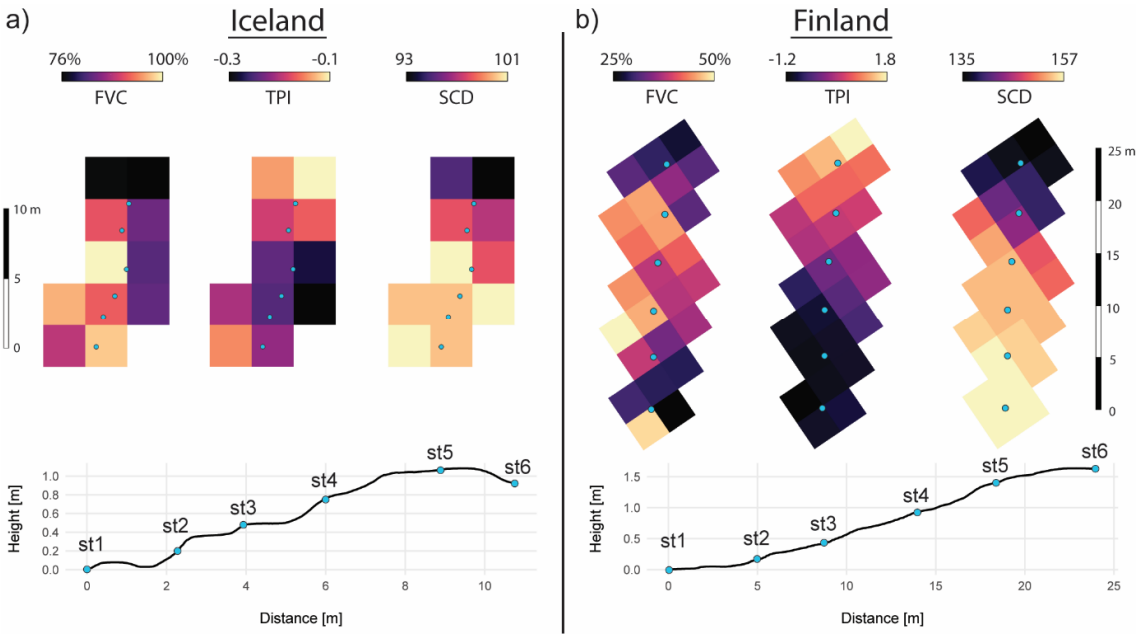

Fig. 38 Cell values of FVC, TPI, SCD surrounding the soil temperature transect for a) Iceland and b) Finland. The high-resolution elevation information of each sensor was acquired from a drone survey and generated DEM (Iceland 2021, Finland 2022).

During the 2021/22 winter in Iceland, soil temperature (ST) measurements from six sensors showed low variation across different topographic positions (Table 11). The ST generally fluctuated around the freezing point, with median values near 0°C, peaks just over 13°C, and trough slightly below freezing. This pattern persisted from early December through to mid-April (Fig. 39). The hollow sensor maintained stable temperatures throughout the winter, while the ridge experienced three significant dips below freezing in 2021 and a sharp cold snap in mid-April 2022 (Fig. 39).

In contrast, the winter of 2022 in Finland presented different thermal profiles. Median temperatures, remained well below freezing, ranging from -4.32°C to -0.45°C. The most extreme temperatures were noted at the ridge: the lowest being -13.4°C and the highest reaching 10°C. The ST variance increased from the hollow probe (St1), at 0.9, to the ridge (St6), at 19. In the hollow, ST stayed just below 0°C and above -2°C with low variability, whereas the ridge exhibited colder temperatures and very higher variability (Fig. 39). From mid to late April, the ridge position underwent freeze-thaw cycles, while the ST in the hollow position began to rise above 0°C in early May.

The ST readings revealed significant microclimatic variation in different topographic positions. Overall, during the freezing period, the ridge locations in both Iceland and Finland showed strong fluctuation above and below the freezing point, whereas the

hollows, especially in Finland, tended to remain around 0°C for extended periods (Fig. 39). In Iceland there was less distinction between the ridge and hollow readings compared to the Finnish sites. Full ST time series in Appendix (Fig. A3, A4).

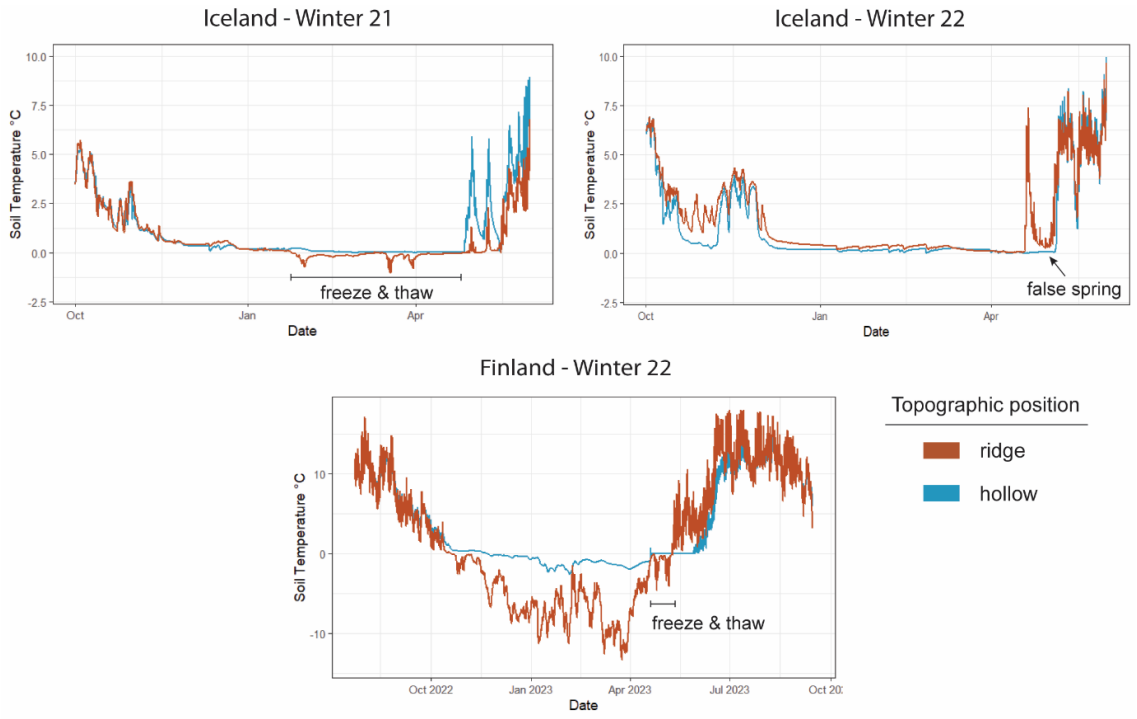

Fig. 39 Soil temperature in the winter season of 2021/22 in Iceland and Finland. The freeze and thaw periods are indicated by temperatures that do not exceed 0°C due to heat from the ground. Exposed vegetation cover is likely to experience freeze and thaw cycles during this period.

Table 11 Soil temperature statistics over the winter periods of 2021/22 in Iceland and Finland. St1 sensor is in the hollow, St 6 at the ridge.

	Iceland Winter 21				**Iceland Winter 22**				**Finland Winter 22**			
Sensor	**Med**	**Min**	**Max**	**Var**	**Med**	**Min**	**Max**	**Var**	**Med**	**Min**	**Max**	**Var**
St1	0.21	-0.07	12.41	7.57	0.37	-0.07	12.41	12.04	-0.45	-1.89	6.26	0.92
St2	0.35	-0.01	13.07	8.19	0.73	-0.01	13.07	11.74	-0.4	-2.62	3.31	1.12
St3	0.21	-0.26	11.90	7.34	0.52	-0.26	11.90	10.35	-1.54	-5.32	4.39	2.73
St4	0.37	-0.39	13.56	8.66	0.98	-0.39	13.56	11.61	-2.1	-6.82	5.03	4.71
St5	0.06	-0.67	12.75	8.27	0.60	-0.67	12.75	10.43	-3.35	-8.72	5.07	10.18
St6	0.32	-1.06	11.68	7.18	0.57	-1.06	11.68	9.71	-4.32	-13.39	10.02	18.96

Topographic influence is particularly apparent when comparing growing degree days (GDD) and freezing degree days (FDD) (Table 12). The GDD values in Iceland were around 33,000 GDD while Finland around 21,000 GDD, with little variation across the transect.

For the FDD a clear increasing trend is observable from the hollow St1 to the ridge St6. In Iceland it ranges from 0 to 169 FDD and in Finland from 1481 to 12,893 FDD.

Table 12 Growing degree days (GDD) and freezing degree days (FDD) for soil temperature logger in Iceland and Finland. St1 probe is in the hollow, St6 at the ridge position.

Sensor	**Ice GDD**	**Fin GDD**	**Ice FDD**	**Fin FDD**
St1	32523	21079	11	1481
St2	33713	19263	0	1991
St3	31974	19593	16	4648
St4	34797	18973	62	5927
St5	31194	18967	123	9239
St6	30571	21565	169	12892

4.5 DISCUSSION

The main aim of this chapter is to investigate the relationship between microclimatic winter conditions, particularly SCD, and the spatial distribution of land cover (vegetation and barren patches) in tundra regions. While efforts were made to select study sites with similar conditions for comparability, the inherent environmental differences between the Icelandic and Finnish sites make direct comparisons challenging. Nevertheless, these contrasting settings allow us to explore how diverse Arctic conditions shape land cover patterns and to gain insights into potential climate transitions and their effects on Arctic ecosystems.

The results revealed contrasting environmental conditions in Iceland and Finland. Generally, in Iceland, SCD levels were low, with mean SCD values ranging from 69 to 103 days among the sites, whereas in Finland, SCD levels were high, with a mean of about 155 days. In Iceland mean FVC distribution is about 70%, whereas in Finland the mean was 40% vegetated. It is important to note that the same FVC value at different sites may not represent identical vegetation levels due to variations in how vegetation and barren values were established for the RECI metric. While this may slightly limit interpretability, the overall impact is expected to be minimal, with Finnish sites likely averaging extreme FVC values due to stronger land cover fragmentation and mixed pixels. The topographic variation in Iceland is smoother with TPI values of up to 0.5 and in Finland steeper of up to 2.0 TPI.

A clear negative correlation between TPI and SCD was observable in Iceland, where hollows were predominantly fully vegetated, and as the position becomes more exposed, the FVC decreased until it reached the highest barren cover distribution at the ridge position. Furthermore, SCD and FVC showed a positive correlation, meaning that with increasing SCD, barren cover decreased. In Finland, the data demonstrated that concave positions (low TPI) presented low FVC until it reached its peak at flat positions (0 TPI) and then declined again towards exposed position (high TPI). At Fin1, the influence of SCD on FVC revealed a bell-shaped curve where 155 SCD represents the peak, whereas site Fin2 at the mountain top showed a negative relationship between SCD and FVC.

In Iceland, soil temperatures showed low variability during the winter months with a maximum of 2°C fluctuation between mid-December and mid-April. Similarly, the number FDD and mesotopographic positions showed minimal variation across the two transects. However, ridges were more likely to experience extensive periods of freeze and thaw cycles during the winter. The harsher climate and steeper topography in Finland contributed to exposure to strong frost activity, particularly at the ridges, which also experienced detrimental freeze and thaw cycles in early spring. In contrast, the hollow positions benefitted from low temperature values and variability due to the thermoregulation of the snow cover.

The discussion begins by describing the site characteristics in Iceland and Finland. Next, the relationships between Fractional Vegetation Cover (FVC), Snow Cover Duration (SCD), and Topographic Position Index (TPI) are examined. This is followed by an analysis of barren cover occurrence in relation to TPI and SCD. Subsequently, soil temperature data are discussed and linked to cryogenic processes. Finally, a future outlook is provided, exploring how projected changes in SCD might impact the studied tundra environments.

4.5.1 Site characteristics Iceland

In Iceland, site characteristics followed the environmental gradient of sea proximity and altitude, with the site closest to the sea revealing the lowest mean SCD value of 69 days. As the distance from the sea increased, the mean SCD value also increased, with Ice2 and Ice3 having mean SCDs of 93 and 103 days, respectively. This trend was expected, as warm air from the sea promotes snow melt, while lower air temperatures at higher altitudes contribute to longer SCD (Semmens et al. 2013).

FVC also followed the environmental gradient, with Ice1 having the highest mean FVC at 74%, followed by Ice2 at 73% and Ice3 at 69%. The bimodal distribution pattern observed for FVC values (Fig. 34b) stems from the classification of the upper boundary of RECI at >2.0, beyond which it started to saturate. Consequently, RECI values over 2.0 were classified as fully vegetated, leading to the distinct peak at 100% FVC distribution. Streeter & Cutler (2020) observed an increase in the number of barren cover patches at higher altitude sites further inland in the study area. However, they noted that the total area of barren cover did not always follow this gradient. The total barren area likely reflects historical differences in stress along the gradient, such as grazing pressure, whereas the number of barren patches could be an indicator of contemporary levels of environmental stress due to their recent formation and dynamic nature, with the ability to either heal or erode further. In contrast, large erosion patches that persist over centuries may not accurately represent current environmental conditions (Streeter & Cutler 2020).

The sites exhibited minimal topographic variation, with low TPI values (-0.5 to 0.7) and surface roughness below 0.5, indicating gentle terrain with limited abrupt elevation changes or prominent features like deep hollows or high ridges.

4.5.2 Site characteristics Finland

In Finland, site characteristics followed the altitudinal gradient, with Fin1 (next to Saana mountain) having a slightly lower SCD of 152 days compared to Fin2 (Saana mountain top) with 158 days. This trend was expected due to lower temperatures at higher altitudes. However, the difference was smaller than anticipated, possibly due to higher wind speeds at higher elevations redistributing snow. For comparison, similar areas described as forb-rich meadows by Niittynen et al. (2020) had an average SCD of 190 days.

FVC also followed the environmental gradient, with Fin1 having a higher mean FVC at 41% compared to 31% for Fin2. This difference is not surprising, as more stressful and geomorphologically active conditions are expected at the mountain top (Hjort & Luoto 2009). However, the generally low FVC values in Finland compared to Iceland were less expected. This can be attributed to the small patch sizes and high land cover diversity within each 9 m^2 sensed pixel. Additionally, the presence of biocrust complicated the determination of the lower boundary RECI values used to define FVC. The biocrust exhibited very low vegetation index values, which differed minimally between barren cover

and lichen-covered boulders/gravel. The high presence of biocrust thus reduced the overall FVC values in the Finnish sites.

The Finnish sites exhibited greater terrain curvature and heterogeneity than Iceland, with TPI ranging from -2 to 2 at Fin1 and -3 to 3 at Fin2, and surface roughness reaching 2 at Fin1 and 3 at Fin2, indicating rugged terrain with distinct features like deep hollows and high ridges typical of an oro-Arctic setting.

4.5.3 Relationship between SCD and TPI

SCD and TPI exhibited a strong negative relationship across all sites, as expected, since hollows are more effective at trapping and protecting snow from redistribution and melt compared to ridges (Litaor et al. 2008). While the role of topographic features on SCD patterns and their variability is well established, the results align with this expectation due to the observed strong relationship. However, Ice1 and Fin2 sites displayed a non-linear relationship between SCD and TPI (Fig. 35a).

In Iceland, Ice1 exhibited a clear negative correlation, with hollows retaining snow for longer durations (of 65 to 103 days) compared to ridges, which retained snow for shorter periods (55–65 days). This difference is likely influenced by the moderating effects of warm sea air temperatures (Table 7).

In Finland, the pattern was similar but more variable due to the harsher climate and more pronounced topography. At Fin2, characterised by greater terrain curvature and ruggedness, SCD on ridges levelled out at approximately 150 days, likely influenced by snow redistribution from strong winds (Föhn & Meister 1983). The higher surface roughness and steep slopes at this site intensified snow movement and melt, contrasting with hollows where snow was retained for longer periods (up to 160 days). As Callaghan et al. (2011d) noted, snow redistribution in ridge areas is a critical factor influencing vegetation dynamics and barren cover formation.

4.5.3 Barren cover occurrence related to TPI and SCD

This study examined how microclimatic factors, specifically SCD and TPI, influence the distribution of barren cover (FVC) in Icelandic and Finnish tundra sites. The results indicate that the relationships between these factors and barren cover distribution vary across sites and environmental stress gradients. A key finding is the tipping point where

SCD transitions from supporting vegetation growth to promoting soil degradation. In Iceland, hollows with SCD below 70 days exhibit low vegetation cover, but once this threshold is exceeded, FVC changes stabilize, and vegetation cover becomes more consistent. In Finland, hollows with SCD around 150–160 days show optimal vegetation growth, but further prolongation leads to nivation and vegetation decline. These thresholds are critical for understanding tundra ecosystem resilience under changing snow regimes (Kelsey et al. 2023, Rixen et al. 2022).

The strong relationship between TPI and FVC indicates the importance of meso-topographic variability as a key factor in landscape development in both environments. In Finland, barren cover patterns varied with TPI and SCD at Fin1, depending on FVC classification. At <10% FVC, barren areas were confined to <-0.5 TPI and >160 SCD, representing truly barren areas driven by nivation. By contrast, at >20% FVC, barren cover extended to ridges and hollows, driven by aeolian erosion. This pattern reflects mixed land cover in a sensed 9 m^2 pixel, combining deflated patches (smaller than nivation patches), vegetation, and biocrust (Fig. 37,Fig. 31g).

TPI vs FVC

In Iceland, land curvature distinctly influenced land cover. Hollow positions (TPI < 0) were predominantly vegetated, while ridges (TPI > 0) were mostly barren (Fig. 37b). A similar division was observed with SCD, where thresholds (63 SCD at Ice1, 92 SCD at Ice2, and 101 SCD at Ice3) (Fig. 37a) aligned with the 0 TPI value (Fig. 35a), marking the transition between concave and convex positions. This suggests that topography may exert a stronger influence on FVC than SCD in these sites.

TPI significantly influenced FVC by shaping soil and vegetation responses to geomorphic processes. In Iceland, hollows consistently supported higher FVC, with Ice2 and Ice3 showing a plateau of vegetation up to TPI = 0, followed by sharp declines on ridges. This pattern reflects how hollows promote vegetation by retaining snow and shielding against harsh weather, whereas ridges are prone to erosion and reduced vegetation cover. This highlights the erosion-prone nature of Andosols, susceptible to deflation and freeze-thaw cycles, are particular sensitive to mesotopographic influence in modulating environmental pressures (Arnalds, 2015).

In Finland, deep hollows were expected to exhibit a negative correlation with FVC due to prolonged snow trapping, while shallower hollows offered beneficial growing conditions. This pattern was evident in Fin2, but Fin1 displayed greater variability in FVC values within hollow positions. Hollows at Fin1 provide both beneficial and detrimental factors, protecting vegetation from harsh weather but also facilitating nivation if snow remains trapped for extended periods (Aalto et al. 2021). Site-specific factors, such as geomorphology and hydrology, play a decisive role in determining whether hollows are conducive to vegetation growth. For instance, hollows in active geomorphic areas with sediment deposition or seasonal water flow may hinder vegetation establishment, as observed at Fin1. In the harsher environment of Fin2, stronger nivation pressures driven by biogeomorphological factors, such as vegetation-cryoturbation interactions, limit vegetation growth across altitudinal zones (Hjort & Luoto 2009).

Unlike this study, Riihimäki et al. (2017) found weak relationships between TPI and aboveground biomass (AGB) in the Kilpisjärvi Alpine tundra, likely due to their use of wider window sizes (50 m and 300 m radii) that smoothed out finer mesotopographic features. This study's use of 20 m radius better captured topographic variability, revealing significant FVC variation and its relationship to mesotopographic factors. These findings emphasise the need for carefully selecting kernel sizes that align with landscape variability.

FVC vs SCD

The relationship between SCD and FVC highlights the critical role of snow cover in shaping tundra vegetation patterns. Longer SCD generally supports vegetation growth by improving thermoregulation and extending moisture availability. However, beyond an optimal threshold, prolonged snow cover may inhibit growth by reducing the growing season.

In Iceland, FVC exhibited a positive linear relationship with SCD across all sites (Fig. 35c), with some variability in hollows (Fig. 36). Ice1 and Ice2 showed a sharp initial increase in FVC with SCD, followed by a plateau in Ice3, suggesting a threshold beyond which additional snow cover offers diminishing benefits. Coastal areas at lower altitudes exhibited lower barren cover than inland sites, likely due to reduced erosion pressure and higher biological productivity from warmer mean temperatures (Streeter & Cutler 2020) (Table 7). However, rapid SCD reductions can disrupt this advantage, as snow cover is

crucial for protecting vegetation in harsh environments (Callaghan et al. 2011d; Wahren et al. 2005). Reduced SCD may decrease functional vegetation variability (Niittynen et al. 2020b), while barren areas lacking vegetation complexity trap less snow, perpetuating environmental stress and erosion (Callaghan et al. 2011d; Wahren et al. 2005).

It is important to consider the difference between the initiation and maintenance of barren cover. The initiation of barren cover may be triggered by a reduction in SCD below a critical threshold, which can lead to decreased vegetation growth and increased soil erosion. Once barren cover is established, its maintenance may be facilitated by the feedback mechanism, where the lack of vegetation and structural complexity further reduces the area's ability to trap snow, thus perpetuating the barren state.

In Finland, FVC patterns were more variable due to differences in vegetation composition and environmental stress. Fin1 displayed an extended bell-shaped curve, peaking at 155 days of SCD, indicative of optimal growing conditions. Beyond this threshold, FVC declined due to shorter growing seasons caused by prolonged snow cover. Fin2, located in a harsher environment, exhibited a steady FVC decline with increasing SCD, with a minor peak at a similar threshold. This difference likely reflects the dominance of stress-resistant species like crowberry and biocrusts at Fin2, which are better adapted to low SCD (Choler 2015; Hejcman et al. 2005).

These findings align with broader research on snow cover’s role on vegetation in cold dependent regions. Jonas et al. (2008) found that faster-growing species emerging with earlier snowmelt in alpine regions, increasing biomass in the Alps. Choler (2015) demonstrated that the snow-free period length drives productivity variations in French alpine grasslands, while summer temperature and precipitation play secondary roles. Similarly, Hejcman et al. (2005) observed that vegetation cover in the Giant Mountains decreases with greater snow depth, though some species adapting to deep snow conditions. They found that snow depth and soil parameters were the key determinants of vegetation patterns

The contrasting SCD responses at Fin1 and Fin2 reflect differences in plant communities and environmental pressures. Fin2's dominance of stress-tolerant species supports a negative SCD-FVC relationship, while Fin1's bell-shaped curve parallels Icelandic trends, where SCD initially promotes vegetation growth before exceeding optimal conditions.

These site-specific responses underscore the complex interplay between snow cover duration, vegetation adaptation, and environmental stressors.

These findings suggest that vegetation in ridge positions benefits from moderate snow cover but plateaus or declines beyond optimal SCD. In hollow positions, vegetation initially thrives with longer SCD but eventually declines due to prolonged snow cover or the dominance of stress-resistant species in harsher environments.

4.5.4 Microclimatic factors controlling cryogenic processes

We expected that snow cover trapped in the hollows provides thermoregulation, protecting vegetation from cryoturbation and the risk of false springs, unlike in ridge areas. In addition, stronger winds in exposed ridge positions bring an additional chill and abrasion effect to the ground cover and further redistribute the snow (Sturm et al. 2001).

In both Iceland and Finland, the insulating properties of snow, which are influenced by topography and snow depth, strongly affected the variance in winter near-surface temperatures (Tyystjärvi et al. 2023). These effects were clearly observable in the two regions, with Iceland exhibiting a smaller difference in SCD between hollows and ridges (8 SCD) on average, while Finland displayed a larger difference (22 SCD) (Fig. 38). In Iceland, soil temperatures near freezing likely led to multiple frequent freeze-thaw cycles in the topsoil, around ridge areas, affecting soil stability and increasing the risk of soil erosion (Arnalds 2015). This is compounded by the low-cohesion and high-water retention of Icelandic Andosols, making them particularly vulnerable to cryoturbation and highly geomorphologically active. It is important to note that the probes were positioned 8 cm deep, suggesting that above-ground vegetation might experience even greater temperature variability due to atmospheric exposure and lower thermal inertia. In other microclimatic studies, such as Niittynen et al. (2024), the commonly used TMS-4 logger measures soil temperature at a depth of 6 cm.

In Finland, the microclimatic data showed a clear decrease in both the median and minimum temperature from the hollow to the ridge position, with an increase in variance towards the ridge. In mid-April, the ridge underwent freeze-thaw cycles for about two weeks. A strong increase in variance was likely related to the depth of snow cover and enhanced thermoregulation stemming from a greater disparity between air and soil temperatures (Kivinen & Rasmus 2015).

Our research confirms the critical role of snow cover in determining both barren and vegetation cover occurrence in tundra environments. This builds upon findings from various studies across Arctic regions. For instance, in the Canadian tundra, Grünberg et al. (2020) revealed a direct correlation between vegetation composition and local variations in snow depth. They found that topsoil temperatures varied significantly depending on vegetation type, with tall shrub tundra having the warmest topsoil, followed by tussock, dwarf shrub, and lichen tundra. These differences were attributed to the varying insulating properties of snow accumulation associated with different vegetation types. Areas with taller vegetation, such as shrubs, trap more snow, leading to better insulation and warmer topsoil temperatures. In contrast, areas with shorter vegetation, like lichens, accumulate less snow, resulting in colder topsoil temperatures and greater temperature variations. Furthermore, Aalto et al. (2017) demonstrated across Fennoscandia how cryogenic land surface processes (cryoturbation, solifluction, nivation) were associated with specific vegetation biomass characteristics. Notably, snow accumulation sites had the lowest aboveground biomass (AGB).

These insights reveal the broader impact of snow cover and biogeomorphological processes on Arctic ecosystems. Such processes not only foster diverse habitats and affect plant resources but also play a pivotal role in plant persistence and species recruitment, thereby significantly influencing community composition and biotic interactions (French 2017). Additionally, these geomorphological influences extend to plant functional traits, providing refugia and consequently altering patterns of occurrence, species richness, and community dynamics (Kemppinen & Niittynen 2022). When geomorphological pressures exceed the threshold conducive to plant establishment, the extent of barren cover increases.

4.5.5 Future Outlook

Changing climatic conditions and snow patterns are expected to significantly impact the tundra ecosystem by altering biological and geomorphological interactions and dynamics (Rixen et al. 2022). Warming in high-latitude regions in Europe is expected to significantly reduce cryogenic activity, with a projected 72% decrease in the periglacial climate realm by 2050 and complete loss by 2100, except at high elevations (Aalto et al. 2017). These processes are closely associated with biomass productivity in high-latitudes. Findings suggest that cold-region land surface processes may reach a critical tipping point in the

future, leading to significant changes in ground conditions and associated atmospheric feedbacks at the landscape scale (Aalto et al. 2021; Aalto et al. 2014).

In Iceland, these effects are likely to be more pronounced due to the rapid warming of the Arctic Ocean, which influences the coastal Arctic regions more intensely (Sasseville et al. 2024; Callaghan et al. 2011b; Callaghan et al. 2011a; Callaghan et al. 2011c). SCD is expected to decrease most rapidly in coastal areas, where mesotopography plays a crucial role due to the retention of snow in hollows (Callaghan et al. 2011c). A reduction in SCD could exacerbate stress-related feedbacks due to diminished protection, persistent winter storms, and the incidence of false springs (Callaghan et al. 2011c; Wahren al et. 2005). The anticipated rise in temperature variability is likely to intensify these stressful conditions, especially in coastal areas where previously protected hollows becoming exposed during winter. Conversely, more inland areas might maintain longer snow cover, potentially delaying these effects.

Reduced sea ice is expected to increase winter storms in the Arctic Ocean (Crawford et al. 2022), and the absence of protective snow cover could lead to increasingly severe impacts on the vegetation cover. Infrequent but severe winter storm events, such as those that occurred in northern Iceland in 1991 and 2019, can have detrimental effects on vegetation (Sigurður Þór Guðmundsson, pers. com.). In 1991, large, vegetated areas were stripped away by sharp ice crystals and high winds, while in 2019, the land was protected by snow cover and widespread damage was inhibited.

In Finland, the impact on SCD is expected to be less pronounced due to its more inland location and colder climate. In Norway, both historic estimates and future projections indicate that increasing temperature and precipitation are associated with substantial reductions in snow cover duration (Pirk et al. 2023).

Reduced SCD will particularly affect vegetation on ridges, particularly if winter warming events that create a "false spring" become more frequent. As a result, plants face an evolutionary trade-off: the benefits of earlier leaf emergence and a longer growing season must be weighed against the risk of tissue damage from exposure to frost activity (Allstadt et al. 2015). Frost damage can offset the benefits of favourable summer conditions, leading to reduced growth even in longer growing seasons (Choler 2018). Additionally, winter warming alters nitrogen dynamics, reducing bioavailable nitrogen for evergreen shrubs in the early growing season, as observed in West Greenland's mesic tundra heath

(Rasmussen et al. 2024). Sudden changes in winter tundra environment also increases the risk of rain on snow events and the formation of thick ice layers within the snowpack or at the ground surface, with particularly severe effects on permafrost, wildlife and society (Hansen et al. 2014).

Conversely, hollow positions could benefit from lower SCD, and areas previously affected by nivation might experience revegetation of barren lands, as it was observed in Alaska since the 1980s (Raynolds et al. 2013). Fin2 could also see an increase in FVC with reduced snow cover. However, to make more accurate predictions local knowledge of plant composition is crucial to understand future trajectories. Aalto et al. (2017) cautioned that warming might have contrasting effects on community compositions depending on the vegetation type and its responsiveness to climate change can vary greatly.

Overall, remote sensing indicates a general greening of the Arctic (Myers-Smith et al. 2020), but snow manipulation experiments show that earlier onset of snowmelt may not lead to increased productivity (Starr et al. 2008). In the long term, Arctic vegetation will likely undergo significant changes due to climate change and local environmental factors. The northward expansion of shrubs and trees (Myers-Smith & Hik 2018; Wolf et al. 2008) could increase productivity. However, this global trend is subject to local variation created by micro- to mesotopographic heterogeneity and associated microclimatic factors, as highlighted by this research. In some areas, vegetation may be damaged by increasing geomorphological pressures and barren cover formation (Bokhorst et al. 2009). The interplay between global processes and local environmental factors will determine the future trajectory of Arctic vegetation under a changing climate. Our findings emphasise the need to consider both global trends and local heterogeneity when assessing the impacts of climate change on tundra ecosystems.

In Iceland, air temperatures around the freezing point, along with a reduction in SCD, are expected to increase winter-related pressures such as cryoturbation and aeolian erosion, which will further reduce soil stability. The vulnerability of Andosols to mechanical disturbance may further intensify soil erosion and increase barren cover. These processes highlight the complex biogeomorphological interactions in Iceland's tundra ecosystems, where changes in climatic conditions and snow cover can significantly impact soil stability and vegetation dynamics. The potential increase in barren cover suggests a

decrease in the resilience of these ecosystems, as they become more susceptible to erosion and less capable of supporting vegetation growth.

In Finland, SCD predictions are more complicated. Milder winter temperatures and shorter SCD could have a minor impact on FVC, but variable early spring temperatures might intensify pressures, favouring stress-resistant plants. Given the Cryosols' resistance to erosion, an increase in barren cover is less likely, while areas in hollows could benefit from lower SCD and enhanced biological productivity. This indicates that Finland's tundra ecosystems may exhibit higher resilience to changing climatic conditions compared to Iceland, as the Cryosols provide a more stable foundation for vegetation growth and are less prone to erosion. A key finding emerging from the study is the ecosystem's adaptive capacity may be tested under variable early spring temperatures, while a shift towards stress-resistant plants or generalist species is suggested.

The findings of this study demonstrate the importance of considering biogeomorphological interactions and ecosystem resilience when assessing the impacts of climate change on tundra environments. The contrasting responses of Iceland and Finland's tundra ecosystems to changes in snow cover duration and temperature highlight the need for site-specific assessments and management strategies.

The findings can be used for areas with specific characteristics, such as exposed positions, low FVC, or low SCD, could be prioritised for erosion control measures. Furthermore, monitoring changes in barren cover and SCD over time could help identify areas where erosion risk is increasing, allowing for proactive management interventions to mitigate potential soil loss and associated ecological impacts.

CHAPTER 5: SOIL MOISTURE AND MESOTOPOGRAPHIC VARIABILITY SHAPE VEGETATION PATTERN AND STRUCTURE

5.1 INTRODUCTION

The climate of the tundra biome is becoming warmer, wetter, and more variable (IPCC 2023; Rantanen et al. 2022; Boisvert & Stroeve 2015). Arctic amplification is causing the region to warm 2 – 4 times faster than the global average (Rantanen et al. 2022; Post et al. 2019) and get wetter. Precipitation rates in the Arctic are similarly disproportionally increasing by 4.5% per degree of global temperature increase, compared to a global average of 1.6-1.9% (Bintanja & Selten 2014). These drastic changes have ecological consequences: broadly, as conditions ameliorate, we expect a 'greening' effect (borealization) as plants respond to improved conditions (Weijers et al. 2018; Vuorinen et al. 2017; Myers-Smith et al. 2011). However, tundra biomes are spatially heterogeneous (patchy) on a landscape scale (Virtanen & Ek 2014), so the ecological response to climate change is likely to vary from place to place. Relatively small differences in topography – common in tundra biomes – will play a key role in structuring the ecological response to climate change, as differences in the shape (curvature) of the land surface determine exposure, aspect, and hydrology, creating sharp microclimatic gradients on relatively small spatial scales. The effect of topography on soil moisture is likely to be particularly important, as small differences in moisture availability can have a disproportionate effect on plant productivity in stressful tundra environments (Kemppinen et al. 2019; Lara et al. 2018; Le Roux et al. 2013). Furthermore, in addition to imposing microclimatic gradients, topographic variation has been shown to amplify the impact of extreme weather events (Suggitt et al. 2011; Bennie et al. 2008). Thus, whilst tundra biomes as a whole are likely to become greener in the future, this effect will be spatially variable; some areas may witness modest changes or even a deterioration in growth conditions. Despite the obvious importance of topography in modulating this process, the interactions of climate, topography and vegetation cover on sub-landscape scales are not well understood.

Topographic variation plays a crucial role in determining the spatial heterogeneity of tundra vegetation (Le Roux & Luoto 2014). Our focus is on mesotopographic variation – i.e. relatively modest changes in relief (1-3 m) across lateral distances of tens to hundreds of metres – as this scale of topographic variation is common in tundra areas and relevant to

the growth and distribution of individual plants. Many tundra biomes were glaciated in the recent geological past, resulting in low-relief landforms such as moraines, drumlins and eskers. Contemporary periglacial and permafrost processes add metre-scale topographic variation. Mesotopographic variation determines important factors such as exposure to desiccating winds, depth and duration of snow cover, geomorphological activity (e.g., the movement of water and sediment via slope processes) and hydrology (Fig. 40). These processes create pronounced microclimatic gradients on small spatial scales, thereby shaping the environment in which plants grow.

A particularly important environmental factor related to mesotopography is soil moisture availability. In tundra biomes, local topographic high points (ridges) are exposed to desiccating winds and drain readily; snow cover is likely to be thin and short-lived (Ch. 4). In contrast, local topographic lows (hollows) are likely to be more sheltered, reducing desiccation by wind (Kemppinen et al. 2018; Müller et al. 2016). Liquid water will accumulate in hollows, as will snow (a vital source of moisture in the spring). Moisture limitation can severely constrain plant growth in tundra biomes, so small scale differences associated with mesotopographic variation are disproportionately important in terms of productivity, morphology, and community composition (Happonen et al. 2019; Niittynen et al. 2018). Future climate change may alter – and possibly accentuate – these gradients. For example, high temporal variability in soil moisture has been shown to be stressful to plants in tundra biomes (Cutler et al. 2023; Kemppinen et al. 2019). An increase in the magnitude and frequency of extreme precipitation events will tend to increase soil moisture variability; the impacts of these changes are likely to be greatest in those areas that already have a tendency towards moisture stress, i.e. ridges. In exceptional circumstances, increased stress will lead to reduced plant productivity and increased susceptibility to soil degradation.

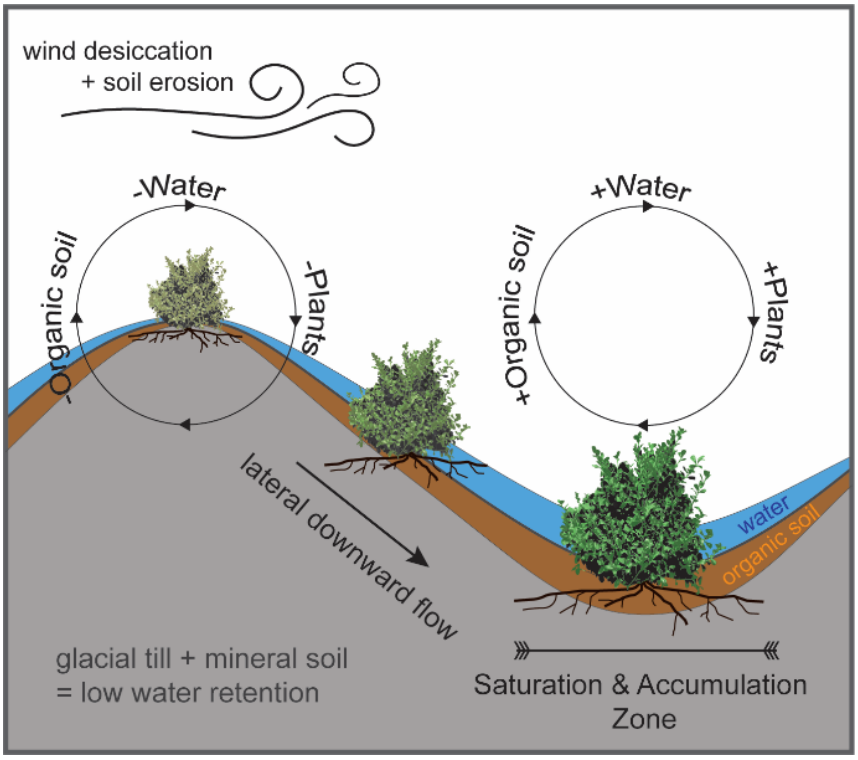

Fig. 40 Illustrates the impact of topography on soil moisture, soil organic carbon, and vegetation properties. In elevated areas like ridges, lateral flow and drainage deplete water, exacerbated by low soil organic content and glacial till with low water retention. Wind activity accelerates evapotranspiration and topsoil desiccation, while soil erosion reduces soil depth. In depressions, accumulated organic soil and stable soil moisture enhance nutrient availability, fostering favourable conditions for vegetation growth. Stressful or beneficial growing conditions are reflected by plant morphology and photosynthetic activity. Modified after Billings (1973), Western et al. (2002) and Kemppinen (2016).

Our understanding of microclimatic conditions, including soil moisture in high-latitude soils, and how their spatial distribution affects environmental stress and affect vegetation growth remains limited. Therefore, this study examined the spatial relationship between soil moisture, mesotopography, and vegetation properties within two tundra ecosystems. The main aims are:

- To understand the spatial variability of soil moisture influenced by mesotopographic variability, which serves as a proxy for microclimate conditions.
- To examine the relationship between microclimatic conditions and vegetation growth, evidenced by alterations in plant community composition, plant vitality, and structure.

To address these aims, we focused our study on three mesotopographic transects situated in two contrasting tundra environments: Iceland and Finland. Iceland, with its warmer climate (mean annual temperature 4°C) and thick volcanic soils, contrasts with

the sites in Finland, which are characterised by a colder climate (mean annual temperature -1.5°C), and thin Cryosols (Chapter 2, Fig. 10, 13). Despite these environmental variations, the amount of precipitation is moderate and similar between the sites of about 500 mm a^{-1}. The vegetation cover and current grazing intensity is similar, allowing meaningful comparison. Sites with different environmental conditions were chosen to encompass a range of climatic and soil conditions, broadening the scope of our research. By studying these different climates, we gain insights into the potential 'borealization' of tundra habitats as the climate ameliorates, with Iceland representing a warmer future for Finland's tundra ecosystems. This allows us to better understand how tundra environments may respond to future climate change scenarios.

Our transects encompassed a series of ridges (local topographic high points) and hollows (local topographic low points). We hypothesised that:

1) Hollow areas are likely to exhibit consistently high soil moisture availability and low soil moisture variability compared to ridges. This disparity is attributed to lateral downflow of soil moisture, desiccation effects from wind exposure, and the scarcity of organic soil content on ridges, all of which contribute to increased environmental stress for plants.

2) Plant community composition and indicators of environmental stress are closely linked to mesotopographic positioning. Hollows, offering beneficial growth conditions, are expected to support higher plant vitality, associated with increased photosynthetic activity and biomass productivity. In contrast, vegetation near or on ridges is presumed to experience heightened stress levels, resulting in a higher proportion of stress-tolerant plant species, and reduced plant vitality of individual species compared to those in hollows.

The research methodology combined very-high-resolution remote sensing imagery with field measurements of soil moisture and vegetation cover. Spatial information was acquired from multispectral uncrewed aerial vehicle (UAV) surveys. The processed orthomosaic, combined with a land cover survey, facilitated supervised classification to categorise plant functional types (PFTs) and calculate vegetation indices. A digital surface model (DSM) was simultaneously generated to classify the terrain into distinct topographic features and calculate the topographic position index (TPI). Combining this

spatial information allowed us to assess plant vitality for PFTs in distinct mesotopographic positions across a landscape.

Additionally, in-situ soil moisture probes were deployed along the mesotopographic transects, providing hourly measurements throughout the year. The vegetation cover over each soil moisture probe was surveyed, along with structural information on dwarf birch, such as plant height, leaf area, and leaf weight (Finnish sites only). The field data gave direct insight into the local soil moisture and vegetation dynamics related to microclimatic conditions.

5.2 STUDY DESIGN

The study areas are located in northeastern Iceland close to Phorshöfn, and in northern Finland, close to Kilpisjärvi. The study plots are located within the investigated sites in the previous chapter, two of them in Ice2 and one in Fin1 (Fig. 31). In the centre of these study plots soil moisture probes were deployed in 2021 – 2023 (Fig. 41).

The study plots were split into a larger area, Y, and a smaller study area, X (Fig. 41). The smaller study areas were limited in size, to ensure comparability between soil measurements, vegetation and spatial data. The X plots were delineated to encompass a single mesotopographic unit comprising a hollow, slope and ridge. In Iceland, the X plots were square, measuring 35 × 35 m for Icex1 and 40 × 40 m for Icex2 (66.138° N, -15.494° E). In Finland, the X plot (Finx, 69.060° N, 20.830° E) measured 50 × 50 m Finx, with the top-left and lower-right corners cut to accommodate steep slopes and to exclude a neighbouring ridge.

The larger Y plots encompassed 11.2 ha in Iceland (Icey) and 5.1 ha in Finland (Finy). This larger area was chosen to evaluate whether the spectral changes observed at a fine scale are also discernible at the landscape level.

We selected our X and Y plots based on the following criteria:

- Hollows are neither waterlogged nor close to water sources.
- Hollows are not exposed to strong nivation pressure (see last Chapter 4).
- The macrotopography surrounding the mesotopographic feature under study should have a consistent, flat surface with little to no slope (only applied to X plots).

- Study plots should have as little barren cover as possible to ensure minimal disruption in soil hydrology and to maximise the chance of capturing a topographic signal (only applied area X).

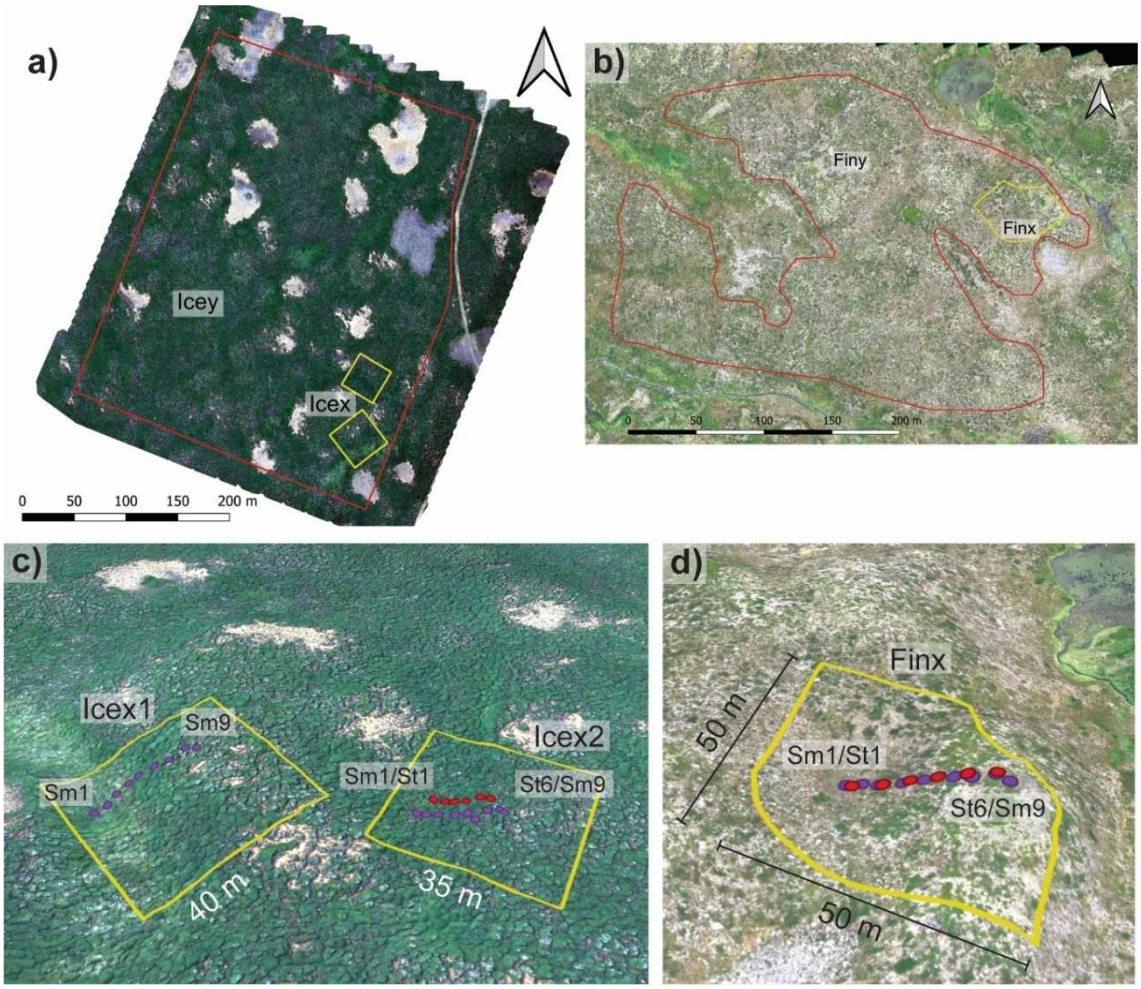

Fig. 41 RGB overview of study areas in a) Iceland and b) Finland. The wider area is denoted as Y the smaller as X. Oblique 3D view of the study sites in c) Iceland and d) Finland. Note the bright spot in the lower left corner, which is a neighbouring hollow exposing boulder and a result from nivation. The terrain was 3x vertically exaggerated to better visualise terrain features. Purple dots (Sm) show locations of soil moisture sensors and red dots (St) shows soil temperature sensors. For the vegetation survey in total four transects were surveyed. Icex1-Sm, Icex2-Sm, Icex2-St and Finx-Sm/St. RGB and DSM are derived from UAV survey.

5.3 METHODS

For each site, mesotopography was derived from digital surface models (DSMs) generated from UAV imagery. This elevation data was used to classify the terrain at the small area (X), while for the wider area (Y) the topographic position index (TPI) was calculated. Soil moisture properties were recorded hourly over a period of approximately one year using

soil moisture probes deployed along a mesotopographic transect. Plant communities were surveyed using quadrats positioned above the deployed probes along the mesotopographic gradient. Additionally, point coordinates of plant functional types (PFTs) were collected, and land cover maps were generated using UAV imagery. Plant vitality information was derived from UAV imagery and calculated vegetation indices.

5.3.1 Soil moisture

5.3.1.1 Soil moisture data collection

Soil moisture was recorded hourly in Iceland over a period of 25 months (Aug 2021 – Sept 2023) and in Finland 12 months (July 2022 – July 2023) (Table 13).

At both sites we established two transects consisting of nine SMT150 soil moisture probes connected with a Delta-T GP2 data logger (Delta-T Devices, Cambridge, UK). The transects were arranged along a mesotopographic elevation gradient ranging from 1 to 2 meters in height and 17 to 27 m in length (Table 13). Probe Sm1 was located in the hollow, and Sm9 was positioned at the ridge. At each site, we carefully removed the topsoil and installed the probes at a depth of 8 cm in Iceland (approximating the depth of the root zone) and a depth of approx. 3 cm in Finland, where the thin soil layer (just a few cm) varied considerably over the topographic transect and limited the depth of the probe placement (Fig. 42). The topsoil was then replaced over the probes to ensure complete coverage while preserving the integrity of the vegetation cover.

Recordings at Icex2 for the year 2022 were shortened, due to redeployment of the instrument to Finland (Table 13). The soil moisture recording in Finland for 2023 was cut short due to a depleted battery. In Iceland at Icex1 probe Sm9 was placed in a microtopographic (cm-scale) elevated feature (thúfur top), and therefore excluded from the analysis, but plotted in the time series. In Finland probe Sm5 was excluded due to malfunction. Substantial rainfall events were identified in the time series when a soil moisture probe recorded a sudden increase of 10% or more in soil moisture content. The onset of snowmelt was also marked and determined when the soil temperature consistently rose above 0°C.

Table 13 Details about logger placement and sensing period.

Transect Logger	Transect length	Height range	Probe depth	Sensing period
Icex1 Sm	16.8 m	1 m	8 cm	26/08/2021 – 19/09/2023
Icex2 Sm	24.2 m	2 m	8 cm	26/08/2021 – 13/06/2022
Finx Sm	26.7 m	1.7 m	~3 cm	23/07/2022 – 10/07/2023

Fig. 42 Soil moisture probes deployed in a) Iceland and b) Finland. Both probes represent position in the hollows. Note the difference in the thickness of organic soil with darker appearance. In Finland after a few centimetres mineral soils were present.

5.3.1.2 Soil moisture analysis

Only soil moisture data from the growing season was analysed. In tundra environments, plant growth usually starts at temperatures above 0°C (Tieszen 1978). The onset of the growing season was based on the soil temperature data from the previous chapter, and defined as the point when any probe along the transect recorded a daily average temperature exceeding 3°C. This period extended until the last probe's daily average temperature fell below this threshold. The 3°C threshold was chosen because it represents the approximate minimum temperature at which biological activity begins, marking the transition from winter dormancy to the growing season. This initial processing resulted in a soil moisture dataset encompassing three growing seasons in Iceland (Icex1 for 22 months and Icex2 for 10 months), and two growing seasons in Finland (Finx1 15 months: (Table 14)).

*Table 14 Period of recorded soil moisture within the growing seasons 2021, 2022 and 2023 in Iceland and Finland. Growing season was defined when a single sensor had an average temperature above 3°C, until the last sensor drops below that threshold. Note, only one complete growing season was recorded in Iceland 2022. * indicates the start and the end of the recording period.*

Period recorded in growing season	2021	2022	2023
Iceland (Icex1 Sm)	27/08* – 31/10	30/04 – 27/11	19/4 – 19/9*
Iceland (Icex2 Sm)	27/08* – 31/10	30/04 – 13/06*	-
Finland (Finx Sm)	-	23/07* – 30/09	11/5 – 10/07*

The median soil volumetric water content (SWC) was derived for each probe and water stress was calculated as the temporal variability of the soil moisture coefficient of variation (CV) (Brown 1998). The CV is calculated by dividing the standard deviation (σ) by the mean and multiplying by 100, providing a percentage that represents the relative variability of the dataset.

$$CV\% = 100\sigma/mean$$

To ensure comparability in the NMDS (Non-metric Multidimensional Scaling) analysis, both CV and median soil moisture were calculated as explanatory environmental variables for identical periods in Icex1 and Icex2 (limited by the sensing period of Icex2). Quartile regression analyses were conducted for each soil moisture transect, including the entire growing season dataset. Quartile regression estimates the relationship between variables at different quantiles, providing a more comprehensive understanding of how soil moisture conditions change across the mesotopographic gradient, rather than just the average effect. This is particularly useful as the influence of soil moisture on vegetation may vary depending on whether soil moisture levels are low, moderate, or high.

5.3.2 Vegetation

5.3.2.1 Vegetation composition survey

A vegetation survey was conducted at 24 quadrats in Iceland (June 2022) and 9 quadrats in Finland (26 July 2022). The quadrats were 1 m^2 and recorded at ~2 m intervals along the mesotopographic slope under study; the centre of each quadrat was placed directly above the soil moisture or temperature probe. In the quadrats, all present plant species were recorded, and their percentage cover was estimated using the Domin scale (Hurford 2006) (Table A9 in Appendix). In Iceland, all the grass-like vegetation was combined into the class ‘Graminoid’. Mosses and lichens were also not classified to the species level.

5.3.2.2 Plant traits data

Plant trait information was collected in Finland. The dwarf birch (*Betula nana*) was selected for plant trait measurement as it is common across the sub-Arctic and present in all quadrats along the transect.

Information on plant height (cm), leaf area (cm^2), leaf dry matter content (LDMC) (dry weight/fresh weight; $g\ g^{-1}$) and SLA (specific leaf area/dry weight; $cm^2\ g^{-1}$) were collected following procedures described in Kemppinen & Niittynen (2022).

Leaf samples were collected on the 26 July 2022 and processed the same day before drying them. Firstly, heights from the soil surface to the highest photosynthetic part (i.e. excluding stem) were measured for three to four individual plants per plot using a ruler. Secondly, two leaf samples from each dwarf birch individual were collected. Only mature leaves without marks or any kind of damage were sampled. Sampled leaves for each plot were put together and kept in zip-lock bags with dampened paper towels. In the laboratory, we kept the samples in the zip-lock bags at 4°C between measurements. Thirdly, the petioles were cut and subsequently weighed using a Mettler AE 100 scale (0.0001 g precision) to measure their fresh weight. Fourth, the leaves were scanned using a Canon CanoScan LiDE 20 scanner (600 dpi resolution) to measure their area. The leaf area was calculated from the scans using the ImageJ software via R with functions from the LeafArea R package (Katabuchi 2015). Finally, the leaves were dried at 70°C for 48 h using VWR VENTI-Line ovens, and then reweighed. The level of observations were individual plants for plant height, individual leaf for leaf area and plot-level means for LDMC and SLA. This resulted in a total of 48 observations of four traits for dwarf birch.

To assess the effect of topographic position on plant trait variables, a one-way analysis of variance (ANOVA) for each trait was conducted. ANOVA was chosen to determine if there were any statistically significant differences between the means of the three topographic positions (hollow, slope, and ridge). This test is appropriate for comparing means across multiple groups and is widely used in ecological studies (Travis, 1998), assuming that the data in each group are normally distributed and have similar spread across all groups. However, due to the small sample size and difficulty in assessing normality, a non-parametric Kruskal-Wallis test, which does not assume normality, was also conducted and revealed similar results. Topographic position was based on the topographic

classification of the X plot (p. 147, Ch. 5.3.3.4), and the plant sampling location (Fig. 62). Four measurements are assigned to hollow, three to slope and five to ridge position.

For traits where ANOVA indicated significant differences ($p < 0.05$) and marginally significant ($p < 0.1$), a post-hoc Tukey's Honest Significant Difference (HSD) test was performed. The Tukey's HSD test allows for multiple pairwise comparisons between group means while controlling for Type I (false positive) error rate (Tukey, 1949). This test is particularly useful in identifying which specific groups differ from each other when the ANOVA suggests an overall difference. The combination of ANOVA and Tukey's HSD provides a robust framework for detecting and characterising differences in plant traits across topographic positions, allowing us to identify patterns of trait variation in relation to landscape features.

5.4.2.1 Plant Community Analysis

To explore the relationships between community composition and environmental variables, non-metric multidimensional scaling (NMDS) with local regressions was performed. NMDS analysis illustrates the differences in species composition and cover (including barren cover and stones) distribution across the surveyed quadrats. Proximity of points in the ordination space indicated similarity between the land cover as well as the presence/absence of species; conversely, points that are more distant from one another represent greater dissimilarity. The surveyed quadrats were assigned to specific topographic positions (hollow, slope, ridge) based on altitude classification (Fig. 62).

To minimise the impact of rare species on the multivariate analysis (Poos & Jackson 2012), taxa present in less than 5% of the quadrats, which equals presence in only one quadrat, were excluded.

NMDS, an ordination method, compresses multidimensional data into a two-dimensional space. Unlike ordination methods that utilise Euclidean distances, NMDS operates on rank orders, offering enhanced flexibility for handling complex and non-linear data relationships (Minchin 1987). It facilitates an intuitive understanding of the spatial relationships among data points (quadrats), preserving their relative distances. This approach effectively illustrates the similarities or differences among quadrats, such as variations in plant community composition across varied topographies, thus aiding in the identification of discernible patterns or clusters.

The NMDS was performed using functions from the *vegan* package in R (Oksanen et al. 2022), employing the *metaMDS* function with Bray dissimilarity and twenty iterations for optimisation. The *envifit* function was subsequently applied to establish the most accurate linear relationship for each environmental variable in relation to the NMDS ordination scores, with the significance of these relationships assessed through permutation testing.

The *ordisurf* function was used to plot smoothed surfaces and linear alignment of soil moisture data onto the ordination space. *Ordisurf* employs a general additive model (GAM), with the environmental data serving as the response variable and the NMDS axes as predictors. In Finland linear alignment was generated for the smoothed surface but there were too few unique covariate combinations (environmental data points) to compute the model effectively. Quadrats (2,6,7,9) were excluded from the GAM due to missing soil moisture data, either due to the failed Sm5 probe or where only St probes were present.

5.3.3 Near-Range Remote sensing

UAV surveys were conducted in the later part of the growing season (23 Aug 2021) in Iceland and during peak growing season in Finland (19 July 2022) (Table 15). Detailed UAV survey information and land cover classification for Iceland is described in Chapter 3. Therefore, only the survey in Finland will be described below.

5.3.3.1 UAV survey Finland

The equipment and survey methodology were the same as those applied in Iceland. A DJI Phantom 4 multispectral (P4m) quadcopter was used, equipped with a Blue (B) (450 nm ± 16 nm); Green (G) (560 nm ± 16 nm); Red (R) (650 nm ± 16 nm); Red-edge (RE) (730 nm ± 16 nm); and Near-infrared (NIR) (840 nm ± 26 nm) sensors (Fig. 43). Flight planning and execution followed the recommendations of the HiLDEN drone network protocol (Assmann et al. 2019). A reflectance target (Mapir Inc., San Diego) was imaged several times during the survey and the image that best resembled the prevailing light conditions was later used for radiometric calibration. Eight ground control points (GCPs) were selected prior to the flight and geolocated with a Spectra Precision ProMark 120 GPS system (Spectra Geospatial, Westminster CO). The surveys were flown along a lawn-mower flight pattern and at an above ground altitude of 70 m, resulting in an average

ground sampling distance of ~5 cm. Images were acquired with 80% front and side overlap and close to solar noon.

Fig. 43 Multispectral UAV and reflectance target used for the aerial survey.

The survey area is at the Fin1 site, as described in the previous chapter. It is situated on a slight slope, ranging from an elevation of 620 to 680 m, with a total length of 800 m. The total area surveyed was 34.5 hectares, split into two flight missions. The surveyed upper part of the slope was used for this study. Flight details are shown in (Table 15) along with the corresponding Icelandic survey.

The UAV processing steps and the generated orthomosaics are the same as described in Chapter 3.

Table 15 UAV survey details of the study area

Location	Date / Time	GCP	Flight altitude	Conditions	Notes
Iceland	23 Aug 2021, 13:53 – 14:36	8	70 m (5 cm spat. resolution)	Inconsistent Cumulus cover - sun mostly obscured	90° gimbal, Lawn-mower flight pattern
Finland	19 July 2022, 12:00 – 13:55	8	70 m (5 cm spat. resolution)	Complete cumulus cover - sun obscured	90° gimbal, Lawn-mower flight pattern

5.3.3.2 Land cover classification

A ground land cover survey was conducted in July 2022 in Kilpisjärvi to collect point coordinates for a supervised classification. For high-precision positional accuracy, a

Spectra Precision ProMark 120 GNSS system with differential GPS (dGPS) capability, comprising a Base and a Rover instrument, was used. In total, 455 points were collected from 16 different land cover classes shown in Table 16. Points were selected based on the judgment of the surveyor, aiming for a representative sample for each class and spatial even distribution. Emphasis was placed on collecting vegetation cover points because vegetation types are more challenging to differentiate than barren cover or water in the UAV orthomosaics.

The collected land cover points were post-processed utilising the Base GPS data and the Spectra Precision Survey Office software to augment positional accuracy. Challenges were encountered with the dGPS system. The software failed to process all of the land cover points, with only a fraction of the data being usable. Possibly due to malfunctioning dGPS devices during recording. Following that process, a total of 292 land cover points were available for analysis.

Table 16 Datapoints collected for different land cover classes. Unprocessed column shows the raw total data collected. The processed column is the datapoints available after post-processing using dGPS.

Land cover	Points unprocessed	Points processed
Dwarf birch	65	46
Biocrust	67	41
Crowberry	55	41
Juniper	50	38
Bilberry	61	34
Mountain heath	29	18
Woolly willow (*Salix lanata*)	7	3
Bilberry mirth (*Vaccinium myrtillus*)	2	1
Grass + Forbs	34	26
Grass	21	11
Wetland	10	6
Moss	14	9
Lichen	5	4
Deflated	23	8
Barren	9	6
Rock	3	-
Total	455	292

The land cover was defined into eight PFT classes, as they were spectrally distinguishable and act as functional groups (Fig. 44): barren (glacial till, rocky surface), biocrust (including lichen and moss), mixed, low-stature shrubs bilberry (*Vaccinium uliginosum*, *-myrtillus, -vitis-idaea*) and mountain heath (*Phyllodoce*), dwarf birch (*Betula nana*), juniper (*Juniperus communis*), crowberry (*Empetrum nigrum*), grass and forbs, wetland (waterlogged soil + *Eriophorum angustifolium, Sphagnum*).

A more detailed classification of the class of low-growing shrubs was complicated due to the frequent co-occurrence of mixed prostrate shrub species and their spectral similarities (Fig. 44e). Similarly, the Grass/Forbs class encompasses multiple species; however, this class is almost absent in the study plots.

A supervised classification method was applied to categorise the land cover into distinct classes. The process began with manual delineation of training and validation areas using collected land cover data points, generated orthomosaics, and field photographs. The selected land cover classes were consistent and clearly distinguishable throughout the surveyed area. This approach ensured an adequate sample size for each class to train and validate the classification model. The manually identified land cover areas were then randomly split, with 70% used as training data and 30% reserved as validation data for accuracy assessment of the supervised classification.

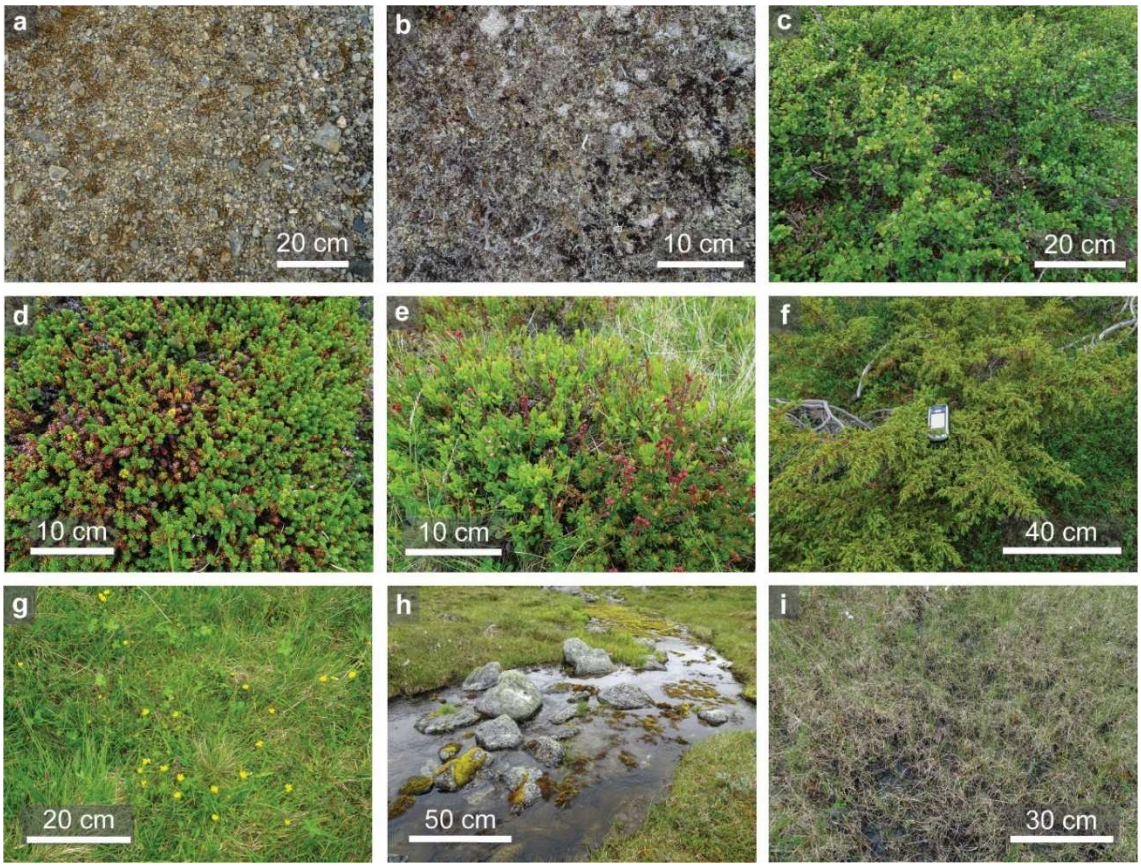

Fig. 44 Land cover types used for classification. a) Barren cover, b) Biocrust, c) Dwarf birch, d) Crowberry, e) Low-stature shrub, f) Juniper, g) Grass/Forbs, h) Water, i) Wetland. Scale at h) is only representative of the bottom of the image, due to the perspective.

The following workflow was applied for the classification (Fig. 45). Spectral bands and indices, including NDVI (Tucker 1979) and RECI (Gitelson et al. 2003), were used due to

their sensitivity to vegetation composition and barren cover identification. DSM was also included, as vegetation composition is influenced by elevation changes. The support vector machine (SVM) classifier was applied, which showed better performance compared to the Random Forest classifier in this setting. The Orfeo ToolBox (OTB) was used in QGIS (3.28) for the classification workflow. Image statistics were computed and included in the model. Training and validation data for each individual class and site was created based on the ground land cover survey and visual interpretation of the very-high-resolution UAV imagery. The SVM model was trained with the training data using the *TrainImageClassifier* tool, with default settings. In this setup, an RBF (Radial Basis Function) kernel was used, which is effective for capturing nonlinear relationships in the data. The cost parameter C=1 balanced the trade-off between maximizing the margin and minimizing misclassification errors, while gamma γ=1 controlled effectively the influence of individual data points. Additionally, the model type was configured as CSVC (C-Support Vector Classification), the standard approach for classification tasks. Afterwards, the *ImageClassifier* was applied using the trained SVM model, image statistics and processed layers for each site. Subsequently for accuracy assessment, a Confusion Matrix was computed with the validation data and the Precision, Recall, F-score and Kappa were calculated for each site (Table 17, 18). These are established metrics in classification assessment. The F-score, a measure that balances precision and recall, is often used to evaluate the performance of binary classification models. Kappa, or Cohen's Kappa, is a statistic that measures inter-rater reliability for categorical items, comparing the observed agreement with the expected agreement by chance (Campbell, 2011).

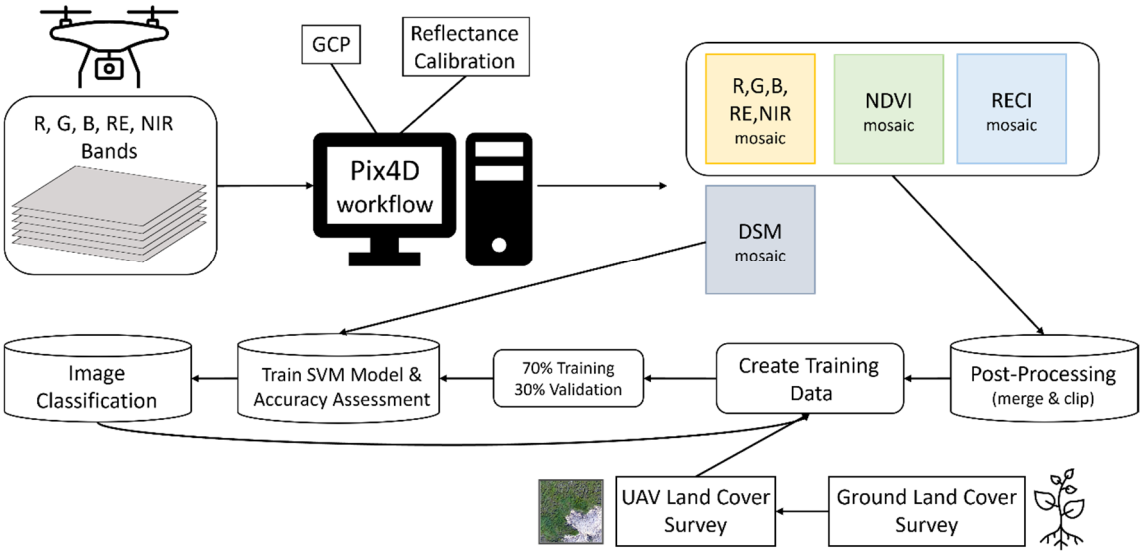

Fig. 45 Workflow from UAV image acquisition to land cover classification. SVM (Support Vector Machine)

Table 17 Confusion matrix of the land cover classification.

	Barren	Grass/ Forbs	Dw. birch	Juniper	Ls-shrub	Crowberry	Biocrust	Water
Barren	3186	0	0	0	0	0	54	0
Grass/Forbs	0	3146	2	38	41	2	11	0
Dwarf birch	0	7	3035	115	60	23	0	0
Juniper	0	79	446	2428	128	158	1	0
Ls-shrub	0	26	28	30	2964	172	20	0
Crowberry	0	8	9	104	273	2843	3	0
Biocrust	26	21	0	0	11	0	3182	0
Water	3	0	0	0	0	0	3	3234

Table 18 Accuracy table of the land cover classification. The Kappa value for all classes is 0.92.

	Barren	Biocrust	Dwarf B.	Crowberry	Ls-shrub	Juniper	Grass/ Forbs	Water
Precision	0.99	0.97	0.86	0.89	0.85	0.89	0.96	1.00
Recall	0.98	0.98	0.94	0.88	0.91	0.75	0.97	1.00
F-score	0.99	0.98	0.90	0.88	0.88	0.82	0.96	1.00

5.3.3.3 Vegetation indices

In this study, vegetation indices were used as proxies for assessing the physiology and vitality of tundra vegetation cover. Changes in the spectral reflectance of vegetation cover can serve as indicators of plant vigour. Vegetation indices have proved to be valuable tools for assessing vegetation vigour, water-stress or biomass quantity (Barton 2012;

Hope et al. 1993; Walker 2003). These indices are particularly useful when focusing on specific facets of plant physiology, such as alterations in pigment content or changes in traits such as leaf-area or structure in response to stress (Barton 2012). Given that plant species exhibit distinct spectral responses to stress, indices were computed for each type of vegetation cover, as delineated by our land cover classification.

The application of the narrow band red-edge (RE) is particularly advantageous for evaluating vegetation stress (Sims & Gamon 2002; Gitelson et al. 2003) (Fig. 46). Zagajewski et al. (2018) investigated the effectiveness of in-situ hyperspectral remote sensing techniques for evaluating the health of vegetation in the high-Arctic. Their findings indicated a strong relationship between pigment-driven spectral indices, measured in narrow bands, and the actual pigment concentrations within the vegetation. RE indices, which hinge on the steepness and position of the RE slope—a transitional phase between the visible red region and the near-infrared (NIR) segment of the electromagnetic spectrum (Gitelson & Merzlyak 1994)—are instrumental. Alterations in the slope and position of this transition zone is notably sensitive to variations in chlorophyll concentration to scattering by the canopy structure (Zagajewski et al. 2017; Carter 1993). The narrow spectral band range has also shown to be a useful indicator of drought stress (Zhu et al. 2021).

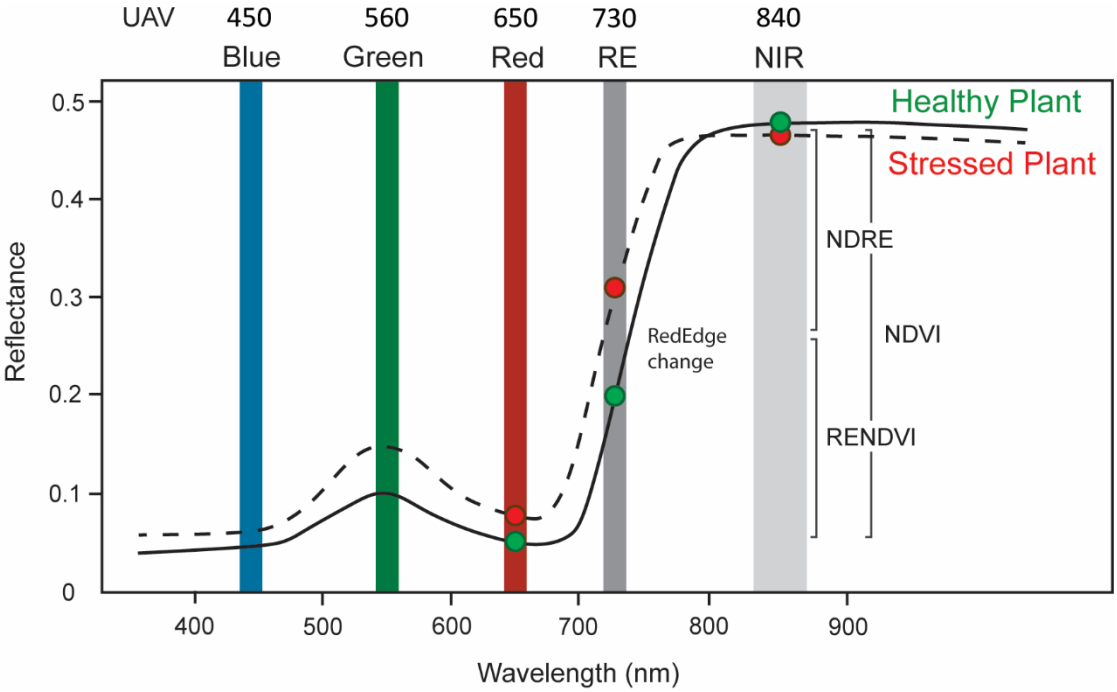

Fig. 46 Generalised spectral change of plants when chlorophyll content gets reduced in different growing stages or as stress response. Notable changes occur in the red-edge region, leading to different outcomes of vegetation indices depending on the ratio of spectral bands. Modified after (Kancheva et al. 2014).

The following three vegetation indices (NDVI, RENDVI, NDRE) chosen for the study were selected based on their useability as proxies for plant physiology and proven applicability in Arctic tundra ecosystems. These indices align with the study's aim of analysing vegetation dynamics influenced by environmental gradients, providing robust tools for assessing vegetation health:

(6) $$NDVI = \frac{NIR - Red}{NIR + Red}$$

(7) $$NDRE = \frac{NIR - RedEdge}{NIR + RedEdge}$$

(8) $$RENDVI = \frac{RedEdge - Red}{RedEdge + Red}$$

The broadband index selected for this analysis was the normalized difference vegetation index (NDVI) (Tucker 1979), which is an established index particularly used for estimating biomass and leaf area index (LAI) (Goswami et al. 2015; Walker 2003; Riedel et al. 2005). Biomass and LAI exhibit exponential relationship with NDVI, suggesting saturation for

higher values of biomass (> 100 g/m^2) and LAI (> 2m^2/m^2) (Goswami et al. 2015). NDVI has low saturation level at values of about 0.8 NDVI (Aalto et al. 2021), making it insensitive to changes in plants with high values.

It is anticipated that the most significant changes occur in the red-edge (RE) range when plants are stressed; therefore, vegetation indices in this region were selected as well (Fig. 46). For narrow-band indices, the normalized difference red edge (NDRE) and red edge NDVI (RENDVI) were chosen, based on the spectral bands available from the UAV survey. The RENDVI is sensitive to changes in chlorophyll content (Gitelson & Merzlyak 1994), making it useful for monitoring slight variations in vegetation health and stress before they are visible in the NDVI. In a study by Zagajewski et al. (2017), RENDVI proved to be the best vegetation index for the high-arctic plant *Dryas octopetala* for upscaling from surface measurements to satellite RapidEye (5m spatial resolution).

Like RENDVI, the NDRE does not saturate quickly and can be also applied to biomass estimation (Sharifi & Felegari 2023). Furthermore, NDRE has proven to be a useful indicator in assessing the nitrogen status of crop canopies, and is related to chlorophyll content and water stress factors (Barnes et al. 2000). It can be a better indicator of crop health in later growth stages where NDVI might become saturated (Nguy-Robertson et al. 2012).

5.3.3.4 Topographic classification

Topographic classification methods integrate the environmental implications of terrain shape and position to represent specific landforms (Bolch & Loibl 2017; Deng 2007). Digital Elevation Models (DEMs) are commonly used to generate indices such as the topographic position index (TPI), local elevation, and relative hill slope position, for terrain classification (Mokarram & Sathyamoorthy 2018). Since the majority of landforms are scale-specific (Mokarram & Sathyamoorthy 2018), it is crucial to use suitable data that reflect the scale of the geomorphic features. Failing to account for this can lead to misrepresentation of terrain and, consequently, misrepresentation of microclimatic conditions such as soil moisture (Kemppinen et al. 2018). To address this issue and accurately depict the topography of each site, high resolution Digital Surface Models (DSMs) data from the UAV survey were used with a GSD of (5 cm).

For the larger Y areas, the TPI (Reu et al. 2013; Jenness 2006) was calculated to indicate convexity or concavity in the landscape, using the approach described in Chapter 4. TPI is useful for capturing the relative position of a point on a landscape, providing information about its elevation in relation to the surrounding area. It helps to identify landforms such as ridges, hollows, or flat/tilted areas, which affect local environmental conditions and thus microclimates. DSMs generated from the UAV surveys were employed to derive TPI, with a window size of 20 m applied in both Iceland and Finland, as it best represented the mesotopographic variability at the desired scale (same window size as the previous chapter).

For the smaller plots X, where the complexity of the terrain features is confined to a small spatial domain, a local elevation classification was used (Hatfield 1999). The plots were classified into hollows, slopes, and ridges based on altitude. Structural features that protruded from the surrounding terrain and were initially classified into a higher elevation class were subsequently reassigned to the preceding elevation class manually. Fig. 47 shows how thúfur or protruding shrubs were categorised within the hollow zone. This classification is based on the rationale that the shrub's root network remains within the depression, thus benefiting from more favourable soil properties.

The Finnish site has been further divided into lower- and upper slope due to slightly steeper topographic profile. The boundaries (in m altitude) are as follows:

Icex1: Hollow <108.8< Slope <109.4< Ridge;
Icex2: Hollow <108.8< Slope <109.4< Ridge;
Finx: Hollow <702.6< Lower Slope <703.1< Upper Slope <703.6< Ridge;

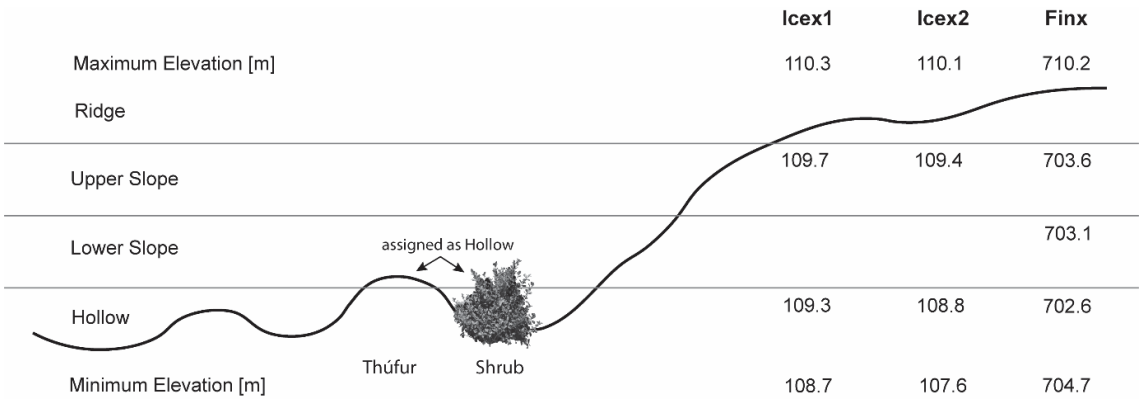

Fig. 47 Classification of topographic zones with boundary values shown for each study site.

5.3.3.5 PFT, Vegetation Indices and Topographic position

The aim was to quantify the vigour of different PFTs in different topographic positions. For the smaller X plots, the PFT were grouped by topographic position and for each topographic position (hollow, slope and ridge) the mean vegetation index (NDVI, RENDVI, NDRE) was calculated.

To determine whether PFTs significantly differ across topographic positions, the Kruskal-Wallis test was applied (McKight & Najab 2010). This non-parametric method assesses differences across multiple groups without presuming any specific distribution. Although it identifies the presence of differences, it does not specify where these differences occur, or the number of group pairs affected. For precise comparisons, Dunn's test was employed for pairwise analysis with Bonferroni adjustment and pairwise Mann-Whitney tests, to identify specific pairs exhibiting stochastic dominance.

For the larger area Y, the TPI served as the indicator for land exposure. Given that both the vegetation indices and TPI are continuous variables, boxplots were plotted to visualize trends for each species.

5.4 RESULTS

5.4.1 Soil moisture

The data on soil moisture revealed a general trend of decreasing moisture from the hollow to the ridge position, although the coefficient of variation (CV) pattern differed between Iceland and Finland (Fig. 48, 49). In Iceland, the mean soil water content (SWC), measured volumetrically, decreased gradually from a 54% mean in the hollow to a 32% mean at the ridge position. Conversely, in Finland, no overall trend was observable in SWC from the hollow to the ridge, with a narrow range from about 19 to 11% (Fig. 48). While the mean decrease in Iceland is notable, the variation in CV values across the Ice1 and Ice2 transect is relatively small, ranging from 12 to 30% CV. In Finland, higher CV values were recorded and a decrease in CV is observable, from 60% CV at the hollow sensors to 30% CV at the ridge sensors (Fig. 49).

The interquartile range plot (Fig. 50) demonstrates a reduction in the range of SWC from hollow to ridge positions. In Finland, the probes Sm1-3 exhibit substantial differences in the range, from completely saturated to almost completely dry conditions, with the

uppermost three probes observing a range of up to 60%. Despite variations, the mean soil moisture content is uniform across the transect. The Icelandic sites did not exhibit a pronounced change in soil moisture range, with the exception of Icex1, where the fourth probe on the slope and the last three probes at the ridge show a lower range. Notably, the mean soil moisture content decreased by approximately 25% from the hollow to the ridge position. At Icex1 the interquartile range is similar across the transect of about 12% while at Icex2 the soil moisture range is increasing from the hollow 10% towards the ridge position 29%.

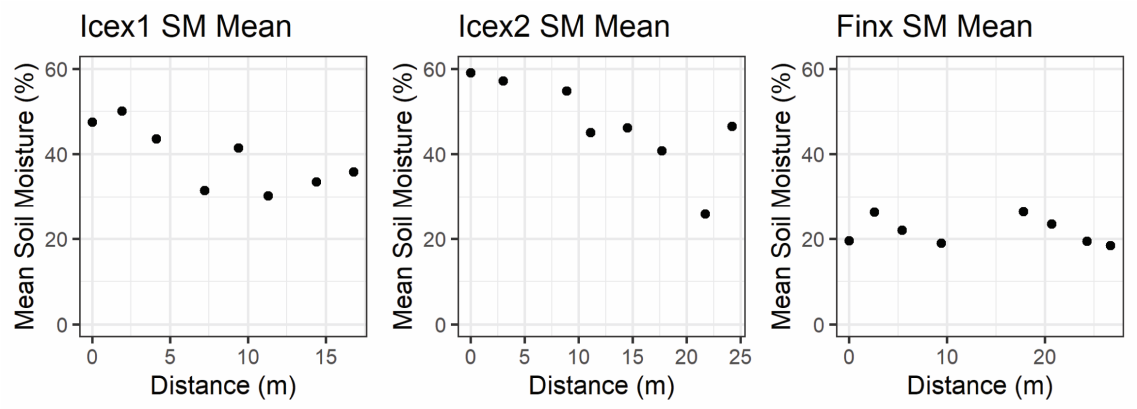

Fig. 48 Mean soil moisture over the growing season for each sensor. Measurements collected along a transect, starting in a hollow (left hand side) and ending on a ridge (right hand side)

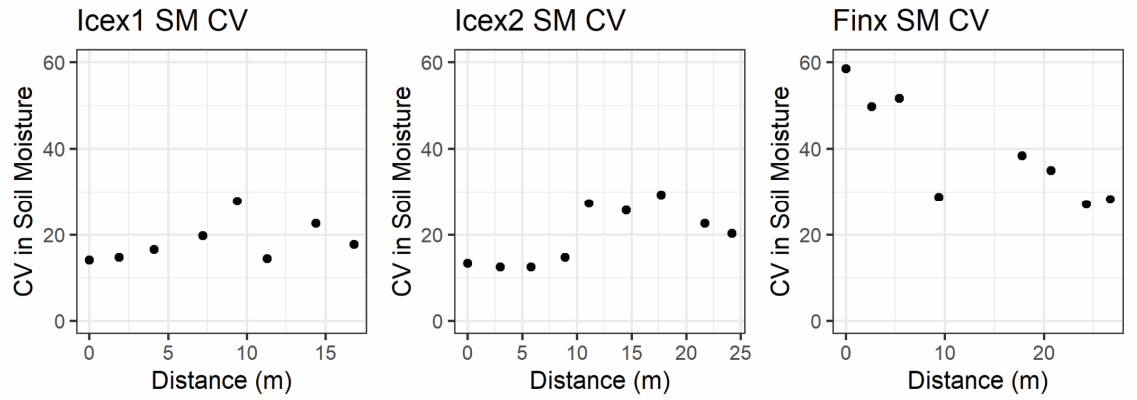

Fig. 49 Coefficient of variance (CV) soil moisture over the growing season for each sensor. Measurements collected along a transect, starting in a hollow (left hand side) and ending on a ridge (right hand side).

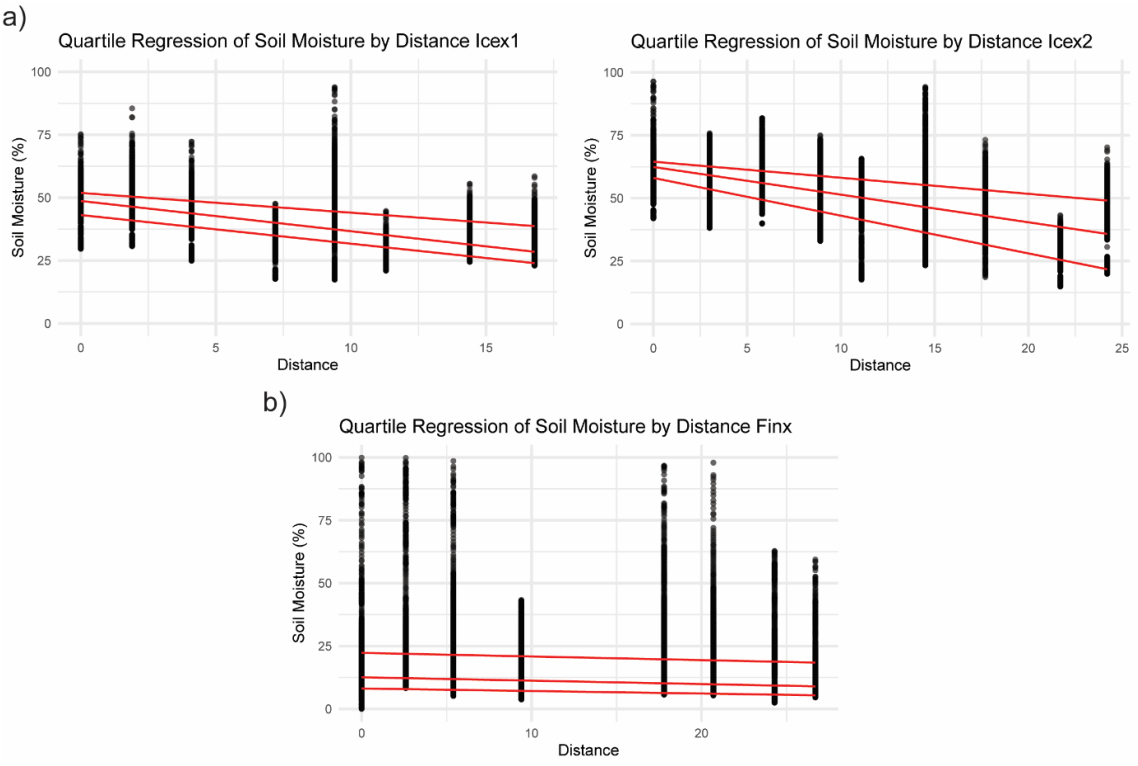

Fig. 50 shows the interquartile regression for soil moisture along the mesotopographic transect. The distance of 0 represents the hollow, with increasing distance moving towards the highest ridge position.

The time series data from Iceland revealed variances in SWC across the transect (Fig. 51, 52). After precipitation events, notably after rapid increases in SWC across all sensors, the sensors in the hollows show a slower decline in soil moisture (Fig. 53). Higher soil moisture levels are recorded in hollows and soil moisture decreases gradually with increasing distance from hollows. Sm9 was placed on a thúfur top, showing low mean SWC of about 13% and very low variability over time (Fig. 51).

In Finland, SWC readings from sensors in hollow, slope and ridge positions showed differences over time, particularly during the early growing season (Fig. 54). The slope and ridge probes exhibited a strong to moderate increase of soil moisture beginning of May (Fig. 53), at the onset of the growing season (Fig. 39). The hollow sensor recorded very high soil moisture levels about two weeks later in early June, and about further two weeks later, overall soil moisture levels and variability rapidly decreased at these probe locations, aligning more closely with those observed by the slope and ridge probes. The hollow position showed a more pronounced loss rate of SWC in comparison to the slope position (Fig. 53). This is particularly evident at Sm1 during the early growing season, where sensors in hollows exhibited a rapid decrease in soil moisture levels. However,

generally the ridge sensor recorded consistently low SWC and variability throughout the growing season (Fig. 54).

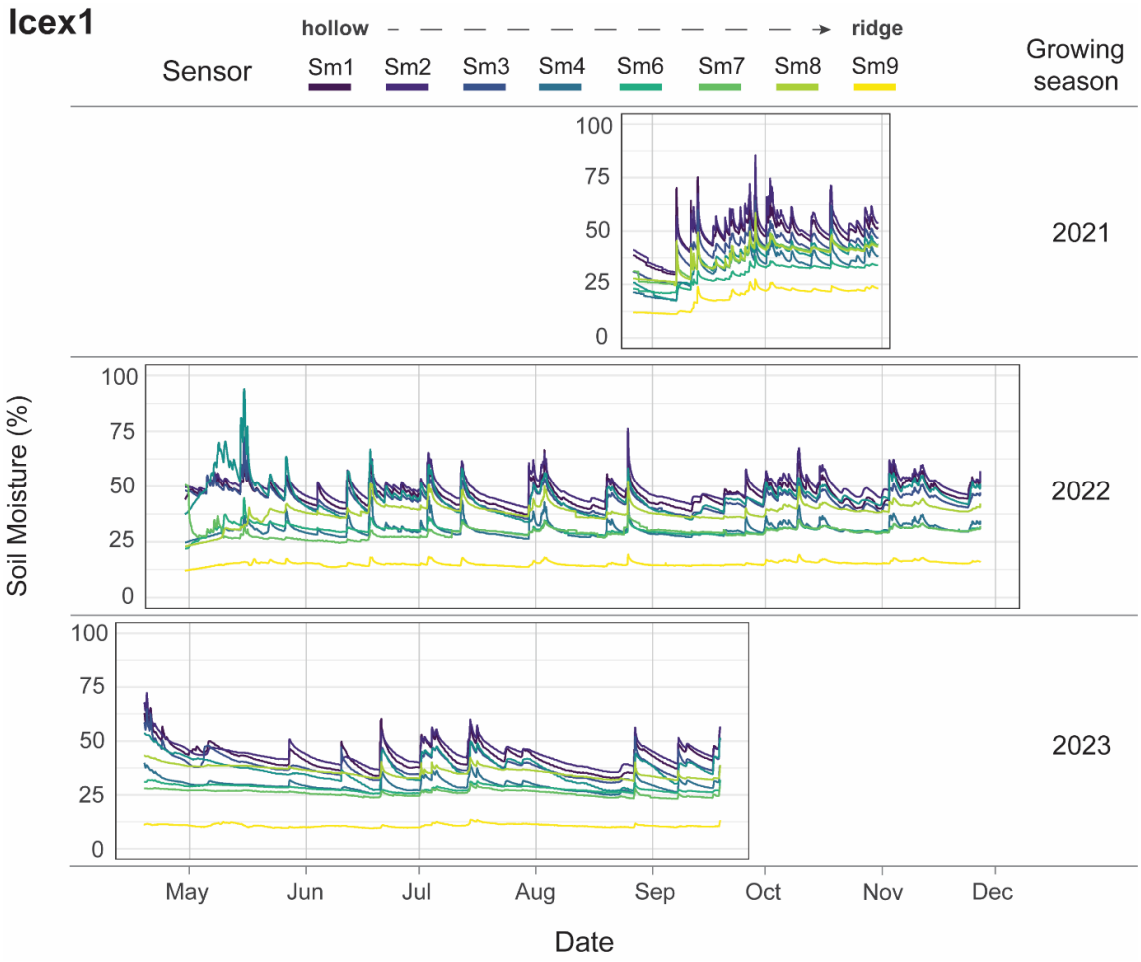

Fig. 51 Soil moisture data for transect at Icex1 in Iceland from sensor in the hollow (dark blue) to ridge (yellow) for the growing season 2021, 2022 and 2023. Note Sm9 was placed at a thúfur top and not included in the analysis.

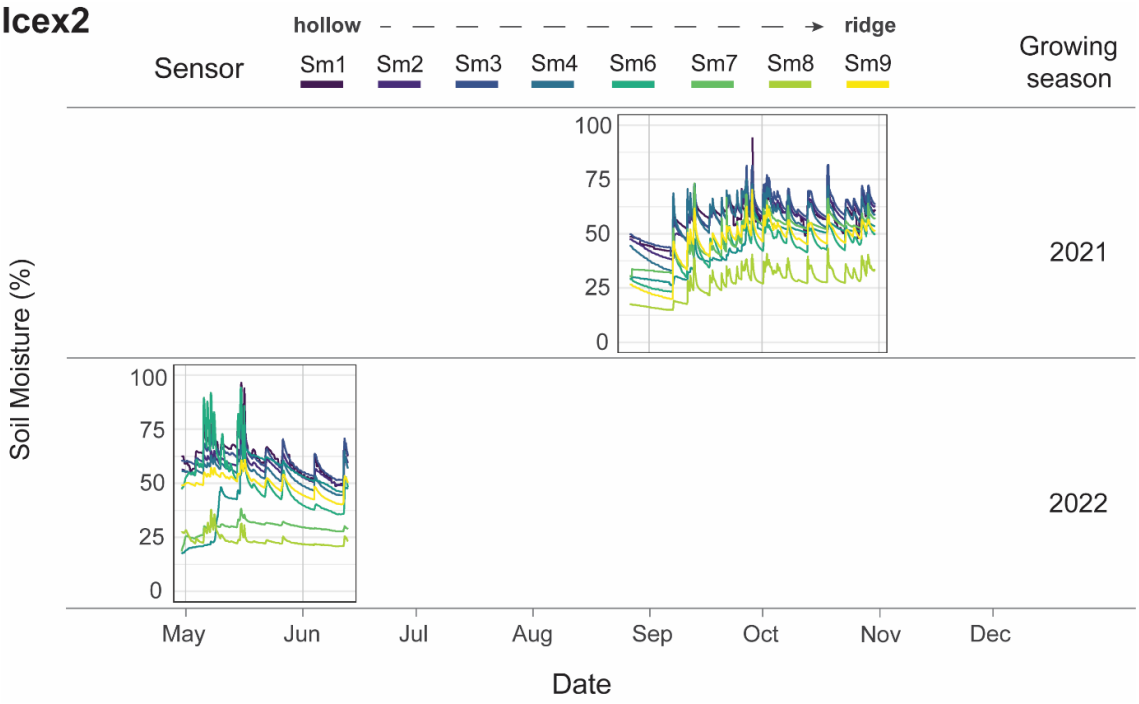

Fig. 52 Soil moisture data from transect at Icex2 from a sensor in the hollow (dark blue) to ridge (yellow) for the growing season 2021 and 2022.

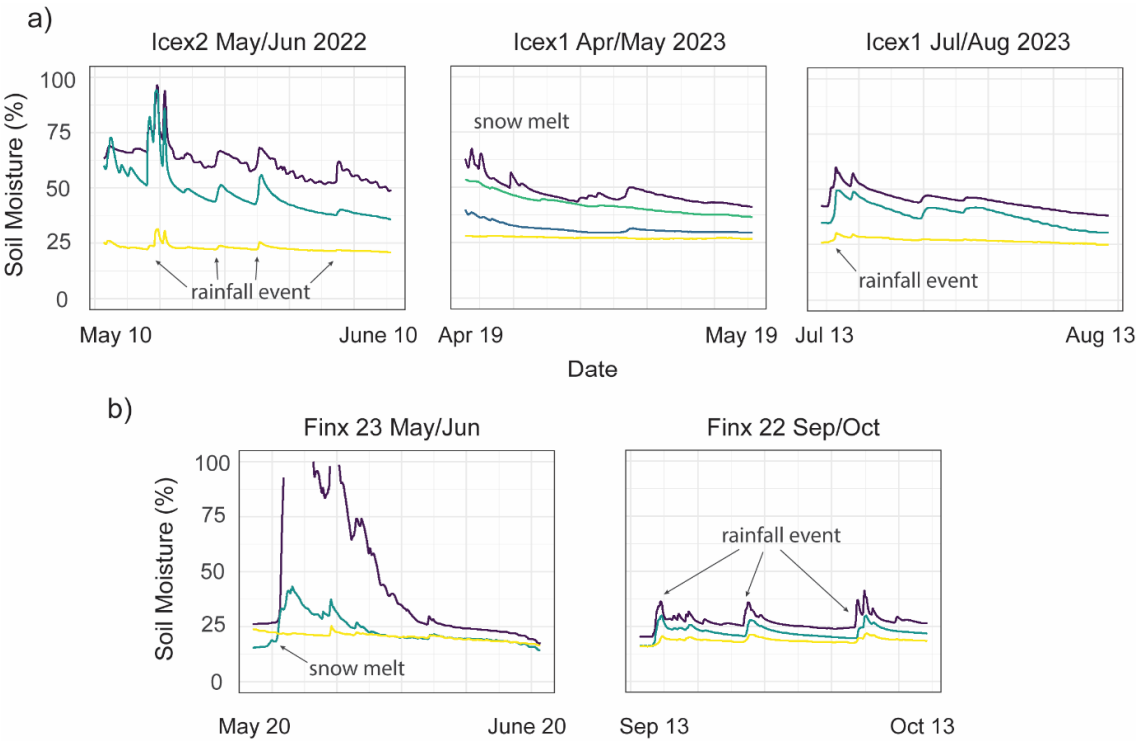

Fig. 53 Soil moisture data for selected periods of a month, a) in Iceland and b) in Finland. The colour indicates topographic position: hollow (purple), slope (blue shades) and ridge (yellow). In Iceland soils proximal to the hollows exhibited a pronounced capacity for accumulating and retaining moisture. This capacity diminished progressively with increased elevation toward the ridge. During the early growing season, observations indicate that probes in the hollows recorded higher soil moisture levels. In Finland, the soils had low capacity to retain water after 'rainfall events', with minor differences between the topographic extremes. In the early

growing season higher soil moisture levels were observed until mid-May for the ridge and until beginning of June for the hollow and slope.

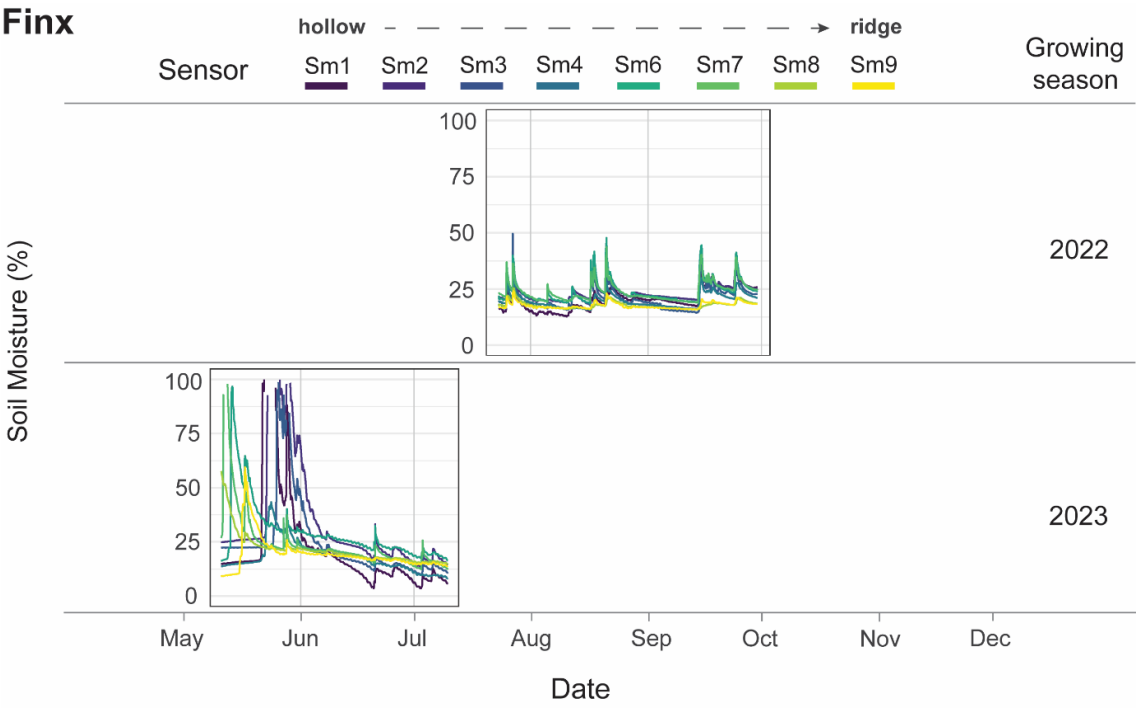

Fig. 54 Soil moisture data from all probes in the hollow (dark purple) to ridge (yellow) for the growing season 2022 and 2023 in Finland. The probe Sm5 was excluded due to malfunction. Note the stark decrease in SWC of Sm1 in the hollow after the snow melt int mid-June.

5.4.2 Vegetation

5.4.2.1 Vegetation abundance

The vegetation survey revealed 17 different plant species in Iceland and 21 in Finland (Fig. 55, 56). The change in plant community composition along the mesotopographic gradient was low to moderate in Iceland and high in Finland.

In Iceland, dwarf birch (*B. nana*) was mainly present in slope positions (Fig. 55). Lichen was found only at the hollow and ridge positions. Moss was evenly distributed with increased abundance at the ridge position. Graminoid cover was highest in the hollows and decreased towards higher positions. Similarly, low-growing shrubs generally decreased towards the ridge, with the exception of crowberry (*Empetrum nigrum*), which was equally present across the transect.

In Finland, graminoid cover, including the sedge *Carex bigelowi*, generally decreased along the transect (Fig. 56). Forbs such as *Solidago virgaurea* follow the same trend. Moss and lichen cover remained consistent across the transect. Low-growing shrubs exhibited varying patterns, with some species like *Vaccinium myrtillus* and *V. vitis-idaea* present at the hollow and slope positions, while others such as *Loiseleuria procumbens* and *V. uliginosum* occurring solely at the ridge. However, the overall abundance of these shrubs decreased towards the ridge, with *E. nigrum* notably dominating this position. As observed in Iceland, the dwarf birch was found predominantly on the slope in Finland. Additionally, bare soil cover and glacial till were mainly found at the ridge with signs of cryogenic and aeolian erosion activity.

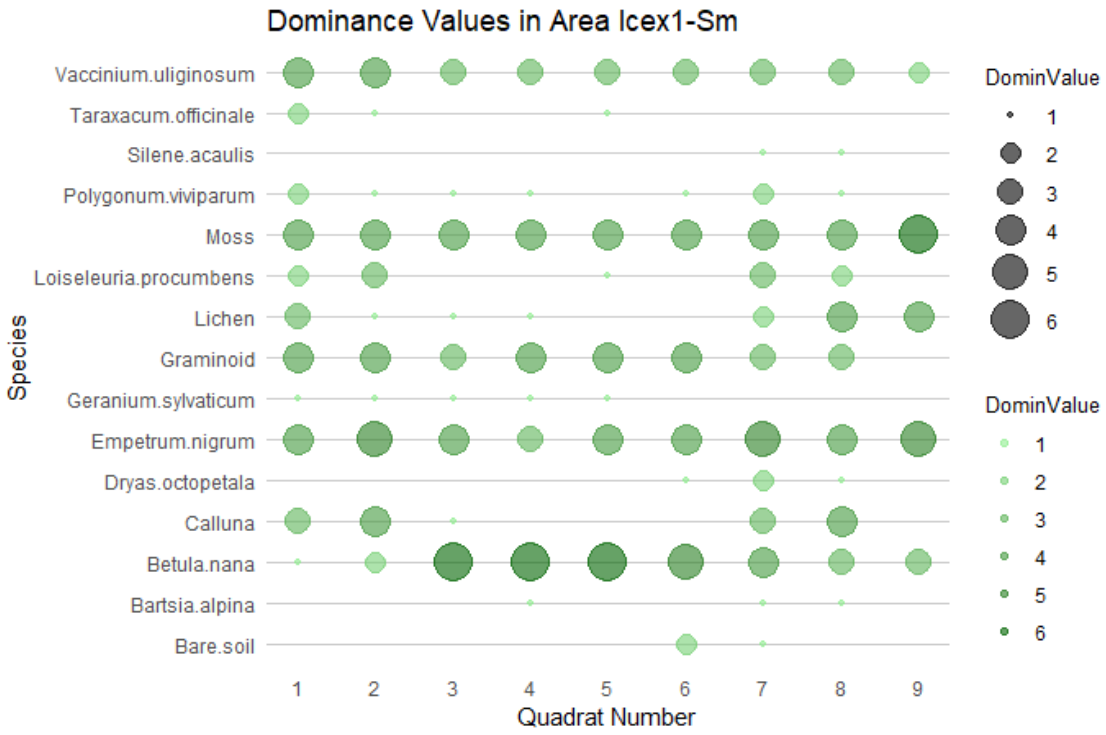

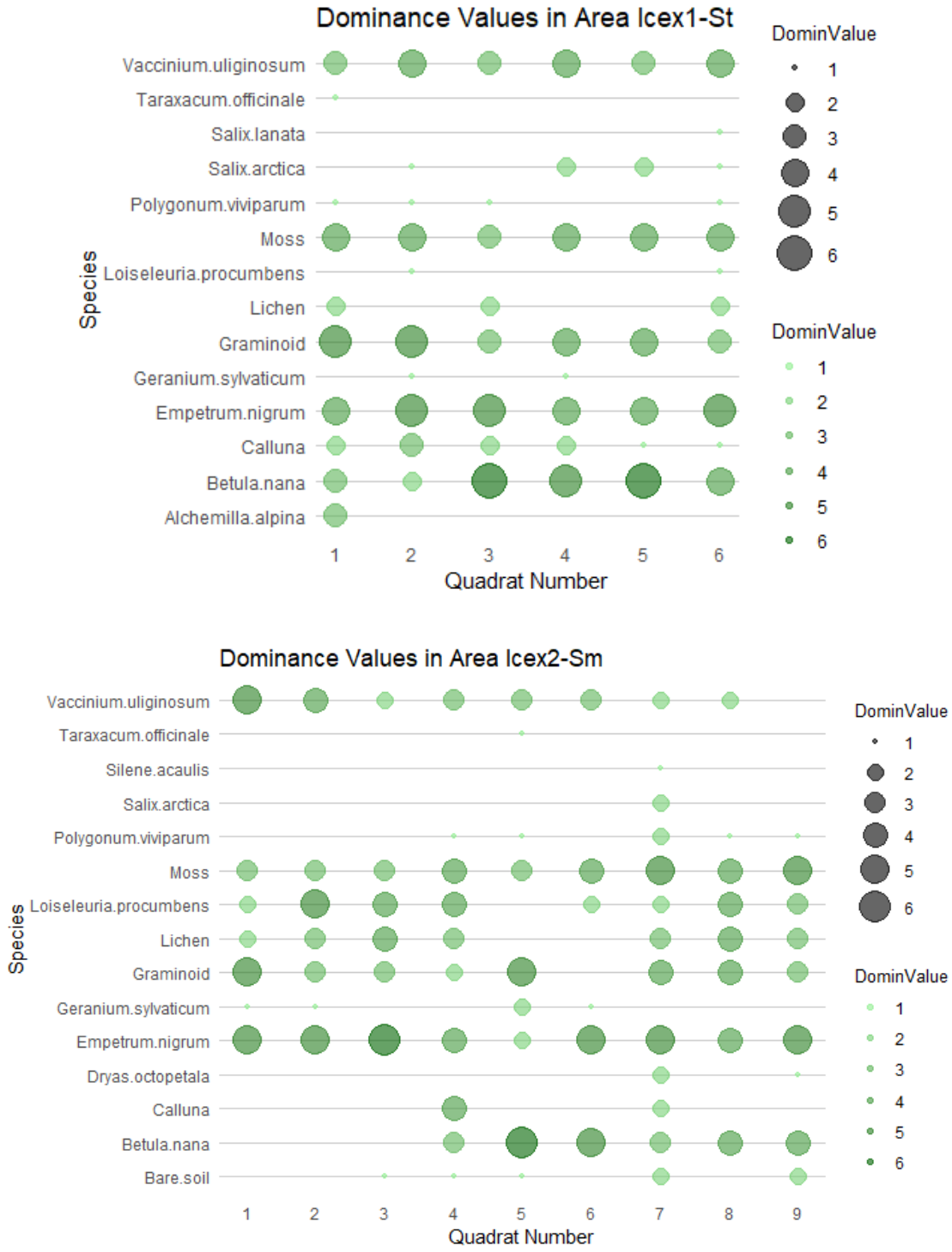

Fig. 55 Vegetation composition at Icex1-Sm, Icex1-St, Icex2-Sm in Iceland. Quadrat numbers range from 1 (hollow) to 9 (ridge).

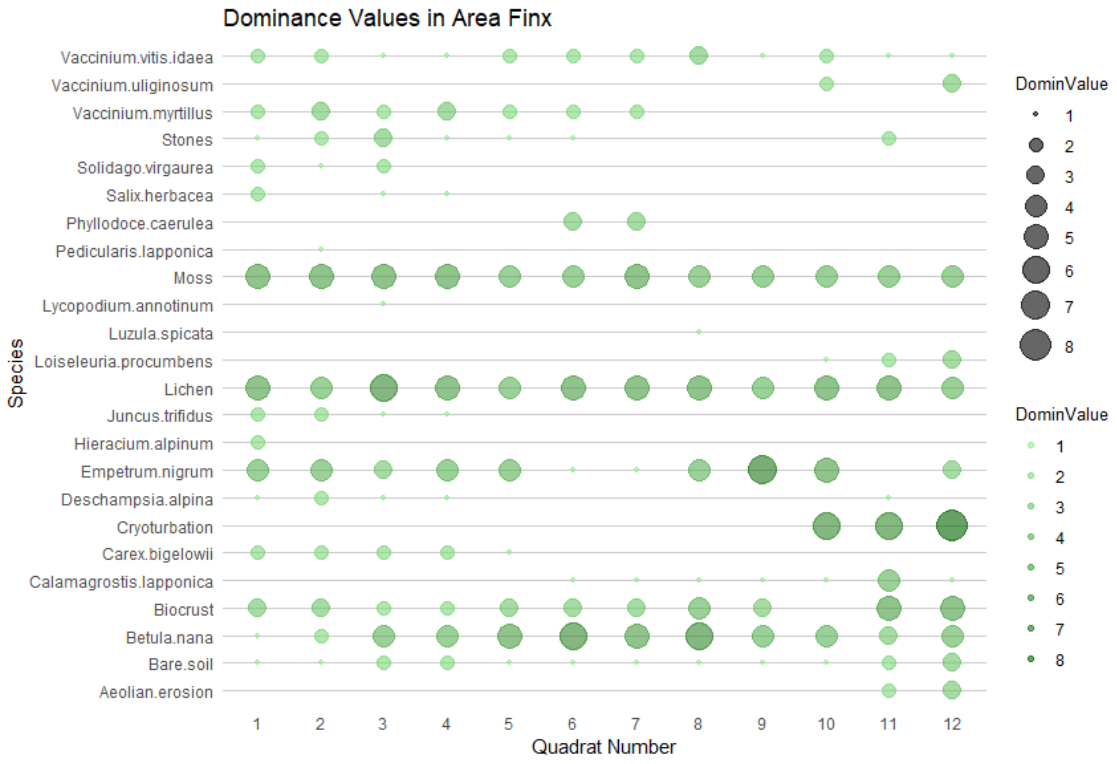

Fig. 56 Vegetation composition at Finx in Finland. Quadrat numbers range from 1 (hollow) to 12 (ridge).

5.4.2.2 Ordination analysis

NMDS visualisation of datasets from both Iceland and Finland implied that species distribution and cover is strongly controlled by the topographic position of each site (Fig. 57) and soil moisture variables as well (Fig. 58). The stress values of 0.1-0.15 indicate a fair fit, while the analysis with a reduced number of quadrats in Finland (Fig. 58c), shows a stress value of 0.02, indicating a good fit.

In Iceland *B. nana* and Lichen were more isolated from the other species (Fig. 57a) with *B. nana* prominently plotting in slope position. Notably, Bare soil plotted closely with *D. octopetala* and *S. acaulis* and together with Lichen they plot close to ridge positions. *G. sylvaticum, Calluna* and Graminoid species plotted closely together in the hollow areas. Moss and *E. nigrum* plotted in the centre adjacent to the ridge positions but also close to slope and hollow.

In Finland, the *B. nana*, Biocrust and Bare soil plotted closely together in the centre, while other forbs, graminoids, and low-growing shrubs plotted around them (Fig. 57b). All of them plotted closely at the slope position. *E. nigrum*, *V. uliginosum, L. procumbens and C.*

lapponica were mainly present at ridge position but widely scattered in the graph. *V. myrtillus*, *D. alpina*, *J. trifidus, S. virgaurea clustered around the hollow positions*.

The linear alignment across both sites and the generated smoothed surface for the SM Median and CV revealed a relationship between the vegetation composition and the SM variable (Fig. 58). In Iceland, the hollows were characterised by low CV and higher SM median values when compared to ridges and slopes, where the CV increased as the median SM decreased. SM median values were similar between slope and ridge, however CV were slightly higher for the ridge positions (Fig. 58a,b).

In Finland the linear alignment revealed a strong relationship between high CV and the hollow position, while the SM median pointing towards the slope quadrats. To note, only eight points were used for the analysis and thus are less representative.

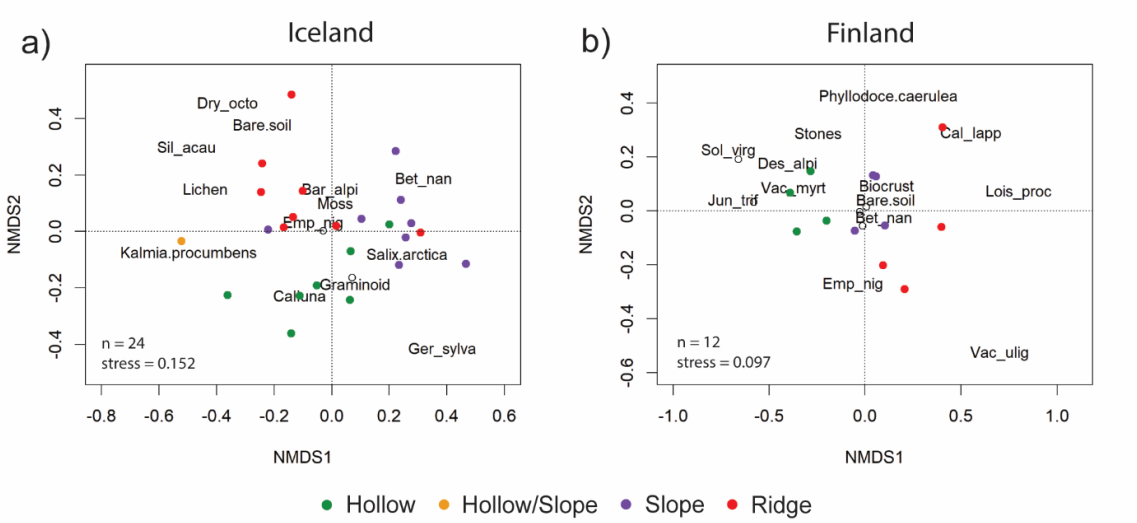

Fig. 57 NMDS plot with vegetation species and land cover (bare soil or stones) for a) Icelandic sites and b) Finnish site, with highlighted topographic position.

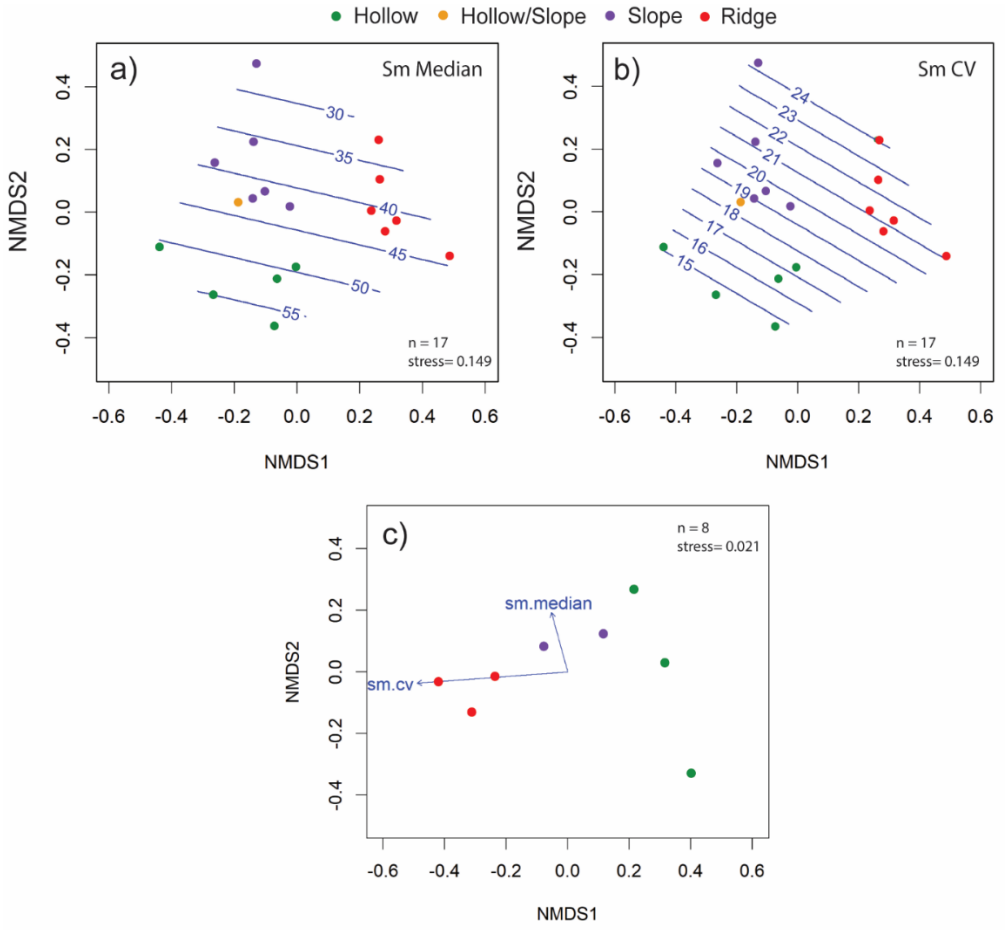

Fig. 58 NMDS plots for Icelandic and Finnish sites, highlighting topographic positions and modelled soil moisture parameters. a) Computed generalised additive model (GAM) with SM median as response variable related to NMDS axes as predictors in Iceland. b) Similarly, computed GAM with SM CV as response variable in Iceland. c) Linear alignment of SM CV and median in Finland.

5.4.2.3 Plant traits

Analysis of plant trait data for dwarf birch (*B. nana*) indicated a correlation between growth form and mesotopographic position but the distribution pattern varied among plant traits (Fig. 59). Only the correlation between mesotopographic position and median height was statistically significant, while leaf area, max height, dry and wet weight had p-values around 0.1. Specific leaf area (SLA) and leaf dry matter content (LDMC) exhibited no relationship related to topographic position (Fig. 60).

The Tukey's HSD post-hoc test revealed that only the median height showed statistically significant differences, specifically between the hollow and ridge positions (Fig. 61). The results showed a decline in both maximum and median shrub heights when moving from the hollow to the ridge, with median heights reducing from 15 cm to 7.5 cm (Fig. 61). Conversely, leaf area shows an increasing trend along the same spatial gradient. Mean

leaf area increased from 0.5 cm^2 in the hollow to around 0.7 cm^2 in slope and ridge position (Fig. 61). While mean dry and wet weight also increase from the hollow with a mean dry weight of 0.025 g and peak at the slope position 0.043 g and then decreases again at the ridge to 0.034 g (Fig. 61).

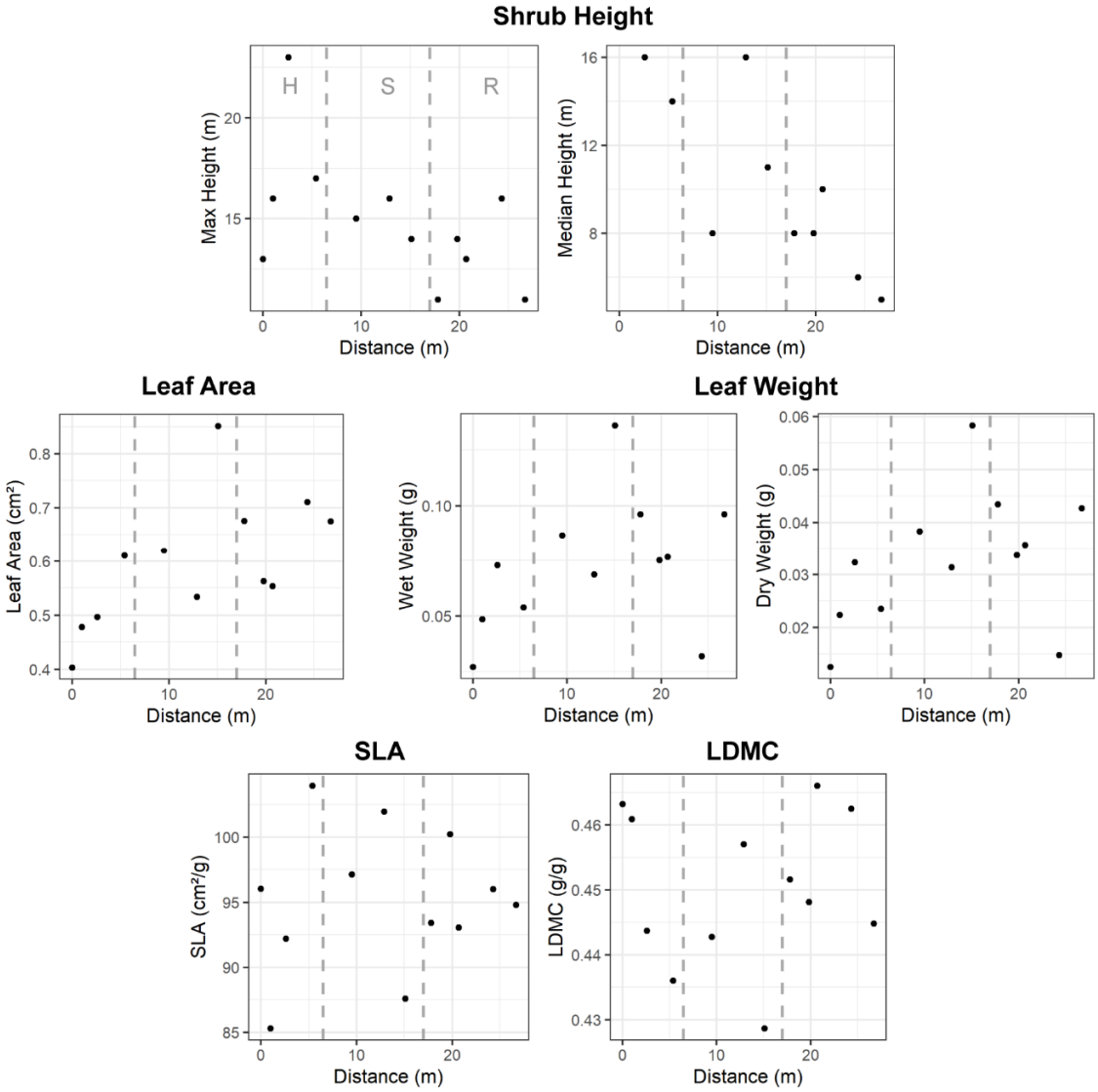

Fig. 59 Plant traits of dwarf birch a) shrub max and median height, b) leaf area, c) wet and dry weight, d) specific leaf area (SLA), e) leaf dry matter content (LDMC). The grey dashed lines indicate the topographic position H = hollow, S = slope, R = ridge.

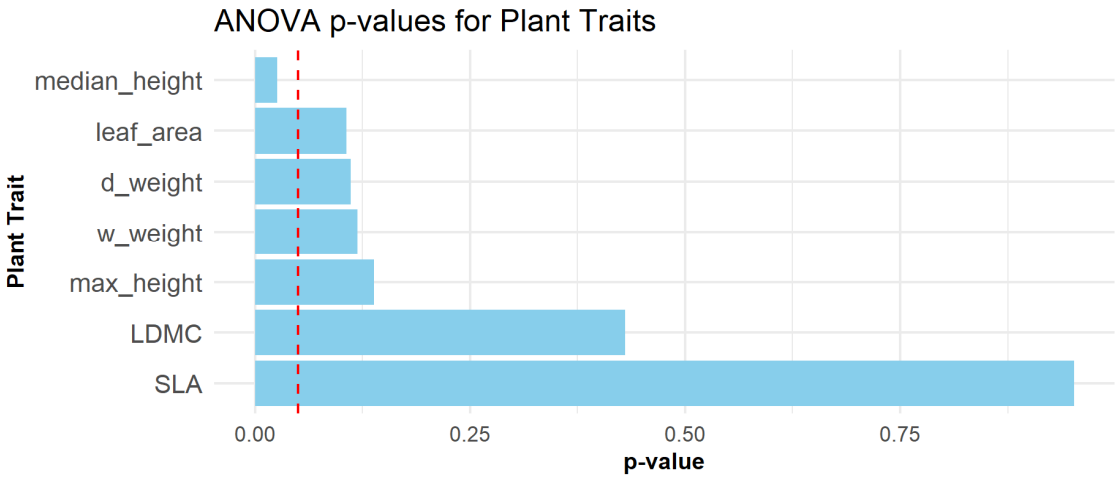

Fig. 60 ANOVA significance test for plant traits related to topographic position. The red dashed line indicates the significance threshold of 0.05 p-value.

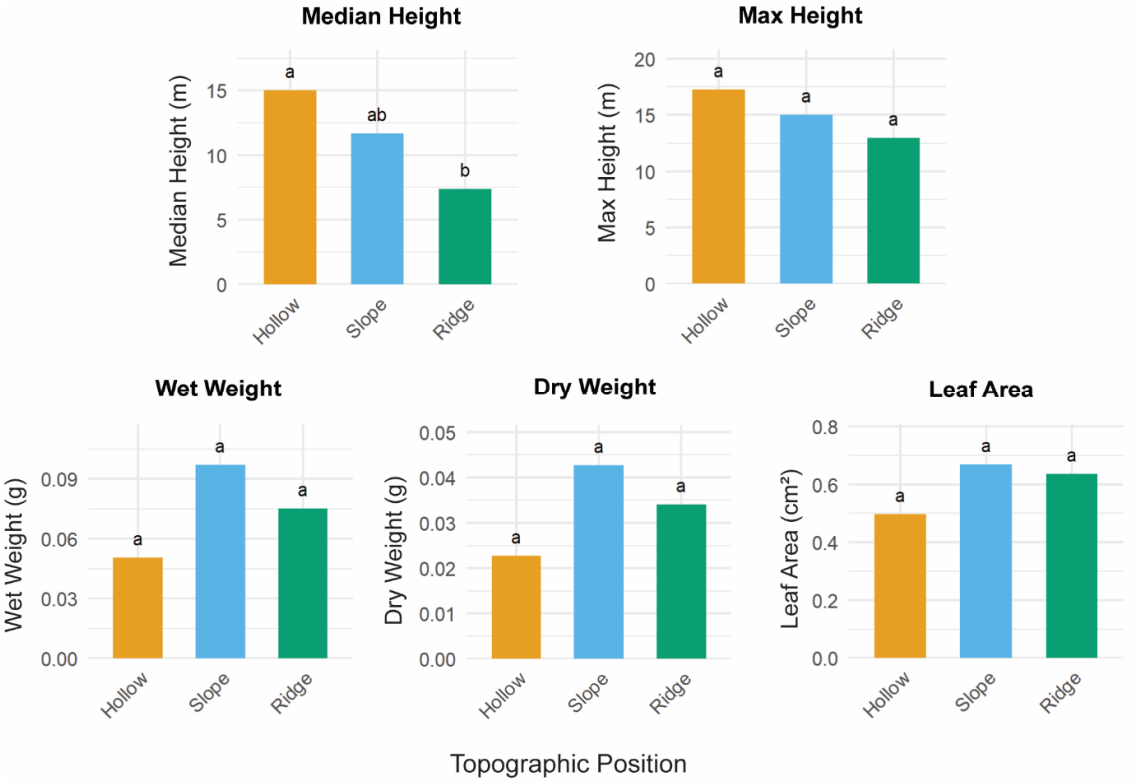

Fig. 61 Means of plant traits across different topographic positions. Significant differences between the topographic positions, as determined by post-hoc Tukey's HSD test, are indicated by the letter annotations. Groups sharing the same letter (e.g., "a") are not significantly different, while groups with different letters (e.g., "a" vs. "b") are significantly different from each other. Groups labelled with "ab" indicate an intermediate group that is not significantly different from either the "a" or "b" group.

5.4.3 PFT composition and vitality

5.4.3.1 X plots

Plant species composition varied across transects and locations in the X plots (Fig. 62). Notably, dwarf birch was predominantly found in hollow and slope positions in both Iceland and Finland, whereas Ls-Veg and crowberry were primarily located at the ridge in Iceland and Finland, respectively (Table 19). Within the same species, there were notable differences in vegetation indices values depending on the position from the hollow (topographic class 1) to the ridge (topographic classes 3/4) positions. Specifically, NDRE frequently exhibited a decline, while NDVI and RENDVI either remained unchanged or increased in value (Table 20).

In Iceland, dwarf birch was primarily found at slope positions or a combination of hollow and slope (Table 19). The Ls-Veg class abundance declined towards the ridge, while the barren cover was exclusively observed at the ridge. Vegetation indices for dwarf birch at hollow and slope positions were similar at Icex1, but values slightly reduced at the ridge, particularly for NDRE (Table 20). At Icex2, dwarf birch showed marginally higher values for all vegetation indices at slope locations, and the same values at hollow and ridge positions. The Ls-Veg class experienced a notable decline in vegetation indices at the ridge, approximately 0.1 in NDVI and 0.02 in NDRE.

In Finland, dwarf birch was more abundant in the hollow position, whereas the Ls-Shrub class was evenly distributed across the X plot, with a slightly higher prevalence at the slope position (Table 19). Crowberry was predominantly found at the ridge and upper slope positions. Biocrust was more prevalent in the hollow and ridge positions, with slightly lower abundance on the slope. The vegetation indices presented contrasting patterns. NDVI and RENDVI values for dwarf birch increased towards the ridge, whereas NDRE values showed a decline (Table 21). Both Ls-Veg and biocrust classes were decreasing towards the ridge. The crowberry class showed minimal variation across the transect, and the distribution of NDVI values was not significantly different among topographic positions.

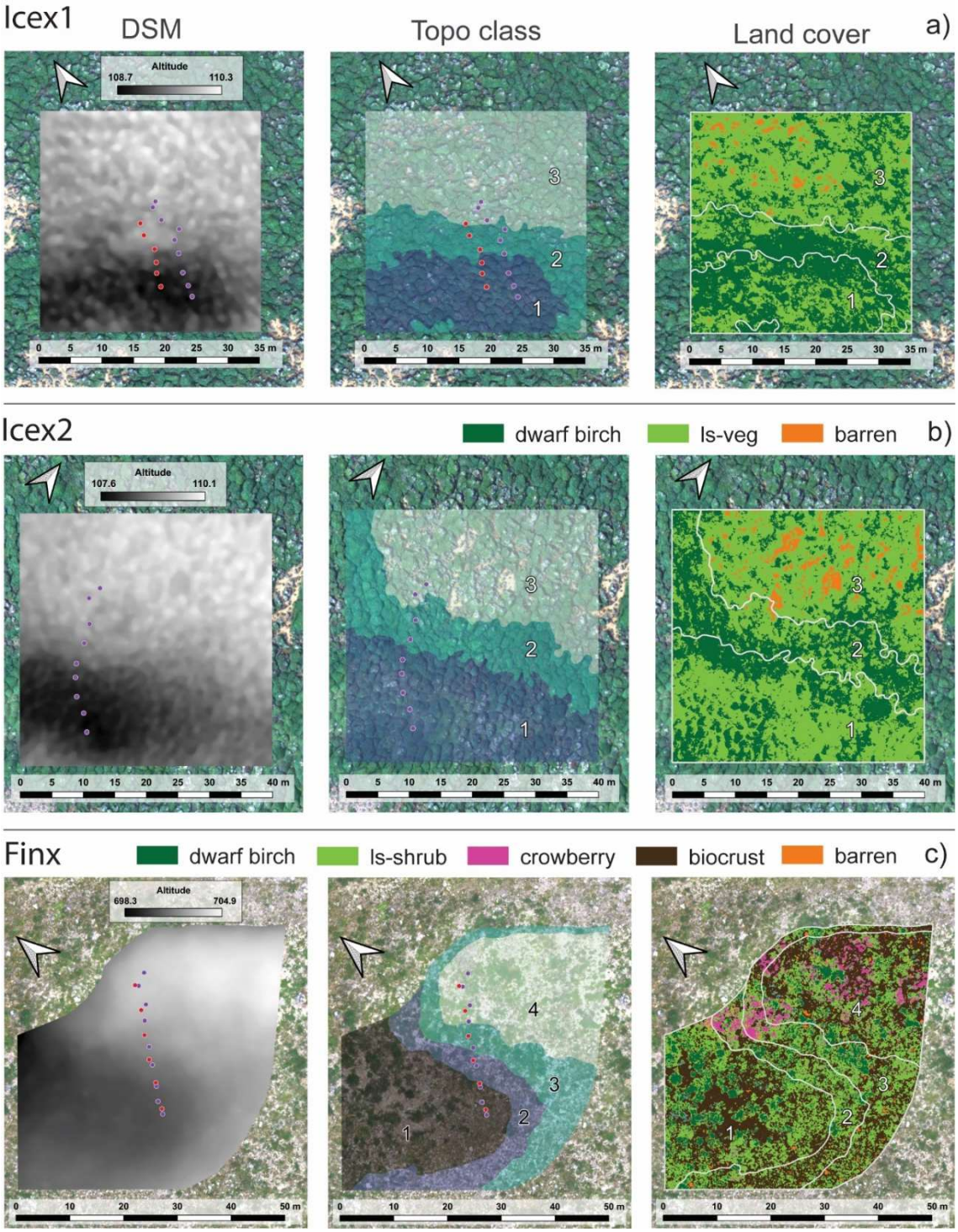

Fig. 62 Topographic and land cover information for study sites in Iceland a) Icex and b) Icex2 and Finland c) Finx. On the left column the DSM is displayed with the altitude range. Red points represent the location of the soil temperature and purple of the soil moisture probes. The second column shows the topographic classification based on elevation ((1) hollow (2) lower slope (Iceland = slope), (3) upper slope, (4) ridge). The last column shows the land cover distribution in the study plots related to topographic position.

Table 19 Proportion of occurrence of each land cover class in relation to topographic position. Topography is classified as follows: 1) hollow, 2) lower slope (Iceland = slope), 3) upper slope, 4) ridge. Only dominant classes are shown in Finx, that is why classes do not sum to 100%.

Proportion of land cover based on topographic position										
	Finx				Icex1			Icex2		
Topo	Dwarf Birch	Ls-Shrub	Crowberry	Biocrust	Dwarf Birch	Ls-Veg	Barren	Dwarf Birch	Ls-Veg	Barren
Hollow	14%	37%	1%	44%	63%	37%	0%	38%	62%	0%
(Lower) Slope	10%	43%	5%	38%	65%	35%	0%	56%	43%	0%
Upper Slope	9%	44%	7%	37%	-	-	-	-	-	-
Ridge	8%	32%	11%	44%	26%	70%	3%	19%	72%	9%

Table 20 Mean vegetation indices of functional land cover types and topographic positions for the study sites in Iceland. The Dunn's test showed that all of the presented values were significantly different in pairwise comparisons between topographic classes, with p-values < 0.05 (Table A11, A12 in Appendix).

Vegetation indices per land cover based on topographic position												
	Icex1						Icex2					
	Dwarf Birch			Ls-Veg			Dwarf Birch			Ls-Veg		
Topo	NDVI	NDRE	RENDVI	NDVI	NDRE	RENDVI	NDVI	NDRE	RENDVI	NDVI	NDRE	RENDVI
Hollow	0.82	0.19	0.75	0.74	0.18	0.64	0.78	0.18	0.70	0.75	0.17	0.66
Slope	0.82	0.20	0.75	0.72	0.18	0.63	0.80	0.19	0.72	0.76	0.18	0.67
Ridge	0.80	0.18	0.73	0.68	0.16	0.58	0.78	0.18	0.70	0.65	0.16	0.56

Table 21 Mean vegetation indices of functional land cover types and topographic positions for the study sites in Finland. The Dunn's test indicated that the majority of vegetation index across topographic classes were significantly different (p-values < 0.05), except for the NDVI values for Crowberry (Table A13 in Appendix).

Vegetation indices per land cover based on topographic position												
Finx												
	Dwarf Birch			Ls-Shrub			Crowberry			Biocrust		
Topo	NDVI	NDRE	RENDVI	NDVI	NDRE	RENDVI	NDVI	NDRE	RENDVI	NDVI	NDRE	RENDVI
Hollow	0.71	0.18	0.60	0.58	0.17	0.46	0.61	0.14	0.51	0.47	0.16	0.34
Lower Slope	0.71	0.17	0.61	0.57	0.16	0.46	0.62	0.14	0.53	0.43	0.15	0.31
Upper Slope	0.72	0.17	0.63	0.58	0.15	0.47	0.61	0.14	0.52	0.42	0.14	0.30

Ridge	0.73	0.17	0.64	0.59	0.15	0.48	0.61	0.14	0.52	0.39	0.13	0.27

5.4.3.2 *Y area*

The distribution of TPI values differed between the two sites (Fig. 63a/b, 65a/b). In Iceland, TPI values ranged from -1 to 1, with a mean of approximately 0, indicating a relatively balanced presence of concave, flat, and convex terrain. In contrast, the Finland site exhibited a broader range of TPI values, spanning from -1 to 2, with a mean of 0.13, suggesting a slightly higher prevalence of convex terrain compared to the Iceland site.

A strong relationship was observed between the land cover distribution and TPI. In Iceland, large proportions of dwarf birch and Ls-Veg were located in the hollow and slope areas (Fig. 63c). The proportion of dwarf birch decreased with increasing TPI. In contrast, Ls-Veg remained high in areas with TPI > 0 but then declined at higher TPI values. Barren cover notably increased in areas with TPI values greater than 0.5. In Finland, Ls-Shrub class exhibited a higher proportion at low TPI values, which gradually diminished for TPI > 0.3 (Fig. 65c). Dwarf birch was primarily located in areas with TPI values between -0.1 and 1.1, with minimal presence at low and extremely high TPI values. This indicates that dwarf birch was mainly found on slopes/flat areas and more at exposed positions towards the ridge. Biocrust peaked at extremely low TPI values and showed a more significant peak at extremely high TPI values. Crowberry was scarcely found in concave and flat areas with TPI values below 0.5. As TPI values increased past this threshold, towards convex terrain, crowberry abundance increased and stabilised, reflecting its presence on ridge positions. The Wetland class was not present in the Y study area.

Upon examining the wider area (Y) using indices of vegetation cover related to TPI, we observed patterns that both align and diverge from those identified in the smaller area, revealing varied responses across different vegetation indices and plant species (Fig. 64, 66). The dwarf birch (Ms-Shrub) class in Iceland demonstrated a uniform distribution of NDVI and RENDVI values across varying TPI levels. In contrast, NDRE values showed a modest reduction of approximately 0.025 towards the ridge, a similar trend that is observed in the Ls-Veg class. The Ls-Veg class displayed a notable increase in NDVI and RENDVI values, by 0.05 and 0.1 respectively, starting from TPI 0.

In Finland, the vegetation indices displayed no clear relationship with TPI, except for the biocrust class, which showed a steady decline in all vegetation indices above approximately -0.5 TPI (Fig. 66). The dwarf birch class exhibited an increase in NDVI and RENDVI values, whereas NDRE demonstrated a steady decrease. The crowberry class revealed some fluctuation in NDVI and RENDVI values above 0 TPI with a marginal rise, while NDRE values remained stable across the TPI range. The Ls-Shrub class, similarly to the dwarf birch, showed an increase in NDVI and RENDVI values, with NDRE progressively decreased from hollow to ridge positions. In contrast, the juniper class exhibited a rise in NDVI and RENDVI values, with NDRE remaining constant until about 0.5 TPI, after which there was a decline.

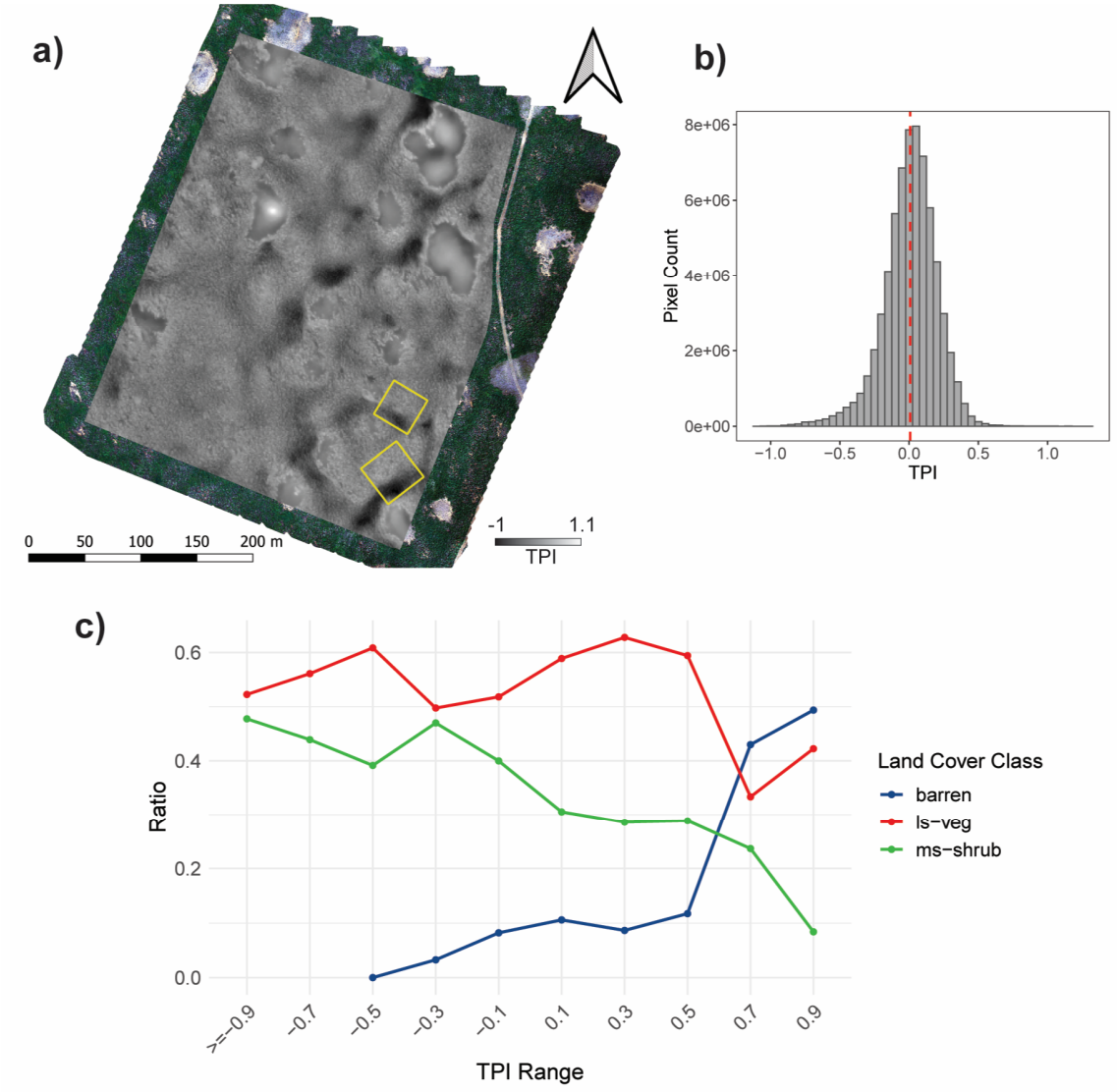

Fig. 63 RGB and TPI map of wider study area Icey including Icex. a) TPI spatial overview of area Icey. The area bounded in yellow represent the X plots Icex1 and Icex2. b) histogram with the TPI distribution of Icey. Dotted red line indicate the mean. c) Distribution of land cover classified in 0.2 TPI bins from starting from -1.1 to 0.9.

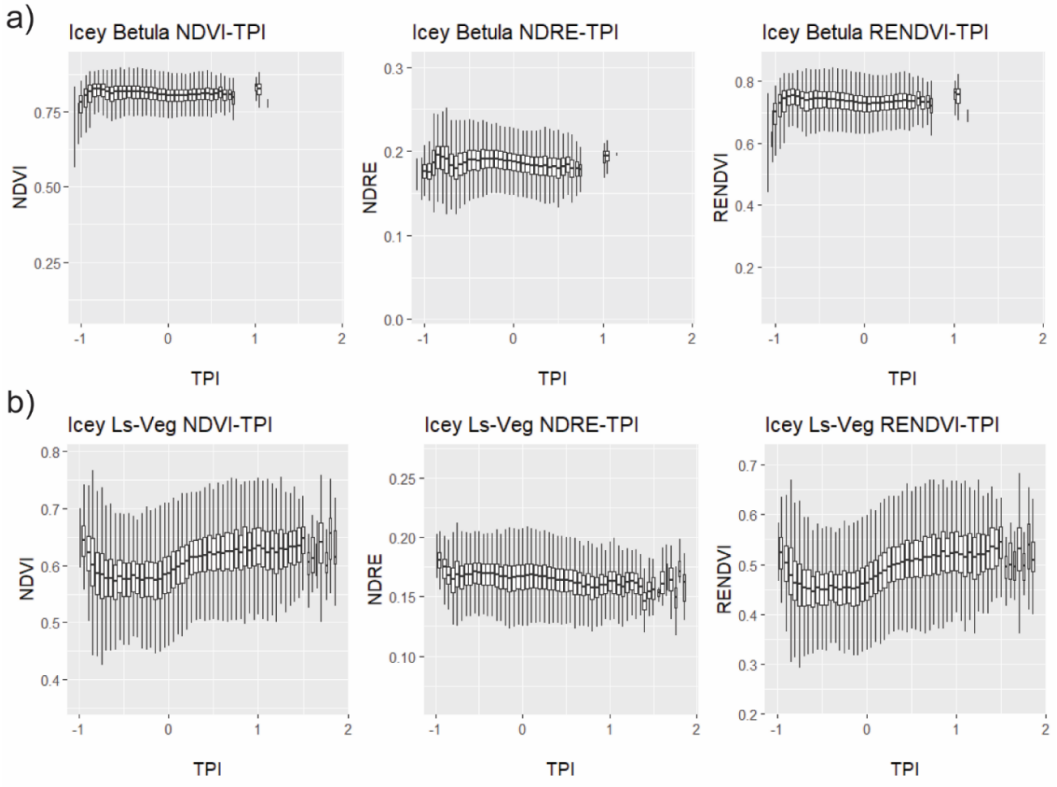

Fig. 64 Vegetation indices are plotted against TPI for each land cover class. a) Dwarf birch and b) Ls-Veg. Each box represents a range of 0.05 TPI, showing the interquartile range, with the median indicated by the horizontal line inside the box. The whiskers extend to the maximum and minimum values within 1.5 times the interquartile range. Outliers beyond this range are excluded.

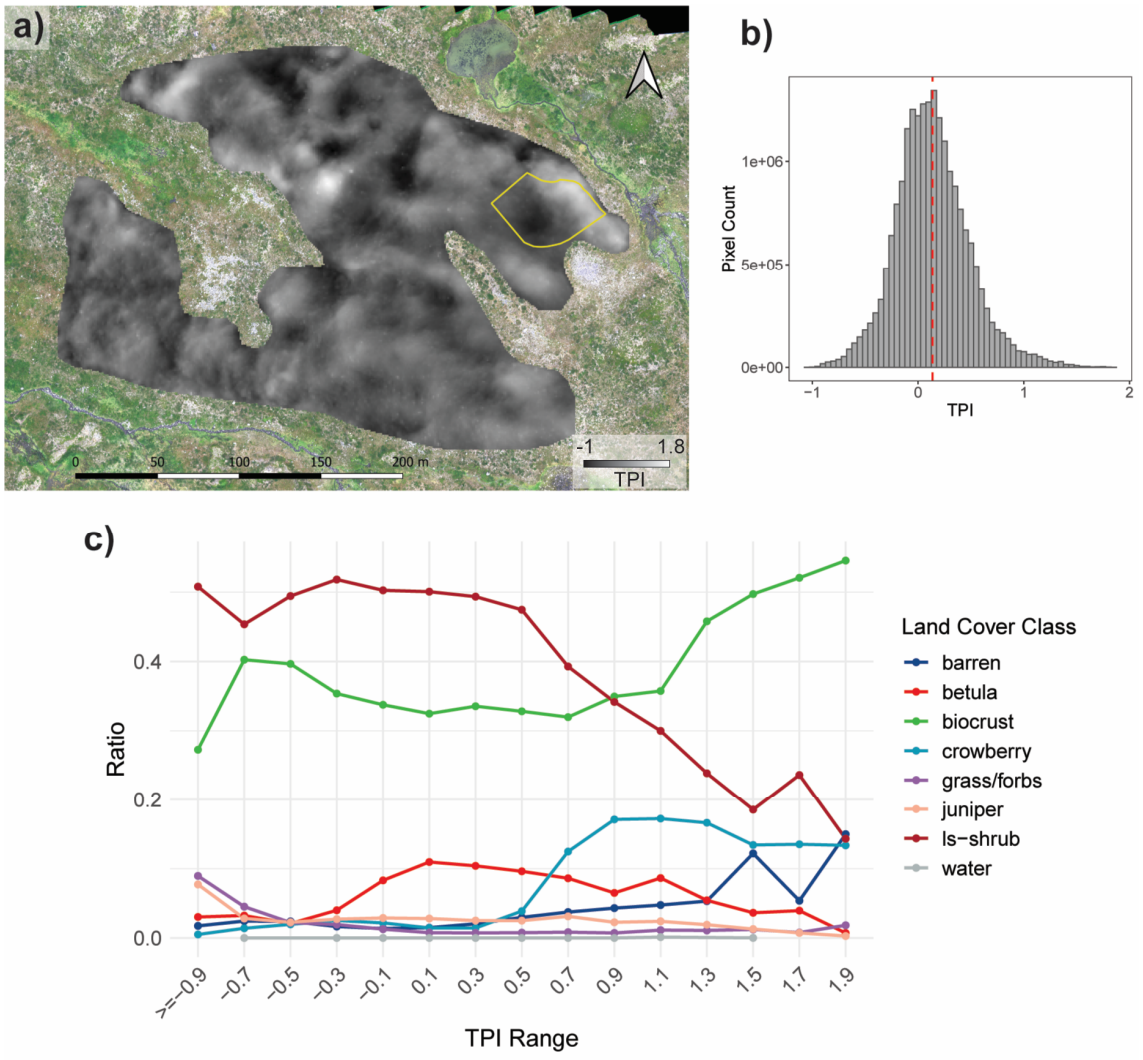

Fig. 65 RGB and TPI map of wider study area Finy including Finx. a) TPI spatial overview of area Finy. The area bounded in yellow represent the X plot Finx. b) Histogram with the TPI distribution of Finy. Dotted red line indicate the mean. c) Distribution of land cover classified in 0.2 TPI bins from starting from -1.1 to 0.9.

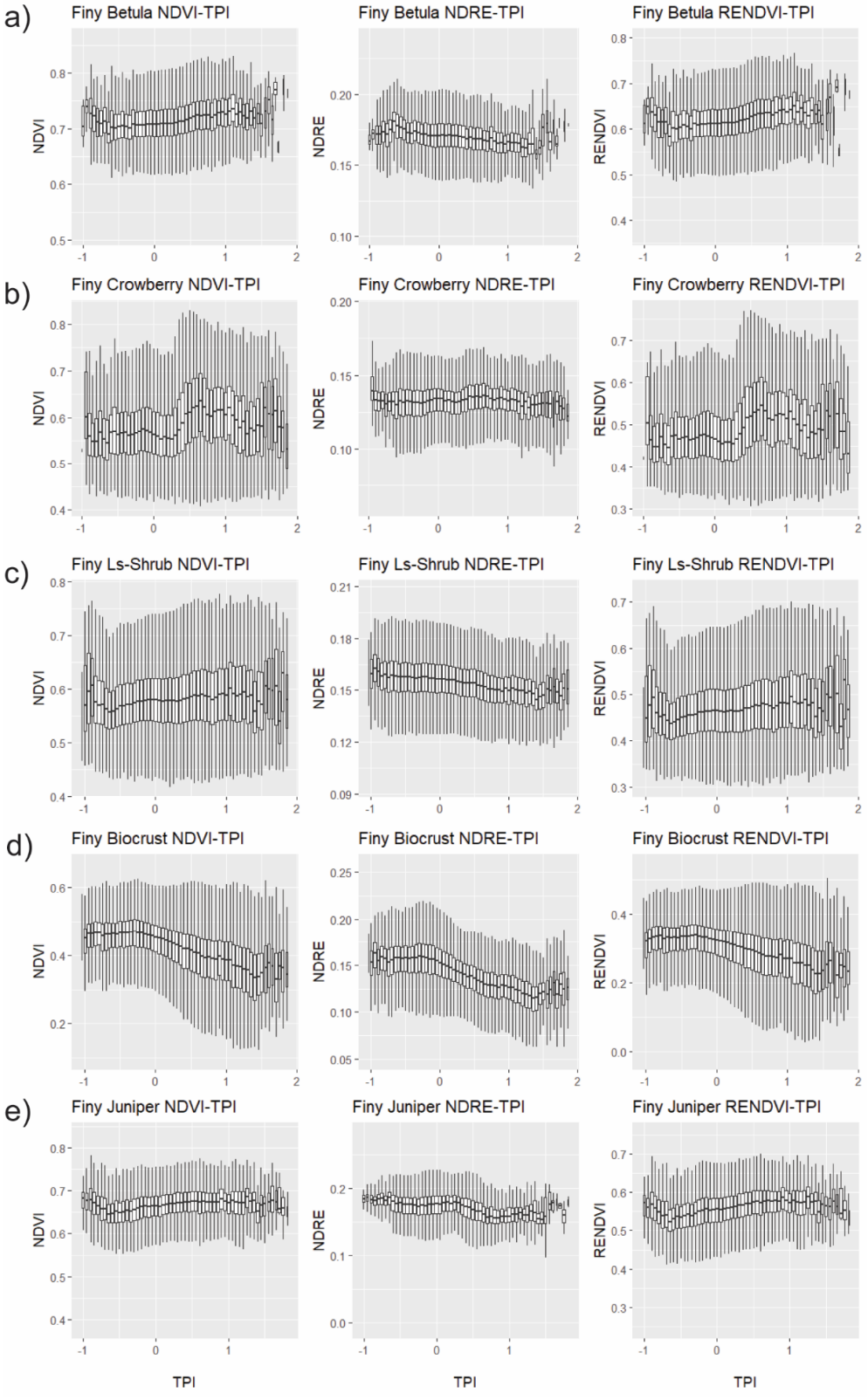

Fig. 66 Vegetation indices are plotted against TPI for each land cover class. a) dwarf birch, b) crowberry, c) Ls-Shrub, d) biocrust, e) juniper. Each box represents a range of 0.05 TPI, showing the interquartile range, with the median indicated by the horizontal line inside the box. The whiskers extend to the maximum and minimum values within 1.5 times the interquartile range. Outliers beyond this range are excluded to minimise noise and enhance clarity of the graphs, aiding in the interpretation of trends.

5.5 DISCUSSION

The objectives of this chapter are to 1) understand how mesotopography affects the spatial variability of soil moisture (as a microclimate proxy) and 2) examine how microclimatic conditions affect vegetation properties, including plant community composition, plant vitality and morphology.

Our results reveal contrasting soil moisture properties and vegetation responses between the study sites. In Iceland, soil moisture was high with low variability (CV), decreasing significantly from hollows to ridges. In Finland, soil moisture was low with higher CV, showing minimal variation mean soil moisture across mesotopographic positions, but notable decrease of CV from hollow to ridge position.

Vegetation composition and plant vigour were correlated with mesotopographic variability at both study sites to a different extent. Low-growing shrubs and graminoid cover generally decreased when moving from hollows to ridges at both locations, except for crowberry, which was restricted to ridges in Finland but evenly distributed along mesotopographic gradients in Iceland. Dwarf birch primarily occupied slopes and hollows, while barren cover was only found on ridges. In Finland, barren cover and biocrusts were more abundant on ridges and to lesser degree in hollows.

Dwarf birch in Finland exhibited morphological responses to the mesotopographic gradient, including reduced height and larger, heavier leaves towards the ridge. These structural adaptations corresponded with landscape-scale vegetation patterns, as evidenced by increased NDVI values with rising TPI (from hollow to ridge) in Finland; however, this trend was not observed in Iceland.

5.5.1 Soil moisture

Soil moisture patterns varied distinctly between Iceland and Finland, driven by differences in soil properties, topography, and seasonal dynamics. In Iceland, mean soil moisture decreased significantly from hollows to ridges (Fig. 50), with a slight increase in the CV. In Finland, mean soil moisture showed minimal variation across the gradient, but CV decreased towards ridges. While Iceland's soil moisture range remained consistent across positions, Finland's hollow and slope positions exhibited a wide range (0–100%), with lower values on ridges.

Seasonal soil moisture patterns also revealed differences between the two sites In Iceland, early growing season probes recorded elevated soil moisture in hollows without reaching saturation (Fig. 53a). Finland's ridges, in contrast, experienced rapid saturation and subsequent drying, followed two weeks later by full saturation in hollows, which retained moisture slightly longer before matching ridge levels (Fig. 53b). This timing difference aligns with snow cover duration (SCD) patterns (Fig. 38). Topsoil moisture (0 – 30 cm depth) was shown to respond strongly to snowmelt (Blankinship et al. 2014). Ridge probes in Finland surpassed 0°C by late May, initiating snowmelt, while hollow positions lagged by about two weeks, delaying moisture availability. In Iceland, the early growing season timing differences between hollows and ridges were less pronounced and varied across plots and seasons.

These findings reflect the influence of mesotopography and soil properties. Iceland's thick Andosols, with high infiltration rates and SOC, effectively retain moisture and exhibit lower CV values (Arnalds 2015). In hollows, thicker soils (>1 m) and anoxic conditions enhance moisture retention, aligning with the presence of Histic Andosols containing 12–20% SOC (Arnalds 2015). Towards ridges, erosion reduces soil thickness and SOC, lowering water retention and increasing variability (Óskarsson et al. 2004). Similarly, Cutler et al. (2023) observed lower soil moisture and higher CV near erosion fronts in southern Iceland with similar soils.

In contrast, Finland's thin Cryosols (a few centimetres thick) lack infiltration capacity and retain little water (Thiffault, 2019; Darmody et al. 2000). Minor differences in soil thickness between positions contribute to small moisture variations, with hollows displaying higher CV due to rapid moisture absorption during rain and subsequent drying. Ridges, with limited moisture absorption, exhibit consistently low moisture levels and lower CV (Fig. 50b). Despite these differences, soil moisture trends were consistent throughout the growing season, with early spikes (Fig. 54) having minimal influence on overall patterns.

The rapid drying of hollows in Finland (Fig. 54), especially after snowmelt, reflects subsoil characteristics. In the neighbouring hollow (light area Fig. 41b next to Finx), nivation processes have inhibited vegetation growth, keeping rocks and pebbles exposed (Le Roux & Luoto 2014; Schöb et al. 2009). In contrast, the monitored hollow (Fig. 41d), with vegetation present, suggests recent revegetation. Results from the previous chapter showed that the monitored hollow has 157 SCD. Such high SCD values were associated

with lower fractional vegetation cover (FVC) and thus can indicate higher nivation pressure. This pressure likely results in thin soils, low SOC, and rapid water loss due to freely, unsorted boulders and pebbles below the surface, causes the rapid loss of water.

These findings also emphasise that caution should be exercised when interpreting soil moisture CV values in larger-scale studies. The CV should be considered alongside total soil moisture levels and other metrics to provide a more comprehensive understanding of soil moisture dynamics, particularly when local factors like geomorphic activity or substrate heterogeneity influence variability (Famiglietti et al. 2008).

5.5.2 Vegetation pattern

Finland exhibited generally higher plant diversity compared to Iceland, likely due to its greater geomorphological diversity and base-rich bedrock (dolomite layer), which create a variety of habitats for rare and highly adapted plant species (Kauhanen 2013). At both sites, vegetation cover was strongly correlated with minor changes in elevation at both study sites, influenced largely by soil moisture. Ordination analysis revealed distinct species assemblages along mesotopographic gradients, with hollow, slope, and ridge positions hosting different communities (Figs. 57, 58). In Iceland, hollows with high soil moisture and low CV supported productive vegetation, whereas Finland's hollows, characterised by higher CV, showed greater variability in vegetation patterns.

These findings align with previous studies that highlight soil moisture as a key determinant of plant community composition and distribution. In northern Finland and Fennoscandia, moist habitats in depressions support higher biomass, species richness, and distinct assemblages compared to drier ridge environments (Kemppinen et al. 2019; Riihimäki et al. 2017; Oksanen & Virtanen 1995). Similarly, in Iceland, high-moisture areas, such as grasslands and wetlands, support productive species (e.g., grasses, sedges, and forbs), while heathlands dominate drier ridges (Arnalds, 2015).

The transition from rich heathland in hollows to poor heathland on ridges was marked by a decline in graminoid and shrub cover and an increase in stress-resistant species such as mosses, lichens, and barren cover (Mörsdorf et al. 2021), albeit with generally very low occurrence of the willow species, as they are preferentially grazed by sheep (Sigurður Þór Guðmundsson, pers. com.). Lichens and moss (notably *Racomitrium lanuginosum*) were found in hollows but were largely restricted to thúfur tops, which exhibited consistently

low soil moisture (Fig. 51). These hummocks created a fine-scale mosaic of microhabitats, adding further variability to soil moisture and vegetation composition. The absence of lichens on slopes may result from shading and litter accumulation by *B. nana* (Fraser et al. 2014).

PFTs and TPI

The distribution of PFTs closely followed the TPI at both sites. In Iceland, dwarf birch abundance decreased from hollows to ridges, while low-stature vegetation (Ls-Veg) persisted up to TPI 0.5 before being replaced by barren cover at higher TPI values. This aligns with the findings of Arnalds et al. (2023) who found that high elevation areas with dry, coarse, thick soils, are susceptible to soil erosion, while moist systems (e.g., wetlands) are more resilient and remain relatively intact in comparison.

In Finland, the relationship between vegetation and topography is more complex due to the presence of more PFT classes. Biocrusts, one of the dominant classes, were more abundant in hollows, slightly decreased in mid-TPI ranges, and increased again on ridges. Their prevalence on ridges reflects the stressful conditions at these locations, such as high exposure, cryogenic activity, and limited soil moisture (Bowker et al. 2014; Cutler 2011; Niittynen et al. 2020a; Kemppinen et al. 2019; Hjort & Luoto 2009). Similarly, barren cover increased with TPI, further indicating harsher environmental conditions.

Ls-Shrub gradually declined as TPI increased, likely due to their sensitivity to environmental gradients, as noted by Kemppinen et al. (2019). In contrast, crowberry was only found at TPI values >= 0.5, known for its resilience to environmental stress and competitive advantage in Arctic ecosystems (Tybirk et al. 2000). The allelopathic effects on neighbouring plants may be weakened by geomorphic disturbances, which could transport allelochemicals deeper into the soil (Bråthen et al. 2010). Crowberry mats can also mediate plant stress by stabilising soil, reducing wind deflation, and enhancing moisture retention (Mod et al. 2014). However, these mats may also reduce nutrient availability, limiting competition from other species.

In both Iceland and Finland, dwarf birch predominantly occupied slope positions. This finding is consistent with other studies, showing that woody plants generally thrive in drier habitats compared to other tundra vegetation type (Kemppinen et al. 2019; Le Ge et al. 2017). However, the dominance of dwarf birch may negatively impact understory

vegetation, as its shading and litter accumulation can suppress shorter plants (Pajunen et al. 2011). This shading effect is potentially contributing to a reduction in species richness in areas where dwarf birch is abundant, such as is observed for lichen, evergreen shrub (*Loiseleuria procumbens, Calluna vulgaris*), and forb (*Polygonum viviparum*) in the Icelandic X plots.

Conversely, forbs, graminoids, and juniper were mainly concentrated in areas with low TPI values (e.g., hollows), where ample soil moisture likely supports their growth. These species' sensitivity to water availability (Abdallah et al. 2020; Kemppinen et al. 2019) explains their restriction to wetter microhabitats.

5.5.3 Vegetation vigour and structure

Dwarf birch showed no change in spectral characteristics related to mesotopography in Iceland, whereas in Finland, NDVI and RENDVI increased from hollow to ridge positions. Besides that, in Finland all shrub classes revealed a general increase in vegetation indices as TPI increased, indicating increased productivity in elevated positions despite generally being less abundant in these locations.

The observed increase in NDVI and RENDVI, alongside the decrease in NDRE, can be explained by the changing ratio among NIR, Red Edge (RE) and Red band reflectance. NDVI and RENDVI rely on Red reflectance, while NDRE uses RE reflectance, which is particularly sensitive to chlorophyll content (Zagajewski et al. 2017). Healthy vegetation exhibits high NIR reflectance and lower Red/RE reflectance, leading to elevated NDVI and RENDVI values. In stressed vegetation, NIR decreases, while RE increases more sharply than Red, producing contrasting NDRE trends (Fig. 46).

In Iceland, the Ls-Veg class, a mix of non-dwarf birch vegetation, showed spectral changes likely linked to shifts in species composition rather than productivity. Species such as *Salix arctica* and *Dryas octopetala* were more abundant on ridges, but limited quadrat data precluded broader conclusions. Larger surveys across TPI gradients would help clarify these patterns.

In Finland, NDVI increases, coupled with declining Ls-Shrub cover, suggest a transition from less productive shrubs to more productive vegetation. Ridge quadrats contained species like *Loiseleuria procumbens* and *Vaccinium uliginosum*, indicating compositional changes. Crowberry dominated areas with TPI > 0.5, likely reflecting its resilience to stress

and its ability to enhance soil moisture retention (Mod et al. 2014). Juniper showed slight NDVI increases across the TPI gradient but was too scarce for reliable interpretation.

Structural data revealed that dwarf birch in Finland decreased in height but had larger, heavier leaves from hollows to ridges. Since NDVI is directly correlated to the leaf area index (LAI) (Goswami et al. 2015), we can conclude that the increase in NDVI can be attributed to the increase in leaf area. This finding was surprising, as we assumed that ridge positions have increased environmental stress conditions and would therefore lower plant vigour, reflected in smaller, less green leaves (Fig. 40). Reasons for the decreased height could be due to lower SCD and therefore increased wind and frost exposure in the winter. Nonetheless, these findings require further investigation due to the small sample size and the low statistical significance of observed changes in leaf structure.

The increase in leaf area and weight may be a result of increased plant productivity related to better access to nutrients through microorganisms or litter quality. Increased dwarf birch presence is positively correlated with a greening trend for RENDVI and NDVI up to a TPI value of 1.1 (Fig. 64, 65), suggesting that higher deciduous shrub cover may lead to changes in nutrient availability and cycling (DeMarco et al. 2014; Buckeridge et al. 2010). However, as soil nutrient availability was not directly measured in this study, the impact of litter quality on nutrient cycling remains speculative and warrants further investigation. Higher nutrient cycling could be also related to increased Biocrust abundance and changing composition at the ridge (Fig. 56, 65). While Biocrust richness was positively correlated with indicators of nitrogen cycling, carbon cycling, and greater ecosystem multifunctionality (Bowker et al. 2014), the impact of Biocrusts on nutrient availability is likely to be less significant compared to the influence of litter quality. Future research could explore the relationship between vegetation indices and shrub abundances across a wider range of topographic positions, vegetation and soil conditions to better understand the potential implications of shrub expansion on nutrient availability in tundra ecosystems.

Vegetation indices showed different trends, particularly NDRE and NDVI/RENDVI. This was especially evident in Finland, where these two metrics showed opposing or misaligned trends (Fig. 66). While studies have demonstrated the suitability of NDRE for biomass estimation (Sharifi & Felegari 2023) and assessing vegetation vigour related to water stress and nitrogen status (Barnes et al. 2000), and NDRE was closely correlated to

NDVI in plant vigour and water stress assessment in southern Iceland (Cutler et al. 2023), it is strongly encouraged to use multiple indices to infer vegetation trends. This is particularly important when hyperspectral information or on the ground data are limited to make more comprehensive interpretations.

5.5.4 Microclimatic impacts on vegetation in Iceland and Fennoscandia

Microclimatic conditions differ markedly between Iceland and Fennoscandia, leading to different vegetation responses and biogeomorphological mechanisms.

In Iceland, Crowberry was intermixed with other tundra vegetation across the terrain, while in Finland, it grew patchily, and only at ridge positions. This was likely due to Iceland's warmer climate and less competition at exposed positions in Finland. Studies in the Arctic (van der Wal & Stien 2014) and the Scandinavian mountain chain (Vowles et al. 2017) indicated that crowberry abundance is higher in warmer locations. Changes in moisture conditions, primarily milder winters and reduced drought stress from frozen ground in spring, also favour evergreen dwarf shrubs like Crowberry. Cold and drought stress can seriously damage these plants (Vuorinen et al. 2017).

These differences can be attributed to the varying growing conditions in the two regions. In Iceland, the warmer macroclimate provides favourable growing conditions across the study area. However, microclimatic conditions differ across mesotopographic gradients in Iceland. Hollows and slope positions offer favourable conditions due to snow insulation (Chaper 4), which provides ample soil moisture during the growing season and generally higher mean soil moisture levels compared to the ridges.

The findings of this study findings suggest that shrub distribution in Iceland may be influenced by soil degradation and erosion, as stress factors related to degradation/erosion (moisture stress, cryoturbation) vary with mesotopographic position. In Iceland, most barren cover is found at elevated positions, where soil moisture levels are low and highly variable near erosion fronts (Cutler et al. 2023). This variability indicated water stress and contributed to lower vigour of graminoids vegetation cover close to eroded areas. In contrast, snow insulation in hollows provides thermoregulation and protects vegetation from wind. Areas without snow cover are subject to temperatures that fluctuate around freezing in winter, promoting freeze-thaw cycles. Icelandic Andosols have high-water holding capacity and low-cohesion; thus, frequent freeze-thaw cycles

lead to substantial reworking and churning of the soils, reducing soil stability (Arnalds, 2015). The additional stress of soil erosion at ridge positions may contribute to the lower presence of dwarf birch, even though soil moisture levels at these locations in Iceland still exceed those in Finland, where dwarf birch is found across the landscape.

Despite the strong differences in soil moisture and temperature conditions between the studied tundra sites, low-growing shrubs such as *V. uliginosum*, *L. procumbens*, *B. nana*, and *E. nigrum* were present in both regions, albeit with higher species richness in Iceland and lower species richness in Finland. This finding supports the results of de la Peña Aguilera (2024), who found that increasing soil moisture and temperature drive local species richness in the Kilpisjärvi region. These species will likely benefit from changing climatic conditions, as they can thrive in a wide range of environmental settings.

In the Finnish study plot, characterised by its colder climate, snow likely plays a more crucial role in shaping local vegetation patterns than soil moisture. This study, corroborating findings from Niittynen et al. (2020a), observed stark differences in winter thermal conditions between hollows and ridges, and comparatively low differences in soil moisture conditions. Similarly, the study of Kemppinen & Niittynen (2022) showed that snow melt and soil and air temperature had the largest impact on plant height. The extreme thermal conditions at both ends of the topographic gradient appear to limit dwarf birch establishment and affect its structure. On exposed ridges, the absence of snow may subject plants to severe winter conditions, such as wind and frost damage, leading to smaller growth forms or precluding establishment altogether. Conversely, in hollows, thick and persistent snow cover might hinder birch colonisation but allows for taller growth forms when established. Dwarf birch was most prevalent at slope positions, where plant traits such as leaf area and weight were highest, suggesting optimal conditions in these intermediate topographic locations. The limited variability in soil moisture across topographic positions and sample size makes it challenging to draw conclusive assessments of its influence on dwarf birch growth.

5.5.5 Soil moisture as a driver of tundra vegetation

Soil moisture is a critical factor in shaping high-latitude vegetation patterns, influencing plant stress and acting as an environmental disturbance factor (Zona et al. 2023; Cutler et al. 2023; Kemppinen et al. 2019; Ackerman et al. 2017; Le Roux et al. 2013). Climate warming in the Arctic has led to disproportionate increases in precipitation (4.5% per

degree of global warming) and decreases in snowfall (Bintanja & Andry 2017), directly affecting soil moisture levels. However, soil moisture distribution is highly heterogeneous, depending on the hydrological conditions influenced by soil depth and properties, which affect the capacity for water infiltration and retention. The underlying subsoil substrate or bedrock is also a major factor, which is not easily identifiable when covered by soil and vegetation. Another important component is the redistribution of water is driven by topography, and as a result more heterogeneous in mountainous than in flatter areas, leading to larger differences in soil moisture levels on a small scale (Engstrom et al. 2005).

Local factors strongly mediate soil moisture patterns, as evidenced at the Finnish study site, where hollow probes quickly lost moisture due to localised drainage processes. Such variability highlights the need for broader measurements across microclimatic zones to draw accurate conclusions. Modelled soil moisture maps, such as those produced by Niittynen et al. (2024), will allow for testing the implications of soil moisture variations on vegetation. However, it should be considered that local heterogeneities in soil moisture conditions may not be captured by broader-scale models. The research by Kemppinen et al. (2018), conducted in the same study area, concluded that soil moisture in high-latitude tundra landscapes exhibits significant fine-scale heterogeneity. High-resolution land surface features predictors, particularly those derived from LiDAR at a 1 m spatial resolution, are essential for accurately estimating soil moisture patterns across these landscapes.

This study highlights the role of mesotopographic variability in shaping soil moisture and vegetation across two tundra regions. While limited in its scope, the findings emphasise the need for further research to understand how mesotopography, soil conditions, and Arctic tundra settings influence soil moisture conditions and thus landscape development.

CHAPTER 6: CONCLUSIONS

This thesis examined the best satellite instruments for monitoring ecological change in Arctic terrestrial regions and explored how microclimatic conditions shape tundra landscapes in sub-Arctic Iceland and oro-Arctic Fennoscandia. These chapters addressed issues such as spectral mixing in soil erosion monitoring and introduced a tool to assess appropriate spatial resolutions for fragmented environments. Furthermore, the dynamics between mesotopography and land cover patterning were explored, as well as the role of soil moisture and temperature in driving biogeomorphological processes.

This final section synthesises the results of Chapters 3–5, identifying best practices for tundra satellite monitoring and the drivers of barren and vegetation cover development in tundra environments. A conceptual microclimatic-land cover model based on the findings from Chapters 4 and 5 is introduced for Iceland and Fennoscandia. The wider implications of the findings are then discussed.

6.1 SOIL EROSION MONITORING

Soil erosion poses a significant threat to affected regions in the Arctic tundra, such as Iceland and Greenland, and should be closely monitored to warn of landscapes crossing irreversible tipping points. However, challenges and limitations arise when using satellite platforms for tundra environmental monitoring. In this study, we were able to show that the use of inappropriate spatial resolutions and vegetation indices can indicate an improvement in landscape condition despite ongoing vegetation cover loss. The extensive expansion of shrubs in the Arctic is fundamentally changing the spectral signature of the landscape, particularly in the NIR band, which is widely used for vegetation indices such as NDVI for landscape cover detection and environmental assessment. This process can mask soil erosion. Barren areas have low values in those spectra, but land cover change due to soil erosion is comparatively slower than the greening signal of shrubification and thus less pronounced in a mixed pixel. In Landsat data most of the erosion patches in Iceland were obscured within a mixed pixel; this hinders accurate monitoring.

PlanetScope has suitable spatial and temporal resolutions (3 m and daily acquisitions), but low spectral resolution. The variability in the data acquisition quality, such as differences in illumination conditions and sensor viewing angles, limits its use. Despite

these limitations, PlanetScope remains a valuable high-resolution dataset with global coverage, providing frequent observations that can be useful for monitoring vegetation dynamics and other land surface changes. Sentinel-2 performed best of the satellite datasets, showing good agreement of NDVI values to the UAV data, good spectral dynamic range and a sufficient spatial resolution to resolve larger barren patches.

To the best of our knowledge, we used for the first time the Shannon evenness index to evaluate pixel mixture. This method could provide useful information when assessing what spatial resolutions are appropriate when monitoring different environments and could inform pixel unmixing approaches. Further testing of this metric with different landscape configurations could increase its applicability. In the studied environment, the amount of information captured increased significantly below 3 m spatial resolution. We therefore emphasise the importance of using UAVs in highly fragmented environments such as the Arctic tundra. The fine-scale land cover variability makes it a difficult terrain to monitor and therefore it is recommended to validate satellite datasets with ground information. Similarly in a recent study of Villoslada et al. (2024) addressed scaling issues in satellite monitoring. They used successfully UAVs to upscale total, leaf, and wood above-ground biomass (AGB) components, as well as topsoil moisture, for subarctic fens with S2 and L8 satellite sources, close to our study site in Finland. Their models showed strong performance, with the best results obtained using S2 data and the red-edge band. The study highlighted the potential for coupling topsoil moisture estimates with AGB predictions beyond the regional scale.

Combining remote sensing data with on the ground information is essential to better comprehend the drivers of erosion and ecosystem change and how these in turn are impacting the environment. For example, in this research, it was possible to link vegetation indices with plant trait information. Interpreting these vegetation indices can be challenging without additional context from ground-based observations. As the Arctic undergoes rapid changes, we need a better understanding of how the changing spectral characteristics of the region are related to ecological and earth surface processes. This is particularly important across different Arctic regions, where the impact of a changing climate can have considerably different effects on biogeomorphological processes. These effects range from land degradation and loss of ecosystem function to the potential 'greening' of the Arctic through increased vegetation growth and shrubification.

Given the challenges of accessing the Arctic, remote sensing will be the primary tool for monitoring tundra ecosystems. Upcoming hyperspectral satellites such as SBG (NASA) and CHIME (ESA) represent a major leap forward. These advanced systems will offer significantly improved spectral information, enabling the capture of the earth's surface in greater detail. The study by Putkiranta et al. (2024) showcased the potential of hyperspectral UAV data in improving estimates of tundra community composition, biomass, and leaf area index (LAI). Such studies pave the way for leveraging hyperspectral satellite datasets for enhanced land cover mapping, biophysical parameter retrieval, and the application of spectral unmixing techniques.

As climate change alters global weather systems, its effect is largely heterogeneous, particularly in the tundra biome where microclimate is strongly mediated by micro- to mesotopography. Microclimate research has become a global discipline, increasingly recognised for its importance in understanding and mitigating the effects of climate change on ecosystems (Kemppinen et al. 2024). Advances in microclimate instruments, including novel field sensors, have made them more accessible and usable for extreme conditions. The region around Kilpisjärvi likely has the most extensive microclimatic monitoring network in the Arctic. A recently released high-resolution dataset modelled from 430 measurement locations covering 300 km^2 at a spatial resolution of 3 m, provides a valuable resource for future theoretical and applied research (Niittynen et al. 2024). Combining monitoring of soil properties such as temperature and moisture, which are critical components for understanding small-scale landscape development, is essential because these factors cannot be accurately sensed remotely at the required temporal and spatial resolutions. For example, detailed microclimate data, such as from Niittynen et al. (2024), could be combined with UAV-derived land cover maps, as in this study. This integration would enable comprehensive analysis of land cover distribution and microclimate relationships, while long-term monitoring could reveal insights into land cover change and microclimate effects. Such knowledge could prove beneficial, as microclimate research has important applications in ecosystem management, particularly in biodiversity conservation. Identifying areas of rapid environmental transformation and protecting microrefugia can help preserve vulnerable species, maintain ecosystem resilience, mitigate the impacts of extreme weather events, and improve ecosystem health and sustainability (Kemppinen et al. 2024).

6.2 MICROCLIMATE AND LANDSCAPE DEVELOPMENT IN ICELAND

The microclimatic conditions in Iceland vary between winter and summer, with distinct effects on landscape processes and vegetation distribution. One main question was to investigate how the distribution of barren cover was related to meso-scale topographic position (hollow, slope and ridge) (TPI) and SCD. The SCD levels were overall relatively low and varied across a short distance (13 km) from the sea towards inland ranging from 69 to 103 days. The topographic variability is rather modest. A clear negative correlation has been detected between the TPI and FVC, with hollows being predominantly fully vegetated and ridges having the highest barren cover distribution (Fig. 67). Conversely, a positive correlation was observed between SCD and FVC, indicating that increasing SCD is associated with lower barren cover. Another research question was understanding the soil thermal conditions during the winter. The Frozen Degree Days (FDD) varied with topographic position, primarily due to differences in snow coverage, although the variability was low during winter. However, on ridges, soil temperatures fluctuated around the freezing point, leading to extended periods of freeze-thaw cycles. This increased cryogenic activity reduces soil stability and likely heightens soil erosion susceptibility due to the properties of Andosols.

During summer, Iceland's warmer macroclimate generally provides favourable growing conditions across the study area. Nevertheless, microclimatic conditions, related to soil moisture, vary along mesotopographic gradients, leading to differences in species richness, diversity, and vegetation distribution. One of the study's research questions was to examine how topography affects the spatial distribution of soil moisture. The results showed considerable variability in mean soil moisture related to mesotopography, with higher moisture values in hollows and lower moisture values on ridges. The soil moisture stress indicator (CV of soil moisture) showed moderately lower values for hollows and higher values for ridges. The signal at the ridge could have been additionally influenced by increased occurrence of bare cover in ridge positions. The study of Cutler et al. (2023) demonstrated that mean soil moisture levels decreased, and CV soil moisture considerably increased towards the erosion front, at the boundary between vegetated and barren areas. This relationship between mesotopographic position, bare cover, and soil moisture dynamics suggests that two areas in the Icelandic landscape experience higher

environmental stress: near erosion fronts and on mesotopographic ridges. These findings may have implications for predicting areas of future erosion.

Another research question was to investigate how plant community composition is structured by mesotopography and whether plant vigour changes over the topographic gradient. Additionally, we aimed to explore if the land cover patterns are related to soil moisture. The results showed that plant community composition was correlated with mesotopographic variability. Low-growing shrubs and graminoid cover generally decreased from hollows to ridges due to more favourable conditions in the hollows. These conditions include snow accumulation, higher SOC, and greater soil depth, all of which contribute to more favourable soil moisture levels. The snow cover provides thermoinsulation during winter, protecting the vegetation and soil from wind and freeze-thaw cycles that cause cryoturbation. In the early growing season, the snow cover melts, providing vital soil moisture. Hollows are better able to retain this moisture, allowing for more stable and higher soil moisture conditions compared to ridges. However, despite the differences in soil moisture between hollows and ridges, in Iceland the soil is relatively thick compared to the oro-Arctic region in Kilpisjärvi with Cryosols, allowing ridges to maintain relatively high soil moisture levels. Towards the ridge position, species richness and diversity decreased but remained comparatively similar to the hollows. Ridges were characterised by a relative increase in abundance of less productive plants such as mosses and lichens and barren cover was only present at the ridges. This pattern is related to harsher environmental conditions, as ridges experience extended periods of freeze-thaw cycles, lower soil moisture levels, high wind speeds, and increased vulnerability to wind erosion due to the low cohesive nature of Andosols, resulting in higher barren cover (Fig. 67). The dominant wind direction from the north, originating from the nearby sea, primarily influence the location of soil erosion. Dwarf birch predominantly occupied slopes, forming dense patches that suppress understory vegetation and showed no changes in spectral characteristics across TPI values. Crowberry was almost evenly distributed along mesotopographic gradients, with a slightly lesser presence on the slopes. NMDS analysis revealed a relationship between topographic position, soil moisture levels, and plant community composition. Generally, hollows exhibited higher soil moisture levels and lower CV, while slope and ridge positions showed lower soil moisture levels and higher CV, revealing increased water stress in these positions and the role of soil moisture in structuring the land cover.

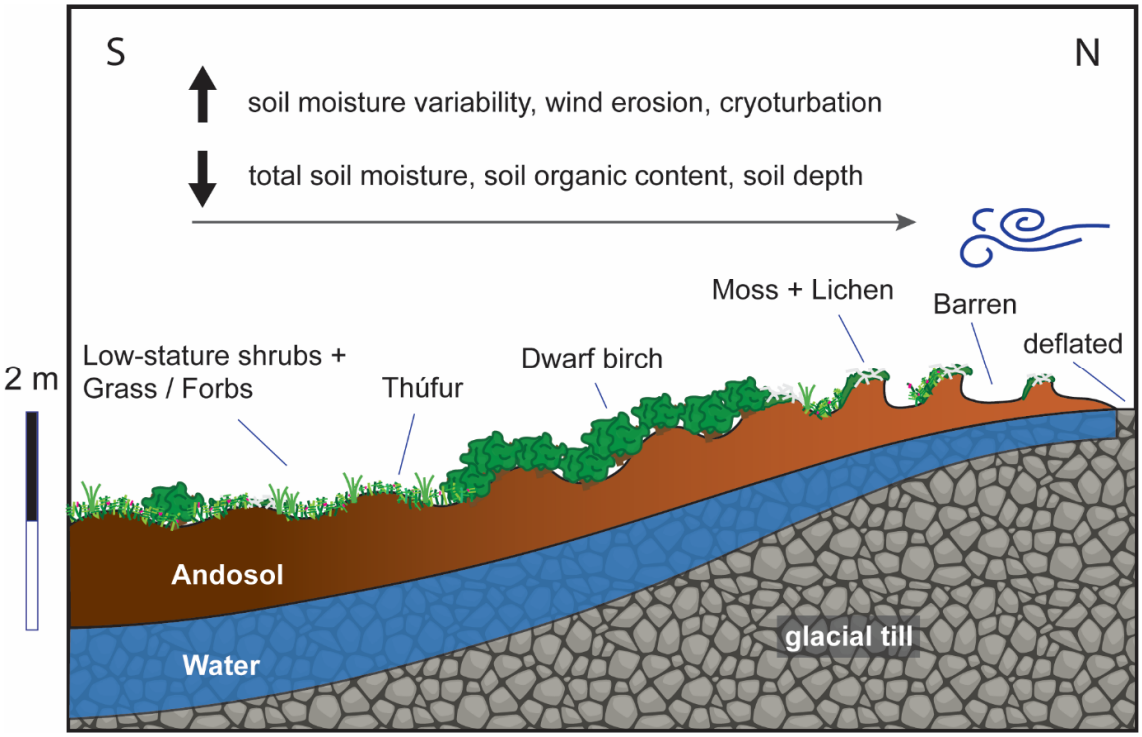

Fig. 67 Conceptual microclimatic landscape development model for Svalbarðshreppur in Iceland.

Our findings have broader implications for understanding the resilience of Iceland's landscape to climate change and the biogeomorphological feedbacks driving soil erosion. Future environmental changes associated with climate change, such as decreased snow cover and increased dwarf birch shrub cover, are mediated by mesotopography. However, the impact of these changes on the Icelandic landscape, particularly in coastal regions, remains unclear. Decreasing snow cover could increase soil erosion vulnerability due to lower thermoregulation and higher exposure to wind erosion and extreme events, while increased medium-stature shrub cover could trap snow, protect vegetation and stabilise soils in the long-term. Furthermore, soil erosion is altering environmental conditions and plant growth, but the specific plants resistant to these pressures have not been established. It is crucial to determine whether dominant spreading plants can stabilise Icelandic soils, with a particular interest in the ability of dwarf birch to reduce soil erosion in Iceland's unique soil conditions. For instance, dwarf birch may stabilise Andosols through its root system or capture snow to increase SCD and reduce erosion pressure in winter ; however, this potential remains uncertain and requires further research.

The study of Streeter & Cutler (2020) demonstrated that small barren patches form around larger barren patches, and the study Cutler et al. (2023) explored a possible

mechanism for this in soil moisture gradients. In our research, we could further show that the initial growth of barren patches probably occurs at ridge positions. To expand knowledge about the erosion dynamics in Iceland, it will be useful to investigate whether breached vegetation cover exposing soil, has the potential to naturally revegetate. The capacity for soil revegetation is particularly crucial to understand in the context of unstable Andosols, which are highly susceptible to deflation and present challenges for vegetation to reestablish due to poor root anchorage. Currently, it is unclear to what extent vegetation can reestablish on these unstable soils. Identifying the specific conditions under which small barren patches might "heal" and revegetate, along with any threshold size and environmental factors that may inhibit this process, is essential. This inquiry is especially important because successful revegetation could foster short-range positive feedback mechanisms that create a pathway towards landscape resilience, counteracting the prevailing negative feedback mechanism of soil erosion (Rietkerk & van de Koppel, 2008). This could be investigated in the future by revisiting the sites to acquire new UAV data and comparing it to the existing dataset, allowing to study of the fine-scale dynamics of these small barren patches over time.

Exploring these processes will enable us to better comprehend the dynamics of erosion patterns and landscape resilience in Iceland. The strong correlation between mesotopography and land cover suggests that the present spatial patterns are a result of underlying terrain heterogeneity rather than Turing patterns emerging from spatial self-organisation. Turing pattern form from scale-dependent feedbacks, which are net feedback effects of short-distance activators (vegetation growth) and long-distance inhibitors (soil erosion) (Rietkerk & van de Koppel 2008). The limited ability of vegetation in hindering soil erosion and potentially revegetation, due to the unstable properties of Andosols, further indicates the absence of the necessary positive feedback for such pattern formation. This hypothesis can be tested in future studies by comparing land cover maps over time to observe changes occurring on the Ms-Shrub – Barren and Ls-Veg – Barren cover boundaries. Additionally, cellular automata models or agent-based models could be used to simulate vegetation-soil interactions and assess pattern formation.

However, the erosion patterns in Iceland likely result from a combination of factors, including localised perturbations due to underlying terrain heterogeneity and to some extent through spatial self-organisation processes. While topography creates areas more

prone to erosion, once erosion begins, it can propagate across the landscape through mechanisms that are partially independent of topography. For instance, the drying out of soil at erosion front edges can facilitate further erosion, regardless of the initial topographic conditions. This terrain variability, coupled with self-propagating erosion processes, creates different resilience responses across the landscape to global stressors. Consequently, a state of multistability emerges, where alternative stable states coexist in spatial domains with varying resilience levels (Fig. 14c) (Rietkerk et al. 2021). This pattern may represent a pathway of resilience, where tipping to a single alternate stable state (e.g., complete desertification) is avoided, and hollow areas serve as refugia for vegetation. This aligns with our observations that hollow positions were consistently fully vegetated, suggesting high resilience to soil erosion in these positions. However, further research and close monitoring are necessary to fully understand the interaction between climate, land cover and topography.

6.3 MICROCLIMATE AND LANDSCAPE DEVELOPMENT IN FENNOSCANDIA

In Finland, the microclimatic conditions during winter and summer exhibited distinct characteristics, impacting landscape processes and vegetation distribution (Fig. 68). As in Iceland, the research question focused on investigating the relationship between barren cover distribution, meso-scale topographic position and SCD. The results indicate that both factors were important in land cover distribution. During winter, Finland experiences high levels of SCD, with an average of approximately 155 days. The topography is more variable compared to the study sites in Iceland, with pronounced topographic landscape features such as hollows and ridges. The study found that barren cover was predominantly located in deep hollows, where nivation pressure inhibits vegetation growth, and on ridges where snow free ridgetops are deflated. Barren cover distribution was more limited in extent compared to Iceland, occurring only in small patches of a few square meters within specific topographic positions. At Fin1 a SCD threshold of about 155 days was identified at which maximum FVC was detected. This value might represent an important biogeomorphological threshold, where growing conditions are met, and beyond which geomorphological pressures increase, limiting vegetation growth. However, at Fin2

in higher altitude lower SCD values were associated with higher FVC, which might stem from the presence of more stress-resistant vegetation composition.

Another important component of the research was to investigate how soil thermal conditions differ with topographic position during the winter. The colder climate, increased snowfall, and steeper topographic variability in Finland contribute to significant differences in frost activity across various topographic positions. Hollows benefit from snow cover and thermoregulation, experiencing low temperature variability, with winter soil temperatures hovering between 0 and -2°C. In contrast, ridges with little to no snow cover exhibit strong temperature variability, with soil temperatures reaching as low as -13.4°C. Moreover, during early spring, these exposed positions experience freeze-thaw cycles, which reduce soil stability and potentially contribute to the development of barren cover.

During the summer period, the study aimed to examine how topography affects the spatial distribution of soil moisture. Finland exhibits low soil moisture levels and comparatively high CV values during the growing season. The analysis revealed low variability in mean soil moisture related to mesotopography, which can be attributed to the thin Cryosols prevalent in the region. These soils have low water retention capacity, resulting in minor soil moisture differences between topographic positions. Counterintuitively, the soil moisture stress indicator (CV) was higher in the hollows than at the ridges. This finding was related to the slightly higher ability of hollows to retain soil moisture compared to ridges. Consequently, the drying process in hollows resulted in more variability in soil moisture readings, while the consistently low soil moisture levels on the ridges led to lower variability. This finding emphasises the need to use multiple soil moisture metrics to assess water conditions.

Examining the influence of mesotopography on plant community composition and vigour, as well as the relationship between land cover patterns and soil moisture, was another research focus. The study found that vegetation composition and plant vigour were correlated with mesotopographic variability (Fig. 68). Ls-shrub and graminoid cover decreased from hollows to ridges, while barren cover and biocrusts were more abundant on ridges and, to a lesser degree, in hollows. Biocrust was present across all topographic positions, becoming proportionally dominant to Ls-shrubs at the ridge positions. Crowberry predominantly occupied ridges, while dwarf birch primarily inhabited slopes

and moderately convex positions. Dwarf birch exhibited morphological responses to the mesotopographic gradient, such as reduced shrub height and larger, heavier leaves towards the ridge. These plant trait changes were also observed at the wider landscape scale, as evidenced by increased NDVI, which is associated with the leaf area index (LAI), with rising TPI from hollow to ridge. Generally, species richness and diversity of vascular plants decreased towards the ridge. Geomorphological features, such as hummocks resulting from cryoturbation or aeolian erosion, were only found at the ridge. This indicates increased environmental stress in these positions, which was mainly attributed to lower snow cover duration. Insufficient soil moisture readings were available to assert a relationship between soil moisture and land cover distribution.

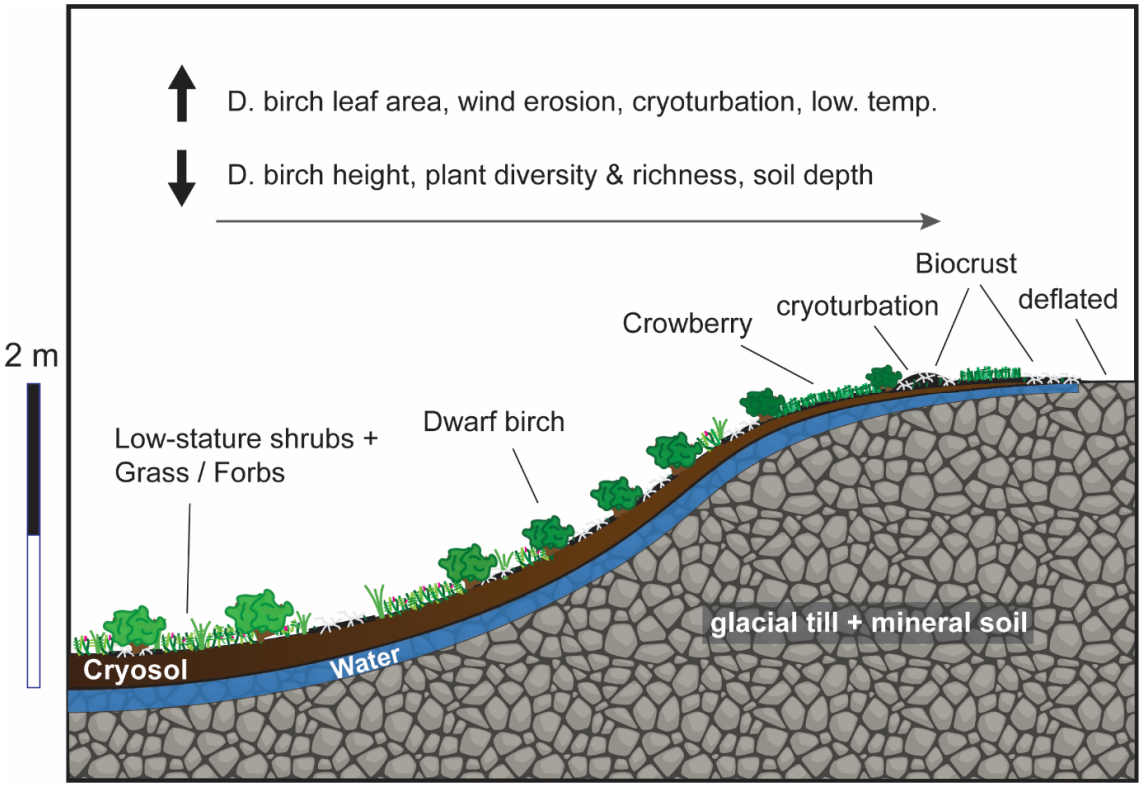

Fig. 68 Conceptual microclimatic landscape development model for Kilpisjärvi in Finland.

In Finland, increased temperatures are likely to contribute to the expansion of woody shrubs while diminishing the cryogenic processes that certain species rely on. However, a shorter SCD could increase spring related pressures, such as tissue damage in the early growing season due to exposure to frost. These shifts in microclimatic conditions will most significantly affect vegetation composition and species richness. The study showed a reduction in species richness and diversity of vascular plants in more exposed terrain. Cold-dependent plants relying on snow cover could be threatened by further SCD

reduction, potentially surviving only in small pockets or being overtaken by generalist species such as *E. nigrum*, which notably dominates ridge areas, and *B. nana*. While these results are speculative due to the small sample size, they align with Niittynen et al. (2018), who demonstrated that shorter SCD tempered the effect of rising temperatures on species richness and led to accelerated rates of local species extinction after a tipping point at 20-30% SCD decrease.

Ridges might continue to have low vegetation cover due to persistent stressful conditions, where plant damage from frost, windblown ice crystals or drought events will pose significant threats. However, the stabilising properties of biocrusts and the compact, cohesive nature of Cryosols provide better protection against soil redistribution by wind compared to the highly erodible Andosols in Iceland. Consequently, the Finnish tundra might be less vulnerable to soil erosion despite reduced snow cover, and previously barren areas affected by nivation might have the opportunity to revegetate through primary succession.

The key species *B. nana* exhibits morphological changes in response to minor topographical variability, potentially indicating alterations in its plant physiology and ecosystem function. Given its widespread distribution across the tundra and its potential implications for global climate feedbacks (such as changing albedo and carbon cycling), local microclimate (soil moisture and temperature) and biogeomorphological processes (including snow trapping, shading, insulation, and soil stabilisation) (Parker et al. 2021; Kemppinen et al. 2021; Juszak et al. 2014; Sturm et al. 2005; Sturm et al. 2001), further research on this species sensitivity and response to microclimatic conditions is vital.

6.4 CURRENT STATE AND FUTURE OUTLOOK

This study demonstrated the complex relationship between microclimates formed by meso-scale landforms and their effects on snow cover duration, soil temperature and moisture in Icelandic and Finnish tundra sites. These microclimatic variables, shaped by landforms, ultimately drive biogeomorphological processes and the distribution of land cover across the tundra landscape. The findings emphasise the importance of considering site-specific environmental factors and stress gradients when assessing the effect of microclimatic variability on vegetation dynamics and landscape development.

Mesotopographic landforms such as hollows, slopes, and ridges play crucial roles in mediating macroclimatic effect, land cover use, and soil development. Each position contributes to creating niche habitats for vegetation while also governing geomorphological processes such as soil and sediment redistribution. Changing climatic conditions and continuous anthropogenic grazing pressure are altering the microclimatic characteristics and may lead to ecological shifts in different topographic positions.

This study suggests that the tundra's response to further reductions in SCD and a warmer, wetter climate will be highly heterogeneous across the biome on both regional and local scales. Although the main spectral signal indicates a 'greening' of the Arctic, associated with shrubification and primary succession, biogeomorphological processes differ significantly across the tundra biome, with major relevance for landscape resilience and future trajectories.

Soil nutrients and microbial activity are crucial factors in Arctic landscape development not covered in this research. Future studies should investigate spatial changes in soil nutrients and their influence on ecosystem processes, especially in the context of Arctic shrubification. Buckeridge et al. (2010) found that tall birch ecosystems have faster nitrogen cycling rates due to higher quality litter inputs, concluding that these litter-related feedbacks may be as important as snow-shrub feedbacks in promoting shrub growth. Conversely, Stark et al. (2023) suggest that evergreen shrub expansion may lead to microbial nutrient limitation, potentially stabilising soil organic matter stocks under warming conditions. These interactions between shrub growth, soil nutrients, and microbial processes are complex, but are essential to understanding landscape development more comprehensively.

Arctic weather extremes are becoming more frequent and intense due to climate change and the region's increased sensitivity to short-term fluctuations. These extremes include more frequent and severe storms, rapid sea ice loss, unprecedented heatwaves, and sudden permafrost thaw events. Such extreme weather patterns, driven by interactions between a wavy tropospheric jet stream, polar vortex displacements, and ongoing Arctic Amplification, have far-reaching implications for both Arctic ecosystems and global climate systems (Overland 2021). The anticipated reduction in snow cover, particularly in coastal regions, could expose vulnerable vegetation to the abrasive effects of high-velocity winds combined with ice crystals. Understanding the impact of reduced snow

cover on vegetation, particularly under stormy conditions, is crucial despite the challenges posed by the infrequency of such events. Studies investigating the insulating properties of snow are therefore important for comprehending these dynamics. For instance, Tyystjärvi et al. (2023) investigated winter near-surface temperatures related to SCD in various Finnish environments. The study found that winter near-surface temperatures in boreal and tundra regions vary significantly based on topography and snow depth: areas with complex terrain and shallow snowpacks had high temperature variability, while flat areas with deep snow showed more stable temperatures. Such research is crucial for assessing the impact of changing snow cover conditions on the energy balance of cold-dependent tundra landscapes.

While the Arctic is currently experiencing global warming, climate models predict a potential drastic cooling of 10-15°C in northern Europe this century. This cooling could occur if the Atlantic Meridional Overturning Circulation (AMOC) crosses a critical tipping point, an event that is becoming increasingly likely (van Westen et al. 2024). Due to this uncertainty in the near-future climate, we need to prepare for a warming and cooling scenario and closely monitor the changes in the high-latitude systems.

The diverse land cover patterns observed between the Icelandic and Finnish sites underscore the need for further research to shed light on the underlying microclimatic mechanisms driving these differences and their potential implications for future land cover changes in the context of climate change scenarios. This study highlights the significance of high-resolution data and sensor quality for effective monitoring of these changes. The integration of these datasets with on the ground information on land cover and soil properties facilitates a more precise evaluation of the complex interactions between microclimates and the tundra environment.

Advancements in UAV technology are enhancing Arctic monitoring capabilities. Emerging cheaper, lighter fixed-wing systems overcome the survey area limitations of common quadcopters, which is crucial given the brief survey windows available in challenging Arctic conditions. The decreasing size and cost of multispectral and hyperspectral sensors, including those with shortwave infrared (SWIR) and thermal infrared (TIR) bands, are making these technologies more accessible to researchers. This enables the study of land cover thermal properties (Yang et al. 2021) and improves soil moisture assessments (Turner et al. 2024). Additionally, UAV-mounted LiDAR systems allow detailed

examination of structural features, such as the relationship between shrub height, topography and snow accumulation (Lamare et al. 2023). Collectively, these developments enhance the validation and accuracy of satellite systems while facilitating more comprehensive tundra studies (Yang et al. 2022).

Moving forward, research efforts should focus on integrating site-specific findings with broader-scale studies to develop a comprehensive understanding of tundra ecosystem responses to changing environmental conditions. By combining local insights with regional and global-scale analyses, we can improve our ability to predict tundra landscape trajectories. This integrated approach will enhance the development of effective conservation and management strategies in the face of climate change challenges.

As physical geographers, our endeavour is to study the earth's surface at various scales and in diverse environments, aspiring to gain insights into landscape formation. By analysing environmental variables and land cover patterns across time and space, we can develop a deeper understanding of environmental processes and identify the nature and trajectory of landscape changes. In this thesis, the objectives were twofold: to enhance our capabilities in Arctic tundra monitoring and to investigate the significance of microclimates in shaping Arctic landscapes across two distinct tundra regions. Through this research, I have come to recognise that I have only begun to explore the complexities of Arctic monitoring and microclimate dynamics. While much work remains to be done, the outcomes of this study offer meaningful contributions to advancing key concepts in environmental monitoring and demonstrating how topography and microclimatic variability influence soil erosion and vegetation dynamics in Iceland and Fennoscandia.

PUBLICATION BIBLIOGRAPHY

Aalto, J.; Niittynen, P.; Riihimäki, H.; Luoto, M. (2021): Cryogenic land surface processes shape vegetation biomass patterns in northern European tundra. In Commun Earth Environ 2 (1). DOI: 10.1038/s43247-021-00292-7.

Aalto, J.; Scherrer, D.; Lenoir, J.; Guisan, A.; Luoto, M. (2018): Biogeophysical controls on soil-atmosphere thermal differences: implications on warming Arctic ecosystems. In Environ. Res. Lett. 13 (7), p. 74003. DOI: 10.1088/1748-9326/aac83e.

Aalto, J.; Harrison, S.; Luoto, M. (2017): Statistical modelling predicts almost complete loss of major periglacial processes in Northern Europe by 2100. In Nature communications 8 (1), p. 515. DOI: 10.1038/s41467-017-00669-3.

Aalto, J.& Luoto, M. (2014): Integrating climate and local factors for geomorphological distribution models. In Earth Surf. Process. Landforms 39 (13), pp. 1729–1740. DOI: 10.1002/esp.3554.

Aalto, J.; Venäläinen, A.; Heikkinen, R. K.; Luoto, M. (2014): Potential for extreme loss in high-latitude Earth surface processes due to climate change. In Geophys. Res. Lett. 41 (11), pp. 3914–3924. DOI: 10.1002/2014GL060095.

Abdallah, M. A. B.; Durfee, N.; Mata-Gonzalez, R.; Ochoa, C. G.; Noller, J. S. (2020): Water Use and Soil Moisture Relationships on Western Juniper Trees at Different Growth Stages. In Water 12 (6), p. 1596. DOI: 10.3390/w12061596.

Ackerman, D.; Griffin, D.; Hobbie, S. E.; Finlay, J. C. (2017): Arctic shrub growth trajectories differ across soil moisture levels. In *Global Change Biol* 23 (10), pp. 4294–4302. DOI: 10.1111/gcb.13677.

Aho, J. & Kalela, O. (1966): The spring migration of 1961 in the Norwegian lemming, Lemmus lemmus (L.), at Kilpisjärvi, Finnish Lapland. Annales Zoologici Fennici, 3(1), 53–65. http://www.jstor.org/stable/23730824.

Ahti, T.; Hämet-Ahti, L. & Jalas, J. (1968): Vegetation zones and their sections in northwestern Europe. Annales Botanici Fennici, 5(3), 169–211. http://www.jstor.org/stable/23724233.

Allstadt, A. J.; Vavrus, S. J.; Heglund, P. J.; Pidgeon, A. M.; Thogmartin, W. E.; Radeloff, V. C. (2015): Spring plant phenology and false springs in the conterminous US during the 21st century. In Environ. Res. Lett. 10 (10), p. 104008. DOI: 10.1088/1748-9326/10/10/104008.

Aldred, O.; Einarsson, Á.; Hlíðberg, Ó. K.; Lárusdóttir, B.; Moreland, J.; Ólafsson, S. (2010): On the precipice: Aerial archaeology in Iceland. Archaeologia Islandica, 8, 111-122.

AMAP, (2017): Snow, Water, Ice and Permafrost in the Arctic (SWIPA) 2017. Arctic Monitoring and Assessment Programme (AMAP), Oslo, Norway. xiv + 269 pp.

Anderson, K.; Gaston, K. J. (2013): Lightweight unmanned aerial vehicles will revolutionize spatial ecology. In Frontiers in Ecol & Environ 11 (3), pp. 138–146. DOI: 10.1890/120150.

Andreatta, D.; Gianelle, D.; Scotton, M.; Dalponte, M. (2022): Estimating grassland vegetation cover with remote sensing: A comparison between Landsat-8, Sentinel-2 and PlanetScope imagery. In Ecological Indicators 141, p. 109102. DOI: 10.1016/j.ecolind.2022.109102.

Angert, A.; Biraud, S.; Bonfils, C.; Henning, C. C.; Buermann, W.; Pinzon, J. et al. (2005): Drier summers cancel out the CO2 uptake enhancement induced by warmer springs. In Proceedings of the National Academy of Sciences of the United States of America 102 (31), pp. 10823–10827. DOI: 10.1073/pnas.0501647102.

Aradóttir, Á.L. (2003): Restoration challenges and strategies in Iceland. Soil Conservation Service of Iceland.

Aradóttir, Á.. L.; Arnalds, Ó.; Archer, S. (1992): Degradation of vegetation and soils (Hnignun grodurs og jardvegs). Græðum Island, soil conservation service yearbook 1991–1992:73–82 (in Icelandic).

Archer, S.; Stokes, C. (2000): Stress, disturbance and change in rangeland ecosystem. In Ó. Arnalds, & S. Archer (Eds.), Rangeland desertification, pp. 17–38. DOI: 10.1007/978-94-015-9602-2.

Arnalds, Ó.; Marteinsdóttir, B.; Brink, Sigmundur H.; Þórsson, J. (2023): A framework model for current land condition in Iceland. In PloS one 18 (7), e0287764. DOI: 10.1371/journal.pone.0287764.

Arnalds, Ó. (2015): The Soils of Iceland. Dordrecht: Springer Netherlands.

Arnalds, Ó.; Thorarinsdottir, E. F.; Thorsson, J.; Waldhauserova, P. D.; Agustsdottir, A. M. (2013): An extreme wind erosion event of the fresh Eyjafjallajökull 2010 volcanic ash. In Scientific reports 3, p. 1257. DOI: 10.1038/srep01257.

Arnalds, Ó (2004): Volcanic soils of Iceland. In CATENA 56 (1-3), pp. 3–20. DOI: 10.1016/j.catena.2003.10.002.

Arnalds, Ó.; Barkarson, B. H. (2003): Soil erosion and land use policy in Iceland in relation to sheep grazing and government subsidies. Environmental Science & Policy, vol. 6, iss. 1, pp. 105-113, ISSN 1462-9011. DOI: 10.1016/S1462-9011(02)00115-6.

Arnalds, O.; Kimble, J. (2001): Andisols of Deserts in Iceland. In Soil Science Soc of Amer J 65 (6), pp. 1778–1786. DOI: 10.2136/sssaj2001.1778.

Arnalds, Ó; Þorarinsdottir, E.F.; Metusalemsson, S.; Jonsson, A; E. Gretarsson, E.; Arnason, A (2001): Soil erosion in Iceland. Soil Conservation Service and Agricultural Research Institute, Iceland.

Arnalds, Ó (2000a): Rangeland Desertification. In Ó. Arnalds, & S. Archer (Eds.), Rangeland desertification, pp. 5–16. DOI: 10.1007/978-94-015-9602-2.

Arnalds, Ó (2000b): The Icelandic 'Rofabard' soil erosion features. In Earth Surf. Process. Landforms 25 (1), pp. 17–28. DOI: 10.1002/(SICI)1096-9837(200001)25:1<17::AID-ESP33>3.0.CO;2-M.

Arnalds, A. (1987): Ecosystem Disturbance in Iceland. In Arctic and Alpine Research 19 (4), p. 508. DOI: 10.2307/1551417.

Arnason, K.; Benediktsson, J. A. (1999): Environmental Mapping Based on High Resolution Remote Sensing Data*, pp. 89–99. DOI: 10.1007/978-3-642-60105-7_8.

Ashcroft, M. B.; Gollan, J. R. (2012): Fine-resolution (25 m) topoclimatic grids of near-surface (5 cm) extreme temperatures and humidities across various habitats in a large (200 × 300 km) and diverse region. In Intl Journal of Climatology 32 (14), pp. 2134–2148. DOI: 10.1002/joc.2428.

Assmann, J. J.; Myers-Smith, I. H.; Kerby, J. T.; Cunliffe, A. M.; Daskalova, G. N. (2020): Drone data reveal heterogeneity in tundra greenness and phenology not captured by satellites. In Environ. Res. Lett . 15 (12), p. 125002. DOI: 10.1088/1748-9326/abbf7d.

Assmann, J. J.; Kerby, J. T.; Cunliffe, A. M.; Myers-Smith, I. H. (2019): Vegetation monitoring using multispectral sensors — best practices and lessons learned from high latitudes. In J. Unmanned Veh. Sys. 7 (1), pp. 54–75. DOI: 10.1139/juvs-2018-0018.

Atar, M.; Shah-Hosseini, R.; Ghaffari, O. (2024): Retrieval of Soil Moisture Using Time Series of Radar and Optical Remote Sensing Data at 10 m Resolution. In : ECRS 2023. ECRS 2023. Basel Switzerland: MDPI, p. 75.

Austrheim, G.; K. Bråthen, R. Ims, A. Mysterud & F. Ødegaard (2010): Alpine environment. In: Environmental conditions and impactsfor Red List species (J. A. Kålås et al., eds.), pp. 107–118, Norwegian Biodiversity Information Centre.

Barbero-Palacios, L.; Barrio, I. C.; García Criado, M.; Kater, I.; Petit Bon, M.; Kolari, T. H. M. et al. (2024): Herbivore diversity effects on Arctic tundra ecosystems: a systematic review. In Environ Evid 13 (1). DOI: 10.1186/s13750-024-00330-9.

Barichivich, J.; Briffa, K.; Myneni, R.; Schrier, G.; Dorigo, W.; Tucker, C. et al. (2014): Temperature and Snow-Mediated Moisture Controls of Summer Photosynthetic Activity in Northern Terrestrial Ecosystems between 1982 and 2011. In Remote Sensing 6 (2), pp. 1390–1431. DOI: 10.3390/rs6021390.

Barkhordarian, A.; Nielsen, D. M.; Olonscheck, D.; Baehr, J. (2024): Arctic marine heatwaves forced by greenhouse gases and triggered by abrupt sea-ice melt. In Commun Earth Environ 5 (1). DOI: 10.1038/s43247-024-01215-y.

Barnes, E.M.; Clarke, T.; Richards, S.E.; Colaizzi, P.D.; Haberland, J.; Kostrzewski, M.; Waller, P.M.; Choi, C.Y.; Riley, E.; Thompson, T.L.; Lascano, R.J.; Li, H.; Moran, M.S.; Robert, P.C.; Rust, R.H.; Larson, W.E. (2000). Coincident detection of crop water stress, nitrogen status and canopy density using ground-based multispectral data. W.E. 504 Precis. Agric. (2010) 11:488–506 123 Larson; Proceedings of the fifth international conference on precision agriculture (2000), Bloomington, MN, USA (Vol. 1619, No. 6).

Barrio, I. C. & Arnalds, Ó (2023): Agricultural Land Degradation in Iceland. In Pereira P.; Muñoz-Rojas M.; Bogunovic I.; Zhao W. (Eds.): A European perspective, vol. 121. Cham:

Springer (The handbook of environmental chemistry Impact of agruculture on soil degradation, 2), pp. 159–177.

Barrio, I. C.; Hik, D. S.; Thórsson, J.; Svavarsdóttir, K.; Marteinsdóttir, B.; Jónsdóttir, I. S. (2018): The sheep in wolf's clothing? Recognizing threats for land degradation in Iceland using state-and-transition models. In Land Degrad Dev 29 (6), pp. 1714–1725. DOI: 10.1002/ldr.2978.

Barton, C. V. M. (2012): Advances in remote sensing of plant stress. In Plant Soil 354 (1-2), pp. 41–44. DOI: 10.1007/s11104-011-1051-0.

Bartsch, A.; Höfler, A.; Kroisleitner, C.; Trofaier, A. (2016): Land Cover Mapping in Northern High Latitude Permafrost Regions with Satellite Data: Achievements and Remaining Challenges. In Remote Sensing 8 (12), p. 979. DOI: 10.3390/rs8120979.

Batista, P. V. G.; Evans, D.; Cândido, B. M.; Fiener, P. (2023): Does soil thinning change soil erodibility? an exploration of long-term erosion feedback systems. Soil, 9(1), 71-88. DOI: 10.5194/soil-9-71-2023.

Beamish, A.; Raynolds, M. K.; Epstein, H.; Frost, G. V.; Macander, M. J.; Bergstedt, H. et al. (2020): Recent trends and remaining challenges for optical remote sensing of Arctic tundra vegetation: A review and outlook. In Remote Sensing of Environment 246, p. 111872. DOI: 10.1016/j.rse.2020.111872.

Belgiu, M. & Drăguţ, L. (2016): Random forest in remote sensing: A review of applications and future directions. In ISPRS J PHOTOGRAMM 114, pp. 24–31. DOI: 10.1016/j.isprsjprs.2016.01.011.

Bennett, J. R.; Shaw, J. D.; Terauds, A.; Smol, J. P.; Aerts, R.; Bergstrom, D. M. et al. (2015): Polar lessons learned: long-term management based on shared threats in Arctic and Antarctic environments. In Frontiers in Ecol & Environ 13 (6), pp. 316–324. DOI: 10.1890/140315.

Bennie, J.; Huntley, B.; Wiltshire, A.; Hill, M. O.; Baxter, R. (2008): Slope, aspect and climate: Spatially explicit and implicit models of topographic microclimate in chalk grassland. In Ecological Modelling 216 (1), pp. 47–59. DOI: 10.1016/j.ecolmodel.2008.04.010.

Berdanier, A. B. & Klein, J. A. (2011): Growing Season Length and Soil Moisture Interactively Constrain High Elevation Aboveground Net Primary Production Ecosystems,14, 963–974, https://doi.org/10.1007/s10021-011-9459-1.

Bergpórsson, P. (1996): Hitafar og gródur [Temperature and vegetation]. pp. 141–164.

Berner, L. T.; Massey, R.; Jantz, P.; Forbes, B. C.; Macias-Fauria, M.; Myers-Smith, I. et al. (2020): Summer warming explains widespread but not uniform greening in the Arctic tundra biome. In Nature communications 11 (1), p. 4621. DOI: 10.1038/s41467-020-18479-5.

Berner, L. T.; Jantz, P.; Tape, K. D.; Goetz, S. J. (2018): Tundra plant above-ground biomass and shrub dominance mapped across the North Slope of Alaska. In Environ. Res. Lett. 13 (3), p. 35002. DOI: 10.1088/1748-9326/aaaa9a.

Bhatt, U. S.; Walker, D. A.; Raynolds, M. K.; Bieniek, P. A.; Epstein, H. E.; Comiso, J. C. et al. (2017): Changing seasonality of panarctic tundra vegetation in relationship to climatic variables. In Environ. Res. Lett. 12 (5), p. 55003. DOI: 10.1088/1748-9326/aa6b0b.

Bhatt, U.; Walker, D.; Raynolds, M.; Bieniek, P.; Epstein, H.; Comiso, J. et al. (2013): Recent Declines in Warming and Vegetation Greening Trends over Pan-Arctic Tundra. In Remote Sensing 5 (9), pp. 4229–4254. DOI: 10.3390/rs5094229.

Bhatt, U. S.; Walker, D. A.; Raynolds, M. K.; Comiso, J. C.; Epstein, H. E.; Jia, G. et al. (2010): Circumpolar Arctic Tundra Vegetation Change Is Linked to Sea Ice Decline. In Earth Interactions 14 (8), pp. 1–20. DOI: 10.1175/2010EI315.1.

Billings, W. D. (1973): Arctic and Alpine Vegetations: Similarities, Differences, and Susceptibility to Disturbance. In BioScience 23 (12), pp. 697–704. DOI: 10.2307/1296827.

Bintanja, R. A. O. (2017): Towards a rain-dominated Arctic. Nature Clim Change 7, 263–267. https://doi.org/10.1038/nclimate3240.

Birks, H. H. (2008): The Late-Quaternary history of arctic and alpine plants. In Plant Ecology & Diversity 1 (2), pp. 135–146. DOI: 10.1080/17550870802328652.

Bintanja, R. & Selten, F (2014): Future increases in Arctic precipitation linked to local evaporation and sea-ice retreat. Nature 509, 479–482. https://doi.org/10.1038/nature13259.

Bjerke, J. W.; Rune Karlsen, S.; Arild Høgda, K.; Malnes, E.; Jepsen, J. U.; Lovibond, S. et al. (2014): Record-low primary productivity and high plant damage in the Nordic Arctic Region in 2012 caused by multiple weather events and pest outbreaks. In Environ. Res. Lett. 9 (8), p. 84006. DOI: 10.1088/1748-9326/9/8/084006.

Bjerke, J. W.; Treharne, R.; Vikhamar-Schuler, D.; Karlsen, S. R.; Ravolainen, V.; Bokhorst, S. et al. (2017): Understanding the drivers of extensive plant damage in boreal and Arctic ecosystems: Insights from field surveys in the aftermath of damage. In The Science of the total environment 599-600, pp. 1965–1976. DOI: 10.1016/j.scitotenv.2017.05.050.

Bjorkman, A.D.; Myers-Smith, I.H.; Elmendorf, S.C. et al. (2018): Plant functional trait change across a warming tundra biome. Nature 562, 57–62. https://doi.org/10.1038/s41586-018-0563-7.

Bjornsson, H.; Jonsson, T.; Gylfadottir, S. S.; Olason, E. O. (2007): Mapping the annual cycle of temperature in Iceland. In metz 16 (1), pp. 45–56. DOI: 10.1127/0941-2948/2007/0175.

Blankinship, J. C.; Meadows, M. W.; Lucas R. G.; Hart, S. C. (2014): Snowmelt timing alters shallow but not deep soil moisture in the Sierra Nevada. Water Resour. Res., 50. DOI:10.1002/2013WR014541.

Boisvert, L. N.; Stroeve, J. C. (2015): The Arctic is becoming warmer and wetter as revealed by the Atmospheric Infrared Sounder. In Geophys. Res. Lett. 42 (11), pp. 4439–4446. DOI: 10.1002/2015GL063775.

Bokhorst, S.; Pedersen, S. H.; Brucker, L.; Anisimov, O.; Bjerke, J. W.; Brown, R. D. et al. (2016): Changing Arctic snow cover: A review of recent developments and assessment of future needs for observations, modelling, and impacts. In Ambio 45 (5), pp. 516–537. DOI: 10.1007/s13280-016-0770-0.

Bokhorst, S. F.; Bjerke, J. W.; Tømmervik, H.; Callaghan, T. V.; Phoenix, G. K. (2009): Winter warming events damage sub-Arctic vegetation: consistent evidence from an experimental manipulation and a natural event. In J. Ecol. 97 (6), pp. 1408–1415. DOI: 10.1111/j.1365-2745.2009.01554.x.

Bolch, T. & Loibl, D. (2017): GIS for Glaciers and Glacial Landforms. In Gis Applications for Socio-Economics and Humanity (Vol. 3, pp. 112-139). Elsevier B.V. DOI: 10.1016/B978-0-12-409548-9.09639-1.

Bowker, M. A.; Maestre, F. T.; Eldridge, D.; Belnap, J.; Castillo-Monroy, A.; Escolar, C.; Soliveres, S. (2014): Biological soil crusts (biocrusts) as a model system in community, landscape and ecosystem ecology. In Biodivers Conserv 23 (7), pp. 1619–1637. DOI: 10.1007/s10531-014-0658-x.

Bramer, I.; Anderson, B. J.; Bennie, J.; Bladon, A. J.; de Frenne, P.; Hemming, D. et al. (2018): Advances in Monitoring and Modelling Climate at Ecologically Relevant Scales 58, pp. 101–161. DOI: 10.1016/bs.aecr.2017.12.005.

Bråthen, K.A.; Fodstad, C.H.; Gallet, C. (2010): Ecosystem disturbance reduces the allelopathic effects of Empetrum hermaphroditum humus on tundra plants. Journal of Vegetation Science 21: 786–795.

Bratsch, S.; Epstein, H.; Buchhorn, M.; Walker, D. (2016): Differentiating among Four Arctic Tundra Plant Communities at Ivotuk, Alaska Using Field Spectroscopy. In Remote Sensing 8 (1), p. 51. DOI: 10.3390/rs8010051.

Bring, A.; Fedorova, I.; Dibike, Y.; Hinzman, L.; Mård, J.; Mernild, S. H. et al. (2016): Arctic terrestrial hydrology: A synthesis of processes, regional effects, and research challenges. In JGR Biogeosciences 121 (3), pp. 621–649. DOI: 10.1002/2015JG003131.

Brown, C. E. (Ed.) (1998): Applied Multivariate Statistics in Geohydrology and Related Sciences. Berlin, Heidelberg: Springer Berlin Heidelberg.

Brown, I. & Ward, R. (1996): The Influence of Topography on Snowpatch Distribution in Southern Iceland: A New Hypothesis for Glacier Formation? In Geografiska Annaler: Series A, Physical Geography 78 (4), pp. 197–207. DOI: 10.1080/04353676.1996.11880467.

Brown, R. D.; Mote, P. W. (2009): The Response of Northern Hemisphere Snow Cover to a Changing Climate*. In J. Climate 22 (8), pp. 2124–2145. DOI: 10.1175/2008jcli2665.1.

Buckeridge, K. M.; Zufelt, E.; Chu, H.; Grogan, P. (2010): Soil nitrogen cycling rates in low arctic shrub tundra are enhanced by litter feedbacks. In Plant Soil 330 (1-2), pp. 407–421. DOI: 10.1007/s11104-009-0214-8.

Buxton, J. E.; Abrams, J. F.; Boulton, C. A.; Barlow, N.; Rangel Smith, C.; van Stroud, S. et al. (2022): Quantitatively monitoring the resilience of patterned vegetation in the Sahel. In Global Change Biol 28 (2), pp. 571–587. DOI: 10.1111/gcb.15939.

Bykov, N. I.; Rygalova, N. V.; Shigimaga, A. A. (2022): Snow cover as a factor of radial growth of woody plants in different habitats of Altai. Acta Biologica Sibirica, 8, 557-569. DOI: 10.5281/zenodo.7726449.

Callaghan, T.V., Cazzolla Gatti, R. & Phoenix, G. (2022): The need to understand the stability of arctic vegetation during rapid climate change: An assessment of imbalance in the literature. Ambio 51, 1034–1044. https://doi.org/10.1007/s13280-021-01607-w.

Callaghan, T. V.; Johansson, M.; Brown, R. D.; Groisman, P. Y.; Labba, N.; Radionov, V. (2011a): Snow, water, ice and permafrost in the Arctic (SWIPA). Climate change and the cryosphere. Oslo: Arctic Monitoring and Assessment Programme.

Callaghan, T. V.; Johansson, M.; Brown, R. D.; Groisman, P. Y.; Labba, N.; Radionov, V. et al. (2011b): Multiple Effects of Changes in Arctic Snow Cover. In AMBIO 40 (S1), pp. 32–45. DOI: 10.1007/s13280-011-0213-x.

Callaghan, T. V.; Johansson, M.; Brown, R. D.; Groisman, P. Y.; Labba, N.; Radionov, V. et al. (2011c): The Changing Face of Arctic Snow Cover: A Synthesis of Observed and Projected Changes. In AMBIO 40 (S1), pp. 17–31. DOI: 10.1007/s13280-011-0212-y.

Callaghan, T. V.; Tweedie, C. E.; Akerman, J.; Andrews, C.; Bergstedt, J.; Butler, M. G. et al. (2011d): Multi-decadal changes in tundra environments and ecosystems: synthesis of the International Polar Year-Back to the Future project (IPY-BTF). In Ambio 40 (6), pp. 705–716. DOI: 10.1007/s13280-011-0179-8.

Callaghan, T. V.; Björn, L. O.; Chernov, Y.; Chapin, T.; Christensen, T. R.; Huntley, B. et al. (2004): Biodiversity, distributions and adaptations of Arctic species in the context of environmental change. In Ambio 33 (7), pp. 404–417. DOI: 10.1579/0044-7447-33.7.404.

Campbell, T. K. F.; Lantz, T. C.; Fraser, R. H. et al. (2021): High Arctic Vegetation Change Mediated by Hydrological Conditions. Ecosystems 24, 106–121. https://doi.org/10.1007/s10021-020-00506-7.

Campbell, J. B. (2011): Introduction to remote sensing. 5th ed. New York, London: Guilford Press.

Candela, S. G.; Howat, I.; Noh, M. J.; Porter, C. C.; Morin, P. J. (2017): ArcticDEM Validation and Accuracy Assessment. In AGU Fall Meeting Abstracts 2017, C51A-0951.

Chernov, Y. I. (1988): The living tundra. Cambridge, New York, New Rochelle: Cambridge University Press (Studies in polar research).

Choler, P. (2018): Winter soil temperature dependence of alpine plant distribution: Implications for anticipating vegetation changes under a warming climate. In Perspectives in Plant Ecology, Evolution and Systematics 30, pp. 6–15. DOI: 10.1016/j.ppees.2017.11.002.

Choler, P. (2015): Growth response of temperate mountain grasslands to inter-annual variations in snow cover duration, Biogeosciences, 12, 3885–3897, https://doi.org/10.5194/bg-12-3885-2015.

Christensen, T. (2013): Arctic terrestrial biodiversity monitoring plan. Akureyri, Iceland: CAFF International Secretariat (CAFF monitoring series report, no. 8).

Chylek, P.; Folland, C.; Klett, J. D.; Wang, M.; Hengartner, N.; Lesins, G.; Dubey, M. K. (2022): Annual Mean Arctic Amplification 1970–2020: Observed and Simulated by CMIP6 Climate Models. In Geophys. Res. Lett. 49 (13), Article e2022GL099371. DOI: 10.1029/2022GL099371.

Cleveland, W. S.; Devlin, S. J. (1988): Locally Weighted Regression: An Approach to Regression Analysis by Local Fitting. In Journal of the American Statistical Association 83 (403), p. 596. DOI: 10.2307/2289282.

Bueno de Mesquita, C. P.; Tillmann, L. S.; Bernard, C. D.; Rosemond, K. C.; Molotch, N. P.; Suding, K. N. (2018): Topographic heterogeneity explains patterns of vegetation response to climate change (1972–2008) across a mountain landscape, Niwot Ridge, Colorado. Arctic, Antarctic, and Alpine Research, 50(1), e1504492. https://doi.org/10.1080/15230430.2018.1504492.

Corenblit, D.; Baas, A. C.W.; Bornette, G.; Darrozes, J.; Delmotte, S.; Francis, R. A. et al. (2011): Feedbacks between geomorphology and biota controlling Earth surface processes and landforms: A review of foundation concepts and current understandings. In Earth-Science Reviews 106 (3-4), pp. 307–331. DOI: 10.1016/j.earscirev.2011.03.002.

Crawford, Alex D.; Lukovich, Jennifer V.; McCrystall, Michelle R.; Stroeve, Julienne C.; Barber, David G. (2022): Reduced Sea Ice Enhances Intensification of Winter Storms over the Arctic Ocean. In J. Climate 35 (11), pp. 3353–3370. DOI: 10.1175/JCLI-D-21-0747.1.

Crimmins, S. M.; Dobrowski, S. Z.; Greenberg, J. A.; Abatzoglou, J. T.; Mynsberge, A. R. (2011): Changes in climatic water balance drive downhill shifts in plant species' optimum elevations. In Science (New York, N.Y.) 331 (6015), pp. 324–327. DOI: 10.1126/science.1199040.

Crochet, P.; Jóhannesson, T.; Jónsson, T.; Sigurðsson, O.; Björnsson, H.; Pálsson, F.; Barstad, I. (2007): Estimating the Spatial Distribution of Precipitation in Iceland Using a Linear Model of Orographic Precipitation. In Journal of Hydrometeorology 8 (6), pp. 1285–1306. DOI: 10.1175/2007JHM795.1.

Cunliffe, A. M.; Assmann, J. J.; Daskalova, G. N.; Kerby, J. T.; Myers-Smith, I. H. (2020): Aboveground biomass corresponds strongly with drone-derived canopy height but weakly with greenness (NDVI) in a shrub tundra landscape. In Environ. Res. Lett. 15 (12), p. 125004. DOI: 10.1088/1748-9326/aba470.

Cutler, N. A.; Kodl, G.; Streeter, R. T.; Thompson, P. I. J.; Dugmore, A. J. (2023): Soil moisture, stressed vegetation and the spatial structure of soil erosion in a high latitude rangeland. In European J Soil Science 74 (4), Article e13393. DOI: 10.1111/ejss.13393.

Cutler, Nick (2011): Vegetation–environment interactions in a sub-arctic primary succession. In Polar Biol 34 (5), pp. 693–706. DOI: 10.1007/s00300-010-0925-6.

Darmody, R. G.; Thorn, C. E.; Dixon, J. C.; Schlyter, P. (2000): Soils and Landscapes of Kärkevagge, Swedish Lapland. In Soil Science Soc of Amer J 64 (4), pp. 1455–1466. DOI: 10.2136/sssaj2000.6441455x.

Davidson, S.; Santos, M.; Sloan, V.; Watts, J.; Phoenix, G.; Oechel, W.; Zona, D. (2016): Mapping Arctic Tundra Vegetation Communities Using Field Spectroscopy and Multispectral Satellite Data in North Alaska, USA. In Remote Sensing 8 (12), p. 978. DOI: 10.3390/rs8120978.

De la Peña Aguilera, P. (2024): Community assembly across Subarctic landscapes - Exploring patterns of diversity. Doctoral thesis, Swedish University of Agricultural Sciences, Uppsala. https://doi.org/10.54612/a.457ae5racn.

DeMarco, J.; Mack, M. C.; Bret-Harte, M. S. (2014): Effects of arctic shrub expansion on biophysical vs. biogeochemical drivers of litter decomposition. In Ecology 95 (7), pp. 1861–1875. DOI: 10.1890/13-2221.1.

Deng, Y. (2007): New trends in digital terrain analysis: landform definition, representation, and classification. In Progress in Physical Geography: Earth and Environment 31 (4), pp. 405–419. DOI: 10.1177/0309133307081291.

Derksen, C.; Brown, R. (2012): Spring snow cover extent reductions in the 2008–2012 period exceeding climate model projections. In Geophys. Res. Lett. 39 (19), Article 2012GL053387. DOI: 10.1029/2012GL053387.

Dialynas, Y. G.; Bastola, S.; Bras, R. L.; Billings, S. A.; Markewitz, D.; Richter, D. deB. (2016): Topographic variability and the influence of soil erosion on the carbon cycle. In Global Biogeochemical Cycles 30 (5), pp. 644–660. DOI: 10.1002/2015GB005302.

Dietz, A. J.; Kuenzer, C.; Gessner, U.; Dech, S. (2012): Remote sensing of snow – a review of available methods. In International Journal of Remote Sensing 33 (13), pp. 4094–4134. DOI: 10.1080/01431161.2011.640964.

Dorigo, W. A.; Wagner, W.; Hohensinn, R.; Hahn, S.; Paulik, C.; Xaver, A.; Gruber, A.; Drusch, M.; Mecklenburg, S.; van Oevelen, P.; Robock, A.; Jackson, T. (2011): The International Soil Moisture Network: a data hosting facility for global in situ soil moisture measurements, Hydrol. Earth Syst. Sci., 15, 1675–1698. DOI: 10.5194/hess-15-1675-2011.

Dugmore, A.; Jackson, R.; Cooper, D.; Newton, A.; Júlísson, Á. D.; Streeter, R. T. et al. (Eds.) (2020): Continuity in the face of a slowly unfolding catastrophe: the persistence of Icelandic settlement despite large-scale soil erosion. Going forward by looking back: Archaeological perspectives on socio-ecological crisis, response, and collapse. With assistance of Riede, F. & Sheets, P..Oxford: Berghahn (p. 162-199 (Catastrophes in context; vol. 3)).

Dugmore, A. J.; Gisladóttir, G.; Simpson, I. A.; Newton, A. (2009): Conceptual Models of 1200 Years of Icelandic Soil Erosion Reconstructed Using Tephrochronology. In Journal of the North Atlantic 2, pp. 1–18. DOI: 10.3721/037.002.0103.

Dugmore, A. J.; Church, M. J.; Buckland, P. C.; Edwards, K. J.; Lawson, I.; McGovern, T. H. et al. (2005): The Norse landnám on the North Atlantic islands: an environmental impact assessment. In Polar Record 41 (1), pp. 21–37. DOI: 10.1017/S0032247404003985.

Dugmore, A. J.; Newton, A. J.; Larsen, G.; Cook, G. T. (2000): Tephrochronology, Environmental Change and the Norse Settlement of Iceland. In Environmental Archaeology 5 (1), pp. 21–34. DOI: 10.1179/env.2000.5.1.21.

Eddudóttir, S. D.; Erlendsson, E.; Gísladóttir, G. (2020): Landscape change in the Icelandic highland: A long-term record of the impacts of land use, climate and volcanism. In Quaternary Science Reviews 240, p. 106363. DOI: 10.1016/j.quascirev.2020.106363.

Eichel, J.; Corenblit, D.; Dikau, R. (2016): Conditions for feedbacks between geomorphic and vegetation dynamics on lateral moraine slopes: a biogeomorphic feedback window. In Earth Surf. Process. Landforms 41 (3), pp. 406–419. DOI: 10.1002/esp.3859.

Eischeid, I.; Soininen, E. M.; Assmann, J. J.; Ims, R. A.; Madsen, J.; Pedersen, Å. Ø. et al. (2021): Disturbance Mapping in Arctic Tundra Improved by a Planning Workflow for Drone Studies: Advancing Tools for Future Ecosystem Monitoring. In Remote Sensing 13 (21), p. 4466. DOI: 10.3390/rs13214466.

Elmendorf, S. C.; Henry, G. H. R.; Hollister, R. D.; Björk, R. G.; Boulanger-Lapointe, N.; Cooper, E. J. et al. (2012): Plot-scale evidence of tundra vegetation change and links to recent summer warming. In Nat. Clim. Chang. 2 (6), pp. 453–457. DOI: 10.1038/nclimate1465.

Engstrom, R.; Hope, A.; Kwon, H.; Stow, D.; Zamolodchikov, D. (2005): Spatial distribution of near surface soil moisture and its relationship to microtopography in the Alaskan Arctic coastal plain. In Hydrology Research 36 (3), pp. 219–234. DOI: 10.2166/nh.2005.0016.

Entekhabi, D.; Njoku, E. G.; O'Neill, P. E.; Kellogg, K. H.; Crow, W. T.; Edelstein, W. N. et al. (2010): The Soil Moisture Active Passive (SMAP) Mission. In Proc. IEEE 98 (5), pp. 704–716. DOI: 10.1109/JPROC.2010.2043918.

Epstein, H. E.; Frost, G. V.; Walker, D. A.; Kwok R. (2015): The Arctic – Declassified high-resolution visible imagery for observing the Arctic. In, State of the Climate in 2014. Bull. Amer. Meteorol. Soc., 96, S142-S143.

Eskandari, R.; Mahdianpari, M.; Mohammadimanesh, F.; Salehi, B.; Brisco, B.; Homayouni, S. (2020): Meta-analysis of Unmanned Aerial Vehicle (UAV) Imagery for Agro-environmental Monitoring Using Machine Learning and Statistical Models. Remote Sensing, 12(21), 3511. DOI: 10.3390/rs12213511.

Eurola, S. (1999): Regionality of our vegetation. Oulanka reports 22:1–116, Oulanka biological station, University of Oulu (in Finnish).

Euskirchen, E. S.; Bennett, A. P.; Breen, A. L.; Genet, H.; Lindgren, M. A.; Kurkowski, T. A. et al. (2016): Consequences of changes in vegetation and snow cover for climate feedbacks in Alaska and northwest Canada. In Environ. Res. Lett. 11 (10), p. 105003. DOI: 10.1088/1748-9326/11/10/105003.

Eysteinsson, T.; Aradottir, Á. (2003): Restoration of birch woodlands in Iceland. In Dubravko Jelčić, Pavlovic G. (Eds.): Kosor J. Prilozi sa Znanstvenog kolokvija 2002. održanog u sklopu 13. Pjesničkih susreta, Drenovci, 08. lipnja 2002. = the papers presented at the scientific conference held in 2002., Otok, 5. listopada 2002, vol. 20047067. Drenovci: Hrašće (Znanstveni kolokvij, svezak 4), pp. 195–209.

Famiglietti, J. S.; Ryu, D.; Berg, A. A.; Rodell, M.; Jackson, T. J. (2008): Field observations of soil moisture variability across scales. In Water Resources Research 44 (1), Article 2006WR005804. DOI: 10.1029/2006WR005804.

Fan, J.; Xu, Y.; Ge, H.; Yang, W. (2020): Vegetation growth variation in relation to topography in Horqin Sandy Land. In Ecological Indicators 113, p. 106215. DOI: 10.1016/j.ecolind.2020.106215.

Fernández, D.; Adermann, E.; Pizzolato, M.; Pechenkin, R.; Rodríguez, C. G.; Taravat, A. (2023): Comparative Analysis of Machine Learning Algorithms for Soil Erosion Modelling Based on Remotely Sensed Data. In Remote Sensing 15 (2), p. 482. DOI: 10.3390/rs15020482.

Fernández, D.; Adermann, E.; Pizzolato, M.; Pechenkin, R.; Rodríguez, C. G. (2022): Remote mapping of soil erosion risk in Iceland. In Int. Arch. Photogramm. Remote Sens. Spatial Inf. Sci. XLVIII-4/W1-2022, pp. 135–141. DOI: 10.5194/isprs-archives-XLVIII-4-W1-2022-135-2022.

Fick, S. E. & Hijmans, R. J. (2017): WorldClim 2: new 1-km spatial resolution climate surfaces for global land areas. In Intl Journal of Climatology 37 (12), pp. 4302–4315. DOI: 10.1002/joc.5086.

Fisk, M. C.; Schmidt, S. K.; Seastedt, T. R. (1998): Topographic patterns of above- and belowground production and nitrogen cycling in Alpine tundra. In Ecology 79 (7), pp. 2253–2266. DOI: 10.1890/0012-9658(1998)079[2253:TPOAAB]2.0.CO;2.

Fitter, A. H. & Raffaelli, D. G. (1999): Advances in Ecological Research, 30. Burlington: Elsevier.

Florinsky, I. V. & Kuryakova, G. A. (1996): Influence of topography on some vegetation cover properties. In CATENA 27 (2), pp. 123–141. DOI: 10.1016/0341-8162(96)00005-7.

Föhn PMB. & Meister R. (1983): Distribution of Snow Drifts on Ridge Slopes: Measurements and Theoretical Approximations. Annals of Glaciology. 1983;4:52-57. DOI:10.3189/S0260305500005231.

Forbes, B. C.; Fauria, M. M.; Zetterberg, P. (2010): Russian Arctic warming and 'greening' are closely tracked by tundra shrub willows. In Global Change Biology 16 (5), pp. 1542–1554. DOI: 10.1111/j.1365-2486.2009.02047.x.

Forbes, B. C. & Kumpula, T. (2009): The Ecological Role and Geography of Reindeer (Rangifer Tarandus) in Northern Eurasia. In Geography Compass. DOI: 10.1111/j.1749-8198.2009.00250.x.

Forkel, M.; Carvalhais, N.; Verbesselt, J.; Mahecha, M.; Neigh, C.; Reichstein, M. (2013): Trend Change Detection in NDVI Time Series: Effects of Inter-Annual Variability and Methodology. In Remote Sensing 5 (5), pp. 2113–2144. DOI: 10.3390/rs5052113.

Fraser, R. H.; Olthof, I.; Lantz, T. C.; Schmitt, C. (2016): UAV photogrammetry for mapping vegetation in the low-Arctic. In Arctic Science 2 (3), pp. 79–102. DOI: 10.1139/as-2016-0008.

Fraser, R. H.; Lantz, T. C.; Olthof, I.; Kokelj, S. V.; Sims, R. A. (2014): Warming-Induced Shrub Expansion and Lichen Decline in the Western Canadian Arctic. In Ecosystems 17 (7), pp. 1151–1168. DOI: 10.1007/s10021-014-9783-3.

Frazier, A. E. & Hemingway, B. L. (2021): A Technical Review of Planet Smallsat Data: Practical Considerations for Processing and Using PlanetScope Imagery. In Remote Sensing 13 (19), p. 3930. DOI: 10.3390/rs13193930.

French, H. M. (2017): The Periglacial Environment. 4 Aufl. [s.l.]: John Wiley and Sons Ltd.

Fretwell, P. T.; Convey, P.; Fleming, A. H.; Peat, H. J.; Hughes, K. A. (2011): Detecting and mapping vegetation distribution on the Antarctic Peninsula from remote sensing data. In Polar Biol 34 (2), pp. 273–281. DOI: 10.1007/s00300-010-0880-2.

Frost, G. V.; Epstein, H. E.; Walker, D. A. (2014): Regional and landscape-scale variability of Landsat-observed vegetation dynamics in northwest Siberian tundra. In Environ. Res. Lett. 9 (2), p. 25004. DOI: 10.1088/1748-9326/9/2/025004.

Frost, G. V.; Epstein, H. E.; Walker, D. A.; Matyshak, G.; Ermokhina, K. (2013): Patterned-ground facilitates shrub expansion in Low Arctic tundra. In Environ. Res. Lett. 8 (1), p. 15035. DOI: 10.1088/1748-9326/8/1/015035.

Furberg, M.; Hondula, D. M.; Saha, M. V.; Nilsson, M. (2018): In the light of change: a mixed methods investigation of climate perceptions and the instrumental record in northern Sweden. In Popul Environ 40 (1), pp. 47–71. DOI: 10.1007/s11111-018-0302-x.

Gamon, J. A.; Huemmrich, K. F.; Stone, R. S.; Tweedie, C. E. (2013): Spatial and temporal variation in primary productivity (NDVI) of coastal Alaskan tundra: Decreased vegetation growth following earlier snowmelt. In Remote Sensing of Environment 129, pp. 144–153. DOI: 10.1016/j.rse.2012.10.030.

García-Ruiz, J. M.; Beguería, S.; Nadal-Romero, E.; González-Hidalgo, J. C.; Lana-Renault, N.; Sanjuán, Y. (2015): A meta-analysis of soil erosion rates across the world. In Geomorphology 239, pp. 160–173. DOI: 10.1016/j.geomorph.2015.03.008.

Geirsdóttir, Á.; Miller, G. H.; Thordarson, T.; Ólafsdóttir, K. B. (2009): A 2000 year record of climate variations reconstructed from Haukadalsvatn, West Iceland. In J Paleolimnol 41 (1), pp. 95–115. DOI: 10.1007/s10933-008-9253-z.

Gergel, S. E. & Turner, M. G. (2017): Learning Landscape Ecology. DOI: 10.1007/978-1-4939-6374-4.

Getzin, S.; Holch, S.; Yizhaq, H.; Wiegand, K. (2022): Plant water stress, not termite herbivory, causes Namibia's fairy circles. Perspectives in Plant Ecology, Evolution and Systematics, Vol. 57. DOI: 10.1016/j.ppees.2022.125698.

Ghilain, N.; Arboleda, A.; Batelaan, O.; Ardö, J.; Trigo, I.; Barrios, J.-M.; Gellens-Meulenberghs, F. (2019): A New Retrieval Algorithm for Soil Moisture Index from Thermal Infrared Sensor On-Board Geostationary Satellites over Europe and Africa and Its Validation. In Remote Sensing 11 (17), p. 1968. DOI: 10.3390/rs11171968.

Giaccone, E.; Luoto, M.; Vittoz, P.; Guisan, A.; Mariéthoz, G.; Lambiel, C. (2019): Influence of microclimate and geomorphological factors on alpine vegetation in the Western Swiss Alps. In Earth Surf. Process. Landforms 44 (15), pp. 3093–3107. DOI: 10.1002/esp.4715.

Giri, C.; Pengra, B.; Long, J.; Loveland, T. R. (2013): Next generation of global land cover characterization, mapping, and monitoring. In International Journal of Applied Earth Observation and Geoinformation 25, pp. 30–37. DOI: 10.1016/j.jag.2013.03.005.

Gisladottir, F. O.; Brink, S. H.; Arnalds, O. (2014): Nytjaland (Icelandic Farmland Database). Agricultural University of Iceland Report, 49.

Gisladottir, F. O.; Arnalds, O.; Gisladottir, G. (2005): The effect of landscape and retreating glaciers on wind erosion in South Iceland. In Land Degrad. Dev. 16 (2), pp. 177–187. DOI: 10.1002/ldr.645.

Gísladóttir, G. (2001): Ecological Disturbance and Soil Erosion on Grazing Land in Southwest Iceland. In A. Conacher (Ed.) Land Degradation 58, pp. 109–126. DOI: 10.1007/978-94-017-2033-5_7.

Gisnås, K.; Etzelmüller, B.; Lussana, C.; Hjort, J.; Sannel, A. B. K.; Isaksen, K. et al. (2017): Permafrost Map for Norway, Sweden and Finland. In Permafrost and Periglac. Process. 28 (2), pp. 359–378. DOI: 10.1002/ppp.1922.

Gitelson, A. A.; Gritz, Y.; Merzlyak, M. N. (2003): Relationships between leaf chlorophyll content and spectral reflectance and algorithms for non-destructive chlorophyll assessment in higher plant leaves. In Journal of plant physiology 160 (3), pp. 271–282. DOI: 10.1078/0176-1617-00887.

Gitelson, A. & Merzlyak, M. N. (1994): Spectral Reflectance Changes Associated with Autumn Senescence of Aesculus hippocastanum L. and Acer platanoides L. Leaves.

Spectral Features and Relation to Chlorophyll Estimation. In Journal of plant physiology 143 (3), pp. 286–292. DOI: 10.1016/S0176-1617(11)81633-0.

Goswami, S.; Gamon, J.; Vargas S.; Tweedie C. (2015): Relationships of NDVI, Biomass, and Leaf Area Index (LAI) for six key plant species in Barrow, Alaska. PeerJ PrePrints 3:e913v1 https://doi.org/10.7287/peerj.preprints.913v1.

Goward, S. N.; Markham, B.; Dye, D. G.; Dulaney, W.; Yang, J. (1991): Normalized difference vegetation index measurements from the advanced very high resolution radiometer. In Remote Sensing of Environment 35 (2-3), pp. 257–277. DOI: 10.1016/0034-4257(91)90017-Z.

Greaves, H. E.; Vierling, L. A.; Eitel, J. U. H.; Boelman, N. T.; Magney, T. S.; Prager, C. M.; Griffin, K. L. (2015): Estimating aboveground biomass and leaf area of low-stature Arctic shrubs with terrestrial LiDAR. In Remote Sensing of Environment 164, pp. 26–35. DOI: 10.1016/j.rse.2015.02.023.

Greipsson, S. (2012): Catastrophic soil erosion in Iceland: Impact of long-term climate change, compounded natural disturbances and human driven land-use changes. In CATENA 98, pp. 41–54. DOI: 10.1016/j.catena.2012.05.015.

Grimes, M.; Carrivick, J. L.; Smith, M. W.; Comber, A. J. (2024): Land cover changes across Greenland dominated by a doubling of vegetation in three decades. In Scientific reports 14 (1), p. 3120. DOI: 10.1038/s41598-024-52124-1.

Grime, J. P. (1977): Evidence for the Existence of Three Primary Strategies in Plants and Its Relevance to Ecological and Evolutionary Theory. The American Naturalist, 111(982), 1169–1194. http://www.jstor.org/stable/2460262.

Grünberg, I.; Wilcox, E. J.; Zwieback, S.; Marsh, P.; Boike, J. (2020): Linking tundra vegetation, snow, soil temperature, and permafrost. In Biogeosciences 17 (16), pp. 4261–4279. DOI: 10.5194/bg-17-4261-2020.

Guay, K. C.; Beck, P. S. A.; Berner, L. T.; Goetz, S. J.; Baccini, A.; Buermann, W. (2014): Vegetation productivity patterns at high northern latitudes: a multi-sensor satellite data assessment. In Global Change Biology 20 (10), pp. 3147–3158. DOI: 10.1111/gcb.12647.

Hall, D. K.; Riggs, G. A.; Salomonson, V. V.; DiGirolamo, N. E.; Bayr, K. J. (2002): MODIS snow-cover products. In Remote Sensing of Environment 83 (1-2), pp. 181–194. DOI: 10.1016/S0034-4257(02)00095-0.

Hall, K. (1998): Nivation or cryoplanation: Different terms, same features? In Polar Geography 22 (1), pp. 1–16. DOI: 10.1080/10889379809377634.

Hansen, B. B.; Isaksen, K.; Benestad, R. E.; Kohler, J.; Pedersen, Å. Ø.; Loe, L. E. et al. (2014): Warmer and wetter winters: characteristics and implications of an extreme weather event in the High Arctic. In Environ. Res. Lett. 9 (11), p. 114021. DOI: 10.1088/1748-9326/9/11/114021.

Happonen, K.; Aalto, J.; Kemppinen, J.; Niittynen, P.; Virkkala, A.-M.; Luoto, M. (2019): Snow is an important control of plant community functional composition in oroarctic tundra. In Oecologia 191 (3), pp. 601–608. DOI: 10.1007/s00442-019-04508-8.

Harris, J. A.; Hollister, R. D.; Botting, T. F.; Tweedie, C. E.; Betway, K. R.; May, J. L. et al. (2022): Understanding the climate impacts on decadal vegetation change in northern Alaska. In Arctic Science 8 (3), pp. 878–898. DOI: 10.1139/as-2020-0050.

Hatfield, D. C. (1999). TopoTools-A collection of topographic modelling tools for ArcINFO. http://proceedings.esri.com/library/userconf/proc00/professional/papers/PAP560/p560.htm (accessed 13.03.2024).

Heindel, R. C.; Culler, L. E.; Virginia, R. A. (2017): Rates and processes of aeolian soil erosion in West Greenland. In The Holocene 27 (9), pp. 1281–1290. DOI: 10.1177/0959683616687381.

Heindel, R. C.; Chipman, J. W.; Virginia, R. A. (2015): The Spatial Distribution and Ecological Impacts of Aeolian Soil Erosion in Kangerlussuaq, West Greenland. In Annals of the Association of American Geographers 105 (5), pp. 875–890. DOI: 10.1080/00045608.2015.1059176.

Hejcman, M.; Dvorak, I. J.; Kocianova, M.; Pavlu, V.; Nezerkova, P.; Vitek, O.; Jenik, J. (2006): Snow Depth and Vegetation Pattern in a Late-melting Snowbed Analyzed by GPS and GIS in the Giant Mountains, Czech Republic. Arctic, Antarctic, and Alpine Research, 38(1), 90–98. https://doi.org/10.1657/1523-0430(2006)038[0090:SDAVPI]2.0.CO;2

Hesselbarth, M. H. K.; Sciaini, M.; With, K. A.; Wiegand, K.; Nowosad, J. (2019): landscapemetrics : an open-source R tool to calculate landscape metrics. In Ecography 42 (10), pp. 1648–1657. DOI: 10.1111/ecog.04617.

Hjort, J. &; Luoto, M. (2009): Interaction of geomorphic and ecologic features across altitudinal zones in a subarctic landscape. In Geomorphology 112 (3-4), pp. 324–333. DOI: 10.1016/j.geomorph.2009.06.019.

Hobson, G. D. (1981): The Polar Continental Shelf :Project. In Journal of Canadian Petroleum Technology 20 (04). DOI: 10.2118/81-04-11.

Holling, C. S. (1973): Resilience and Stability of Ecological Systems. In Annu. Rev. Ecol. Syst. 4 (1), pp. 1–23. DOI: 10.1146/annurev.es.04.110173.000245.

Hope, A. S.; Kimball, J. S.; Stow, D. A. (1993): The relationship between tussock tundra spectral reflectance properties and biomass and vegetation composition. In International Journal of Remote Sensing 14 (10), pp. 1861–1874. DOI: 10.1080/01431169308954008.

Huang, Z.; Cao, C.; Chen, W.; Xu, M.; Dang, Y.; Singh, R. et al. (2020): Remote Sensing Monitoring of Vegetation Dynamic Changes after Fire in the Greater Hinggan Mountain Area: The Algorithm and Application for Eliminating Phenological Impacts. In Remote Sensing 12 (1), p. 156. DOI: 10.3390/rs12010156.

Huete, A; Didan, K.;, Miura, T.; Rodriguez E.P.; X Gao, L.G Ferreira L.G. (2002): Overview of the radiometric and biophysical performance of the MODIS vegetation indices. Remote Sensing of Environment, vol. 83, iss. 1–2, pp. 195-213. DOI: 10.1016/S0034-4257(02)00096-2.

Huete, A. R. & Tucker, C. J. (1991): Investigation of soil influences in AVHRR red and near-infrared vegetation index imagery, International Journal of Remote Sensing, 12:6, 1223-1242. DOI: 10.1080/01431169108929723.

Hugelius, G.; Strauss, J.; Zubrzycki, S.; Harden, J. W.; Schuur, E. A. G.; Ping, C.-L. et al. (2014): Estimated stocks of circumpolar permafrost carbon with quantified uncertainty ranges and identified data gaps. In Biogeosciences 11 (23), pp. 6573–6593. DOI: 10.5194/bg-11-6573-2014.

Huggett, R. J. & Cheesman, J. (2002): Topography and the environment. Harlow: Prentice Hall.

Huntington, H. P. (2013): Provisioning and Cultural Services. In Arctic Biodiversity Assessment - Status and Trends in Arctic Biodiversity, 484–519. Akureyri, Iceland: Conservation of Arctic Flora and Fauna (CAFF).

Hurford, C. (2006): Minimising Observer Error. In: Hurford, C., Schneider, M. (eds) Monitoring Nature Conservation in Cultural Habitats. Springer, Dordrecht. DOI: 10.1007/1-4020-3757-0_10.

Ilmatieteen laitos / The Finnish Meteorological Institute (2024): Climatological Data Finland. Retrieved from: https://en.ilmatieteenlaitos.fi/download-observations. (accessed 15 March 2024)

Inderjit; Callaway, R. M.; Meron, E. (2021): Belowground feedbacks as drivers of spatial self-organization and community assembly. In Physics of life reviews 38, pp. 1–24. DOI: 10.1016/j.plrev.2021.07.002.

Iversen, C. M.; Sloan, V. L.; Sullivan, P. F.; Euskirchen, E. S.; McGuire, A. D.; Norby, R. J. et al. (2015): The unseen iceberg: plant roots in arctic tundra. In The New phytologist 205 (1), pp. 34–58. DOI: 10.1111/nph.13003.

Jackson, T. (2004): Vegetation water content mapping using Landsat data derived normalized difference water index for corn and soybeans. In Remote Sensing of Environment 92 (4), pp. 475–482. DOI: 10.1016/j.rse.2003.10.021.

Jenness J. (2006): Topographic Position Index, v. 1.3a. Jenness Enterprises. http://www.jennessent.com/arcview/tpi.htm (accessed 01.12.2023).

Jia G. J.; Epstein H. E.; Walker D. A. (2003): Greening of arctic Alaska, 1981–2001 Geophys. Res. Lett. 30 2067. https://doi.org/10.1029/2003GL018268.

Jonas, T.; Rixen C.; Sturm M. and Stoeckli V. (2008): How alpine plant growth is linked to snow cover and climatevariability, J. Geophys. Res., 113, G03013, doi:10.1029/2007JG000680.

Jones, H. G. (2001): Snow-vegetation interactions in tundra environments. Snow ecology: an interdisciplinary examination of snow-covered ecosystems. Cambridge University Press, Cambridge, 378 pp.

Ju, J. & Masek, J. G. (2016): The vegetation greenness trend in Canada and US Alaska from 1984–2012 Landsat data. In Remote Sensing of Environment 176, pp. 1–16. DOI: 10.1016/j.rse.2016.01.001.

Juszak, I.; Erb, A. M.; Maximov, T. C.; Schaepman-Strub, G. (2014): Arctic shrub effects on NDVI, summer albedo and soil shading. In Remote Sensing of Environment 153, pp. 79–89. DOI: 10.1016/j.rse.2014.07.021.

Kaarlejärvi, E.; Eskelinen, A.; Olofsson, J. (2017): Herbivores rescue diversity in warming tundra by modulating trait-dependent species losses and gains. In Nature communications 8 (1), p. 419. DOI: 10.1038/s41467-017-00554-z.

Kancheva R.; Borisova D.; Georgiev G. (2014): Chlorophyll assessment and stress detection from vegetation optical properties. Ecological Engineering and Environment Protection, 1, 34-43.

Katabuchi, M. (2015): LeafArea : an R package for rapid digital image analysis of leaf area. In Ecological Research 30 (6), pp. 1073–1077. DOI: 10.1007/s11284-015-1307-x.

Kauhanen, H. O. (2013): Mountains of Kilpisjarvi Host An Abundance of Threatened Plants in Finnish Lapland. In Bot Pac 2 (1), pp. 43–52. DOI: 10.17581/bp.2013.02105.

Ke, Y.; Im, J.; Lee, J.; Gong, H.; Ryu, Y. (2015): Characteristics of Landsat 8 OLI-derived NDVI by comparison with multiple satellite sensors and in-situ observations. In Remote Sensing of Environment 164, pp. 298–313. DOI: 10.1016/j.rse.2015.04.004.

Kearney, M. R. (2020): How will snow alter exposure of organisms to cold stress under climate warming? In Global Ecol Biogeogr 29 (7), pp. 1246–1256. DOI: 10.1111/geb.13100.

Kéfi, S.; Guttal, V.; Brock, W. A.; Carpenter, S. R.; Ellison, A. M.; Livina, V. N. et al. (2014): Early warning signals of ecological transitions: methods for spatial patterns. In PloS one 9 (3), e92097. DOI: 10.1371/journal.pone.0092097.

Kelsey, K. C.; Pedersen, S. H.; Leffler, A. J.; Sexton, J. O.; Feng, M.; Welker, J. M. (2021): Winter snow and spring temperature have differential effects on vegetation phenology and productivity across Arctic plant communities. In Global Change Biol 27 (8), pp. 1572–1586. DOI: 10.1111/gcb.15505.

Kelsey, K. C.; Pedersen, S. H.; Leffler, A. J.; Sexton, J. O.; Welker, J. M. (2023): Snow and Vegetation Seasonality Influence Seasonal Trends of Leaf Nitrogen and Biomass in Arctic Tundra. Ecosphere 14(5): e4515. DOI: 10.1002/ecs2.4515.

Kemppinen, J.; Lembrechts, J. J.; van Meerbeek, K.; Carnicer, J.; Chardon, N. I.; Kardol, P. et al. (2024): Microclimate, an important part of ecology and biogeography. In Global Ecol Biogeogr, Article e13834. DOI: 10.1111/geb.13834.

Kemppinen, J. & Niittynen, P. (2022): Microclimate relationships of intraspecific trait variation in sub-Arctic plants. In Oikos 2022 (12), Article e09507. DOI: 10.1111/oik.09507.

Kemppinen, J.; Niittynen, P.; Happonen, K.; Roux, P. C.; Aalto, J.; Hjort, J. et al. (2022): Geomorphological processes shape plant community traits in the Arctic. In Global Ecol Biogeogr, Article geb.13512. DOI: 10.1111/geb.13512.

Kemppinen, J.; Niittynen, P.; Virkkala, A.-M.; Happonen, K.; Riihimäki, H.; Aalto, J.; Luoto, M. (2021): Dwarf Shrubs Impact Tundra Soils: Drier, Colder, and Less Organic Carbon. In Ecosystems 24 (6), pp. 1378–1392. DOI: 10.1007/s10021-020-00589-2.

Kemppinen, J.; Niittynen, P.; Aalto, J.; Le Roux, P. C.; Luoto, M. (2019): Water as a resource, stress and disturbance shaping tundra vegetation. In Oikos 128 (6), pp. 811–822. DOI: 10.1111/oik.05764.

Kemppinen, J.; Niittynen, P.; Riihimäki, H.; Luoto, M. (2018): Modelling soil moisture in a high-latitude landscape using LiDAR and soil data. In Earth Surf. Process. Landforms 43 (5), pp. 1019-1031. DOI: 10.1002/esp.4301.

Keshava N. & Mustard, J. F. (2002): "Spectral unmixing," in IEEE Signal Processing Magazine, vol. 19, no. 1, pp. 44-57, DOI: 10.1109/79.974727.

King, L. & Seppälä, M. (1987): Permafrost Thickness and Distribution in Finnish Lapland - Results of Geoelectrical Soundings , Polarforschung, Bremerhaven, Alfred Wegener Institute for Polar and Marine Research & German Society of Polar Research, 57 (3), pp. 127-147 .

Kivinen, S. & Rasmus, S. (2015): Observed cold season changes in a Fennoscandian fell area over the past three decades. In Ambio 44 (3), pp. 214–225. DOI: 10.1007/s13280-014-0541-8.

Kivinen, S.; Kaarlejärvi, E.; Jylhä, K.; Räisänen, J. (2012): Spatiotemporal distribution of threatened high-latitude snowbed and snow patch habitats in warming climate. In Environ. Res. Lett. 7 (3), p. 34024. DOI: 10.1088/1748-9326/7/3/034024.

Kizyakov, A. & Leibman, M. O. (2016): Cryogenic relief-formation processes: a review of 2010–2015 publications. In KZ (4). DOI: 10.21782/KZ1560-7496-2016-4(45-58).

Kleman, J.; Hättestrand, C.; Borgström, I.; Stroeven, A. (1997): Fennoscandian palaeoglaciology reconstructed using a glacial geological inversion model. In J. Glaciol. 43 (144), pp. 283–299. DOI: 10.3189/S0022143000003233.

Kok, J. F.; Parteli, E. J. R.; Michaels, T. I.; Karam, D. B. (2012): The physics of wind-blown sand and dust. In Reports on progress in physics. Physical Society (Great Britain) 75 (10), p. 106901. DOI: 10.1088/0034-4885/75/10/106901.

Kolasa, J. (1989): Ecological Systems in Hierarchical Perspecitive: Breaks in Community Structure and Other Consequences. In Ecology 70 (1), pp. 36–47. DOI: 10.2307/1938410.

Krenz, J.; Greenwood, P.; Kuhn, N.J. (2019): Soil Degradation Mapping in Drylands Using Unmanned Aerial Vehicle (UAV) Data. Soil Syst. 3, 33. DOI: 10.3390/soilsystems3020033.

Kropp, H.; Loranty, M. M.; Natali, S. M.; Kholodov, A. L.; Rocha, A. V.; Myers-Smith, I. et al. (2021): Shallow soils are warmer under trees and tall shrubs across Arctic and Boreal ecosystems. In Environ. Res. Lett. 16 (1), p. 15001. DOI: 10.1088/1748-9326/abc994.

Kumar, M.; Männistö, M. K.; van Elsas, J. D.; Nissinen, R. M. (2016): Plants impact structure and function of bacterial communities in Arctic soils. In Plant Soil 399 (1-2), pp. 319–332. DOI: 10.1007/s11104-015-2702-3.

Lagergren, F.; Björk, R. G.; Andersson, C.; Belušić, D.; Björkman, M. P.; Kjellström, E. et al. (2024): Kilometre-scale simulations over Fennoscandia reveal a large loss of tundra due to climate warming. In Biogeosciences 21 (5), pp. 1093–1116. DOI: 10.5194/bg-21-1093-2024.

Laidler, G. J.; Treitz, P. M.; Atkinson, D. M. (2008): Remote Sensing of Arctic Vegetation: Relations between the NDVI, Spatial Resolution and Vegetation Cover on Boothia Peninsula, Nunavut. In ARCTIC 61 (1), p. 1. DOI: 10.14430/arctic2.

Lamare, M.; Domine, F.; Revuelto, J.; Pelletier, M.; Arnaud, L.; Picard, G. (2023): Investigating the Role of Shrub Height and Topography in Snow Accumulation on Low-Arctic Tundra using UAV-Borne Lidar. In J. Hydrometeor 24 (5), pp. 853–871. DOI: 10.1175/JHM-D-22-0067.1.

Landsat collection 2 (2021). Version 1.0: January 7, 2021; Version 1.1: January 15, 2021. With assistance of U.S. Geological Survey. Reston, VA (Fact Sheet, 2021-3002). Available online at https://pubs.usgs.gov/publication/fs20213002.

Langford, Z.; Kumar, J.; Hoffman, F.; Norby, R.; Wullschleger, S.; Sloan, V.; Iversen, Colleen (2016): Mapping Arctic Plant Functional Type Distributions in the Barrow Environmental Observatory Using WorldView-2 and LiDAR Datasets. In Remote Sensing 8 (9), p. 733. DOI: 10.3390/rs8090733.

Lara, M. J.; McGuire, A. D.; Euskirchen, E. S.; Genet, H.; Yi, S.; Rutter, R. et al. (2020): Local-scale Arctic tundra heterogeneity affects regional-scale carbon dynamics. In Nature communications 11 (1), p. 4925. DOI: 10.1038/s41467-020-18768-z.

Lara, M. J.; Nitze, I.; Grosse, G.; Martin, P.; McGuire, A. D. (2018): Reduced arctic tundra productivity linked with landform and climate change interactions. In Scientific reports 8 (1), p. 2345. DOI: 10.1038/s41598-018-20692-8.

Ge, L.; Lafleur, P. M.; Humphreys, E. R. (2017): Respiration from Soil and Ground Cover Vegetation Under Tundra Shrubs. In Arctic, Antarctic, and Alpine Research 49 (4), pp. 537–550. DOI: 10.1657/AAAR0016-064.

Le Roux, P. C.& Luoto, M. (2014): Earth surface processes drive the richness, composition and occurrence of plant species in an arctic-alpine environment. In J Veg Sci 25 (1), pp. 45–54. DOI: 10.1111/jvs.12059.

Le Roux, P. C.; Aalto, J.; Luoto, M. (2013): Soil moisture's underestimated role in climate change impact modelling in low-energy systems. In Global Change Biol 19 (10), pp. 2965–2975. DOI: 10.1111/gcb.12286.

IPCC, 2023: Climate Change 2023: Synthesis Report. Contribution of Working Groups I, II and III to the Sixth Assessment Report of the Intergovernmental Panel on Climate Change [Core Writing Team, H. Lee and J. Romero (eds.)]. IPCC, Geneva, Switzerland. DOI: 10.59327/IPCC/AR6-9789291691647.

Lembrechts, J. J.; Lenoir, J. (2020): Microclimatic conditions anywhere at any time! In Global Change Biol 26 (2), pp. 337–339. DOI: 10.1111/gcb.14942.

Lenton, T. M.; Abrams, J. F.; Bartsch, A.; Bathiany, S.; Boulton, C. A.; Buxton, J. E. et al. (2024): Remotely sensing potential climate change tipping points across scales. In Nature communications 15 (1), p. 343. DOI: 10.1038/s41467-023-44609-w.

Letterly, A.; Key, J.; Liu, Y. (2018): Arctic climate: changes in sea ice extent outweigh changes in snow cover. In The Cryosphere 12 (10), pp. 3373–3382. DOI: 10.5194/tc-12-3373-2018.

Leutner, B.; Horning, N.; Schwalb-Willmann, J. (2019): RStoolbox: Tools for Remote Sensing Data Analysis. *R package version 0.2, 6*. DOI: 10.32614/CRAN.package.RStoolbox.

Liaw, A. & Wiener, M. (2002): Classification and Regression by Randomforest. R News, 2, 18-22. http://CRAN.R-project.org/doc/Rnews/. (Accessed January 2024)

Lidmar-Bergström, K. & Näslund, J. O. (2002): Landforms and uplift in Scandinavia. In SP 196 (1), pp. 103–116. DOI: 10.1144/GSL.SP.2002.196.01.07.

Liljequist, G. H. (1993): High latitudes. A history of Swedish Polar travels and research. Stockholm: Swedish Polar Research Secretariat in collaboration with Streiffert.

Litaor, M. I.; Williams, M.; Seastedt, T. R. (2008): Topographic controls on snow distribution, soil moisture, and species diversity of herbaceous alpine vegetation, Niwot Ridge, Colorado. In J. Geophys. Res. 113 (G2), Article 2007JG000419. DOI: 10.1029/2007JG000419.

Liu, N.; Budkewitsch, P.; Treitz, P. (2017): Examining spectral reflectance features related to Arctic percent vegetation cover: Implications for hyperspectral remote sensing of Arctic tundra. In Remote Sensing of Environment 192, pp. 58–72. DOI: 10.1016/j.rse.2017.02.002.

Livensperger, C.; Steltzer, H.; Darrouzet-Nardi, A.; Sullivan, P. F.; Wallenstein, M.; Weintraub, M. N. (2019): Experimentally warmer and drier conditions in an Arctic plant community reveal microclimatic controls on senescence. In Ecosphere 10 (4), Article e02677. DOI: 10.1002/ecs2.2677.

Loranty, M. M.; Goetz, S. J.; Beck, P. S. A. (2011): Tundra vegetation effects on pan-Arctic albedo. In Environ. Res. Lett. 6 (2), p. 24014. DOI: 10.1088/1748-9326/6/2/024014.

Lu, D.; Weng, Q. (2007): A survey of image classification methods and techniques for improving classification performance. In International Journal of Remote Sensing 28 (5), pp. 823–870. DOI: 10.1080/01431160600746456.

Lundquist, J. D.; Lott, F. (2008): Using inexpensive temperature sensors to monitor the duration and heterogeneity of snow-covered areas. In Water Resources Research 44 (4), Article 2008WR007035. DOI: 10.1029/2008WR007035.

Maclean, Ilya M. D.; Duffy, J. P.; Haesen, S.; Govaert, S.; de Frenne, P.; Vanneste, T. et al. (2021): On the measurement of microclimate. In Methods Ecol Evol 12 (8), pp. 1397–1410. DOI: 10.1111/2041-210X.13627.

Magurran, A. E.; Baillie, S. R.; Buckland, S. T.; Dick, J. M.; Elston, D. A.; Scott, E. M. et al. (2010): Long-term datasets in biodiversity research and monitoring: assessing change in ecological communities through time. In Trends in ecology & evolution 25 (10), pp. 574–582. DOI: 10.1016/j.tree.2010.06.016.

Mallen-Cooper, M.; Graae, B. J.; Cornwell, W. K. (2021): Lichens buffer tundra microclimate more than the expanding shrub Betula nana. In Annals of botany 128 (4), pp. 407–418. DOI: 10.1093/aob/mcab041.

Markkula, I.; Turunen, M.; Rasmus, S. (2019): A review of climate change impacts on the ecosystem services in the Saami Homeland in Finland. In Science of The Total Environment 692, pp. 1070–1085. DOI: 10.1016/j.scitotenv.2019.07.272.

Marston, R. A. (2010): Geomorphology and vegetation on hillslopes: Interactions, dependencies, and feedback loops. In Geomorphology 116 (3-4), pp. 206–217. DOI: 10.1016/j.geomorph.2009.09.028.

Marteinsdóttir, B.; Barrio, I. C.; Jónsdóttir, I. S. (2017): Assessing the ecological impacts of extensive sheep grazing in Iceland. In IAS 30, pp. 55–72. DOI: 10.16886/IAS.2017.07.

Martin, A. C.; Jeffers, E. S.; Petrokofsky, G.; Myers-Smith, I.; Macias-Fauria, M. (2017): Shrub growth and expansion in the Arctic tundra: an assessment of controlling factors using an evidence-based approach. In Environ. Res. Lett. 12 (8), p. 85007. DOI: 10.1088/1748-9326/aa7989.

Massa, C.; Bichet, V.; Gauthier, É.; Perren, B. B.; Mathieu, O.; Petit, C. et al. (2012): A 2500 year record of natural and anthropogenic soil erosion in South Greenland. In Quaternary Science Reviews 32, pp. 119–130. DOI: 10.1016/j.quascirev.2011.11.014.

Matthes, H.; Rinke, A.; Miller, P.A. et al. (2012): Sensitivity of high-resolution Arctic regional climate model projections to different implementations of land surface processes. Climatic Change 111, 197–214. https://doi.org/10.1007/s10584-011-0138-1.

McFadden, J. P.; Chapin, F. S.; Hollinger, D. Y. (1998): Subgrid-scale variability in the surface energy balance of arctic tundra. In Journal of Geophysical Research Atmospheres 103 (D22), 28,947-28,961. DOI: 10.1029/98JD02400.

McKight, P. E.; Najab, J. (2010): Kruskal-Wallis Test. In Irving B. Weiner, W. Edward Craighead (Eds.): The Corsini encyclopedia of psychology. 4th ed. Hoboken NJ: Wiley, p. 1.

Meltofte, H. (2013): Arctic biodiversity assessment. Status and trends in arctic biodiversity synthesis. Akuryeri: Conservation of Arctic Flora and Fauna (CAFF).

IPCC, 2019: Polar Regions. In: IPCC Special Report on the Ocean and Cryosphere in a Changing Climate [H.-O. Pörtner, D.C. Roberts, V. MassonDelmotte, P. Zhai, M. Tignor, E. Poloczanska, K. Mintenbeck, A. Alegría, M. Nicolai, A. Okem, J. Petzold, B. Rama, N.M. Weyer (eds.)]. Cambridge University Press, Cambridge, UK and New York, NY, USA, pp. 203-320. https://doi.org/10.1017/9781009157964.005.

Metcalfe, D. B.; Hermans, T. D. G.; Ahlstrand, J.; Becker, M.; Berggren, M.; Björk, R. G. et al. (2018): Patchy field sampling biases understanding of climate change impacts across the Arctic. In Nature ecology & evolution 2 (9), pp. 1443–1448. DOI: 10.1038/s41559-018-0612-5.

Michaelides, R. J.; Schaefer, K.; Zebker, H. A.; Parsekian, A.; Liu, L.; Chen, J. et al. (2019): Inference of the impact of wildfire on permafrost and active layer thickness in a discontinuous permafrost region using the remotely sensed active layer thickness (ReSALT) algorithm. In Environ. Res. Lett. 14 (3), p. 35007. DOI: 10.1088/1748-9326/aaf932.

Miles, V. V.; Esau, I. (2016): Spatial heterogeneity of greening and browning between and within bioclimatic zones in northern West Siberia. In Environ. Res. Lett. 11 (11), p. 115002. DOI: 10.1088/1748-9326/11/11/115002.

Minchin, P. R. (1987): An evaluation of the relative robustness of techniques for ecological ordination. In Vegetatio 69 (1-3), pp. 89–107. DOI: 10.1007/BF00038690.

Mod, H. K. & Luoto, M. (2016): Arctic shrubification mediates the impacts of warming climate on changes to tundra vegetation. In Environ. Res. Lett. 11 (12), p. 124028. DOI: 10.1088/1748-9326/11/12/124028.

Mod, H. K.; Le Roux, P. C.; Luoto, M. (2014): Outcomes of biotic interactions are dependent on multiple environmental variables. In J Veg Sci 25 (4), pp. 1024–1032. DOI: 10.1111/jvs.12148.

Mokarram, M. & Sathyamoorthy, D. (2018): A review of landform classification methods. In Spat. Inf. Res. 26 (6), pp. 647–660. DOI: 10.1007/s41324-018-0209-8.

Montandon, L. M. & Small, E. E. (2008): The impact of soil reflectance on the quantification of the green vegetation fraction from NDVI. Remote Sensing of Environment, Vol. 112, Iss. 4, pp. 1835-1845, ISSN 0034-4257. DOI: 10.1016/j.rse.2007.09.007.

Moreno-de Las Heras, M.; Saco, P. M.; Willgoose, G. R.; Tongway, D. J. (2011): Assessing landscape structure and pattern fragmentation in semiarid ecosystems using patch-size distributions. In Ecological applications : a publication of the Ecological Society of America 21 (7), pp. 2793–2805. DOI: 10.1890/10-2113.1.

Morin, P.; Porter, C.; Cloutier, M.; Howat, I.; Noh, M.-J.; Willis, M. et al. (2016): ArcticDEM; A Publically Available, High Resolution Elevation Model of the Arctic. In EGU General Assembly Conference Abstracts, EPSC2016-8396.

Mörsdorf, M. A.; Ravolainen, V. T.; Yoccoz, N. G.; Thórhallsdóttir, T. E.; Jónsdóttir, I. S. (2021): Decades of Recovery From Sheep Grazing Reveal No Effects on Plant Diversity Patterns Within Icelandic Tundra Landscapes. In Front. Ecol. Evol. 8, Article 602538. DOI: 10.3389/fevo.2020.602538.

Mott, R.; Vionnet, V.; Grünewald, T. (2018): The Seasonal Snow Cover Dynamics: Review on Wind-Driven Coupling Processes. In Front. Earth Sci. 6, Article 197, p. 409470. DOI: 10.3389/feart.2018.00197.

Musacchio, M.; Silvestri, M.; Romaniello, V.; Casu, M.; Buongiorno, M. F.; Melis, M. T. (2024): Comparison of ASI-PRISMA Data, DLR-EnMAP Data, and Field Spectrometer Measurements on “Sale ‘e Porcus”, a Salty Pond (Sardinia, Italy). In Remote Sensing 16 (6), p. 1092. DOI: 10.3390/rs16061092.

Müller, M.; Schwab, N.; Schickhoff, U.; Böhner, J.; Scholten, T. (2016): Soil Temperature and Soil Moisture Patterns in a Himalayan Alpine Treeline Ecotone. In Arctic, Antarctic, and Alpine Research 48 (3), pp. 501–521. DOI: 10.1657/AAAR0016-004.

Myers-Smith, I. H.; Kerby, J. T.; Phoenix, G. K.; Bjerke, J. W.; Epstein, H. E.; Assmann, J. J. et al. (2020): Complexity revealed in the greening of the Arctic. In Nat. Clim. Chang. 10 (2), pp. 106–117. DOI: 10.1038/s41558-019-0688-1.

Myers-Smith, I. H.; Hik, D. S. (2018): Climate warming as a driver of tundra shrubline advance. In J Ecol 106 (2), pp. 547–560. DOI: 10.1111/1365-2745.12817.

Myers-Smith, I. H.; Elmendorf, S. C.; Beck, P. S. A.; Wilmking, M.; Hallinger, M.; Blok, D. et al. (2015): Climate sensitivity of shrub growth across the tundra biome. In Nat. Clim. Chang. 5 (9), pp. 887–891. DOI: 10.1038/NCLIMATE2697.

Myers-Smith, I. H.; Forbes, B. C.; Wilmking, M.; Hallinger, M.; Lantz, T.; Blok, D.; Tape, K. D.; Macias-Fauria, M.; Sass-Klaassen, U.; Levesque, E.; Boudreau, S.; Ropars, P.; Hermanutz, L.; Trant, A.; Collier, L. S.; Weijers, S.; Rozema, J.; Rayback, S. A.; Schmidt, N. M.; ... Hik, D. S. (2011): Shrub expansion in tundra ecosystems: dynamics, impacts and research priorities. Environmental Research Letters, 6(4), 1 - 15. DOI: 10.1088/1748-9326/6/4/045509.

NASA, Landsat Missions. https://www.usgs.gov/landsat-missions (accessed June 2024)

Nguy-Robertson, A.; Gitelson, A.; Peng, Y.; Viña, A.; Arkebauer, T.; Rundquist, D. (2012): Green Leaf Area Index Estimation in Maize and Soybean: Combining Vegetation Indices to Achieve Maximal Sensitivity. In Agronomy Journal 104 (5), pp. 1336–1347. DOI: 10.2134/agronj2012.0065.

Niittynen, P.; Salminen, H.; Peña-Aguilera, P.; Aalto, J.; Alahuhta, J.; Luoto, M. et al. (2024): A Gridded Microclimate Dataset from a Sub-Arctic Biodiversity Hotspot in Finland. bioRxiv, 2024-03. DOI: 10.1101/2024.03.30.587419.

Niittynen, P.; Heikkinen, R. K.; Aalto, J.; Guisan, A.; Kemppinen, J.; Luoto, M. (2020a): Fine-scale tundra vegetation patterns are strongly related to winter thermal conditions. In Nat. Clim. Chang. 10 (12), pp. 1143–1148. DOI: 10.1038/s41558-020-00916-4.

Niittynen, P.; Heikkinen, R. K.; Luoto, M. (2020b): Decreasing snow cover alters functional composition and diversity of Arctic tundra. In Proceedings of the National Academy of Sciences of the United States of America 117 (35), pp. 21480–21487. DOI: 10.1073/pnas.2001254117.

Niittynen, P.; Heikkinen, R. K.; Luoto, M. (2018): Snow cover is a neglected driver of Arctic biodiversity loss. In Nat. Clim. Chang. 8 (11), pp. 997–1001. DOI: 10.1038/s41558-018-0311-x.

Niittynen, P. & Luoto, M. (2018): The importance of snow in species distribution models of arctic vegetation. In Ecography 41 (6), pp. 1024–1037. DOI: 10.1111/ecog.03348.

NOAA, AVHRR Imager. https://coastwatch.noaa.gov/cwn/instruments/avhrr.html (accessed June 2024).

Nuttall, M. (1998): Protecting the Arctic. Indigenous peoples and cultural survival. Amsterdam: Harwood Academic Publ (Studies in environmental anthropology, vol. 3).

Oberbauer, S. F.; Elmendorf, S. C.; Troxler, T. G.; Hollister, R. D.; Rocha, A. V.; Bret-Harte, M. S. et al. (2013): Phenological response of tundra plants to background climate variation tested using the International Tundra Experiment. In Philosophical transactions of the Royal Society of London. Series B, Biological sciences 368 (1624), p. 20120481. DOI: 10.1098/rstb.2012.0481.

Oksanen, J. et al. (2022): Vegan: community ecology package. R package version 2.6-4. https://CRAN.R-project.org/package=vegan. (Accessed February 2024)

Oksanen, L. & Virtanen, R. (1995): Geographical ecology of northernmost Fennoscandia. Helsinki: Finnish Zoological and Botanical Publishing Board (Acta Botanica Fennica, no. 153).

Ólafsdóttir, R. & Guòmundsson, H. J. (2002): Holocene land degradation and climatic change in northeastern Iceland. In The Holocene 12 (2), pp. 159–167. DOI: 10.1191/0959683602hl531rp.

Ólafsdóttir, R.; Schlyter, P.; Haraldsson, H. V. (2001): Simulating icelandic vegetation cover during the holocene implications for long-term land degradation. In Geografiska Annaler: Series A, Physical Geography 83 (4), pp. 203-215. DOI: 10.1111/j.0435-3676.2001.00155.x.

Ólafsson, H.; Furger, M.; Brümmer, B. (2007): The weather and climate of Iceland. In metz 16 (1), pp. 5–8. DOI: 10.1127/0941-2948/2007/0185.

Olofsson, J.; Kitti, H.; Rautiainen, P.; Stark, S.; Oksanen, L. (2001): Effects of Summer Grazing by Reindeer on Composition of Vegetation, Productivity and Nitrogen Cycling. In Ecography 24(1), pp. 13–24. DOI: 10.1034/j.1600-0587.2001.240103.x.

Olofsson, J.; Stark, S.; Oksanen, L. (2004): Reindeer influence on ecosystem processes in the tundra. In Oikos 105 (2), pp. 386–396. DOI: 10.1111/j.0030-1299.2004.13048.x.

Orndahl, K. M.; Ehlers, L. P. W.; Herriges, J. D.; Pernick, R. E.; Hebblewhite, M.; Goetz, S. J. (2022): Mapping tundra ecosystem plant functional type cover, height and aboveground biomass in Alaska and northwest Canada using unmanned aerial vehicles. In Arctic Science, Article AS-2021-0044. DOI: 10.1139/AS-2021-0044.

Óskarsson, H.; Arnalds, Ó.; Gudmundsson, J.; Gudbergsson, G. (2004): Organic carbon in Icelandic Andosols: geographical variation and impact of erosion. In CATENA 56 (1-3), pp. 225–238. DOI: 10.1016/j.catena.2003.10.013.

Overland, J. E. (2021): Rare events in the Arctic. Climatic Change 168, 27. DOI: 10.1007/s10584-021-03238-2.

Overland, J. E.; Dethloff, K.; Francis, J. A.; Hall, R. J.; Hanna, E.; Kim, S.-J. et al. (2016): Nonlinear response of mid-latitude weather to the changing Arctic. In Nature Climate Change, 6 (11), pp. 992–999. DOI: 10.1038/nclimate3121.

Pajunen, A. M.; Oksanen, J.; Virtanen, R. (2011): Impact of shrub canopies on understorey vegetation in western Eurasian tundra. In J Veg Sci 22 (5), pp. 837–846. DOI: 10.1111/j.1654-1103.2011.01285.x.

Pal, M. (2005): Random forest classifier for remote sensing classification. In International Journal of Remote Sensing 26 (1), pp. 217–222. DOI: 10.1080/01431160412331269698.

Pape, R.; Löffler, J. (2012): Climate change, land use conflicts, predation and ecological degradation as challenges for reindeer husbandry in northern Europe: what do we really know after half a century of research? In AMBIO: A Journal of the Human Environment 41 (5), pp. 421–434. DOI: 10.1007/s13280-012-0257-6.

Parker, T.C.; Thurston, A.M.; Raundrup, K. et al. (2021): Shrub expansion in the Arctic may induce large-scale carbon losses due to changes in plant-soil interactions. Plant Soil 463, 643–651. https://doi.org/10.1007/s11104-021-04919-8.

Pattison, R. R.; Jorgenson, J. C.; Raynolds, M. K.; Welker, J. M. (2015): Trends in NDVI and Tundra Community Composition in the Arctic of NE Alaska Between 1984 and 2009. In Ecosystems 18 (4), pp. 707–719. DOI: 10.1007/s10021-015-9858-9.

Pearce, R. (2001): Plant Freezing and Damage. In Annals of botany 87 (4), pp. 417–424. DOI: 10.1006/anbo.2000.1352.

Peña-Aguilera, P.; Schmidt, N. M.; Stewart, L.; Parisy, B.; van der Wal, R.; Lindman, L. et al. (2023): Consistent imprints of elevation, soil temperature and moisture on plant and arthropod communities across two subarctic landscapes. In Insect Conserv Diversity 16 (5), pp. 684–700. DOI: 10.1111/icad.12667.

Pessi, I. S.; Viitamäki, S.; Virkkala, A.-M.; Eronen-Rasimus, E.; Delmont, T. O.; Marushchak, M. E. et al. (2022): In-depth characterization of denitrifier communities across different soil ecosystems in the tundra. In Environmental microbiome 17 (1), p. 30. DOI: 10.1186/s40793-022-00424-2.

Petit Bon, M.; Inga, G. K.; Jónsdóttir, I. S.; Utsi, T. A.; Soininen, E. M.; Bråthen, K. A. (2020): Interactions between winter and summer herbivory affect spatial and temporal plant nutrient dynamics in tundra grassland communities. In Oikos 129 (8), pp. 1229–1242. DOI: 10.1111/oik.07074.

Peng, J.; Loew, A.; Merlin, O.; Verhoest, N. E. C. (2017): A review of spatial downscaling of satellite remotely sensed soil moisture. In Reviews of Geophysics 55 (2), pp. 341–366. DOI: 10.1002/2016RG000543.

Pettorelli, N.; Laurance, W. F.; O'Brien, T. G.; Wegmann, M.; Nagendra, H.; Turner, W. (2014): Satellite remote sensing for applied ecologists: opportunities and challenges. In Journal of Applied Ecology 51 (4), pp. 839–848. DOI: 10.1111/1365-2664.12261.

Phoenix, G. K.; Bjerke, J. W. (2016): Arctic browning: extreme events and trends reversing arctic greening. In Global Change Biology 22 (9), pp. 2960–2962. DOI: 10.1111/gcb.13261.

Pichon, B.; Donnet, S.; Gounand, I.; Kéfi, S. (2024): Estimating distances to tipping points from dryland ecosystem images. DOI: 10.1101/2024.02.20.581244.

Teixeira Pinto, C.; Jing, X.; Leigh, L. (2020): Evaluation Analysis of Landsat Level-1 and Level-2 Data Products Using In Situ Measurements. In Remote Sensing 12, 2597. DOI: 10.3390/rs12162597.

Pirk, N.; Aalstad, K.; Yilmaz, Y. A.; Vatne, A.; Popp, A. L.; Horvath, P. et al. (2023): Snow-vegetation-atmosphere interactions in alpine tundra. DOI: 10.5194/bg-2023-21.

Poesen, J. (2018): Soil erosion in the Anthropocene: Research needs. In Earth Surf. Process. Landforms 43 (1), pp. 64–84. DOI: 10.1002/esp.4250.

Poley, L. G. & McDermid, G. J. (2020): A Systematic Review of the Factors Influencing the Estimation of Vegetation Aboveground Biomass Using Unmanned Aerial Systems. In Remote Sensing 12 (7), p. 1052. DOI: 10.3390/rs12071052.

Poos, M. S. & Jackson, D. A. (2012): Addressing the removal of rare species in multivariate bioassessments: The impact of methodological choices. In Ecological Indicators 18, pp. 82–90. DOI: 10.1016/j.ecolind.2011.10.008.

Portal, G.; Jagdhuber, T.; Vall-llossera, M.; Camps, A.; Pablos, M.; Entekhabi, D.; Piles, M. (2020): Assessment of Multi-Scale SMOS and SMAP Soil Moisture Products across the Iberian Peninsula. In Remote Sensing 12 (3), p. 570. DOI: 10.3390/rs12030570.

Porter, C.; Morin, P.; Howat, I.; Noh, M.-J.; Bates, B.; Peterman, K. et al. (2018): ArcticDEM, Version 3. DOI: 10.7910/DVN/OHHUKH.

Post, E.; Alley, R. B.; Christensen, T. R.; Macias-Fauria, M.; Forbes, B. C.; Gooseff, M. N. et al. (2019): The polar regions in a 2°C warmer world. In Science advances 5 (12), eaaw9883. DOI: 10.1126/sciadv.aaw9883.

Post, E.; Steinman, B. A.; Mann, M. E. (2018): Acceleration of phenological advance and warming with latitude over the past century. In Scientific reports 8 (1), p. 3927. DOI: 10.1038/s41598-018-22258-0.

Putkiranta, P.; Räsänen, A.; Korpelainen, P.; Erlandsson, R.; Kolari, T. H.M.; Pang, Y. et al. (2024): The value of hyperspectral UAV imagery in characterizing tundra vegetation. In Remote Sensing of Environment 308, p. 114175. DOI: 10.1016/j.rse.2024.114175.

Rantanen, M.; Kämäräinen, M.; Niittynen, P.; Phoenix, G. K.; Lenoir, J.; Maclean, I. et al. (2023): Bioclimatic atlas of the terrestrial Arctic. In Scientific data 10 (1), p. 40. DOI: 10.1038/s41597-023-01959-w.

Rango A. (1997). The response of areal snow cover to climate change in a snowmelt–runoff model. Annals of Glaciology. 25:232-236. DOI:10.3189/S0260305500014099.

Rantanen, M.; Karpechko, A. Y.; Lipponen, A.; Nordling, K.; Hyvärinen, O.; Ruosteenoja, K. et al. (2022): The Arctic has warmed nearly four times faster than the globe since 1979. In Commun Earth Environ 3 (1). DOI: 10.1038/s43247-022-00498-3.

Räsänen, A.; Juutinen, S.; Aurela, M.; Virtanen, T. (2019): Predicting aboveground biomass in Arctic landscapes using very high spatial resolution satellite imagery and field sampling. In International Journal of Remote Sensing 40 (3), pp. 1175–1199. DOI: 10.1080/01431161.2018.1524176.

Rasmussen, L. H.; Danielsen, B. K.; Elberling, B.; Ambus, P.; Björkman, M. P.; Rinnan, R.; Andresen, L. C. (2024): Nitrogen immobilization could link extreme winter warming events to Arctic browning. In Soil Biology and Biochemistry 191, p. 109319. DOI: 10.1016/j.soilbio.2024.109319.

Rast, M.; Nieke, J.; Adams, J.; Isola, C.; Gascon, F. (2021): Copernicus Hyperspectral Imaging Mission for the Environment (Chime). In : 2021 IEEE International Geoscience and Remote Sensing Symposium IGARSS: IEEE.

Raynolds, M. K.; Walker, D. A. (2016): Increased wetness confounds Landsat-derived NDVI trends in the central Alaska North Slope region, 1985–2011. In Environ. Res. Lett. 11 (8), p. 85004. DOI: 10.1088/1748-9326/11/8/085004.

Raynolds, M.; Magnússon, B.; Metúsalemsson, S.; Magnússon, S. (2015): Warming, Sheep and Volcanoes: Land Cover Changes in Iceland Evident in Satellite NDVI Trends. In Remote Sensing 7 (8), pp. 9492–9506. DOI: 10.3390/rs70809492.

Raynolds, M. K.; Walker, D.A.; Ambrosius, K. J.; Brown, J.; Everett, K. R.; Kanevskiy, M.; Kofinas, G. P.; Romanovsky, V. E.; Shur, Y.; Webber P. J. (2014): Cumulative geoecological effects of 62 years of infrastructure and climate change in ice-rich permafrost landscapes, Prudhoe Bay Oilfield, Alaska. Global Change Biology 20: 1211–1224. DOI: 10.1111/gcb.12500.

Raynolds, M. K.; Walker, D. A.; Verbyla, D.; Munger, C. A. (2013): Patterns of Change within a Tundra Landscape: 22-year Landsat NDVI Trends in an Area of the Northern Foothills of the Brooks Range, Alaska. In Arctic, Antarctic, and Alpine Research 45 (2), pp. 249–260. DOI: 10.1657/1938-4246-45.2.249.

Raynolds, M. K.; Walker, D. A.; Epstein, H. E.; Pinzon, J. E.; Tucker, C. J. (2012): A new estimate of tundra-biome phytomass from trans-Arctic field data and AVHRR NDVI. In Remote Sensing Letters 3 (5), pp. 403–411. DOI: 10.1080/01431161.2011.609188.

Raynor, E. J.; Gersie, S. P.; Stephenson, M. B.; Clark, P. E.; Spiegal, S. A.; Boughton, R. K. et al. (2021): Cattle Grazing Distribution Patterns Related to Topography Across Diverse Rangeland Ecosystems of North America. In Rangeland Ecology & Management 75, pp. 91–103. DOI: 10.1016/j.rama.2020.12.002.

Reu, J. de; Bourgeois, J.; Bats, M.; Zwertvaegher, A.; Gelorini, V.; Smedt, P. de et al. (2013): Application of the topographic position index to heterogeneous landscapes. In Geomorphology 186, pp. 39–49. DOI: 10.1016/j.geomorph.2012.12.015.

Riedel, S. M.; Epstein, H. E.; Walker, D. A. (2005): Biotic controls over spectral reflectance of arctic tundra vegetation. In International Journal of Remote Sensing 26 (11), pp. 2391–2405. DOI: 10.1080/01431160512331337754.

Rietkerk, M.; Bastiaansen, R.; Banerjee, S.; van de Koppel, J.; Baudena, M.; Doelman, A. (2021): Evasion of tipping in complex systems through spatial pattern formation. In Science (New York, N.Y.) 374 (6564), eabj0359. DOI: 10.1126/science.abj0359.

Rietkerk, M. & van de Koppel, J. (2008): Regular pattern formation in real ecosystems. In Trends in ecology & evolution 23 (3), pp. 169–175. DOI: 10.1016/j.tree.2007.10.013.

Rietkerk, M.; Dekker, S. C.; Ruiter, P. C. de; van de Koppel, J. (2004): Self-organized patchiness and catastrophic shifts in ecosystems. In Science (New York, N.Y.) 305 (5692), pp. 1926–1929. DOI: 10.1126/science.1101867.

Rietze, N.; Assmann, J. J.; Plekhanova, E.; Naegeli, K.; Damm, A.; Maximov, T. C. et al. (2024): Summer drought weakens land surface cooling of tundra vegetation. In Environ. Res. Lett. 19 (4), p. 44043. DOI: 10.1088/1748-9326/ad345e.

Riihimäki, H.; Heiskanen, J.; Luoto, M. (2017): The effect of topography on arctic-alpine aboveground biomass and NDVI patterns. In International Journal of Applied Earth Observation and Geoinformation 56, pp. 44–53. DOI: 10.1016/j.jag.2016.11.005.

Riley, S. J.; DeGloria S. D.; Elliot R. (1999): A terrain ruggedness index that quantifies topographic heterogeneity. Intermountain Journal of Sciences, vol. 5 iss. (1-4):23-27.

Rixen, C.; Høye, T. T.; Macek, P.; Aerts, R.; Alatalo, J. M.; Anderson, J. T. et al. (2022): Winters are changing: snow effects on Arctic and alpine tundra ecosystems. In Arctic Science 8 (3), pp. 572–608. DOI: 10.1139/as-2020-0058.

Romano, N.; Szabó, B.; Belmonte, A.; Castrignanò, A.; Ben-Dor, E.; Francos, N.; Nasta, P. (2023): Chapter 6. Mapping soil properties for UAS-based environmental monitoring. DOI: 10.1016/B978-0-323-85283-8.00010-2.

Rundgren, M.; Ingólfsson, Ó. (1999): Plant survival in Iceland during periods of glaciation? In Journal of Biogeography 26 (2), pp. 387–396. DOI: 10.1046/j.1365-2699.1999.00296.x.

Sadler, J. P. (1999): Biodiversity on oceanic islands:a palaeoecological assessment. In Journal of Biogeography 26 (1), pp. 75–87. DOI: 10.1046/j.1365-2699.1999.00285.x.

Salminen, H.; Tukiainen, H.; Alahuhta, J.; Hjort, J.; Huusko, K.; Grytnes, J.-A. et al. (2023): Assessing the relation between geodiversity and species richness in mountain heaths and tundra landscapes. In Landscape Ecology 38 (9), pp. 2227–2240. DOI: 10.1007/s10980-023-01702-1.

Sasseville, V.; Langlois, A.; Brucker, L.; Johnson, C. A. (2024): Patterns and trend analysis of rain-on-snow events using passive microwave satellite data over the Canadian Arctic Archipelago since 1987. In J. Hydrometeor. DOI: 10.1175/JHM-D-22-0218.1.

Scheffer, M.; Carpenter, S.; Foley, J. A.; Folke, C.; Walker, B. (2001): Catastrophic shifts in ecosystems. In Nature 413 (6856), pp. 591–596. DOI: 10.1038/35098000.

Schöb, C.; Kammer, P. M.; Choler, P.; Veit, H. (2009): Small-scale plant species distribution in snowbeds and its sensitivity to climate change. In Plant Ecol 200 (1), pp. 91–104. DOI: 10.1007/s11258-008-9435-9.

Schuur, E. A. G.; McGuire, A. D.; Schädel, C.; Grosse, G.; Harden, J. W.; Hayes, D. J. et al. (2015): Climate change and the permafrost carbon feedback. In Nature 520 (7546), pp. 171–179. DOI: 10.1038/nature14338.

Semmens, K.A.; Ramage, J.M.; Bartsch, A.; Liston, G.E. (2013): Early snowmelt events: detection, distribution, and significance in a major sub-arctic watershed. Environmental Research Letters, 8. DOI: 10.1088/1748-9326/8/1/014020.

Seppälä, M. (2004): Wind as a geomorphic agent in cold climates. New York: Cambridge University Press (Studies in polar research).

Sharifi, A. & Felegari, S. (2023): Remotely sensed normalized difference red-edge index for rangeland biomass estimation. In Aircraft Engineering and Aerospace Technology 95 (7), pp. 1128–1136. DOI: 10.1108/AEAT-07-2022-0199.

She, X.; Zhang, L.; Cen, Y.; Wu, T.; Huang, C.; Baig, M. H. A. (2015): Comparison of the Continuity of Vegetation Indices Derived from Landsat 8 OLI and Landsat 7 ETM+ Data among Different Vegetation Types. Remote Sensing, 7(10), 13485-13506. DOI: 10.3390/rs7101348

Sjogren, E. (1973): Icelandic, Miscellaneous, Arsrit Skograektarfelags Islands 1972/1973., (52–69), The microclimate in woodland and scrub in Haukadalur and Vaglaskogur [Iceland].

Siewert, M. B.; Olofsson, J. (2020): Scale-dependency of Arctic ecosystem properties revealed by UAV. In Environ. Res. Lett. 15 (9), p. 94030. DOI: 10.1088/1748-9326/aba20b.

Sigurdsson, S. (1977): Birki d Islandi [Birch in Iceland]. Reykjavík: Skógarmál, 146-172 pp. 146–172.

Silvertown, J.; Araya, Y.; Gowing, D. (2015): Hydrological niches in terrestrial plant communities: a review. In J. Ecol. 103 (1), pp. 93–108. DOI: 10.1111/1365-2745.12332.

Simpson, I. A.; Dugmore, A. J.; Thomson, A.; Vésteinsson, O. (2001): Crossing the thresholds: human ecology and historical patterns of landscape degradation. In CATENA 42 (2-4), pp. 175–192. DOI: 10.1016/S0341-8162(00)00137-5.

Sims, D. A. & Gamon, J. A. (2002): Relationships between leaf pigment content and spectral reflectance across a wide range of species, leaf structures and developmental stages. In Remote Sensing of Environment 81 (2-3), pp. 337–354. DOI: 10.1016/S0034-4257(02)00010-X.

Smith, K. E.; Burrows, M. T.; Hobday, A. J.; King, N. G.; Moore, P. J.; Sen Gupta, A. et al. (2023): Biological Impacts of Marine Heatwaves. In Annual review of marine science 15, pp. 119–145. DOI: 10.1146/annurev-marine-032122-121437.

Sonesson, M. & Callaghan, T. V. (1991): Strategies of survival in plants of the Fennoscandian tundra. In Arctic, vol. 44, pp. 95-105. DOI: 10.14430/arctic1525.

Song, C. & Woodcock, C. E. (2003): Monitoring forest succession with multitemporal Landsat images: factors of uncertainty. In IEEE Transactions on Geoscience and Remote Sensing, vol. 41, no. 11, pp. 2557-2567. DOI: 10.1109/TGRS.2003.818367.

Song, XP.; Hansen, M.C.; Stehman, S.V. et al. (2018). Global land change from 1982 to 2016. Nature 560, 639–643. DOI: 10.1038/s41586-018-0411-9.

Sotille, M. E.; Bremer, U. F.; Vieira, G.; Velho, L. F.; Petsch, C.; Simões, J. C. (2020): Evaluation of UAV and satellite-derived NDVI to map maritime Antarctic vegetation. In Applied Geography 125, p. 102322. DOI: 10.1016/j.apgeog.2020.102322.

Spitzer, C. M.; Wardle, D. A.; Lindahl, B. D.; Sundqvist, M. K.; Gundale, M. J.; Fanin, N.; Kardol, P. (2022): Root traits and soil micro-organisms as drivers of plant-soil feedbacks within the sub-arctic tundra meadow. In J. Ecol. 110 (2), pp. 466–478. DOI: 10.1111/1365-2745.13814.

Stark, S.; Kumar, M.; Myrsky, E. et al. (2023): Decreased Soil Microbial Nitrogen Under Vegetation ‘Shrubification’ in the Subarctic Forest–Tundra Ecotone: The Potential Role of Increasing Nutrient Competition Between Plants and Soil Microorganisms. Ecosystems 26, 1504–1523. https://doi.org/10.1007/s10021-023-00847-z

Starr, G.; Oberbauer, S. F.; Ahlquist, L. E. (2008): The Photosynthetic Response of Alaskan Tundra Plants to Increased Season Length and Soil Warming. In Arctic, Antarctic, and Alpine Research 40 (1), pp. 181–191. DOI: 10.1657/1523-0430(06-015)[STARR]2.0.CO;2.

Steindorsson, S. (1962) On the age and immigration of the Icelandic flora. Societas Scientiarum Islandica, 35.

Stewart, K. J.; Grogan, P.; Coxson, D. S.; Siciliano, S. D. (2014): Topography as a key factor driving atmospheric nitrogen exchanges in arctic terrestrial ecosystems. In Soil Biology and Biochemistry 70, pp. 96–112. DOI: 10.1016/j.soilbio.2013.12.005.

Stoessel, M.; Moen, J.; Lindborg, R. (2022): Mapping cumulative pressures on the grazing lands of northern Fennoscandia. In Scientific reports 12 (1), p. 16044. DOI: 10.1038/s41598-022-20095-w.

Stow, D. A.; Hope, A.; McGuire, D.; Verbyla, D.; Gamon, J.; Huemmrich, F. et al. (2004): Remote sensing of vegetation and land-cover change in Arctic Tundra Ecosystems. In Remote Sensing of Environment 89 (3), pp. 281–308. DOI: 10.1016/j.rse.2003.10.018.

Strahler, A. H.; Strahler, A. N. (2005): Physical geography. Science and systems of the human environment. 3rd ed. New York: J. Wiley.

Streeter, R. T.; Cutler, N. A. (2020): Assessing spatial patterns of soil erosion in a high-latitude rangeland. In Land Degrad Dev 31 (15), pp. 2003–2018. DOI: 10.1002/ldr.3585.

Streeter, R.; Dugmore, A. J.; Lawson, I. T.; Erlendsson, E.; Edwards, K. J. (2015): The onset of the palaeoanthropocene in Iceland: Changes in complex natural systems. In The Holocene 25 (10), pp. 1662–1675. DOI: 10.1177/0959683615594468.

Streeter, R.; Dugmore, A. (2014): Late-Holocene land surface change in a coupled social–ecological system, southern Iceland: a cross-scale tephrochronology approach. In Quaternary Science Reviews 86, pp. 99–114. DOI: 10.1016/j.quascirev.2013.12.016.

Streeter, R.; Dugmore, A. J.; Vésteinsson, O. (2012): Plague and landscape resilience in premodern Iceland. In Proceedings of the National Academy of Sciences of the United States of America 109 (10), pp. 3664–3669. DOI: 10.1073/pnas.1113937109.

Stroeven, A. P.; Hättestrand, C.; Kleman, J.; Heyman, J.; Fabel, D.; Fredin, O. et al. (2016): Deglaciation of Fennoscandia. In Quaternary Science Reviews 147, pp. 91–121. DOI: 10.1016/j.quascirev.2015.09.016.

Sturm, M. & Wagner, A M. (2010): Using repeated patterns in snow distribution modeling: An Arctic example. In Water Resources Research 46 (12), Article 2010WR009434. DOI: 10.1029/2010WR009434.

Sturm, M.; Douglas, T.; Racine, C.; Liston, G. E. (2005): Changing snow and shrub conditions affect albedo with global implications. In J. Geophys. Res. 110 (G1), Article 2005JG000013. DOI: 10.1029/2005JG000013.

Sturm, M.; Holmgren, J.; McFadden, J. P.; Liston, G. E.; Chapin, F. Stuart; R.; Charles H. (2001): Snow–Shrub Interactions in Arctic Tundra: A Hypothesis with Climatic Implications. In J. Climate 14 (3), pp. 336–344. DOI: 10.1175/1520-0442(2001)014<0336:SSIIAT>2.0.CO;2.

Subhatu, A.; Speranza, C. I.; Zeleke, G.; Roth, V.; Lemann, T.; Herweg, K.; Hurni, H. (2018): Interrelationships between terrace development, topography, soil erosion, and soil dislocation by tillage in Minchet Catchment, Ethiopian Highlands. In Land Degrad Dev 29 (10), pp. 3584–3594. DOI: 10.1002/ldr.3109.

Suggitt, A. J.; Gillingham, P. K.; Hill, J. K.; Huntley, B.; Kunin, W. E.; Roy, D. B.; Thomas, C. D. (2011): Habitat microclimates drive fine-scale variation in extreme temperatures. In Oikos 120 (1), pp. 1-8. DOI: 10.1111/j.1600-0706.2010.18270.x.

Suvanto, S.; Le Roux, P. C.; Luoto, M. (2014): Arctic-alpine vegetation biomass is driven by fine-scale abiotic heterogeneity. In Geografiska Annaler: Series A, Physical Geography, n/a-n/a. DOI: 10.1111/geoa.12050.

Tape, K. D.; Hallinger, M.; Welker, J. M.; Ruess, R. W. (2012): Landscape Heterogeneity of Shrub Expansion in Arctic Alaska. In Ecosystems 15 (5), pp. 711–724. DOI: 10.1007/s10021-012-9540-4.

Tarnocai, C.; Canadell, J. G.; Schuur, E. A. G.; Kuhry, P.; Mazhitova, G.; Zimov, S. (2009): Soil organic carbon pools in the northern circumpolar permafrost region. In Global Biogeochemical Cycles 23 (2), Article 2008GB003327. DOI: 10.1029/2008GB003327.

Thiffault, E. (2019): Boreal forests and soils 36 (36), pp. 59–82. DOI: 10.1016/B978-0-444-63998-1.00005-7.

Thomas, D. N. (Ed.) (2020): Arctic ecology. Hoboken NJ: Wiley-Blackwell. pp. 103-132.

Thompson, P. I. J.; Dugmore, A. J.; Newton, A. J.; Streeter, R. T.; Cutler, N. A. (2022a): Variations in tephra stratigraphy created by small-scale surface features in sub-polar landscapes. In Boreas 51 (2), pp. 317–331. DOI: 10.1111/bor.12557.

Thompson, D. R.; Basilio, R.; Brosnan, I.; Cawse-Nicholson, K.; Chadwick, K. D.; Guild, L. et al. (2022b): Ongoing Progress Toward NASA's Surface Biology and Geology Mission. In : IGARSS, pp. 5007–5010.

Thomson, E. R.; Spiegel, M. P.; Althuizen, I. H. J.; Bass, P.; Chen, S.; Chmurzynski, A. et al. (2021): Multiscale mapping of plant functional groups and plant traits in the High Arctic using field spectroscopy, UAV imagery and Sentinel-2A data. In Environ. Res. Lett. 16 (5), p. 55006. DOI: 10.1088/1748-9326/abf464.

Thordarson, T. & Larsen, G. (2007): Volcanism in Iceland in historical time: Volcano types, eruption styles and eruptive history. In Journal of Geodynamics 43 (1), pp. 118–152. DOI: 10.1016/j.jog.2006.09.005.

Thorsson, J. (2008): Desertification of high latitude ecosystems: Conceptual models, time-series analyses and experiments. (PhD thesis). Texas A&M University.

Tian, F.; Fensholt, R.; Verbesselt, J.; Grogan, K.h; Horion, S.; Wang, Y. (2015): Evaluating temporal consistency of long-term global NDVI datasets for trend analysis. In Remote Sensing of Environment 163, pp. 326–340. DOI: 10.1016/j.rse.2015.03.031.

Tieszen, L. L. (1978): Photosynthesis in the Principal Barrow, Alaska, Species: A Summary of Field and Laboratory Responses. In Larry L. Tieszen (Ed.): Vegetation and Production Ecology of an Alaskan Arctic Tundra. New York, NY: Springer-Verlag New York (Ecological Studies, Analysis and Synthesis, 29), pp. 241–268. DOI: 10.1007/978-1-4612-6307-4_10.

Tømmervik, H.; Bjerke, J. W.; Gaare, E.; Johansen, B.; Thannheiser, D. (2012): Rapid recovery of recently overexploited winter grazing pastures for reindeer in northern Norway. In Fungal Ecology 5 (1), pp. 3–15. DOI: 10.1016/j.funeco.2011.08.002.

Trahan, M. W. & Schubert, B. A. (2016): Temperature-induced water stress in high-latitude forests in response to natural and anthropogenic warming. In Global Change Biol 22 (2), pp. 782–791. DOI: 10.1111/gcb.13121.

Traustason, B. & Snorrason, A. (2008): Spatial distribution of forests and woodlands in Iceland in accordance with the CORINE land cover classification. In Icelandic Agricultural Sciences, vol. 21, pp. 39–47.

Travis, J. (1998): Experiments in Ecology: Their Logical Design and Interpretation Using Analysis of Variance. A. J. Underwood. In The Quarterly Review of Biology 73 (4), pp. 534–535. DOI: 10.1086/420505.

Tsang, L.; Durand, M.; Derksen, C.; Barros, A. P.; Kang, D.-H.; Lievens, H. et al. (2022): Review article: Global monitoring of snow water equivalent using high-frequency radar remote sensing. In The Cryosphere 16 (9), pp. 3531–3573. DOI: 10.5194/tc-16-3531-2022.

Tucker, C. J. (1979): Red and photographic infrared linear combinations for monitoring vegetation. In Remote Sensing of Environment 8 (2), pp. 127–150. DOI: 10.1016/0034-4257(79)90013-0.

Tukey J. W. (1949): Comparing individual means in the analysis of variance. Biometrics. 5(2):99-114. PMID: 18151955. DOI: 10.2307/3001913.

Turetsky, M. R.; Abbott, B. W.; Jones, M. C.; Walter, A. K.; Olefeldt, D.; Schuur, E. A. G. et al. (2019): Permafrost collapse is accelerating carbon release. In Nature 569 (7754), pp. 32–34. DOI: 10.1038/d41586-019-01313-4.

Turner, D.; Cimoli, E.; Lucieer, A.; Haynes, R. S.; Randall, K.; Waterman, M. J. et al. (2024): Mapping water content in drying Antarctic moss communities using UAS -borne SWIR imaging spectroscopy. In *Remote Sens Ecol Conserv* 10 (3), pp. 296–311. DOI: 10.1002/rse2.371.

Tybirk, K.; Nilsson, M.-C.; Michelsen, A.; Kristensen, H. L.; Shevtsova, A.; Strandberg, T. M. et al. (2000): Nordic Empetrum Dominated Ecosystems: Function and Susceptibility to Environmental Changes. In AMBIO: A Journal of the Human Environment 29 (2), pp. 90–97. DOI: 10.1579/0044-7447-29.2.90.

Tyystjärvi, V. A.; Niittynen, P.; Kemppinen, J.; Luoto, M.; Rissanen, T.; Aalto, J. (2023): Variability and drivers of winter near-surface temperatures over boreal and tundra landscapes. The Cryosphere, 18, pp. 403–423. DOI: 10.5194/tc-18-403-2024.

Tyystjärvi, V.; Kemppinen, J.; Luoto, M.; Aalto, T.; Markkanen, T.; Launiainen, S. et al. (2022): Modelling spatio-temporal soil moisture dynamics in mountain tundra. In Hydrological Processes 36 (1), Article e14450. DOI: 10.1002/hyp.14450.

Vajda, S. (1950): The Mathematical Theory of Communication. By Claude E. Shannon and Warren Weaver. Pp. 117 $2.50. 1949. (University of Illinois Press, Urbana). In Math. Gaz. 34 (310), pp. 312–313. DOI: 10.2307/3611062.

Valanne, K.; Patomäki, J.; Kalela, O. (1968): Box-nesting birds in timber-line forests at Kilpisjärvi, Finnish Lapland. In Annales Zoologici Fennici, vol. 5, iss,4, pp. 401–408. http://www.jstor.org/stable/23731413.

Vali, A.; Comai, S.; Matteucci, M. (2020): Deep Learning for Land Use and Land Cover Classification Based on Hyperspectral and Multispectral Earth Observation Data: A Review. In Remote Sensing 12 (15), p. 2495. DOI: 10.3390/rs12152495.

van der Wal, R. & Stien, A. (2014): High-arctic plants like it hot: a long-term investigation of between-year variability in plant biomass. In Ecology 95 (12), pp. 3414–3427. DOI: 10.1890/14-0533.1.

van der Wal, R. (2006): Do herbivores cause habitat degradation or vegetation state transition? Evidence from the tundra. In Oikos 114 (1), pp. 177–186. DOI: 10.1111/j.2006.0030-1299.14264.x.

van Westen, R. M.; Kliphuis, M.; Dijkstra, H. A. (2024): Physics-based early warning signal shows that AMOC is on tipping course. In Science advances 10 (6), eadk1189. DOI: 10.1126/sciadv.adk1189.

van Zuijlen, K.; Roos, R. E.; Klanderud, K.; Lang, S. I.; Asplund, J. (2020): Mat-forming lichens affect microclimate and litter decomposition by different mechanisms. In Fungal Ecology 44, p. 100905. DOI: 10.1016/j.funeco.2019.100905.

Veðurstofa Íslands, (accessed Mar 2022, Feb 2024). Climatological Data. Icelandic Meteorological Office. Retrieved from: http://en.vedur.is/climatology/data/http://en.vedur.is/climatology/data/.

Viles, H. (2020): Biogeomorphology: Past, present and future. In Geomorphology 366, p. 106809. DOI: 10.1016/j.geomorph.2019.06.022.

Villoslada, M.; Berner, L. T.; Juutinen, S.; Ylänne, H.; Kumpula, T. (2024): Upscaling vascular aboveground biomass and topsoil moisture of subarctic fens from Unoccupied Aerial Vehicles (UAVs) to satellite level. In The Science of the total environment 933, p. 173049. DOI: 10.1016/j.scitotenv.2024.173049.

Vincent, W. F.; Callaghan, T. V.; Dahl-Jensen, D.; Johansson, M.; Kovacs, K. M.; Michel, C. et al. (2011): Ecological Implications of Changes in the Arctic Cryosphere. In AMBIO 40 (S1), pp. 87–99. DOI: 10.1007/s13280-011-0218-5.

Virtanen, R.; Oksanen, L.; Oksanen, T.; Cohen, J.; Forbes, B. C.; Johansen, B. et al. (2016): Where do the treeless tundra areas of northern highlands fit in the global biome system: toward an ecologically natural subdivision of the tundra biome. In Ecology and evolution 6 (1), pp. 143–158. DOI: 10.1002/ece3.1837.

Virtanen, T. & Ek, M. (2014): The fragmented nature of tundra landscape. In International Journal of Applied Earth Observation and Geoinformation 27, pp. 4–12. DOI: 10.1016/j.jag.2013.05.010.

Virtanen, R.; Luoto, M.; Rämä, T.; Mikkola, K.; Hjort, J.; Grytnes, J.-A.; Birks, H. J. B. (2010): Recent vegetation changes at the high-latitude tree line ecotone are controlled by geomorphological disturbance, productivity and diversity. In Global Ecol Biogeogr 19 (6), pp. 810–821. DOI: 10.1111/j.1466-8238.2010.00570.x.

Vowles, T.; Gunnarsson, B.; Molau, U.; Hickler, T.; Klemedtsson, L.; Björk, R. G. (2017): Expansion of deciduous tall shrubs but not evergreen dwarf shrubs inhibited by reindeer in Scandes mountain range. In J Ecol 105 (6), pp. 1547–1561. DOI: 10.1111/1365-2745.12753.

Vuorinen, K. E. M.; Oksanen, L.; Oksanen, T.; Pyykönen, A.; Olofsson, J.; Virtanen, R. (2017): Open tundra persist, but arctic features decline-Vegetation changes in the warming Fennoscandian tundra. In Global Change Biol 23 (9), pp. 3794–3807. DOI: 10.1111/gcb.13710.

Wahren, C.-H. A.; Walker, M. D.; Bret-Harte, M. S. (2005): Vegetation responses in Alaskan arctic tundra after 8 years of a summer warming and winter snow manipulation

experiment. In Global Change Biol 11 (4), pp. 537-552. DOI: 10.1111/j.1365-2486.2005.00927.x.

Walker, D. A.; Daniëls, F. J. A.; Alsos, I.; Bhatt, U. S.; Breen, A. L.; Buchhorn, M. et al. (2016): Circumpolar Arctic vegetation: a hierarchic review and roadmap toward an internationally consistent approach to survey, archive and classify tundra plot data. In Environ. Res. Lett. 11 (5), p. 55005. DOI: 10.1088/1748-9326/11/5/055005.

Walker, M. D.; Wahren, C. H.; Hollister, R. D.; Henry, G. H. R.; Ahlquist, L. E.; Alatalo, J. M. et al. (2006): Plant community responses to experimental warming across the tundra biome. In Proceedings of the National Academy of Sciences of the United States of America 103 (5), pp. 1342–1346. DOI: 10.1073/pnas.0503198103.

Walker, D. A.; Raynolds, M. K.; Daniëls, F. J.A.; Einarsson, E.; Elvebakk, A.; Gould, W. A. et al. (2005): The Circumpolar Arctic vegetation map. In J Veg Sci 16 (3), pp. 267–282. DOI: 10.1111/j.1654-1103.2005.tb02365.x.

Walker, B.; Holling, C. S.; Carpenter, S. R.; Kinzig, A. P. (2004): Resilience, Adaptability and Transformability in Social-ecological Systems. In E&S 9 (2). DOI: 10.5751/ES-00650-090205.

Walker, D. A. (2003): Phytomass, LAI, and NDVI in northern Alaska: Relationships to summer warmth, soil pH, plant functional types, and extrapolation to the circumpolar Arctic. In J. Geophys. Res. 108 (D2). DOI: 10.1029/2001JD000986.

Walker, D. A.; Halfpenny, J. C.; Walker, M. D.; Wessman, C. A. (1993): Long-Term Studies of Snow-Vegetation Interactions. In BioScience 43 (5), pp. 287–301. DOI: 10.2307/1312061.

Wang, J. A.; Sulla-Menashe, D.; Woodcock, C. E.; Sonnentag, O.; Keeling, R. F.; Friedl, M. A. (2020): Extensive land cover change across Arctic-Boreal Northwestern North America from disturbance and climate forcing. In Global Change Biol 26 (2), pp. 807–822. DOI: 10.1111/gcb.14804.

Waddington, J.M. & Roulet, N.T. (1996): Atmosphere-wetland carbon exchanges: Scale dependency of CO2 and CH4 exchange on the developmental topography of a peatland. Global Biogeochemical Cycles 10: doi: 10.1029/95GB03871.

Wang, H.; Li, Z.; Cao, L.; Feng, R.; Pan, Y. (2021). Response of NDVI of Natural Vegetation to Climate Changes and Drought in China. Land, 10(9), 966. DOI: 10.3390/land10090966.

Wang, P.; Limpens, J.; Mommer, L.; van Ruijven, J.; Nauta, A. L.; Berendse, F. et al. (2017): Above- and below-ground responses of four tundra plant functional types to deep soil heating and surface soil fertilization. In J. Ecol. 105 (4), pp. 947–957. DOI: 10.1111/1365-2745.12718.

Wang, X.; Zi, H.; Wang, J.; Guo, X.; Zhang, Z.; Yan, T. et al. (2023): Grazing-induced changes in soil microclimate and aboveground biomass modulate freeze–thaw processes in a Tibetan alpine meadow. In Agriculture, Ecosystems & Environment 357, p. 108659. DOI: 10.1016/j.agee.2023.108659.

Wegmann, M.; Orsolini, Y.; Zolina, O. (2018): Warm Arctic–cold Siberia: comparing the recent and the early 20th-century Arctic warmings. In Environ. Res. Lett. 13 (2), p. 25009. DOI: 10.1088/1748-9326/aaa0b7.

Weijers, S.; Myers-Smith, I. H.; Löffler, J. (2018): A warmer and greener cold world: summer warming increases shrub growth in the alpine and high Arctic tundra. In Erdkunde 72 (1), pp. 63–85. DOI: 10.3112/erdkunde.2018.01.04.

Weiss, A. D.: Topographic Position and Landform Analysis (poster), ESRI User Conference, San Diego, USA, 2001.

White, E. P.; Brian J. E.; Jessica L. G. (2008): On Estimating the Exponent of Power-Law Frequency Distributions. In Ecology 89 (4), pp. 905–912. PMID: 18481513. DOI: 10.1890/07-1288.1.

Widhalm, B.; Bartsch, A.; Leibman, M.; Khomutov, A. (2017): Active-layer thickness estimation from X-band SAR backscatter intensity. In The Cryosphere 11 (1), pp. 483–496. DOI: 10.5194/tc-11-483-2017.

Williams, C. J.; McNamara, J. P.; Chandler, D. G. (2009): Controls on the temporal and spatial variability of soil moisture in a mountainous landscape: the signature of snow and complex terrain. In Hydrol. Earth Syst. Sci. 13 (7), pp. 1325–1336. DOI: 10.5194/hess-13-1325-2009.

Winkler, Daniel E.; Chapin, Kenneth J.; Kueppers, Lara M. (2016): Soil moisture mediates alpine life form and community productivity responses to warming. In Ecology 97 (6), pp. 1553–1563. DOI: 10.1890/15-1197.1.

With, K. A. (2019): Landscape Effects on Ecosystem Structure and Function. In Kimberly A. With (Ed.): Essentials of landscape ecology. Oxford: Oxford University Press (Oxford workshop series), pp. 512–546.

Wolf, A.; Callaghan, T. V.; Larson, K. (2008): Future changes in vegetation and ecosystem function of the Barents Region. In Climatic Change 87 (1-2), pp. 51–73. DOI: 10.1007/s10584-007-9342-4.

Woodcock, C. E. & Strahler A. H. (1987). The factor of scale in remote sensing. Remote Sensing of Environment, Vol. 21, Iss. 3, pp. 311-332. DOI: 10.1016/0034-4257(87)90015-0.

Woollett, J.; Ólafsson, S.; Ævarsson, U.; Adderley, W.; Þórsdóttir, K.; Sigurgeirsson, M.; Gisladottir, G.; Dupont-Hébert, C. (2014): Svalbarðsrannsóknir 2013: Bægisstaðir, Hjálmarvík, Kúðá, Svalbarð, Sjóhúsavík og Skriða / Archaeological Fieldwork at Svalbarð, NE Iceland 2013: Bægisstaðir, Hjálmarvík, Kúðá, Svalbarð, Sjóhúsavík og Skriða.

Xu, D & Guo X. (2014): Compare NDVI Extracted from Landsat 8 Imagery with that from Landsat 7 Imagery. American Journal of Remote Sensing. Vol. 2, No. 2, pp. 10-14. DOI: 10.11648/j.ajrs.20140202.11

Xu, L.; Myneni, R. B.; Chapin III, F. S.; Callaghan, T. V.; Pinzon, J. E.; Tucker, C. J. et al. (2013): Temperature and vegetation seasonality diminishment over northern lands. In Nature Clim Change 3 (6), pp. 581–586. DOI: 10.1038/nclimate1836.

Yan, Y.; Yan, R.; Wang, X.; Xu, X.; Xu, D.; Jin, D. et al. (2019): Grazing affects snow accumulation and subsequent spring soil water by removing vegetation in a temperate grassland. In The Science of the total environment 697, p. 134189. DOI: 10.1016/j.scitotenv.2019.134189.

Yang, D.; Morrison, B. D.; Davidson, K. J.; Lamour, J.; Li, Q.; Nelson, P. R. et al. (2022): Remote sensing from unoccupied aerial systems: Opportunities to enhance Arctic plant ecology in a changing climate. In J. Ecol. 110 (12), pp. 2812–2835. DOI: 10.1111/1365-2745.13976.

Yang, D.; Meng, R.; Morrison, B. D.; McMahon, A.; Hantson, W.; Hayes, D. J. et al. (2020): A Multi-Sensor Unoccupied Aerial System Improves Characterization of Vegetation Composition and Canopy Properties in the Arctic Tundra. In Remote Sensing 12 (16), p. 2638. DOI: 10.3390/rs12162638.

Yao, Y (2024): Pattern and change of NDVI and their environmental influencing factors for 1986–2019 in the Qinling-Daba Mountains of central China. Frontiers in Forests and Global Change, Vol 7. DOI: 10.3389/ffgc.2024.1372488.

Zagajewski, B.; Kycko, M.; Tømmervik, H.; Bochenek, Z.; Wojtuń, B.; Bjerke, J. W.; Kłos, A. (2018): Feasibility of hyperspectral vegetation indices for the detection of chlorophyll concentration in three high Arctic plants: Salix polaris, Bistorta vivipara, and Dryas octopetala. In Acta Soc Bot Pol 87 (4). DOI: 10.5586/asbp.3604.

Zagajewski, B.; Tømmervik, H.; Bjerke, J.; Raczko, E.; Bochenek, Z.; Kłos, A. et al. (2017): Intraspecific Differences in Spectral Reflectance Curves as Indicators of Reduced Vitality in High-Arctic Plants. In Remote Sensing 9 (12), p. 1289. DOI: 10.3390/rs9121289.

Zelnik, Y. R. & Meron, E. (2018): Regime shifts by front dynamics. In Ecological Indicators 94, pp. 544–552. DOI: 10.1016/j.ecolind.2017.10.068.

Zhang, R.; Wang, H.; Fu, Q.; Rasch, P. J.; Wu, M.; Maslowski, W. (2021): Understanding the Cold Season Arctic Surface Warming Trend in Recent Decades. In Geophys. Res. Lett. 48 (19), Article e2021GL094878. DOI: 10.1029/2021GL094878.

Zhang, W.; Miller, P. A.; Smith, B.; Wania, R.; Koenigk, T.; Döscher, R. (2013): Tundra shrubification and tree-line advance amplify arctic climate warming: results from an individual-based dynamic vegetation model. In Environ. Res. Lett. 8 (3), p. 34023. DOI: 10.1088/1748-9326/8/3/034023.

Zhao, Z.; Frenne, P. de; Peñuelas, J.; van Meerbeek, K.; Fornara, D. A.; Peng, Y. et al. (2022): Effects of snow cover-induced microclimate warming on soil physicochemical and biotic properties. In Geoderma 423, p. 115983. DOI: 10.1016/j.geoderma.2022.115983.

Zhu, K.; Sun, Z.; Zhao, F.; Yang, T.; Tian, Z.; Lai, J. et al. (2021): Relating Hyperspectral Vegetation Indices with Soil Salinity at Different Depths for the Diagnosis of Winter Wheat Salt Stress. In Remote Sensing 13 (2), p. 250. DOI: 10.3390/rs13020250.

Zinger, L.; Shahnavaz, B.; Baptist, F.; Geremia, R. A.; Choler, P. (2009): Microbial diversity in alpine tundra soils correlates with snow cover dynamics. In The ISME journal 3 (7), pp. 850–859. DOI: 10.1038/ismej.2009.20.

Žížala, D.; Juřicová, A.; Zádorová, T.; Zelenková, K.; Minařík, R. (2019): Mapping soil degradation using remote sensing data and ancillary data: South-East Moravia, Czech Republic. In European Journal of Remote Sensing 52 (sup1), pp. 108–122. DOI: 10.1080/22797254.2018.1482524.

Zona, D.; Lafleur, P. M.; Hufkens, K.; Gioli, B.; Bailey, B.; Burba, G. et al. (2023): Pan-Arctic soil moisture control on tundra carbon sequestration and plant productivity. In Global Change Biol 29 (5), pp. 1267–1281. DOI: 10.1111/gcb.16487.

APPENDIX

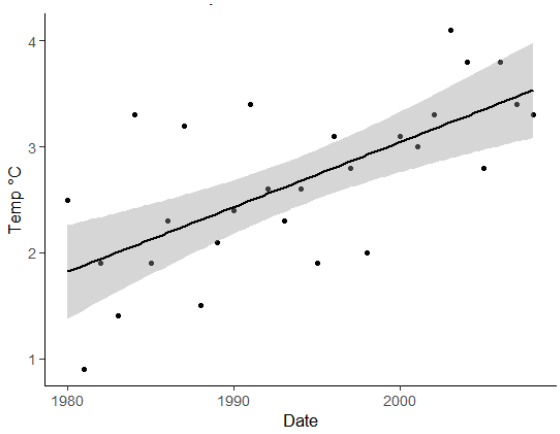

Fig. A1 Temperature change in N-Iceland Raufarhöfn for the period 1980-2008. LOESS curve fitted to mean annual temperature with 95% confidence interval.

Table A1 Satellite datasets downloaded from respective platforms.

Satellite	Product ID	Type	Source
PlanetScope	*20210901_123636_17_2407_3B_AnalyticMS*	*Level 3B*	*planet.com*
	20210901_123638_47_2407_3B_AnalyticMS	*Level 3B*	
	20210901_114920_66_2440_3B_AnalyticMS	*Level 3B*	
Sentinel-2	*S2A_MSIL2A_20210901T130301_N0301_R038_T28WDU_20210901T154212*	*Level 2a*	*scihub.copernicus.eu*
Landsat-8	*LC08_L2SP_217014_20210808_20210819_02_T1*	*Collection 2, Level 2, Tier 1*	*earthexplorer.usgs.gov*
	LC08_L2SP_218014_20210831_20210909_02_T1	*Collection 2, Level 2, Tier 1*	

Table A2 Accessed GEE databases for time series analysis.

GEE database
USGS Landsat 8 Collection 2 Tier 1 TOA Reflectance
USGS Landsat 7 Collection 2 Tier 1 TOA Reflectance
USGS Landsat 5 TM Collection 2 Tier 1 TOA Reflectance

Table A3 Aerial photos used from LMI.

Flight location and path	Photo Number	Date
91 - Balafell-Melrakkanes	F-8070	01/07/1980

Table A4 Mean SHEI values for surveyed sites and different spatial resolutions (from Fig. 29)

Site	Spatial resolution [m]									
	0.5	**1**	**3**	**5**	**10**	**20**	**30**	**50**	**100**	**150**
As	0.36	0.49	0.63	0.69	0.75	0.80	0.77	0.72	0.69	0.66
Gs3	0.40	0.56	0.69	0.70	0.68	0.64	0.65	0.68	0.69	0.70
Sval1	0.41	0.57	0.65	0.64	0.62	0.61	0.62	0.65	0.66	0.65
Gs1	0.42	0.59	0.70	0.71	0.70	0.70	0.73	0.78	0.84	0.83
Reveg	0.32	0.43	0.52	0.55	0.58	0.65	0.72	0.81	0.88	0.82
Gs4	0.35	0.50	0.63	0.66	0.68	0.71	0.75	0.80	0.85	0.83
Gs2	0.36	0.50	0.63	0.66	0.69	0.74	0.80	0.85	0.89	0.83
Sval9	0.31	0.43	0.56	0.60	0.63	0.69	0.75	0.84	0.90	0.94
Sval8	0.24	0.33	0.43	0.47	0.53	0.61	0.66	0.78	0.88	0.99
Sval3	0.28	0.39	0.53	0.57	0.62	0.66	0.73	0.81	0.86	0.91
Sval7	0.29	0.41	0.56	0.61	0.68	0.76	0.80	0.85	0.88	0.87
Sval6	0.32	0.42	0.54	0.58	0.63	0.70	0.78	0.86	0.94	0.99
Mean	0.34	0.47	0.59	0.62	0.65	0.69	0.73	0.78	0.82	0.82

Table A5 ID of used PlanetScope imagery for fractional vegetation cover calculation.

	PlanetScope Data for FVC
Iceland	20220817_115827_61_2276_3B_AnalyticMS_8b
	20220817_115825_33_2276_3B_AnalyticMS_8b
Finland	20220730_095405_61_249c_3B_AnalyticMS_8b

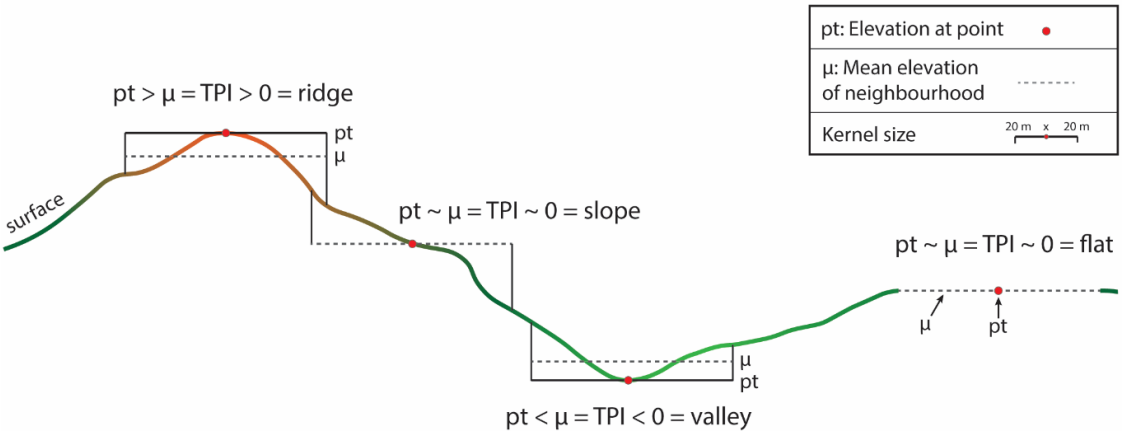

Fig. A2 Concept of the topographic position index (TPI). Positive TPI values are indicative of ridges, while negative values represent hollows. TPI values around 0 correspond to plains or straight slopes. Landforms are sensitive to scale and are depending on the kernel size.

Table A6 SCD statistics for each study site.

SCD	Mean	Median	Min	Max	SD	Variance
Fin1	152	154	122	180	7.5	56.3
Fin2	158	157	132	195	9.9	98.8
Ice1	69	67	50	106	9.1	82.9
Ice2	93	94	61	120	7.1	51.1
Ice3	103	104	74	138	8.1	65.8

Table A7 FVC statistics for each study site.

FVC	Mean	Median	Min	Max	SD	Variance
Fin1	0.46	0.45	0	1	0.16	0.02
Fin2	0.34	0.33	0	1	0.15	0.02
Ice1	0.72	0.77	0	1	0.22	0.05
Ice2	0.69	0.74	0	1	0.20	0.04
Ice3	0.62	0.65	0	1	0.24	0.06

Table A8 TPI statistics for each study site.

TPI	Mean	Median	Min	Max	SD	Variance
Fin1	0.12	0.10	-3.86	4.20	0.78	0.61
Fin2	0.08	0.01	-5.54	6.35	1.36	1.85
Ice1	0.01	0.01	-0.73	1.11	0.17	0.03
Ice2	0.01	0.02	-1.17	1.17	0.17	0.03
Ice3	0.02	0.03	-1.51	1.84	0.21	0.04

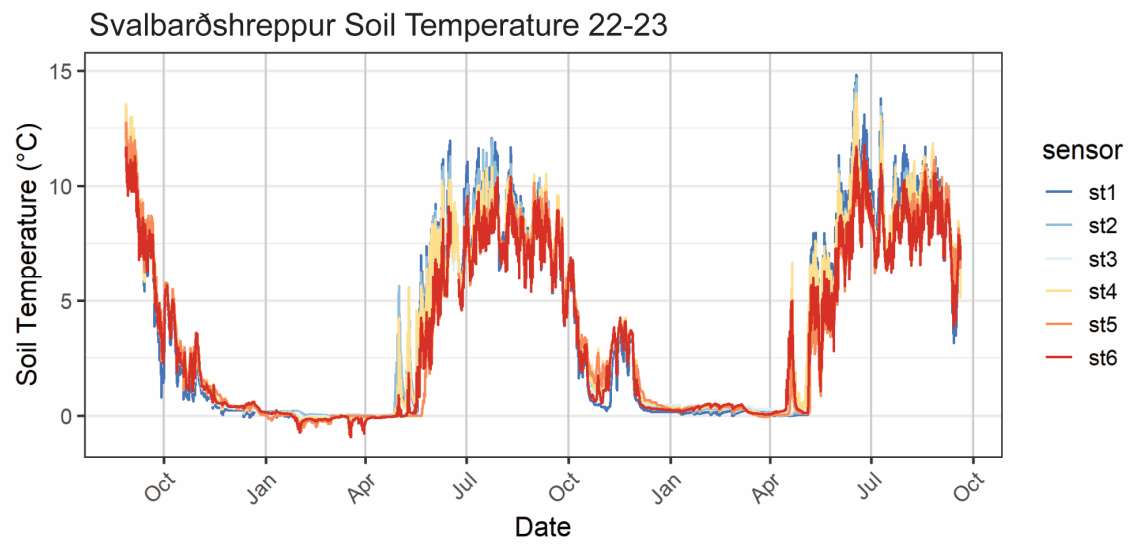

Fig. A3 A4 Soil temperature time series from study plot Icex2 in Svalbarðshreppur. St1 probe is located in the hollow St6 at the ridge.

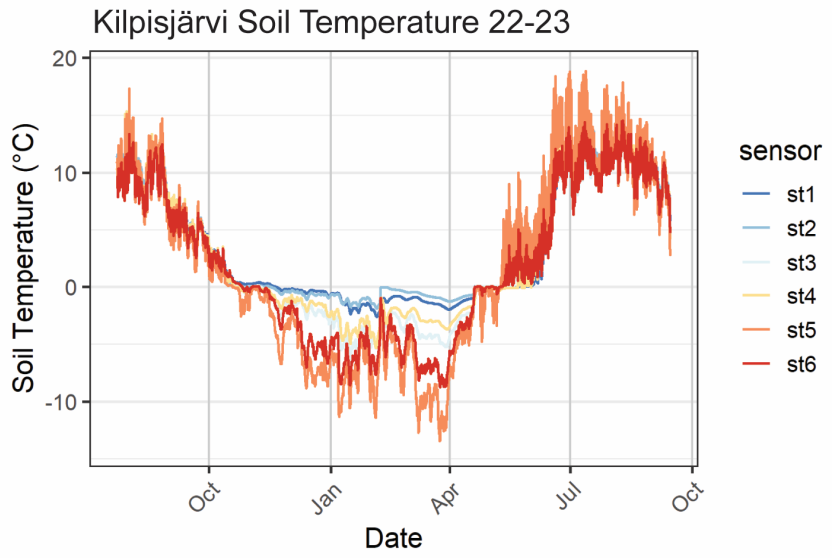

Fig. A4 Soil temperature time series from study plot Finx in Kilpisjärvi. St1 probe is located in the hollow St6 at the ridge.

Table A9 Domin Scale and percentage vegetation cover.

Domin scale	Range (%)	Mid-range value (%)
10	91-100	96
9	76-90	83
8	51-75	63
7	34-50	42
6	26-33	30
5	11-25	18
4	5-10	8
3	1-4	3
2	<1 (several individuals)	0.5
1	<1 (few individuals)	0.3

Table A10 ANOVA results for plant trait.

Metric	**Df**	**Sum Sq**	**Mean Sq**	**F value**	**Pr(>F)**	**signif**
Wet weight	2	0.003761	0.0018803	2.718	0.119	
	9	0.006225	0.0006917			
Dry weight	2	0.0007063	0.0003532	2.836	0.111	
	9	0.001121	0.0001246			
Leaf area (cm^2)	2	0.06259	0.0313	2.914	0.106	
	9	0.09665	0.01074			
SLA (cm^2/g)	2	3.5	1.77	0.049	0.952	
	9	322.2	35.81			
LDMC	2	0.0002618	0.0001309	0.928	0.43	
	9	0.00127	0.0001411			
Median height	2	91.73	45.87	6.439	0.0259	*
	7	49.87	7.12			
Max height	2	40.17	20.083	2.485	0.138	
	9	72.75	8.083			

Table A11 Dunns test for site Icex1 on vegetation index distribution for tested land cover compared to different topographic positions. 1) hollow, 2) slope, 3) ridge. The Asterisk indicates if comparison is significant.

Land cover	Veg Index	Comparison Topo position	Z	P_adj	signif
ls-veg	ndvi	1 - 2	28.973	2.1675E-184	*
ls-veg	ndvi	1 - 3	162.082	0	*
ls-veg	ndvi	2 - 3	109.803	0	*
ls-veg	ndre	1 - 2	15.678	3.19782E-55	*
ls-veg	ndre	1 - 3	191.245	0	*
ls-veg	ndre	2 - 3	151.707	0	*
ls-veg	rendvi	1 - 2	28.751	1.3117E-181	*
ls-veg	rendvi	1 - 3	147.456	0	*
ls-veg	rendvi	2 - 3	97.031	0	*
betula	ndvi	1 - 2	-13.597	6.21568E-42	*
betula	ndvi	1 - 3	171.538	0	*
betula	ndvi	2 - 3	176.584	0	*
betula	ndre	1 - 2	-20.223	9.16849E-91	*
betula	ndre	1 - 3	176.608	0	*
betula	ndre	2 - 3	187.602	0	*
betula	rendvi	1 - 2	-12.109	1.41626E-33	*
betula	rendvi	1 - 3	145.558	0	*
betula	rendvi	2 - 3	150.371	0	*

Table A12 Dunn's test for site Icex2 on vegetation index distribution for tested land cover compared to different topographic positions. 1) hollow, 2) slope, 3) ridge. The Asterisk indicates if comparison is significant.

Land cover	Veg Index	Comparison Topo position	Z	P_adj	signif
ls-veg	ndvi	1 - 2	-62.689	0	*
ls-veg	ndvi	1 - 3	293.093	0	*
ls-veg	ndvi	2 - 3	286.174	0	*
ls-veg	ndre	1 - 2	-92.4218	0	*
ls-veg	ndre	1 - 3	226.505	0	*
ls-veg	ndre	2 - 3	266.194	0	*
ls-veg	rendvi	1 - 2	-52.676	0	*
ls-veg	rendvi	1 - 3	288.776	0	*
ls-veg	rendvi	2 - 3	272.649	0	*
betula	ndvi	1 - 2	-94.7	0	*
betula	ndvi	1 - 3	-5.747	1.36363E-08	*
betula	ndvi	2 - 3	72.7143	0	*
betula	ndre	1 - 2	-84.5	0	*
betula	ndre	1 - 3	30.966	2.2957E-210	*

betula	ndre	2 - 3	100.275	0	*
betula	rendvi	1 - 2	-88.8404	0	*
betula	rendvi	1 - 3	-13.1042	4.67584E-39	*
betula	rendvi	2 - 3	60.652	0	*

Table A13 Dunn's test for site Finx on vegetation index distribution for tested land cover compared to different topographic positions. 1) hollow, 2) lower slope, 3) upper slope, 4) ridge. The Asterisk indicates if comparison is significant.

Land cover	Veg Index	Comparison Topo position	Z	P_adj	signif
betula	ndvi	1 - 2	-7.557	1.23557E-13	*
betula	ndvi	1 - 3	-39.679	0	*
betula	ndvi	2 - 3	-25.074	2.8509E-138	*
betula	ndvi	1 - 4	-72.147	0	*
betula	ndvi	2 - 4	-48.093	0	*
betula	ndvi	3 - 4	-22.496	1.3499E-111	*
betula	ndre	1 - 2	68.339	0	*
betula	ndre	1 - 3	134.453	0	*
betula	ndre	2 - 3	48.894	0	*
betula	ndre	1 - 4	156.364	0	*
betula	ndre	2 - 4	57.535	0	*
betula	ndre	3 - 4	5.761	2.51369E-08	*
betula	rendvi	1 - 2	-18.858	7.51558E-79	*
betula	rendvi	1 - 3	-60.926	0	*
betula	rendvi	2 - 3	-32.376	1.7714E-229	*
betula	rendvi	1 - 4	-95.605	0	*
betula	rendvi	2 - 4	-55.782	0	*
betula	rendvi	3 - 4	-22.407	1.006E-110	*
biocrust	ndvi	1 - 2	102.2	0	*
biocrust	ndvi	1 - 3	156.678	0	*
biocrust	ndvi	2 - 3	37.577	0	*
biocrust	ndvi	1 - 4	265.997	0	*
biocrust	ndvi	2 - 4	104.602	0	*
biocrust	ndvi	3 - 4	68.0179	0	*
biocrust	ndre	1 - 2	118.733	0	*
biocrust	ndre	1 - 3	212.245	0	*
biocrust	ndre	2 - 3	68.375	0	*
biocrust	ndre	1 - 4	345.787	0	*
biocrust	ndre	2 - 4	149.849	0	*
biocrust	ndre	3 - 4	80.033	0	*
biocrust	rendvi	1 - 2	88.142	0	*
biocrust	rendvi	1 - 3	126.356	0	*

biocrust	rendvi	2 - 3	25.234	5.0883E-140	*
biocrust	rendvi	1 - 4	220.563	0	*
biocrust	rendvi	2 - 4	83.398	0	*
biocrust	rendvi	3 - 4	59.886	0	*
crowberry	ndvi	1 - 2	-6.259	1.16474E-09	*
crowberry	ndvi	1 - 3	-1.599	0.329478409	
crowberry	ndvi	2 - 3	8.720	8.32155E-18	*
crowberry	ndvi	1 - 4	-0.211	1	
crowberry	ndvi	2 - 4	12.526	1.61214E-35	*
crowberry	ndvi	3 - 4	3.484	0.001479342	*
crowberry	ndre	1 - 2	6.925	1.30607E-11	*
crowberry	ndre	1 - 3	19.411	1.85543E-83	*
crowberry	ndre	2 - 3	21.396	4.3516E-101	*
crowberry	ndre	1 - 4	24.534	1.8868E-132	*
crowberry	ndre	2 - 4	32.467	9.4024E-231	*
crowberry	ndre	3 - 4	10.744	1.89781E-26	*
crowberry	rendvi	1 - 2	-7.259	1.17218E-12	*
crowberry	rendvi	1 - 3	-3.395	0.002056561	*
crowberry	rendvi	2 - 3	7.402	4.01576E-13	*
crowberry	rendvi	1 - 4	-2.483	0.039073018	*
crowberry	rendvi	2 - 4	10.261	3.1781E-24	*
crowberry	rendvi	3 - 4	2.487	0.038698273	*
ls-shrub	ndvi	1 - 2	10.67	4.21503E-26	*
ls-shrub	ndvi	1 - 3	-4.4301	2.82456E-05	*
ls-shrub	ndvi	2 - 3	-13.817	6.07255E-43	*
ls-shrub	ndvi	1 - 4	-33.662	6.195E-248	*
ls-shrub	ndvi	2 - 4	-38.917	0	*
ls-shrub	ndvi	3 - 4	-26.961	1.2578E-159	*
ls-shrub	ndre	1 - 2	90.390	0	*
ls-shrub	ndre	1 - 3	171.473	0	*
ls-shrub	ndre	2 - 3	62.457	0	*
ls-shrub	ndre	1 - 4	212.877	0	*
ls-shrub	ndre	2 - 4	95.857	0	*
ls-shrub	ndre	3 - 4	35.192	7.9145E-271	*
ls-shrub	rendvi	1 - 2	-3.124	0.005345018	*
ls-shrub	rendvi	1 - 3	-31.453	1.1468E-216	*
ls-shrub	rendvi	2 - 3	-24.082	1.1624E-127	*
ls-shrub	rendvi	1 - 4	-67.089	0	*
ls-shrub	rendvi	2 - 4	-54.349	0	*
ls-shrub	rendvi	3 - 4	-32.396	9.4232E-230	*